
A proteomic approach to investigate agronomic traits in barley using the genetic variation of mapping populations

Dissertation

Zur Erlangung des akademischen Grades
Doctor rerum naturalium (Dr. rer. nat.)

vorgelegt der

Naturwissenschaftlichen Fakultät I
Biowissenschaften
der Martin-Luther-Universität Halle-Wittenberg

von

Frau Katja Witzel

Geboren am 07.04.1978 in Nordhausen

Gutachter/in

1. Prof. Dr. Klaus Humbeck
2. Priv. Doz. Dr. Hans-Peter Mock
3. Assoc. Prof. Dr. Christine Finnie

Halle/Saale, den 11.09.2008

1. Abstract	1
2. Introduction	4
2.1. Approaches for crop improvement using mapping populations.....	4
2.2. Maturation and germination of barley grains	7
2.3. Adaptation to salt stress and characteristics of salinity tolerance	8
2.3.1. Physiology of salt stress	9
2.3.2. Plant strategies for adaptation to salt stress.....	11
2.3.3. Targets for improving salt tolerance in plants.....	11
Control of salt uptake and transport	11
Protection against osmotic stress	12
Promotion of plant growth in saline soil	13
2.4. Proteomics for the dissection of stress responses.....	13
2.5. Scientific aims of the work.....	15
3. Materials and Methods	17
3.1. Plant material.....	17
3.1.1. Barley genotypes and mapping populations.....	17
3.1.2. Plant growth in hydroponic culture and salinity treatments.....	17
3.1.3. Growth measurements.....	18
3.2. Protein extraction methods and concentration measurements.....	18
3.2.1. Extraction of water-soluble protein fraction from mature grains.....	18
3.2.2. Extraction of storage proteins from mature grains.....	18
3.2.3. Protein extraction from roots.....	19
3.2.4. Enrichment and extraction of plasma membrane proteins from roots	19
Enrichment of plasma membranes by two-phase partitioning method	19
Enrichment of hydrophobic proteins by batch reversed-phase chromatography	20
3.2.5. Determination of protein concentration in crude mixtures	21
3.3. Protein separation methods.....	21
3.3.1. SDS-PAGE.....	21
3.3.2. Two-dimensional gel electrophoresis.....	21
3.4. Visualization of proteins and image acquisition.....	22
3.4.1. Colloidal Coomassie Brilliant Blue staining.....	22
3.4.2. Ruthenium staining	22
3.4.3. Silver staining.....	23
3.5. Relative quantitation of proteins and peptides	23
3.5.1. Image analysis of 2-dimensional gel patterns	23
3.5.2. Label-free quantitation of tryptic peptides	23
Protein digest preparation.....	23
Liquid chromatography and mass spectrometry configuration.....	24
Data processing and protein identification.....	24
3.5.3. Western blotting	24
3.6. Protein identification	25
3.6.1. Peptide mass fingerprinting by MALDI-TOF MS.....	25
3.6.2. <i>De novo</i> sequencing of peptides by tandem MS/MS	25

3.7.	Molecular cloning techniques.....	26
3.7.1.	Bacterial strains, vectors and oligonucleotides	26
3.7.2.	RNA preparation and Northern blot analysis.....	27
3.7.3.	DNA preparation and Southern blot analysis.....	28
3.8.	Plant transformation	28
3.9.	Statistical analysis	28
3.9.1.	Cluster analysis of protein patterns	28
3.9.2.	Quantitative trait loci analysis for protein expression.....	29
3.9.3.	Principle component analysis of peptide profiles derived from LC-based mass spectrometry	29
4.	Results.....	30
4.1.	Grain protein profiling of the Brenda x HS213 mapping population.....	30
4.1.1.	Construction of a protein reference map from barley cv. Brenda mature grains	30
4.1.2.	Expression profiling of proteins in mature grains.....	32
	Analysis of the water-soluble protein fraction of barley grains from the first experiment.....	33
	Analysis of the water-soluble protein fraction of barley grains from the second experiment.....	37
	Calculation of QTL for protein expression	40
	Analysis of alcohol-soluble grain storage proteins	45
4.2.	Grain proteome analysis of accessions from the Oregon Wolfe Barley mapping population differing in salt stress response	48
4.2.1.	Comparative proteome profiling	48
4.2.2.	Identification of candidate proteins by mass spectrometry	51
4.2.3.	Cloning and overexpression of candidate proteins	53
4.3.	Proteome analysis of accessions from the Steptoe Morex mapping population with contrasting response towards salt stress at different developmental stages	57
4.3.1.	Comparative proteome profiling of mature grains	57
	Identification of candidate proteins by mass spectrometry	60
	Cloning and overexpression of candidate proteins	61
4.3.2.	Assessment of salt tolerance at the seedling stage of the Steptoe and Morex parental lines	62
4.3.3.	Cultivar-specific and salt stress-affected protein expression in roots of Steptoe and Morex	64
4.3.4.	Identification of progeny lines showing a similar response towards salt stress at the seedling stage as the parent lines.....	75
4.3.5.	Plasma membrane protein expression in roots of Steptoe and Morex subjected to salt stress	76
	Enrichment of plasma membranes using two-phase partitioning method	77
	Identification of plasma membrane proteins by LC-based mass spectrometry ..	78
	Comparative analysis of the plasma membrane proteome of Steptoe and Morex roots under salt stress conditions	83
5.	Discussion	89
5.1.	Detection of QTL for protein expression in mature grains of the Brenda x HS213 mapping population	89

5.2.	Proteome analysis of mature grains from contrasting genotypes reveals candidate proteins conferring salt tolerance during germination.....	91
5.2.1.	Candidate proteins retrieved in the Oregon Wolfe Barley population.....	91
5.2.2.	Candidate proteins detected in the Steptoe Morex population.....	95
5.3.	Hydroponic long-term salt stress experiments using the parent genotypes of the Steptoe Morex population confirm the results of the germination assay	100
5.4.	Root proteome analysis of the parent lines of the Steptoe Morex population after salt stress treatment reveals cultivar-specific protein expression	102
5.4.1.	Proteins non-responsive to salt stress treatment.....	105
5.4.2.	Proteins showing the same regulation in both genotypes upon treatment	106
5.4.3.	Proteins exhibiting a cultivar-specific regulation upon treatment	110
5.5.	Identification of accessions from the Steptoe Morex population with contrasting response towards salinity treatment.....	113
5.6.	Proteome analysis of root plasma membranes reveals salt stress-responsive protein expression	114
5.6.1.	Identification of plasma membrane proteins from barley root tissue.....	114
5.6.2.	Salt-induced changes in the plasma membrane proteome of barley genotypes with contrasting response towards salinity stress.....	116
5.7.	Summary: what are the characteristics of a salt tolerant barley genotype and how can salt tolerance be improved?	119
6.	References	122
7.	Abbreviations.....	135
8.	Acknowledgements.....	137
9.	Curriculum vitae	139
10.	Affirmation.....	143
11.	Appendix	144

1. Abstract

In recent years, the complete genome sequences of model (*Arabidopsis thaliana*) and crop plants (*Oryza sativa*) as well as an enormous number of plant expressed sequence tags (EST) have become available. This huge information resource is utilized for the determination of the function of many genes simultaneously in 'Functional Genomics' approaches including global transcript and protein profiling together with the employment of mutant and transgenic plants. In order to assign the location of a gene in the genome, gene expression studies can be combined with genomic marker analysis in 'Genetical Genomics' approaches. In this thesis both types of studies were applied for the determination of grain protein composition and for analysing salt stress mechanisms at the germination and at the seedling stage in barley.

Barley (*Hordeum vulgare*) is an important cereal crop grown both for the feed and malting industries. Hence, there is a high interest to gain deeper insight into the determinants of nutritional quality and abiotic stress tolerance at the molecular level in order to improve the assessment of new traits. The GABI-SEED II project at the IPK Gatersleben used barley as a model plant representing cool season cereals for gene and protein expression as well as for marker-based fingerprinting of related lines with the aim to identify trait-related genes using quantitative trait loci (QTL) analysis. For the characterization of a set of doubled haploid introgression lines presenting a wild barley genome (*Hordeum spontaneum* HS213) within a modern cultivar background (*H. vulgare* cv. Brenda), 2-dimensional (D) gel electrophoresis was employed for the analysis of protein content and composition of mature grains. In two independently grown sets of plants, about 70 QTL for protein expression were detected and subjected to mass spectrometry-based identification. Although only few QTL signals could be recovered due to variances in growing conditions between both sets, results demonstrate the high technical reproducibility in detecting single features in the overall protein complement that can be achieved by 2-D gel electrophoresis. For the second set of plants, which was more robust in terms of growth conditions, most pQTL were classified as metabolism and disease/defence related proteins, making them relevant for future molecular breeding projects. Among the cereals, barley is considered as notably salt tolerant and cultivars display considerable variability in tolerance towards salt stress. In fact, the parental lines of the Oregon Wolfe Barley (OWB) mapping population and the parents of the Steptoe Morex (SM) mapping population display contrasting salt stress response during germination under salinity stress. With the objective to investigate the determinants of salt tolerance at the germination

stage the grain proteome of those lines was compared. In order to limit the number of possible candidate proteins and to rule out proteins not involved in salt tolerance mechanisms, four progeny lines were added to the analysis that showed an even stronger trait for salt response than the parent lines in the respective population. As a result, 6 and 7 protein spots were identified differing in expression between groups of salt tolerant and salt sensitive genotypes in the OWB and the SM population, respectively. More abundant in salt tolerant cultivars were proteins that play a role in NADPH generation and the synthesis of ABA-responsive proteins. To test their functionality, stable transformation studies in a salt sensitive barley cultivar ('Golden Promise') using promoters, which drive ubiquitous and endosperm-specific expression, were initiated.

Hydroponic salt stress experiments using the parent lines of the SM mapping population confirmed the results of the germination assays and revealed a higher tolerance of the Morex parent towards salinity treatment than the Steptoe parent. In order to identify proteins conferring salt tolerance and to understand the regulation of protein expression and protein function during salt stress, the proteome of roots from both genotypes under control and salt stress conditions (100 mM and 150 mM NaCl) was investigated by 2-D gel electrophoresis. MS-based identification was successful for 28 protein spots that were grouped according to their expression into classes of cultivar-specific, salt stress-responsive or cultivar-specific salt stress-responsive proteins. Promising candidates for increasing salt tolerance in barley include proteins involved in the detoxification of reactive oxygen species and protein synthesis.

Roots regulate the ion and nutrient uptake, transport and regulation of water status and here, proteins in the lipid bilayer of plasma membranes are of great biological importance. For an in-depth characterisation of proteins embedded in or attached to plasma membranes, these proteins were investigated in a subcellular proteomics approach. Aqueous two-phase partitioning method for the enrichment of plasma membranes was applied, followed by reversed-phase chromatography for the additional enrichment of hydrophobic integral membrane proteins. Membrane proteins are not amenable to classical 2-D gel electrophoresis and therefore, identification and quantitation of proteins was accomplished by label-free liquid chromatography-based mass spectrometry method. The proteome profiling of barley root plasma membrane proteins yielded in the identification of about 160 proteins. Out of these, 56 % had one or more predicted transmembrane domain. However, it is very likely that the remaining soluble proteins have been coenriched with plasma membrane proteins due to a close interaction of both, like membrane-anchored GTP-binding proteins and ADP-

ribosylation factors functioning in signalling pathways and targeting to the plasma membrane. Subsequent to the proteome profiling, samples from the salt sensitive and the salt tolerant barley cultivar under control and stress conditions were compared. Alterations in the plasma membrane proteome demonstrate a genotype-specific response towards salt stress by modulating transport activities, signalling processes and protein turnover rate.

2. Introduction

2.1. Approaches for crop improvement using mapping populations

Plants are exposed to various biotic and abiotic stress factors under field conditions and yield reduction caused by these stresses can make up to 50 % (Vij and Tyagi, 2007). In the past, researchers used a gene-by-gene approach to identify genes conferring tolerance but since stress tolerance or biomass production in general is a multigenic trait, those networks are not understood entirely.

Complete genome sequences and large-scale EST sequencing projects from various model and crop plants facilitated the use of tools that aid in the determination of gene functions. These approaches are summarized as 'Functional Genomics'. The progress made in recent years in exploring the genome resulted in the generation of methods, such as microarrays, 2-D gel electrophoresis and yeast two-hybrid, for high-throughput analysis of the transcriptome, proteome and metabolome (Figure 1).

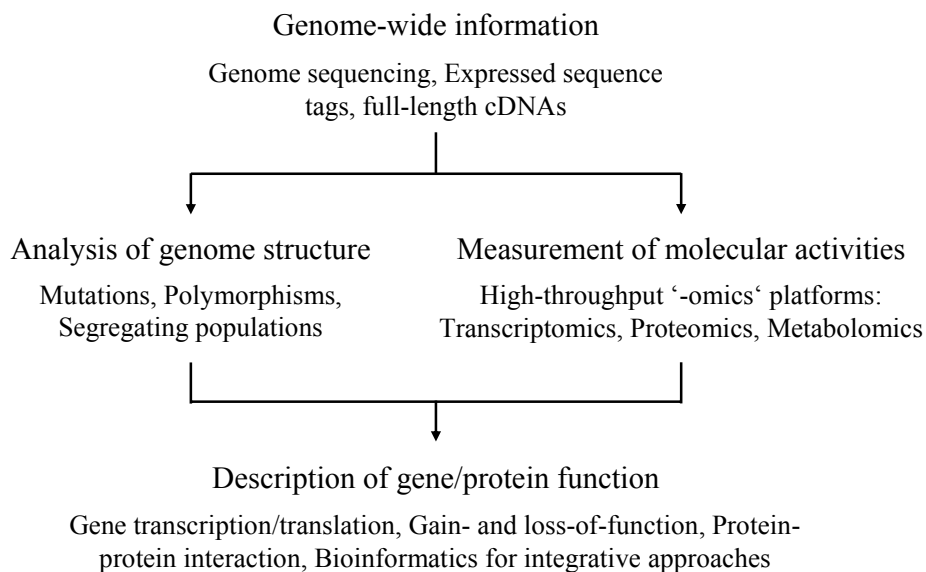


Figure 1: The 'Functional Genomics' approaches aim at the understanding of gene and protein functions and interactions using global expression profiling. The availability of sequence information provides the basis for the application of transcript and protein profiling in conjunction with mutant or transgenic genotypes. For processing the large quantity of generated data sets, bioinformatic methods are used.

From the literature several examples are known where 'Functional Genomics' was applied for unravelling biosynthetic pathways or stress response mechanisms. For the investigation of gene-to-metabolite networks, transcriptomics and metabolomics can be applied in conjunction

as shown in a recent study on *Arabidopsis* plants overexpressing a MYB transcription factor (Tohge et al., 2005). Transcriptome analysis of about 22,000 genes on DNA microarrays and metabolome analysis of 1,800 putative metabolites yielded in the identification of new genes involved in flavonoid biosynthesis. When leaf extracts of four *Arabidopsis* genotypes were subjected to gas chromatography/mass spectrometry, results indicated that each genotype possessed a distinct ‘metabolite phenotype’ (Fiehn et al., 2000). Proteome analysis using 2-D gel electrophoresis of an *Arabidopsis* mutant with disturbed cell division indicated an elevated protein expression of stress-responsive proteins (Lee et al., 2008). In global gene expression profiling studies during abiotic stress treatment, stress-inducible genes were identified enabling the elucidation of stress response mechanisms (reviewed in Vij and Tyagi, 2007).

When breeding for favourable agronomic traits, the distribution of the genome in the progeny can be followed by molecular marker analysis. In order to assign the genomic region to a phenotype, ‘Functional Genomics’ is then extended to ‘Genetical Genomics’. The term ‘Genetical Genomics’ was introduced by Jansen and Nap (2001) and outlines a strategy for unravelling metabolic, regulatory or developmental pathways by merging genetics with genomics. Gene expression data from related individuals in a segregating population are treated as inherited quantitative trait and molecular marker data of each individual can be used to map this trait on the genome by quantitative trait loci (QTL) analysis (Figure 2). Since the publication of this strategy in 2001, this approach has been utilized for the dissection of complex traits in yeast, mouse as well as human cell lines with great success and therefore, the application in the field of plant biology has been attempted (reviewed in de Koning and Haley, 2005; Li and Burmeister, 2005; Varshney et al., 2005; Vij and Tyagi, 2007).

The improvement of crop plants aims especially at the increase in biomass production at different developmental stages as well as biotic and abiotic stress tolerance. A valuable natural genetic resource for these targeted breeding strategies are mapping populations derived from two parents with phenotypic differences for any given trait that can be scored for each individual of the resulting population, such as grain weight, fruit composition, transcript abundance or protein expression. Using mapping populations displaying variability of the trait of interest and that have been genotyped with molecular markers, these physiological traits can be related to the genome locations of genes affecting the trait. In a segregating population, the respective trait can be more pronounced in progeny lines as it is in one of the parental lines. This phenomenon is called transgression and results in the dispersion of genes between the parents increasing or decreasing the trait of interest in some individuals where all the

alleles increasing or decreasing the trait have been combined (Prioul et al., 1997). One example for transgression is presented in Figure 3. Here, the parental lines as well as the offspring lines of the Oregon Wolfe Barley population were tested for salt tolerance during germination and some of the progeny revealed a stronger trait for salt response as compared to the parents (Weidner et al., 2005).

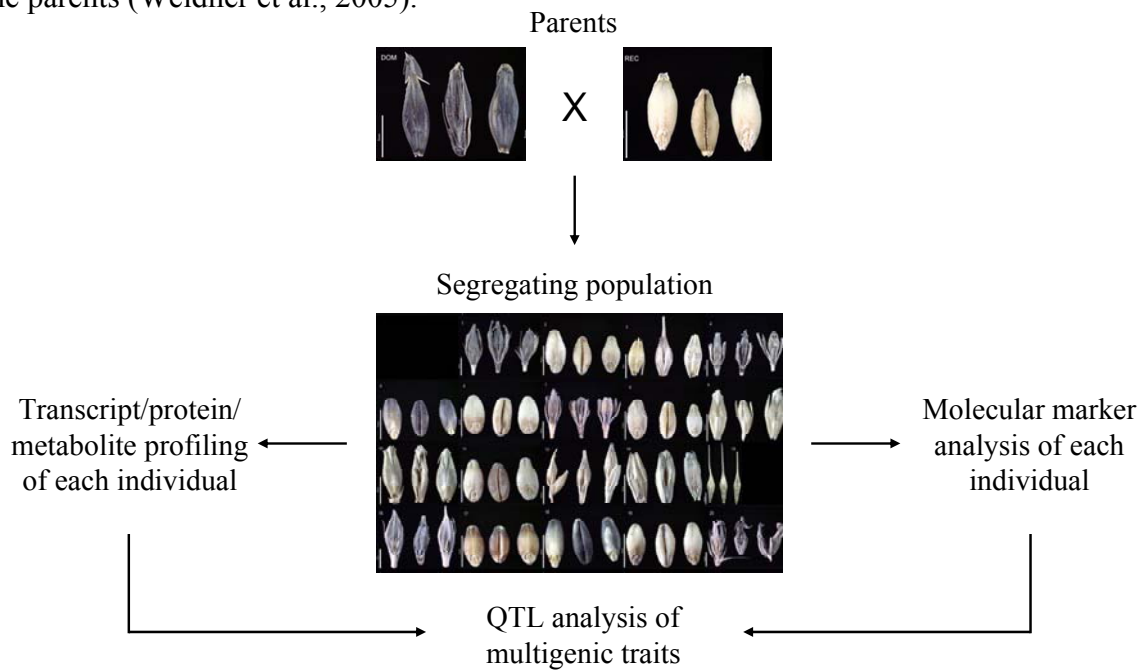


Figure 2: Transcript, protein and metabolite profiling as well as molecular marker analysis of individuals from a segregating population enables QTL analysis for the identification of influential transcripts, proteins or metabolites in ‘Genetical Genomics’ approaches. To generate a segregating population two barley marker stocks are crossed to generate the F1 progeny and homozygous double haploid genotypes are produced. The F1 progeny is self-crossed for a number of times or backcrossed with one parent to generate an advanced backcross population (Tanksley and Nelson, 1996). Each individual is genotyped by molecular markers and subjected to microarray, proteome and/or metabolite analysis (Jansen and Nap, 2001). Using this strategy, the expression profile of a given mRNA, protein or metabolite can be related to its underlying genetic components and genetic map positions by QTL analysis. Pictures from accessions of the Oregon Wolfe Barley mapping population are courtesy of Dr Niels Stein, IPK.

It is also possible to introduce only a relatively small number of genes into genomes and this is achieved in advanced backcross populations (Tanksley and Nelson, 1996). In order to introduce favourable traits into crop species, the genomes of wild relatives are exploited by crossing an elite variety with a wild species. Offspring generations are backcrossed several times with the crop variety and genotyped with polymorphic molecular markers.

In recent years, the amount of functionally characterized genes, expressed sequence tags and genome sequencing projects increased rapidly. Today, about 500,000 EST sequences are

annotated for barley in public databases (www.ncbi.nlm.nih.gov, 25. April 2008). This huge information resource for the development of molecular markers derived from these sequences and the generation of high-density genomic marker maps accelerated the rise of QTL analysis. Since gene expression is a quantitative trait that can be scored for each individual of a population, it can be integrated for QTL analysis.

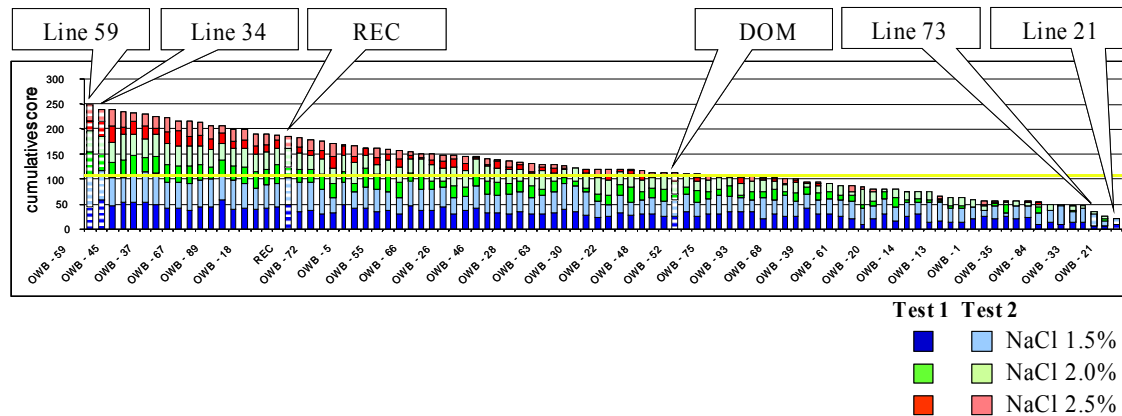


Figure 3: Germination assay for salt tolerance using the OWB mapping population. The germination rate was scored in two independent experiments and the cumulative score is given in the diagram. The parent REC displayed a higher tolerance towards salinity during germination, whereas the DOM parent was more sensitive towards stress treatment. From all progeny lines tested, 24 % reacted even more tolerant than REC and 49 % were more sensitive than DOM. The diagram is taken from Weidner et al. (2005).

Keurentjes and co-workers have used 160 lines from a recombinant inbred line population derived from a cross of *Arabidopsis thaliana* cv. Landsberg *erecta* with cv. Cape Verde Island, determined from each line the transcript levels of about 24,000 genes on DNA microarrays and genotyped each line with 144 molecular markers (Keurentjes et al., 2007). By treating gene expression as inherited factor, the data set was used for QTL analysis and revealed a total of 4,523 QTL for gene expression in this population. This data set provided the basis for the construction of regulatory networks as shown for genes associated with flowering time. In a global transcript profiling approach, West et al. analysed transcripts of 211 recombinant inbred lines from a population derived from a cross between *A. thaliana* cv. Bayreuth-0 and cv. Shahdara and detected about 36,000 eQTL (West et al., 2007).

2.2. Maturation and germination of barley grains

Grains of crop plants, such as rice, maize or barley, are highly valuable for the nutrition of humans and livestock as they contain a high percentage of sugars, starch, storage proteins and fatty acids. Most of these major compounds are synthesized at the onset of grain maturation

and are stored to serve the developing embryo during grain germination (Figure 4). While a large number of the genes responsible for the synthesis of these compounds are known, the regulatory networks that determine protein composition, grain size or weight are not fully understood. In order to unravel these networks in barley, large-scale analysis of gene and protein expression was targeted on grain maturation and germination. During barley grain maturation, different regulators are active in embryo and endosperm (Sreenivasulu et al., 2006). In the developing embryo, abscisic acid (ABA) signalling pathways induce the synthesis of storage proteins conferring desiccation tolerance, such as dehydrins and late embryogenesis abundant (LEA) proteins. In the endosperm ABA-related genes induce the synthesis of starch and storage proteins, while ethylene signalling influences the expression of proteases and leads to programmed cell death in this tissue leaving cell structure intact. Recent results indicate that the phytohormone-responsive transcription factors controlling grain germination are synthesised already during late maturation (Sreenivasulu et al., 2008).

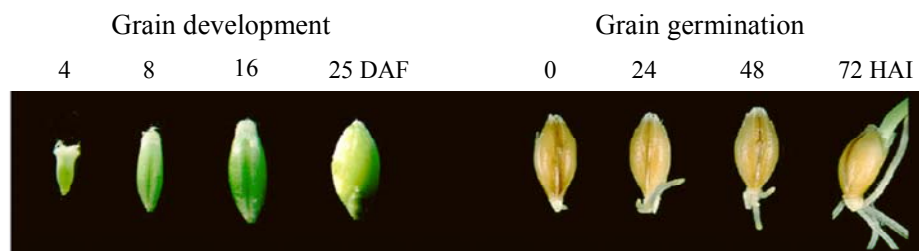


Figure 4: Key stages of grain development and germination in barley. The endosperm development is divided into the pre-storage, storage and desiccation phase. Upon the uptake of water, the embryonic axis is extended and the radicle protrudes (DAF, days after fertilisation; HAI, hours after imbibition). The picture is taken from Sreenivasulu et al. (2008).

While ABA concentration is highest during maturation and dormancy, gibberellic acid (GA) concentration increases at the stage of imbibition and germination. GA-responsive gene expression leads to the mobilisation of storage compounds to serve as C and N source for the embryo (Bewley, 1997). New synthesised proteins during germination confer oxidative stress and desiccation tolerance (Bønsager et al., 2007).

2.3. Adaptation to salt stress and characteristics of salinity tolerance

In addition to drought and extreme temperatures, salinity is one of the most severe abiotic stress factors threatening agriculture worldwide. More than 800 million hectares of land are salt-affected and this makes 6 % of the world's total land area (Munns, 2005). With an

increasing demand for food production for the growing world population, improving salt tolerance of crops is an important issue.

2.3.1. Physiology of salt stress

The physiology of salt stress responses in different plant species is well described and dramatic differences in salt tolerance between species are found. The effect of soil salinity on growth of salt sensitive lupin, salt tolerant barley and two halophytes is shown in Figure 5. Lupin is one of the most salt sensitive crops and plants of this species will not survive salinity concentrations higher than 100 mM NaCl, while barley, one of the most salt tolerant crops, will produce a reduced yield under these conditions (Munns et al., 2002). Kaller grass and saltbush are two Australian halophytes that can tolerate NaCl concentrations higher than 250 mM NaCl.

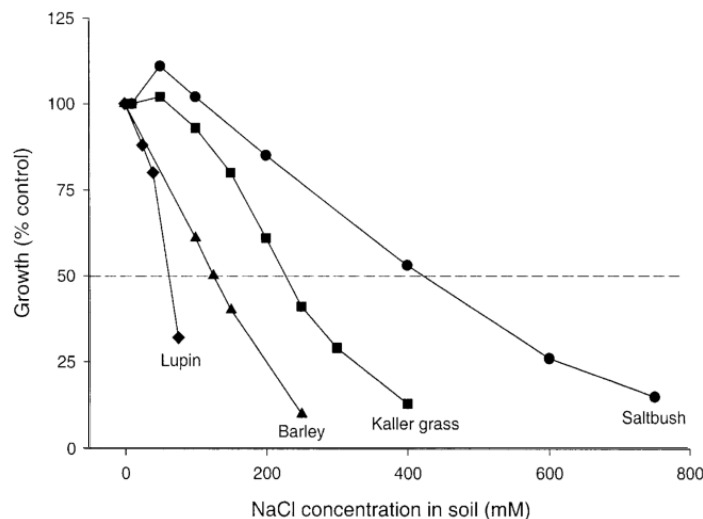


Figure 5: Inhibition of plant growth by soil salinity in four species showing different degrees of tolerance. Lupin is highly sensitive towards salinity, whereas barley can tolerate elevated levels of NaCl. Kaller grass and saltbush are halophytes that can cope with salt at concentrations in the range of seawater. The diagram is taken from Munns et al. (2002).

In general, high levels of Ca^{2+} , Mg^{2+} , SO_4^{2-} and NaCl characterize soil salinity, while effects of Na^+ solely are referred to as sodicity. Since NaCl concentration plays the major role on saline soils, sodicity is equalled with salinity in most cases. Elevated levels of salt negatively influence porosity as well as water permeability of the soil and lower the osmotic potential because of the higher concentration of ions in the soil increasing the electrical conductivity. For that reason, the effect of salinity on plant growth can be divided into two phases: the first phase is described as osmotic stress and the second phase as salt-specific stress (Munns, 2005). In the first phase the ability of the plant to take up water is reduced and the cellular and

metabolic processes involved are common to drought. While the osmotic potential decreases, cell expansion and cell wall synthesis, protein synthesis, stomatal conductance as well as photosynthetic activity are inhibited, while solute and ABA accumulation is induced. The salt building up within the plant at this early stage of salinity stress is below toxic levels in growing cells and it is hypothesised that it is actually beneficial as it might be taken up into the expanding vacuole for osmotic adjustment (Fricke, 2004).

In the second phase of salinity stress the salt inside the plant causes growth inhibition due to its toxicity. With the uptake of water, salts are transported with the transpiration stream to leaves where concentration is gradually increasing as the water evaporates. Na^+ enters the roots passively by moving down an electrochemical-potential gradient, while Cl^- entry is restricted by a negative plasma membrane potential (Figure 6).

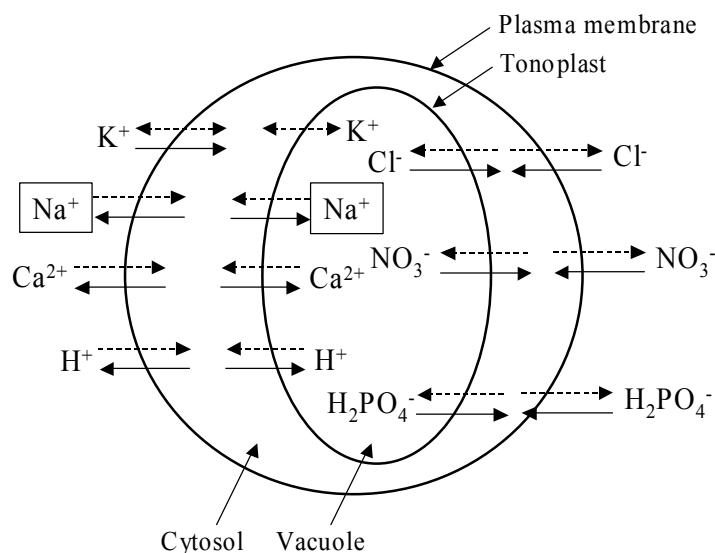


Figure 6: Ion transport processes in the plant cells. To maintain ion concentrations optimal for metabolic activities, ions are transported passively (dashed arrows) or actively (solid arrows). K^+ is accumulated passively by the cytosol and the vacuole and can be taken up when intracellular concentrations are low. Na^+ and Ca^{2+} are actively removed from the cytosol into the vacuole and the apoplast. Acidity of the vacuole and the extracellular medium is caused by the transport of protons out of the cytosol. Anions are taken up into the cytosol in an active manner (Taiz and Zeiger, 2006).

When the capability of the vacuole to sequester ions is exceeded, ion concentration is rapidly increasing in the cytosol. From the cytosol, Na^+ ions are pumped outside the cell to the apoplast and accumulate in the cell walls (Figure 7). As concentrations in the cell wall increase, the cell will shrink and dehydrate. Secondary effects caused by ion toxicity are the generation of reactive oxygen species (ROS) damaging cell membrane structures, proteins and DNA.

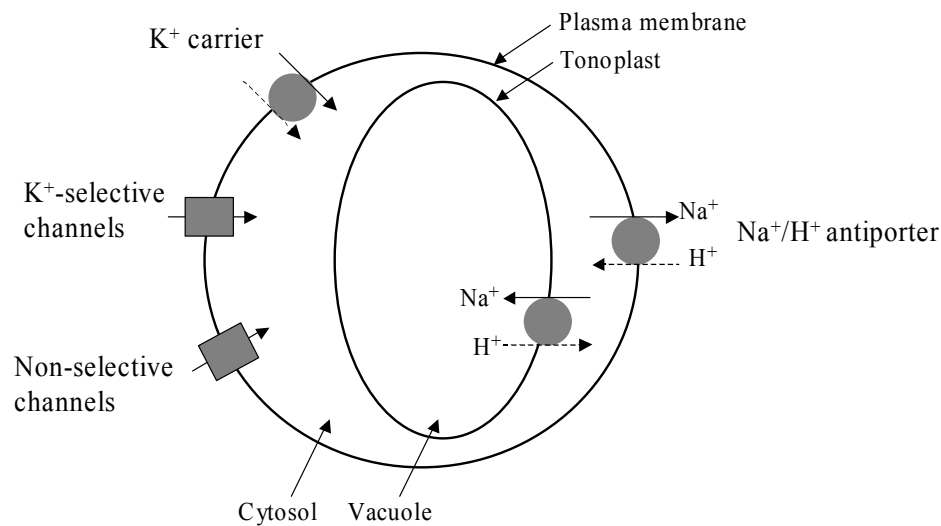


Figure 7: Mechanisms of Na^+ transport in cells of higher plants. Selective and non-selective cation transporters and channels as well as antiporter activity mediate the uptake of sodium ions. The Na^+/H^+ antiporter mediates compartmentalization into the vacuole (Munns et al., 2002).

2.3.2. Plant strategies for adaptation to salt stress

Mechanisms for conferring tolerance in the phase of Na^+ toxicity can be grouped into two main types: minimizing the entry of salt into the plant and minimizing the concentration of salt in the cytosol. Low salt accumulation in leaves can be achieved by salt exclusion in several ways: (i) reduced salt uptake by root cells, (ii) inhibition of loading of Na^+ to the xylem, (iii) unloading of salt from the xylem and (iv) unloading of salt from the phloem to avoid the transport to growing tissues of the shoot (Munns, 2002; Munns et al., 2006). In order to maintain physiological conditions at the cellular level, Na^+ is exported from the cytosol via Na^+/H^+ antiporters that are driven by the proton gradient across the plasma membrane. Also intracellular sequestration in the vacuole is achieved by Na^+/H^+ antiporters driven by the pH gradient across the tonoplast (reviewed in Munns et al., 2002).

2.3.3. Targets for improving salt tolerance in plants

Possible candidate genes for increasing salt tolerance can be divided into three main groups: (i) those that mediate salt uptake and transport, (ii) those that have osmotic or protective function and (iii) those that promote plant growth in saline soil (reviewed in Munns, 2005).

Control of salt uptake and transport

As mentioned before, Na^+ can be transported via selective K^+ - and non-selective channels as well as Na^+/H^+ antiporter. In order to maintain ion homeostasis under salinity stress, some of these genes for cation transport were used for transgenic experiments. The capability to

increase salt tolerance was shown for a Na^+/H^+ antiporter from the tonoplast, *AtNHX1*. Arabidopsis plants overexpressing *AtNHX1* were able to grow and set seed at 200 mM NaCl, whereas control plants were limited to 100 mM NaCl (Apse et al., 1999). Also overexpression of the plasma membrane Na^+/H^+ antiporter *SOS1* conferred salt tolerance in Arabidopsis as roots of transgenic plants grew more quickly on saline soil, thereby increasing plant survival from 17 to 43 % (Shi et al., 2003). HKT (high-affinity K^+ transporter) mediate Na^+ specific or Na^+/K^+ transport by regulating the root-to-shoot transport of Na^+ through the removal of Na^+ from the xylem sap as it flows to the shoot (Huang et al., 2008). It could be shown in Arabidopsis that down regulation of *AtHKT1* significantly increases salt sensitivity (Rus et al., 2004).

Attempts were made to increase the capacity of proton pumps in order to sustain the proton gradient across the membranes. The electrochemical gradient driving H^+ antiporters is created across the plasma membrane by P-type H^+ -ATPases pumping protons into the apoplast and across the tonoplast by V-type H^+ -ATPases and pyrophosphatase that pump protons into the vacuole (Munns, 2005). Overexpression of the vacuolar pyrophosphatase *AtAVPI* enabled transgenic plants to grow on 250 mM NaCl (Gaxiola et al., 2001).

Protection against osmotic stress

Genes functioning in osmotic stress responses usually occur under multiple stress factors, such as drought, salinity or low temperature. Osmotic adjustment under stress conditions can be achieved by the accumulation of solutes, such as sugars, organic acids, polyols and nitrogen-containing compounds like amino acids and proteins (reviewed in Ashraf and Harris, 2004). With the increasing compartmentalisation of ions in the vacuole during salinity stress, solutes accumulate in the cytosol to maintain an equal water potential within the cell. The production of solutes such as glycinebetaine, proline, sorbitol, mannitol and sucrose enables the plant to maintain growth at a reduced rate by adjusting the positive turgor pressure that is needed for cell growth. Although at high concentrations, these compounds do not interfere with enzyme function and are therefore termed 'compatible solutes'. Proteins that are expressed upon water-deficit belong to the group of LEA proteins. Under osmotic stress, but also in the desiccation phase of grain maturation, these proteins aid to stabilize the integrity of other proteins. ROS formed on the onset of osmotic stress need to be detoxified to prevent oxidation of membrane lipids, proteins or DNA. Enzymes that scavenge ROS include superoxide dismutase, catalase, ascorbate peroxidase and others (Mittler et al., 2004).

Transgenic approaches with genes functioning in the removal of ROS are highlighted in the 'Discussion' section.

Accumulation of solutes in transgenic approaches is achieved by modulating biosynthetic pathways. Proline is naturally accumulated under stress in all plant species. However, increased concentration up to fourfold and a concomitant increase in salt tolerance was shown for the overexpression of Δ -1-pyrroline-5-carboxylate synthetase in tobacco when the feedback inhibition was circumvented by a modified transgene (Hong et al., 2000). Also overexpression of mannitol and trehalose synthesis increased salt tolerance (Abebe et al., 2003; Garg et al., 2002).

Promotion of plant growth in saline soil

Candidate genes conferring salt tolerance by increasing growth rate could modulate signalling processes like hormones, transcription factors or protein kinases. But since these processes are fairly complex, overexpression studies will cause a variety of effects that might not be related to salt stress specifically. Transgenic rice overexpressing a Ca^{2+} -dependent protein kinase exhibited greater tolerance towards salinity (Saijo et al., 2000). Interestingly, in these transgenic plants genes were induced responding to salinity and drought, but not to cold, indicating that downstream pathways are different between osmotic stress and cold stress.

Between 1993 and 2003, 68 publications described an increase of plant salt tolerance when the expression of a single gene was modulated in a transgenic approach using *Arabidopsis*, rice, tobacco or other species (reviewed in Flowers, 2004). Salt tolerance is a multigenic trait with numerous genes involved. Transgenic plants contribute to the understanding of salt tolerance mechanisms; however the alteration of a single gene might not seem sufficient to enhance overall tolerance. Stress responses appear as a concerted expression change of numerous genes and proteins and in order to detect these global expression patterns, transcriptomics and proteomics are applied. By analysing the expression of several hundred gene or protein species at once, it is possible to generate interaction networks.

2.4. Proteomics for the dissection of stress responses

Large-scale gene expression analysis on the genome and transcriptome level resulted in the generation of vast amount of DNA sequences. But in order to elucidate gene function, the investigation of the gene product, the protein, is inevitable. The term proteomics comprehends the functional analysis of the protein complement from an organism, organ or tissue.

Proteomics dates back to the 1970s when the reliable method of 2-dimensional gel electrophoresis made the separation of crude protein mixtures possible (O'Farrell, 1975). But at that time, there was no instrumentation available to determine the proteins identity at a large scale and with high sensitivity. These limitations were removed in the 1990s by the development of ionisation methods for mass spectrometry suitable for biomolecules, like matrix-assisted laser desorption ionisation and electrospray ionisation mass spectrometry. Today, proteomics is far more complex than the identification of protein spots on 2-D gels. It also covers the analysis of post-translational modifications, such as phosphorylation and glycosylation, enzymatic assays for the functional determination, localisation studies of gene products and promoter activity as well as protein-protein interactions, such as yeast two-hybrid (Pandey and Mann, 2000). At the moment, the standard workflow for the separation, quantitation and identification of proteins in a complex mixture is 2-D gel electrophoresis in conjunction with mass spectrometry (Figure 8).

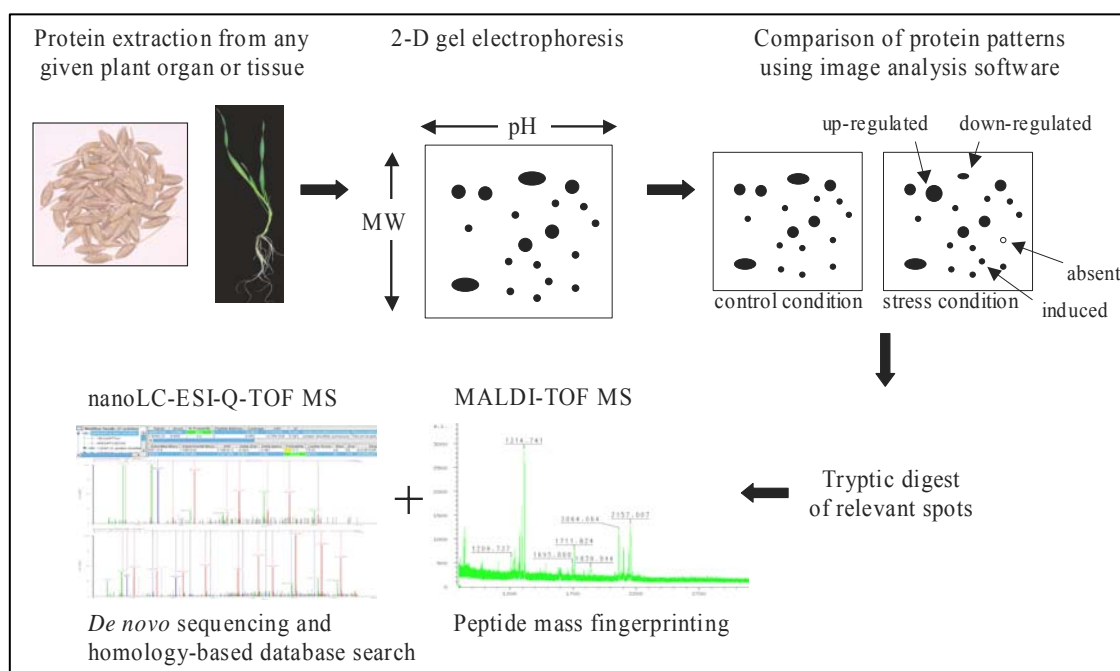


Figure 8: Two-dimensional gel electrophoresis for protein separation and quantitation coupled with mass spectrometry for protein identification. Protein extracts are separated in the first dimension according to the isoelectric point using immobilised pH gradients and in the second dimension according to the molecular weight (MW) using sodium dodecyl sulfate polyacrylamide gel electrophoresis (SDS-PAGE). The resulting gel patterns are compared and spot volumina quantified by image analysis software. Spots with alterations in expression are collected from the 2-D gel and digested with trypsin. The tryptic peptides are analysed by mass spectrometry. For the identification via peptide mass fingerprinting, the acquired peptide masses are compared with theoretical digests of proteins annotated in public databases. Using tandem mass spectrometry, the amino acid sequences of the tryptic peptides are determined and subjected to homology-based database search.

Due to continuing enhancements in protein resolution, loading capacity, staining methods and image analysis software, 2-D gel electrophoresis was applied for the analysis of plant proteins with great success. Databases were constructed containing all expressed proteins from plant organs and cell organelles from various species. The analysis of leaf, silique and seedling of the model plant *Arabidopsis* resulted in the identification of about 3,000 proteins using 2-D gel electrophoresis and MALDI-TOF MS (Giavalisco et al., 2005). Applying a similar approach, 140 proteins were identified from the wheat leaf proteome (Donnelly et al., 2005) and about 200 proteins were found in protein extracts of barley grains (Østergaard et al., 2002). This method has also been used to analyse the protein complement under biotic and abiotic stress conditions, such as cold (Amme et al., 2006), drought (Salekdeh et al., 2002), UV light (Casati et al., 2005), fungal (Campo et al., 2004) and bacterial infections (Jorin et al., 2006). The effect of salinity stress, especially in crop plants, was investigated in several studies. Various tissues were analysed in response to salt stress, *e.g.* rice leaves (Salekdeh et al., 2002), rice leaf lamina (Parker et al., 2006), tobacco leaves (Dani et al., 2005), rice roots (Chitteti and Peng, 2007; Moons et al., 1995; Yan et al., 2005), wheat roots (Wang et al., 2008) and *Arabidopsis* roots (Jiang et al., 2007). These studies revealed valuable insight into species- as well as tissue-specific stress responses and proved that 2-D gel electrophoresis is an adequate tool for large-scale analysis of protein expression.

Nevertheless, it should be noted that 2-D gel electrophoresis has some limitations. In contrast to gene profiling, where several thousands of transcripts can be analysed at once, even high-resolution 2-D gels can resolve about 1,000 proteins and these are only the high abundant protein species in a crude mixture. Furthermore, extremely acidic and basic proteins are not amenable to 2-D gel electrophoresis using conventional pH gradients ranging from 3 to 10. For the analysis of proteins belonging to these groups, other methods have been established, like liquid chromatography-based methods for the separation of peptides. Using 2-D gels, application of prefractionation techniques and narrow-range pH gradients improved the resolution considerably.

2.5. Scientific aims of the work

Barley is a major crop and there is a high interest in unravelling the determinants of grain nutritional quality and increasing the plants ability to grow under unfavourable environmental conditions. In this thesis, several aspects of elucidating agronomic traits of barley are addressed using 'Functional Genomics' and 'Genetical Genomics' approaches.

The proteome analysis of introgression lines developed from a cross between a modern breeding line and a wild type variety (Li et al., 2005) was embedded within the GABI-SEED II project at IPK Gatersleben. The aim of this project was the characterization of this mapping population in order to find trait-related proteins. The protein composition of mature grains from two independently grown sets of introgression lines should be analysed and subsequently protein patterns should be subjected to QTL analysis.

Salinity is a serious threat for agriculture and among the cereals barley is considered to be one of the most salt tolerant. Germination on saline soil is an important agronomic trait and in order to find proteins that confer salt tolerance at the germination stage, the grain proteome of barley accessions with contrasting response towards salinity should be compared. Two different mapping populations were selected for this approach, the Oregon Wolfe Barley population developed to map phenotypic traits and the Steptoe Morex population developed to map agronomic traits.

Furthermore, the root proteome of the parent lines of the Steptoe Morex population should be investigated. Both lines display a contrasting response towards salinity treatment at the seedling stage. With the objective to identify proteins conferring tolerance at this developmental stage, both genotypes should be used for long-term hydroponic stress experiments and analysed for alterations in the protein complement of root tissue.

Candidate proteins derived from the comparative proteome analysis of barley genotypes with contrasting response towards salinity either at the germination stage or at the seedling stage should be functionally tested in overexpression studies using a salt sensitive barley cultivar.

In a subcellular proteomics approach, plasma membranes from roots of Steptoe and Morex should be isolated and investigated. The aim was to perform a profiling of the plasma membrane proteome and a comparative protein profiling of both genotypes based on the expression of integral or peripheral plasma membrane proteins.

3. Materials and Methods

3.1. Plant material

3.1.1. Barley genotypes and mapping populations

The following barley cultivars and accessions of mapping populations were analysed at different developmental stages: *Hordeum vulgare* cv. Brenda, the cv. Brenda x *H. spontaneum* HS213 population (Li et al., 2005), accessions from the Oregon Wolfe Barley (OWB) population including the parent lines *Hv* cv. DOM and cv. REC (Costa et al., 2001) as well as accessions from the Steptoe Morex (SM) population including the parent lines *Hv* cv. Steptoe and cv. Morex (Han et al., 1997). The barley cultivar ‘Golden Promise’ was used as host plant for gene transfer experiments.

3.1.2. Plant growth in hydroponic culture and salinity treatments

Plant culture and stress treatments were carried out according to Walia et al. (2006) with some modifications. Barley grains were rinsed and placed on filter paper dampened with 0.1 % Previcur N (Bayer CropScience, Langenfeld, Germany) for 5-7 days at 4 °C to break dormancy. Afterwards grains were transferred to the growth chamber for germination at 22/20 °C for 16/8 h light/dark, respectively, for 2 days. Seedlings were transferred to Biolaston (PVC) that were soaked in 1:1 diluted modified Hoagland’s solution (Hoagland and Arnon, 1950) (3 mM KH₂PO₄, 1 mM MgSO₄, 1 mM CaCl₂*2H₂O, 25 µM H₃BO₃, 2 µM MnSO₄, 2 µM ZnSO₄, 0.5 µM CuSO₄, 0.5 µM Na₂MoO₄*2H₂O, 0.1 mM Fe-EDTA, 1 mM H₂SO₄, 8 mM NH₄NO₃ with the pH adjusted to 7.0 using KOH) and cultivated at 22/20 °C for 16/8 h, respectively. After 3 days, the seedlings were transferred to the hydroponic system with modified Hoagland’s solution and acclimated there for 2 more days. The hydroponic system was covered with a perforated plate that held the plants and plants grew under continuous air supply to the solution. Growing conditions were the following: 350 µEinstein of light intensity, 18/16 °C for 14/10 h, 70 % humidity with constant air supply to the nutrient solution. For reasons of stable supply with nutrients, the solutions were exchanged every other day. Salinity treatment started with the addition of 50 mM NaCl to all groups except to the control plants. After two days, 100 mM NaCl was added to all groups, except to the control and the 50 mM NaCl treated plants. The salt concentration in the nutrient solution was increased up to 250 mM following this scheme (see Figure 39). Four days after the highest

NaCl concentration was applied, plants were harvested either for protein extraction or for the determination of growth parameters.

3.1.3. Growth measurements

The following biometric data were determined for 20 plants from each cultivar grown under control conditions or at different salt concentrations (50, 100, 150, 200, 250 mM NaCl) in three independent experiments: length, fresh weight and dry weight of secondary and tertiary shoot as well as of root. The relation of relative growth inhibition was calculated from means of control and stress measurements.

3.2. Protein extraction methods and concentration measurements

3.2.1. Extraction of water-soluble protein fraction from mature grains

Water-soluble proteins were extracted from mature grains following the protocol of Østergaard et al. (2002). In short, approximately 1 g of grains was homogenized under liquid nitrogen in a cooled mortar to flour. Aliquots of 250 mg flour were thawed in 1250 µl of low salt buffer (5 mM Tris/HCl pH 7.5, 1 mM CaCl₂) and incubated for 30 min at 4 °C on a shaker. After centrifugation step (Mikro 22R, Hettich, Tuttlingen, Germany; 15 min, 4 °C, 36,000 x g) the supernatant was mixed with 4 volumes of ice-cold acetone and incubated at – 20 °C for 2 h. Proteins were sedimented by centrifugation (5 min, 4 °C, 36,000 x g) and dried in a vacuum centrifuge (Concentrator 5301, Eppendorf, Hamburg, Germany). The pellet was dissolved in lysis buffer (8 M urea, 2 % CHAPS, 20 mM DTT, 0.5 % IPG buffer) by incubating for 1 h at 37 °C on a shaker. Insoluble material was pelleted by centrifugation (15 min, room temperature, 36,000 x g).

3.2.2. Extraction of storage proteins from mature grains

The prolamin fraction was extracted from mature grains. One hundred mg of flour was extracted in 1.5 ml acetone in an ultrasonic bath at room temperature for 15 min to remove excess of starch present in grains. After a centrifugation step (5 min, room temperature, 31,800 x g), the pellet was dried using a vacuum centrifuge and resuspended in 500 µl 55 % 2-propanol for 30 min in an ultrasonic bath. The sample was centrifuged at 31,800 x g for 5 min at 4 °C and the volume of the supernatant was determined. The supernatant was dried in a vacuum centrifuge and solubilised with buffer A (8 M urea, 2 % CHAPS, 20 mM DTT, 0.5 % IPG buffer) to the same volume as before drying by incubating for 1 h at 37 °C on a shaker. Insoluble material was pelleted by centrifugation (15 min, room temperature).

3.2.3. Protein extraction from roots

The extraction of proteins from roots were performed following TCA/acetone precipitation method (Amme et al., 2005). Briefly, the frozen root material was homogenized under liquid nitrogen to a fine powder. One part (approximately 1 g) of this material was mixed with 10 parts of TCA/acetone solution (10 % w/v TCA, 0.07 % w/v 2-mercaptoethanol in acetone) and incubated for 45 min at -20°C . The precipitate was pelleted and washed twice with 0.07 % w/v 2-mercaptoethanol in acetone. The protein pellet was dried in a vacuum centrifuge and dissolved in buffer A (8 M urea, 2 % CHAPS, 20 mM DTT, 0.5 % IPG buffer) at 37°C for 1 h under shaking conditions. Insoluble material was removed by centrifugation at room temperature for 15 min.

3.2.4. Enrichment and extraction of plasma membrane proteins from roots

Enrichment of plasma membranes by two-phase partitioning method

The enrichment of plasma membranes was accomplished following the protocol of Santoni (2007), with minor modifications for root tissue. Approximately 30 g of frozen root tissue was vacuum infiltrated with homogenisation buffer (50 mM MOPS, 5 mM EDTA, 330 mM sucrose, pH 7.5 with KOH; added before use: 5 mM DTT, 5 mM ascorbate, 0.6 % (w/v) polyvinylpolypyrrolidone, Complete mini proteinase inhibitor (Roche, Mannheim, Germany) and homogenized with a blender. The solution was filtered through 2 layers of Miracloth (Calbiochem, Darmstadt, Germany) and debris was pelleted by centrifugation (Beckman centrifuge with JA-14 rotor, BeckmanCoulter, Fullerton, USA; $10,000 \times g$, 4°C , 15 min). The supernatant was transferred to ultracentrifugation vials and centrifuged at $50,000 \times g$ for 50 min at 4°C (Beckman ultracentrifuge with 70Ti rotor). The resulting supernatant was referred to as cytosolic fraction, the pellet as microsomal fraction. The pellet was resuspended using a brush in plasma membrane (PM) buffer (330 mM sucrose, 5 mM potassium phosphate buffer with pH 7.8; added before use: 1 mM DTT, 0.1 mM EDTA) and loaded onto a prepared two-phase system consisting of 6.4 % (w/w) Dextran T500, 6.4 % (w/w) PEG 3350, 300 mM sucrose, 5 mM potassium phosphate buffer, 5 mM KCl and H_2O to fill up. All following steps were carried out at 4°C . A 24 g system consisted of 18 g aqueous polymers and 6 g microsomal fraction and for one extraction of root plasma membranes, four 2-phase systems were prepared and stored at 4°C over night. For the first extraction round, 6 g of microsomal fraction was added to the first system and 6 ml of PM buffer was added to the second, mixed by inverting and followed by centrifugation at $1000 \times g$ for 7 min at 4°C . The

upper phase of system 2 was loaded onto the lower phase of system 1 and the upper phase of system 1 was loaded onto the lower phase of system 2 (Figure 9). Both systems and two more systems, where the PM buffer was added with the adequate amount of the exchanged upper phases, were centrifuged as before. The upper phase of system 3 was replaced with the upper phase of system 2 and yielded the final upper phase after centrifugation. The upper phase of system 2 was added to the lower phase of system 1. After centrifugation, the resulting lower phase was collected and referred as endomembrane fraction. The upper phase of system 4 was loaded onto the lower phase of system 3. After a centrifugation step, the resulting upper phases were pooled and referred as plasma membrane fraction. To both membrane fractions 1 volume (Vol) of PM buffer was added and samples were centrifuged at $100,000 \times g$ for 60 min at 4°C . Pellets were resolved with a brush in PM buffer, homogenized and stored at -80°C .

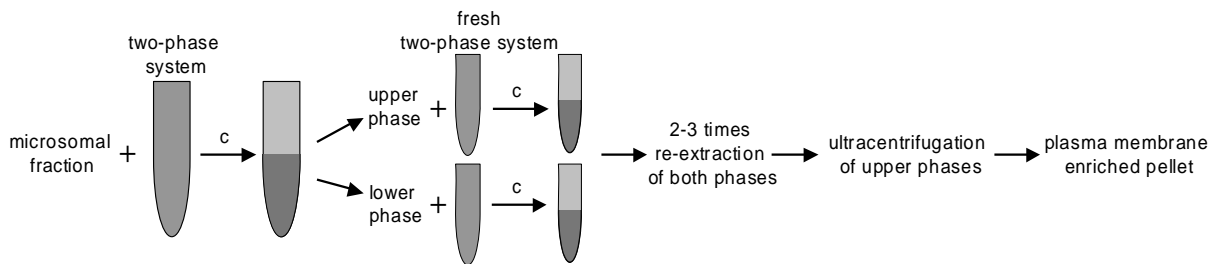


Figure 9: The method of aqueous two-phase partitioning. The microsomal fraction is added to the prepared two-phase system. After a centrifugation step, the upper phase becomes enriched with PM and the lower phase with endomembranes. Each phase is enriched using complementary fresh phases and membranes in the final upper and lower phase are pelleted by centrifugation.

Enrichment of hydrophobic proteins by batch reversed-phase chromatography

For the removal of soluble proteins using reversed-phase chromatography, the protocol of Hynek et al. (2006) was applied. Prior to reversed-phase chromatography, proteins were chloroform/methanol-precipitated to remove lipids. One Vol of plasma membrane fraction was mixed with 1 Vol chloroform and 4 Vol methanol. The solution was centrifuged at room temperature for 2 min at maximum speed. One Vol of methanol was added to the lower phase and centrifuged as before. The pellet was dried at room temperature and resuspended in SDS-buffer (50 mM MES, 50 mM Tris, 0.5 % w/v SDS, 1 mM EDTA, pH 7.3).

Batch reversed-phase chromatography was performed with Handee Micro-spin columns (Pierce Thermo Scientific, Pittsburgh, USA), filled with approximately 100 μl of Nucleosil 300-5 C4 (Macherey-Nagel, Düren, Germany). Columns were washed with 100 μl 2-propanol

and centrifuged at 1000 x g for 1 min at room temperature. After equilibration with 100 µl 0.15 % TFA, 100 µg delipidated membrane proteins were loaded onto the column. The flow-through was collected and the column was washed with 0.15 % TFA. Proteins were serially eluted with 100 µl 49 %, 50 %, 51 % and 90 % 2-propanol. Fractions were dried in a vacuum centrifuge and dissolved in SDS-buffer.

3.2.5. Determination of protein concentration in crude mixtures

The methods for determining the protein concentrations were chosen according to the amount of protein and the buffer they were dissolved in. Proteins dissolved in SDS-containing buffer were determined with the Bradford method (Bradford, 1976). When protein pellets were resolubilised in buffer containing CHAPS and DTT, the 2-D Quant Kit (GE Healthcare, München, Germany) was used following the manufacturer's instructions. Plasma membrane protein content was determined using the Popov assay and BSA as a reference (Popov et al., 1975).

3.3. Protein separation methods

3.3.1. SDS-PAGE

SDS-PAGE of membrane proteins was performed with precasted 4-12 % Bis-Tris NuPAGE gels (Invitrogen, Karlsruhe, Germany) following the manufacturer's instructions.

3.3.2. Two-dimensional gel electrophoresis

Isoelectric focusing and subsequent SDS-PAGE was accomplished as described in Schlesier and Mock (2006). Dependent on the separation and staining method, different concentrations of proteins were used. For cCBB stain, 200 µg or 500 µg protein mixture were loaded by rehydration on immobilized pH gradient (IPG) strips of 13 cm or 24 cm in length, respectively. When the fluorescent stain Ruthenium II tris (bathophenanthroline disulfonate) (RuBP) was applied, 100 µg or 300 µg total protein were isoelectrically focused on IPG strips of 13 cm or 24 cm in length, respectively. For isoelectric focusing, pH gradients of 3-10 or 3-11 were used. The separation on an IPGphor II unit (GE Healthcare) was performed with the following parameters for IPG strips of 13 cm in length: 14 h rehydration, 1 h gradient to 250 V, 1 h gradient to 500 V, 1 h gradient to 4,000 V and 5.30 h 4,000 V with a total of about 25 kVh. When 24 cm IPG strips were used, the following parameters were applied: 12 h rehydration, 2 h gradient to 150 V, 2 h gradient to 300 V, 2 h gradient to 1,000 V, 3 h gradient to 3,000 V, 3 h gradient to 6,000 V and 10 h 6,000 V with a total of approximately 80 kVh.

After IEF, strips were equilibrated in buffer A (50 mM Tris/HCl, pH 8.8, 6 M urea, 30 % v/v glycerin, 2 % w/v SDS, 20 mM DTT, 0.01 % bromphenol blue) and additionally in buffer B (50 mM Tris/HCl, pH 8.8, 6 M urea, 30 % v/v glycerin, 2 % w/v SDS, 135 mM iodoacetamide, 0.01 % bromphenol blue) for 15 min each. The strips were then placed on top of an 11.25 % SDS polyacrylamide gel and covered with 0.5 % agarose. Separation in the second dimension was performed using a Hoefer S600 (GE Healthcare) or a DaltSix apparatus (GE Healthcare). Afterwards, gels were washed for 5 min with water and proteins were visualized.

3.4. Visualization of proteins and image acquisition

3.4.1. Colloidal Coomassie Brilliant Blue staining

After 2-D gel electrophoresis, gels were incubated for 10 min in 5 % phosphoric acid under shaking conditions. The gels were then stained using GelCodeBlue Stain Reagent (Pierce Thermo Scientific) following the manufacturer's instructions. Image acquisition was performed using a UMAX Power Look III scanner (Umax Systems, Willich, Germany) with the MagicScan software (v4.5, Umax).

3.4.2. Ruthenium staining

The fluorescent stain was synthesized as described in Rabilloud et al. (2001). Briefly, 0.2 g of potassium pentachloro aquo ruthenate ($K_2Cl_5Ru.H_2O$; Alfa Aesar, Karlsruhe, Germany) was dissolved in 20 ml of boiling water under reflux. To the solution, 0.8 g bathophenanthroline disulfonate was added and kept under reflux for additional 20 min. To the mixture 5 ml of 500 mM sodium ascorbate solution was then added and incubated refluxing for further 20 min. The solution was chilled on ice and the pH was adjusted to 7.0 with NaOH. The volume was then adjusted to 26 ml, making a final concentration of about 20 mM of the ruthenium(II)-tris-(bathophenanthroline-disulphonate) (RuBP) staining solution. Aliquots were stored at $-20\text{ }^\circ\text{C}$.

For protein staining the protocol of Lamanda et al. (2004) was applied with minor modifications. Gels were incubated in 30 % ethanol, 10 % acetic acid overnight at $4\text{ }^\circ\text{C}$ for fixation and washed four times for 30 min with 20 % ethanol. Staining was performed with $1\text{ }\mu\text{M}$ RuBP solution in 20 % ethanol for six h in the dark under shaking conditions. Gels were washed for 10 min with water and destained in 40 % ethanol, 10 % acetic acid overnight at $4\text{ }^\circ\text{C}$. Prior to scanning, the gels were equilibrated twice in water for 10 min.

Image acquisition was accomplished using the Fuji FLA-5100 (FujiFilm, Tokyo, Japan) with the Image Reader FLA-5000 v1.0 software. Scanning parameters were: resolution 100 μm , 16 bit picture, excitation wavelength 473 nm, emission filter 580 nm.

3.4.3. Silver staining

SDS-PAGE gels were fixed for 30 min in solution 1 (40 % ethanol, 10 % acetic acid) and washed with water three times for 5 min. The sensitizing reaction was performed with solution 2 (0.8 M NaOAc, 33 % v/v ethanol, 0.2 % w/v $\text{Na}_2\text{S}_2\text{O}_3$, 3.12 % v/v glutardialdehyde) for 30 min, followed by three washing steps with water. For silver reaction the gels were incubated in solution 3 (0.25 % AgNO_3) for 20 min and after an additional washing step the development was performed for 2-5 min in solution 4 (236 mM Na_2CO_3 , 0.2% v/v formaldehyde). The reaction was stopped with solution 5 (43.5 mM $\text{Na}_2\text{-EDTA}$). The image acquisition of stained gels was performed in the same way as for cCBB stained gels.

3.5. Relative quantitation of proteins and peptides

3.5.1. Image analysis of 2-dimensional gel patterns

For the 2-D image analysis, the Progenesis software (Nonlinear Dynamics, Newcastle upon Tyne, United Kingdom) was applied using the default parameters. The parameters for Phoretix 2D Evolution and Progenesis PG220 were: background subtraction method was 'mode of non-spot' with margin 45, spot matching with vector box size 12 and search box size 64, normalization method was total spot volume multiplied by 100 and spot filtering (area > 300, volume > 1500). Progenesis PG240 was used with the following parameters: background subtraction method was 'Progenesis background', spot-matching mode was property based, minimum spot area for spot detection: 16, normalization method was total spot volume multiplied by total area and spot filtering (area > 300, volume > 1500)

3.5.2. Label-free quantitation of tryptic peptides

Protein digest preparation

Thirty μg of plasma membrane proteins were delipidated (see 3.2.4) and the pellet was solubilised in 50 μl 0.1 % RapiGest SF (Waters, Eschborn, Germany) under shaking conditions for 1 h at 37 $^\circ\text{C}$, 10 min at 80 $^\circ\text{C}$ and 5 min at 95 $^\circ\text{C}$. The tryptic digest was

performed following the manufacturer's instructions. LC-MS analyses were performed using 2 μ l (approximately 0.3 μ g) of the protein digest. All samples were analysed in triplicate.

Liquid chromatography and mass spectrometry configuration

Liquid chromatography (LC) of tryptic peptides was performed as described in Vissers et al. (2007) with minor modifications. A NanoAcquity system (Waters) was equipped with a 20 mm x 180 μ m Symmetry (5 μ m) C₁₈ precolumn and a 150 mm x 75 μ m BEH (1.7 μ m) C₁₈ analytical reversed phase column. The samples were transferred to the precolumn and afterwards the peptides were separated with a gradient of 3 – 40 % acetonitrile over 100 min. The lock mass, glufibrino peptide solution (100 fmol/ μ l, Waters), was delivered from the auxiliary pump of the NanoAcquity pump with a constant flow rate of 600 nl/min to the reference sprayer of the NanoLockSpray source.

Mass spectrometry (MS) analysis of tryptic peptides was performed using a Q-TOF Premier mass spectrometer (Waters) operating in v-mode and positive nanoelectrospray ion mode (Vissers et al., 2007). Source temperature was set to 80 °C and cone gas flow to 50 l/h. The voltage of 2.8 kV was applied for the nanoflow probe tip. Accurate mass LC-MS data were collected in an alternating low energy (MS) and elevated energy mode of acquisition (MS^E) using MassLynx v4.1 (Waters). The spectral acquisition time in each mode was 1 s with a 0.02 s interscan delay. In MS mode, data were collected at constant collision energy of 4 eV. In MS^E mode, the collision energy was ramped from 10 to 28 eV during each 1 s data collection cycle with one complete cycle of low and elevated energy data acquired every 2.04 s.

Data processing and protein identification

The continuum LC-MS^E data were processed (ion detection, clustering, and normalization) and searched using ProteinLynx GlobalServer v2.3 (Waters). Protein identifications were obtained with the embedded ion accounting algorithm of the software and searching the SwissProt *Viridiplantae* and TrEMBL *Poales* database.

3.5.3. Western blotting

Immunoblotting analysis of plasma membrane proteins was performed as described in Hynek et al. (2006). Antibodies were kindly provided by Anja Thoe Fuglsang (Royal Veterinary and Agricultural University, Denmark) and Maarten Chrispeels (University of California, San Diego, USA).

3.6. Protein identification

3.6.1. Peptide mass fingerprinting by MALDI-TOF MS

Spots selected for protein identification from the water-soluble protein fraction of mature grains as well as from root tissue were excised manually or automatically (Proteiner SP, Bruker Daltonics, Bremen, Germany) from 2-D gels, washed and digested with trypsin as described in Witzel et al. (2007).

Proteins from the alcohol-soluble protein fraction of mature grains were processed as follows: after the washing step spots were reduced with 10 mM DTT in 25 mM ammonium bicarbonate for 1 h at 55 °C under shaking conditions. Afterwards, the solution was replaced by 55 mM iodoacetamide in 25 mM ammonium bicarbonate and the spot was incubated for 45 min at room temperature under shaking conditions in the dark. The gel plug was washed with 25 mM ammonium bicarbonate for 10 min, with 10 mM ammonium bicarbonate/50 % acetonitrile for 30 min and with 25 mM ammonium bicarbonate over night at 5 °C. After the final washing step with 10 mM ammonium bicarbonate/50 % acetonitrile for 30 min the spot was dried and digested with trypsin as outlined before.

The acquisition of Peptide Mass Fingerprint data was performed on a REFLEX III MALDI-TOF mass spectrometer (Bruker Daltonics) operating in reflector mode. Spectra were calibrated using external calibration and subsequent internal mass correction. Protein identification was performed with the MASCOT search engine (Matrix Science, London, United Kingdom) searching for *Viridiplantae* in the NCBI nonredundant protein sequence database and barley EST Gene Index in the TIGR database. Parameters for the search were the following: monoisotopic mass accuracy 100-200 ppm tolerance, missed cleavages 1, allowed variable modifications: oxidation (Met), propionamide (Cys) and carbamidomethyl (Cys).

3.6.2. *De novo* sequencing of peptides by tandem MS/MS

When the identification via MALDI-TOF MS failed, samples were subjected to analysis by nanoLC-ESI-Q-TOF MS/MS and *de novo* sequencing according to Amme et al. (2006). The MS/MS spectra searches were conducted to a protein *Viridiplantae* index of the nonredundant NCBI database and the barley EST Gene Index in the TIGR database. A 10 ppm peptide, 0.1 Da fragment tolerance, one missed cleavage and variable oxidation (Met) and propionamide (Cys) were used as the search parameters. BLAST homology and similarity

searches were conducted with a protein *Viridiplantae* index of the nonredundant NCBI database.

3.7. Molecular cloning techniques

3.7.1. Bacterial strains, vectors and oligonucleotides

Escherichia coli strains XL-1 Blue (Stratagene, La Jolla, USA) and One Shot® TOP10F' (Invitrogen) were used for plasmid transformation and propagation. *Agrobacterium tumefaciens* strain AGL1 was used for plant transformation (Hensel et al., 2008).

The vector pCRBlunt (Invitrogen) was used for cloning of PCR products. Subsequently, constructs for plant transformation were ligated into pUbi-ABM (DNA Cloning Service, Hamburg, Germany) for ubiquitin-driven expression (Christensen and Quail, 1996) and into Lig154(pNOS+PaG) for α -gliadin driven expression (Vickers et al., 2006). The binary vector for *Agrobacterium* transformation of barley plants was p6d35S (Hausmann and Toepfer, 1999). The vectors pUbi-ABM, Lig154(pNOS+PaG) and p6d35S were kindly provided by Drs Götz Hensel and Axel Himmelbach, IPK.

The list of oligonucleotides used for gene amplification and for the generation of probes for Southern and Northern blotting is given in Table 1.

Cloning of genes and transformation of bacteria were performed using standard techniques (Sambrook and Russell, 2001).

Table 1: Oligonucleotides used for amplification and probe synthesis. The created restriction sites are underlined.

Number	Sequence	Name
1	5'-CGG <u>GGA ATT CAT</u> GGC GTC GCA GAA GTT C-3'	5'-primer glucose/ribitol dehydrogenase homolog (HS09N23) in pUbi-AB
2	5'-GAT <u>GAA GCT TTG</u> ACG ATG GTA CCA CCG T-3'	3'-primer glucose/ribitol dehydrogenase homolog (HS09N23) in pUbi-AB
3	5'- <u>CC CGG</u> GAT GGC GTC GCA GAA GTT C-3'	5'-primer glucose/ribitol dehydrogenase homolog (HS09N23) in Lig145(NOS+PaG)
4	5'- <u>CC CGG</u> GTG ACG ATG GTA CCA CCG T-3'	3'-primer glucose/ribitol dehydrogenase homolog (HS09N23) in Lig145(NOS+PaG)
5	5'-GAT <u>TGG ATC CAT</u> GGC TCT CAC CAG AAT T-3'	5'-primer cytosolic 6-phosphogluconate dehydrogenase (HI05J23) in pUbi-AB
6	5'-CGC <u>GAA GCT TTT</u> AGA TCT TCG AGT TCG C-3'	3'-primer cytosolic 6-phosphogluconate dehydrogenase (HI05J23) in pUbi-AB
7	5'- <u>CC CGG</u> GAT GGC TCT CAC CAG AAT T-3'	5'-primer cytosolic 6-phosphogluconate dehydrogenase (HI05J23) in Lig145(NOS+PaG)

8	5'- <u>CC CGG GTT</u> AGA TCT TCG AGT TCG C-3'	3'-primer cytosolic 6-phosphogluconate dehydrogenase (HI05J23) in Lig145(NOS+PaG)
9	5'- <u>GAA TTC</u> ATG TCC CAA AGC TTG TTC C-3'	5'-primer glucose/ribitol dehydrogenase homolog (HO26C23S) in pUbi-AB
10	5'- <u>GTC GAC TCA</u> CAG TCT TGA TTT GAG C-3'	3'-primer glucose/ribitol dehydrogenase homolog (HO26C23S) in pUbi-AB
11	5'-TGG TCC <u>CCG GGA</u> TGT CCC AAA GCT TG-3'	5'-primer glucose/ribitol dehydrogenase homolog (HO26C23S) in Lig145(NOS+PaG)
12	5'-TGG TCC <u>CCG GGT</u> CAC AGT CTT GAT TTG-3'	3'-primer glucose/ribitol dehydrogenase homolog (HO26C23S) in Lig145(NOS+PaG)
13	5'-TGG TCG <u>AAT TCA</u> TGA CCA TGA TTA CGC CAA GCG C-3'	5'-primer cytosolic 6-phosphogluconate dehydrogenase (HS09M23R) in pUbi-AB
14	5'-TGG TCA <u>AGC TTC</u> TAC GGG CGC TCC TGG TTG-3'	3'-primer cytosolic 6-phosphogluconate dehydrogenase (HS09M23R) in pUbi-AB
15	5'-TGG TCC <u>CCG GGA</u> TGA CCA TGA TTA CGC CAA GC-3'	5'-primer cytosolic 6-phosphogluconate dehydrogenase (HS09M23R) in Lig145(NOS+PaG)
16	5'-TGG TCC <u>CCG GGC</u> TAC GGG CGC TCC TG-3'	3'-primer cytosolic 6-phosphogluconate dehydrogenase (HS09M23R) in Lig145(NOS+PaG)
17	5'-ATC GGA CGA TTG CGT CGC A-3'	5'-primer hygromycin probe for Southern blotting
18	5'-TAT CGG CAC TTT GCA TCG GC-3'	3'-primer hygromycin probe for Southern blotting

3.7.2. RNA preparation and Northern blot analysis

RNA extractions from leaves and mature grains of transgenic and wild type barley plants was performed using peqGOLD RNAPureTM (PEQLAB, Erlangen, Germany) reagent following the manufacturer's instructions.

For Northern blotting, 20 µg of total RNA was separated on a 1.5 % (w/v) agarose gel containing 1 x MEN (20 mM MOPS, 5 mM sodiumacetate, 1 mM EDTA, pH 7.0) and 16 % formaldehyde. The RNA was transferred to a GeneScreen Plus® NR Hybridization transfer membrane (Perkin Elmer, Waltham, USA) using capillary blotting with 20 X SSC buffer (3 M NaCl, 300 mM sodium citrate*2H₂O) over night. The RNA was fixed via UV cross-linking and hybridised with the respective ³²P-dCTP labelled probe in Church buffer (0.25 mM sodium phosphate buffer, 1 mM EDTA, 1 % BSA, 7 % SDS) over night. Radioactive labelling of the probe was carried out using High Prime labelling kit (Roche). After washing with 2 x SSC buffer hybridisation signals were detected with BAS 2000 Bio-Imaging Analyser (FujiFilm).

3.7.3. DNA preparation and Southern blot analysis

DNA from leaf material was prepared as follows: 200 mg of leaf was homogenized in liquid nitrogen and supplemented with 800 µl extraction buffer (1 % N-lauryl sarcosine, 100 mM Tris/HCl, pH 8, 10 mM EDTA, 100 mM NaCl). After adding 800 µl phenol/chloroform/isoamylalcohol (25:24:1) the solution was centrifuged at maximum speed at room temperature. The DNA in the supernatant was precipitated with 80 µl 3 M sodium acetate and 800 µl 2-propanol. The solution was centrifuged again, the pellet was washed with 70 % ethanol and then dissolved in TE buffer (10 mM Tris, 1 mM EDTA) containing 40 µg/ml RNase.

For Southern blotting, 30 µg of DNA was digested with *Hind*III and separated on a 0.8 % agarose gel. The gel was equilibrated in 0.4 N NaOH and DNA was transferred to HybondTM-N⁺ (GE Healthcare) membrane through capillary blotting with 0.4 N NaOH over night. Hybridisation of the membrane with the respective probe was performed as described for Northern blotting procedure.

3.8. Plant transformation

The stable transformation of immature barley embryos was a service of the Plant Reproductive Biology group at IPK and was accomplished as described in Hensel et al. (2008).

3.9. Statistical analysis

3.9.1. Cluster analysis of protein patterns

Protein expression data was extracted from the image analysis software as background-subtracted spot volume. Dr Marc Strickert from the Data Inspection group at IPK performed the cluster analysis of 2-D gel patterns. The data table containing the spot volumes that were detected on all 2-D gels was quantile normalized (Bolstad et al., 2003), log₂ transformed and z-score transformed in order to create a homogeneous data set for subsequent analysis. A grouping of the normalized experiments was obtained by using the Cluster v3.0 software package (de Hoon et al., 2004) using hierarchical clustering with average linkage (Eisen et al., 1998). The clustering results were visualized by means of the Java Treeview v1.1.0 open source software (Saldanha, 2004).

3.9.2. Quantitative trait loci analysis for protein expression

Protein expression data was extracted from the image analysis software as background-subtracted spot volume. The mean of three technical replicates per sample was quantile normalized (Bolstad et al., 2003) and log₂ transformed (Dr Marc Strickert, Data Inspection group, IPK). Dr Christof Pietsch from the Gene and Genome Mapping group at IPK performed QTL analysis for protein expression. An advanced backcross population comprising 181 doubled haploid lines between the spring barley variety ‘Brenda’ and the *H. spontaneum* accession HS213 was genotyped with 60 microsatellite markers (Li et al., 2005) and 30 unpublished single nucleotide polymorphism markers. Single marker regression was used for QTL analysis using QTL Cartographer v1.7. A LOD score of ≥ 3 was used as a significance threshold for QTL detection. It should be noted that due to linkage disequilibrium of some molecular markers within the population, a proportion of QTL could not be allocated to a specific genetic location. Therefore, these markers were combined into haplotypes (see Table A3 in the Appendix).

3.9.3. Principle component analysis of peptide profiles derived from LC-based mass spectrometry

PCA was applied in order to assess the technical and biological variability of peptide profiles. Dr Marc Strickert from the Data Inspection group at IPK performed PCA of LC-separated tryptic peptides from plasma membrane proteins. The intensity data from each EMRT cluster was exported from ProteinLynx GlobalServer v2.3 (Waters) and loaded into CSVed v1.4.4 (<http://csved.sjfrancke.nl/index.html>). To reduce the number of missing values, the 5,000 EMRT clusters with highest intensity were selected for PCA and missing values still present were replaced by the number of 1. Subsequently, the data set was lg transformed and PCA was performed using R software (www.R-project.org).

4. Results

4.1. Grain protein profiling of the Brenda x HS213 mapping population

4.1.1. Construction of a protein reference map from barley cv. Brenda mature grains

Within the scope of the comparative protein profiling of the introgression lines derived from barley cv. Brenda and *H. spontaneum* HS213 cross, a reference map of soluble proteins from the Brenda parent was established. Soluble proteins from mature grains were extracted employing a protocol optimised for barley grains (Østergaard et al., 2002). Here, the release of storage proteins, dominating 2-D gel patterns, is suppressed and the analysis of proteins relevant for developmental processes is permitted. Extracted proteins were separated by 2-D gel electrophoresis in the first dimension using isoelectric focussing (IEF) and in the second dimension by SDS-PAGE. For the construction of the reference map, 217 highly abundant and reproducible protein spots were collected manually from 2-D gels for mass spectrometry-based identification (Figure 10).

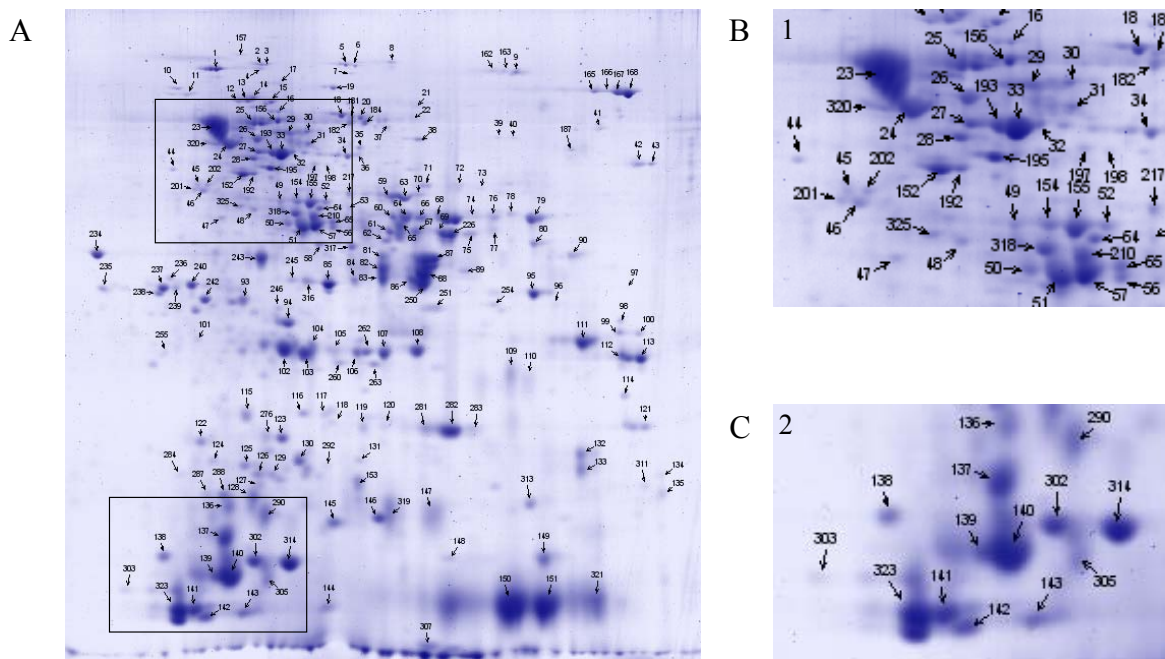


Figure 10: Proteins selected for identification of the water-soluble proteome of barley (cv. Brenda) grains (A). The protein extract of the water-soluble fraction was separated using a pH gradient from 3-10 in the first dimension and a 12.5 % SDS-PAGE for the second dimension. The proteins were visualized by colloidal Coomassie Brilliant Blue (cCBB) staining. Two regions of the 2-D gel were enlarged in B and C. An enlarged view on the complete 2-D gel and the list of identified proteins is provided in Figure A1 and Table A1 in the Appendix section.

After tryptic in-gel digest, the proteins were analysed by MALDI-TOF MS, on the basis of peptide mass fingerprinting, and LC-ESI-Q-TOF MS, employing homology-based database search of amino acid sequences. Out of 187 successfully identified spots, 87 proteins were found unique and the rest could be assigned to a total of 34 proteins (Table A1 in the Appendix). The most abundant proteins on 2-D gels were isoforms of LEA proteins. These proteins were identified in 13 spots covering a broad range from approximately 15-80 kDa and from pH 5-9 based on their location on the 2-D map. A further example of the complexity of protein expression was heat shock protein 70 (Hsp 70) that was found in 10 spots with isoforms of similar biochemical properties.

All identified proteins were grouped by their functional annotation according to established criteria (Bevan et al., 1998) (Figure 11).

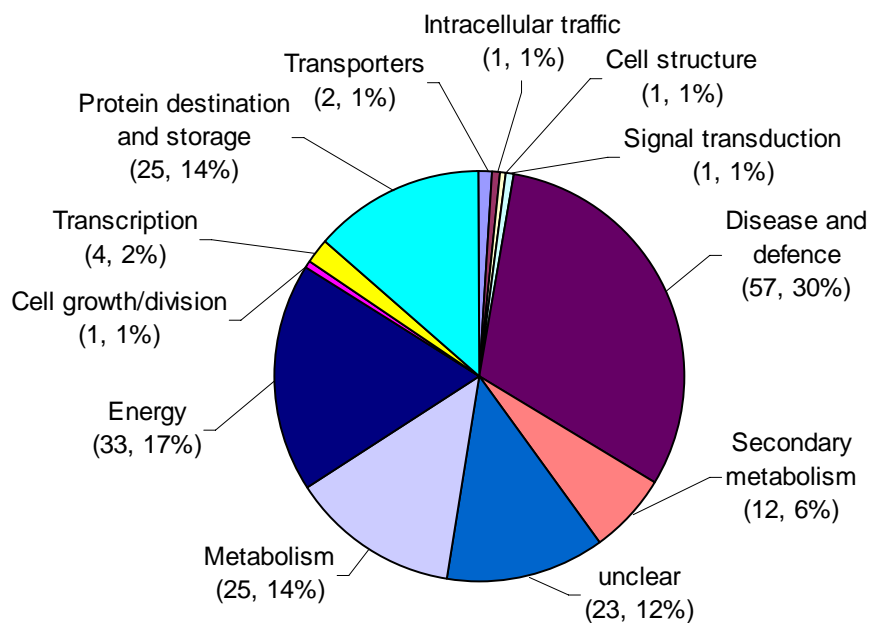


Figure 11: Functional classification of *Hv* cv. Brenda grain proteins. The list of the identified proteins and their classification is given in Table A1.

Most proteins (57 proteins, 30 %) belong to the group of disease/defence and are related to defence, stress and detoxification processes. The second largest group (33 proteins, 17 %) represents proteins involved in energy production such as glycolysis, TCA and pentose phosphate pathway. A further major group, comprising 25 protein spots (14 %), are metabolic enzymes functioning in carbohydrate, amino acid or nucleotide processes. Proteins grouped under protein destination and storage (25 proteins, 14 %) include folding, targeting and proteolysis.

4.1.2. Expression profiling of proteins in mature grains

The comparative protein profiling of introgression lines obtained by crossing the elite variety *H. vulgare* cv. Brenda with the wild type *H. spontaneum* was embedded into the GABI-SEED II project. Employing a ‘Genetical Genomics’ approaches in this project, these lines were extensively characterized on the genome, transcript, protein and phenotypic level. By treating these parameters as inherited factors, QTL analysis of the whole segregating population enables the identification of trait-related genes and pathways for molecular breeding strategies. Because of the uniform background and low percentage of introgressions from the wild type genome in the offspring lines, this population is suitable to study genes and regulatory networks in barley grains, turning a crop plant into a model plant. The construction of the Brenda x HS213 mapping population by members of the Gene and Genome Mapping group at IPK is depicted in Figure 12. Sets of lines were grown in two consecutive years and mature grains were used for the protein profiling of soluble proteins.

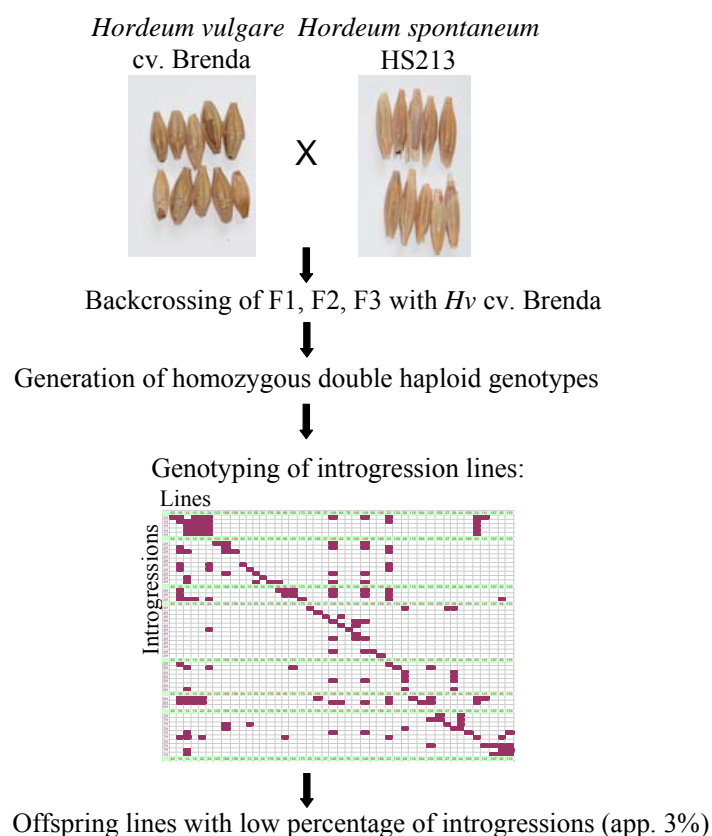


Figure 12: Construction of the Brenda x HS213 doubled-haploid advanced backcross mapping population. The German spring barley cultivar ‘Brenda’ served as the recurrent parent and the wild species line ‘HS213’ as the donor line. The resulting population was backcrossed with ‘Brenda’ three times and genotyped with 60 microsatellite markers (Li et al., 2005) and 30 single nucleotide polymorphism markers. Mature grains from introgression lines were made available for proteome analysis by courtesy of the Gene and Genome Mapping group and the Molecular Genetics group from IPK.

Analysis of the water-soluble protein fraction of barley grains from the first experiment

The first experiment consisted of 53 introgression lines (ILs) growing in three different batches in phytochambers under controlled conditions with the Brenda parent growing in each batch. The reason for splitting the first experiment into batches was the limited availability of phytochambers at that time. Grains from three plants per line were pooled and the soluble protein fraction was extracted. To ensure technical reproducibility of protein separation, three 2-D gels per sample were produced. After IEF using 13 cm immobilised pH gradient (IPG) strips and SDS-PAGE, proteins were visualized with colloidal Coomassie Brilliant Blue and spot patterns were compared using image analysis software. In this comparison, the protein pattern of each IL was matched to the Brenda pattern and spots with differential expression were selected for mass spectrometry-based identification, assuming that the change in spot abundance is related to the respective introgression in this line. The quantification of spot abundance is a critical step in the workflow and this was conducted using Phoretix 2D Evolution software (NonLinear Dynamics, United Kingdom). For spot detection, background subtraction, warping, matching and spot normalisation the default parameters of the software were applied. In order to exclude background signals, spot filter criteria were used as described in the Materials and Methods section (3.5.1).

Overall, 700-800 spots were detected on 2-D gels of grain proteins and mean values of normalized spot volume from the technical replicates were used for comparison. Spots were selected for identification based on a threshold of at least 1.5-fold change in ratio of abundance. From the first batch, consisting of 22 introgression lines, 449 spots were selected for identification. The second and third batch included 20 and 11 lines and based on the comparison, 521 and 238 spots were excised from the gels for mass spectrometry analysis, respectively. On average, 20-30 proteins with change in abundance between the Brenda parent and the IL were detected in the first experiment. In combination with protein spots from the grain proteome mapping, a number of 1,533 spots were digested and tryptic peptides were analysed by MALDI-TOF MS. Due to the limited entry number of barley in public databases, only 50 % of all spots were identified by peptide mass fingerprinting (Figure 13A). Remaining samples were then subjected to LC-ESI-Q-TOF MS for *de novo* sequencing of tryptic peptides and homology-based database search. Here, additional 40 % of protein spots could be identified (Figure 13B).

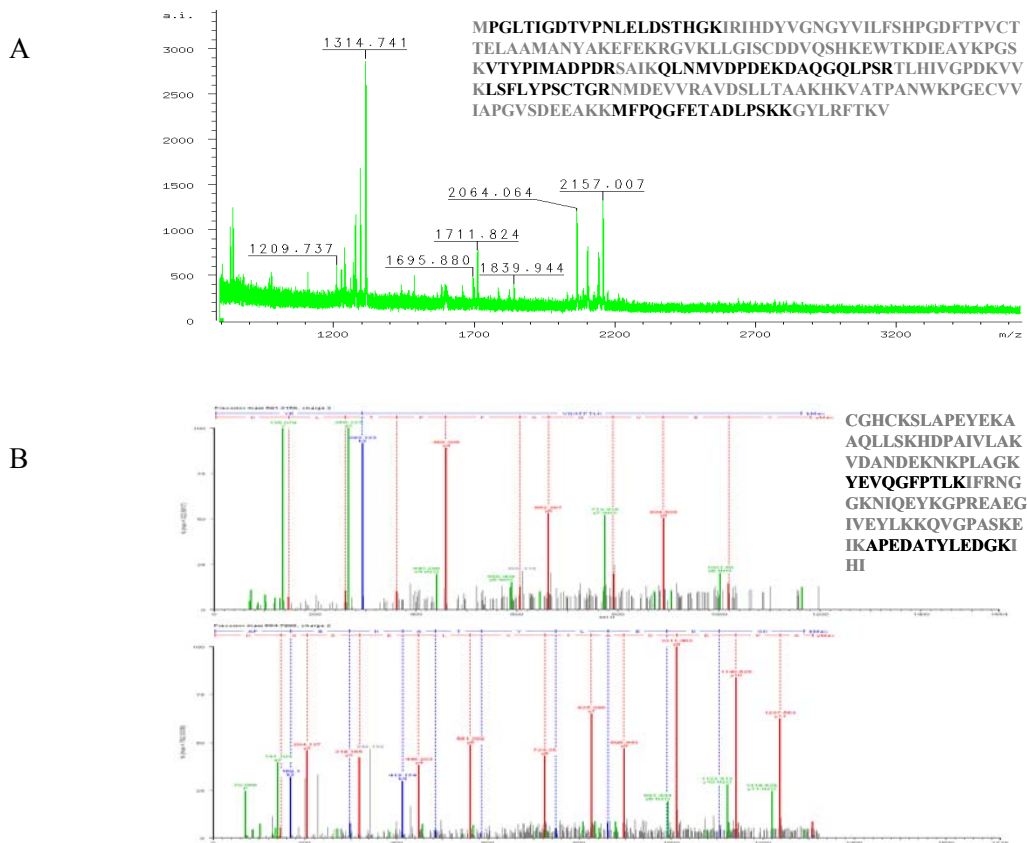


Figure 13: Identification of proteins by mass spectrometry. A: MALDI-TOF spectrum of tryptic digestion from a spot identified as peroxiredoxin (gi:1694833). Given are protein sequence (in grey) and matching tryptic peptides (in black). B: ESI-MS/MS spectra of the m/z 591.3158 ($M+H$)⁺ (upper panel) and m/z 654.7998 ($M+H$)⁺ (lower panel) peptide ions derived from in-gel tryptic digestion of a spot identified as protein disulfide isomerase (gi: 4803450). Indicated are protein sequence (in grey) and tryptic peptides identified by LC-ESI-Q-TOF-MS. Peptide mass fingerprinting as well as blast homology and similarity searches were conducted against the *Viridiplantae* index of the NCBI nr database.

To ensure the spots identity, each spot selected from the ILs was compared with the identity of respective spot from the Brenda mapping approach. If the identity differed or identification failed at all, the spot was rejected from the data set. Using these filter criteria, the resulting data set was reduced to 1,106 protein spots. An example of differential protein expression between IL and the Brenda parent is given in Figure 14.

With the aim of facilitating the interpretation of this large-scale data set and to represent the data in their biological context, differential protein expression was visualized with the Vanted software (<http://vanted.ipk-gatersleben.de>). Using identifiers from public databases (NCBI, TIGR, UniProt, KEGG, GO), it is possible to show data in the context of their underlying biological networks by mapping the data onto existing metabolic pathways. The application

of this tool for the visualization of single protein expression differences in the introgression lines was successful (Figure 15).

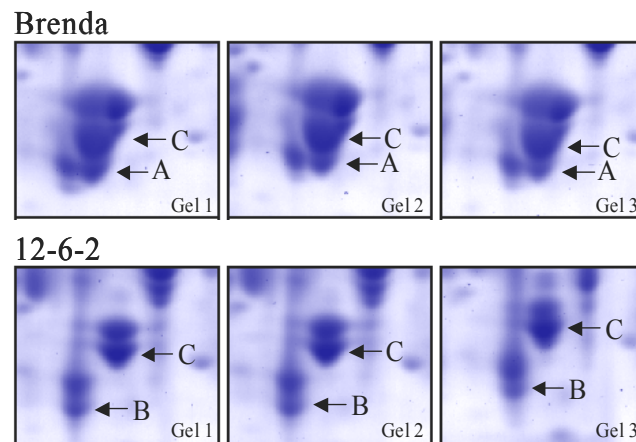


Figure 14: Spot expression varying between the Brenda parent and introgression line 12-6-2. Spot A was identified as peroxidase 1 and is present only on 2-D gels from Brenda grain proteins. Identification of spot B lead to a seed maturation protein PM34 and this spot was only detected in line 12-6-2. Spot C was identified as aldose reductase and the spot abundance was 3.4 fold higher in the Brenda parent compared to 12-6-2.

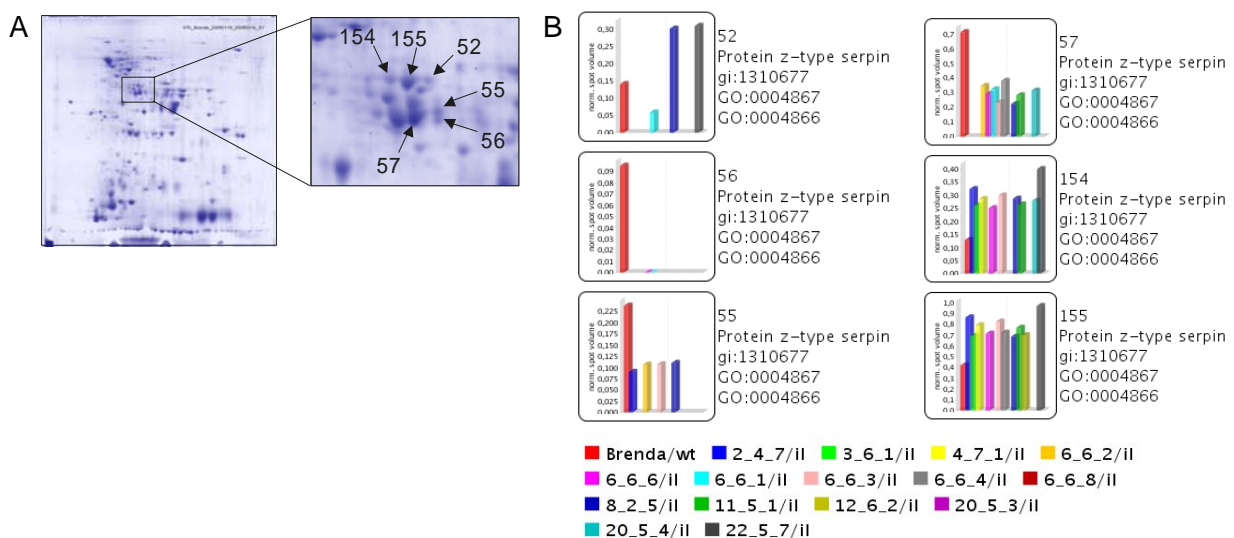


Figure 15: Visualisation of differential protein expression using Vanted software. Six proteins spots on 2-D gels led to the identification of z-type serpins (A). In order to find isoform-specific differential expression among introgression lines, the expression of proteins was followed in a subset of introgression lines (B). Given are number and identifier for each z-type serpin spot shown in A. Values in the diagram represent the normalized spot volume as mean of three replicates. Only lines are presented in the diagrams where the protein expression differed significantly from the Brenda parent. Visualisation of protein expression data was performed using Vanted v1.0 (<http://vanted.ipk-gatersleben.de>; Christian Klukas, Network Analysis Group, IPK).

But due to the poor number of plant- and tissue-specific KEGG pathways as well as lacking gene ontology terms for various barley grain proteins, the mapping of proteomic data onto metabolic pathways did not yield in a better understanding of differential protein expression in the introgression lines. This sparse information also did not allow the analysis of protein isoforms detected on 2-D gels with differential abundance in introgression or parent line.

In order to estimate the environmental effects on the protein complement due to the splitting of the first experiment into three batches, the gel patterns of the three Brenda lines from each batch were compared. For quantitation of spot volumes, a recently released and enhanced version of Phoretix, termed SameSpots (NonLinear Dynamics), was used which implements identical spot outlines, improved spot matching and statistical tools. Principle component analysis (PCA) on protein spots ($p < 0.05$) revealed a greater distance between the third batch and the remaining two batches (Figure 16). The result strongly points towards a high environmental influence on the grain proteome not only of the Brenda parent but also of ILs grown in the third batch.

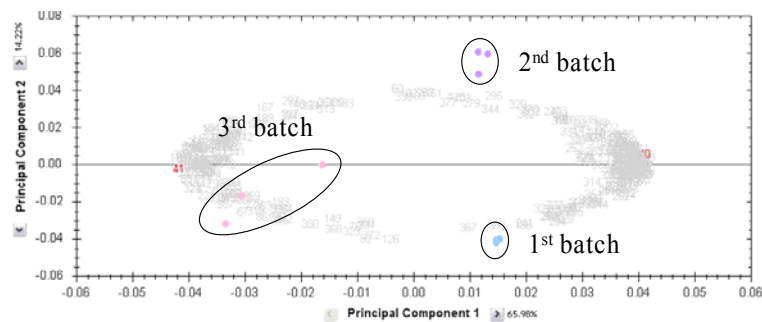


Figure 16: Environmental influence on the protein expression of barley cv. Brenda, grown in three different batches. PCA of protein spots from three replicates per sample display the greatest separation between 2-D gels of the third batch and the remaining two batches. Used for calculation were only spots with $p < 0.05$.

This assumption was further supported by cluster analysis of the overall gel patterns of ILs. For that, all 2-D gels from the first experiment were processed with the SameSpots software to ensure highest matching and best spot quantification. The cluster analysis revealed a strong separation of ILs based on the batches they were grown in (Figure 17).

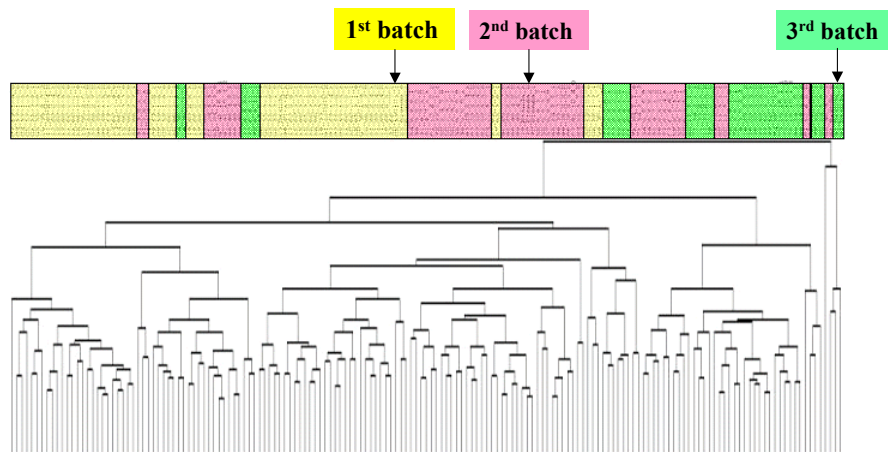


Figure 17: Cluster analysis of 2-D gel patterns from the first experiment (Dr Marc Strickert, Data Inspection group, IPK). The overall protein patterns detected on three replicate 2-D gels per sample were used for cluster analysis in order to determine the degree of similarity among the three growing batches. Two-D gels from ILs that were grown in the first batch are colour coded in yellow, the second batch in magenta and the third batch in green. Arrows indicate the position of the Brenda parent in the respective batch.

Analysis of the water-soluble protein fraction of barley grains from the second experiment

The second experiment consisted of 45 ILs grown in one single batch and this provided the prerequisite for more robust data set as compared to the first experiment. For the analysis of this second set, the protein separation on large-format 2-D gels (IPG strips of 24 cm in length) was established. In contrast to the conventional mid-scale 2-D gels (IPG strips of 13 cm in length), this improvement resulted in an enhanced resolution due to the longer running distance and also to a better visualisation of low-abundant proteins due to higher loading capacity (Figure 18). Overall, in the comparative profiling a total of 3,890 differentially expressed proteins spots were detected as differentially expressed in comparison to Brenda, reflecting the improved protein separation on large-format 2-D gels.

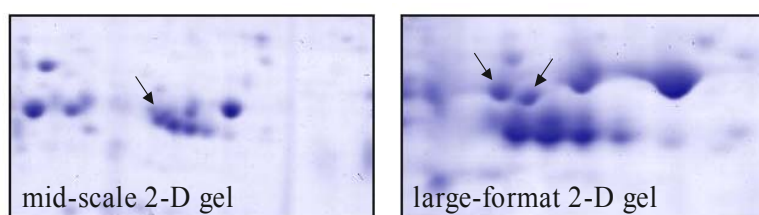


Figure 18: Protein separation on 2-D gels using mid-scale (13 cm IPG strips, left) and large-format 2-D gels (24 cm IPG strips, right). Close-up views on same scale visualize enhancements in protein separation on large-format 2-D gels (arrow).

Due to the high number of detected differential abundances, identification of all selected spots via mass spectrometry did not seem reasonable. Instead, this large data set was used for multivariate analysis in a clustering approach using the overall 2-D gel patterns of ILs and the Brenda parent. Following this approach the high technical reproducibility of 2-D gel electrophoresis was confirmed as most of the technical replicates from one sample clustered together (Figure 19).

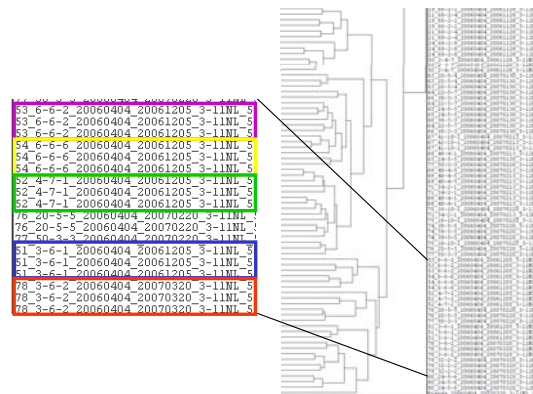


Figure 19: Cluster analysis of the protein patterns confirmed a high reproducibility of 2-D gel electrophoresis of three technical replicates from one sample (Dr Marc Strickert, Data Inspection group, IPK). Grouped in coloured boxes are technical replicates from one IL.

A significant correlation in clustering of 2-D gel patterns derived from ILs grown in the two consecutive years could not be found, probably due to the variances in growth conditions. To a large extent, the results of the cluster analysis from the second set confirmed the outcome of the direct comparison as lines with a low number of differentially expressed protein spots are located closer in the cladogram to the parent Brenda. But also it was noticed that the number of introgressions does not determine the position in the cladogram. There are ILs with a high number of insertions showing a more similar pattern as compared to Brenda than other lines with a comparable number of introgressions (Figure 20). This could indicate the influence of environmental effects on the protein pattern, but also the expression of a variable number of genes underlying these introgressions.

To assess the general impact of environmental factors on the whole data set, the grain proteome of the Brenda parent harvested in all sets and in both experiments was compared on large format 2D-gels. PCA revealed a strong separation between batches as well as experiments and confirmed the results of cluster analysis (Figure 21). Overall, the first two batches from the first experiment are located closer together as compared to the third batch from the same experiment and to the second experiment. Influences of growth conditions

differing from one year to the other can be expected and would not necessary devaluate the data set. The isolated position of the third batch led to the exclusion of lines grown in this batch from the subsequent QTL analysis for protein expression (pQTL).

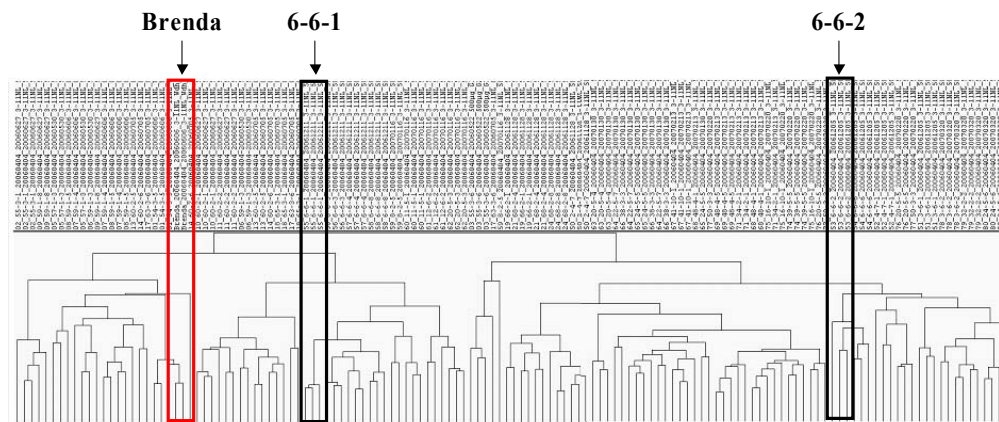


Figure 20: Cluster analysis of 2-D gel patterns from the second experiment (Dr Marc Strickert, Data Inspection group, IPK). Shown are the positions of the parent line Brenda and two ILs in the cladogram, based on 2-D gel protein patterns. Lines 6-6-1 and 6-6-2 were genotyped with about 17 and 9 introgressions at molecular marker positions, respectively.

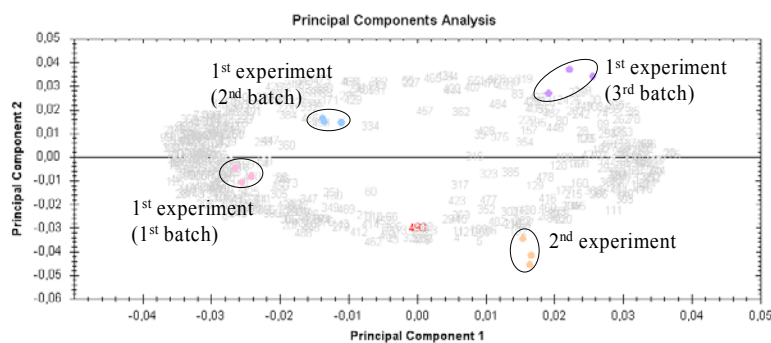


Figure 21: PCA of protein expression from the Brenda parent grown in three batches in the first experiment and in one batch in the second experiment. Protein spots from three technical replicates per sample demonstrate a considerable variation between batches as well as experiments. Spots were included in PCA that showed a significant change in expression at $p < 0.05$ as given by the image analysis software.

Summary of the protein profiling from mature grains of the Brenda x HS213 mapping population

At this point, the results of the comparative protein profiling are summarized shortly. Offspring lines from the Brenda x HS213 mapping population were grown in two consecutive years in phytochambers. Due to space limitations in the first year, the lines were divided into three batches with the Brenda parent growing in each batch. The water-soluble protein fraction from grains was analysed by 2-D gel electrophoresis and revealed a strong grouping of the protein profiles into the respective batches the plants were grown in. In the second year,

plants were grown in a single batch and this resulted in a more consistent data set with lower environmental influence.

Initially, this mapping population was analysed for QTL that control agronomic traits (Li et al., 2005). Under field conditions QTL for grain yield, heading date, ear length malting quality and others were detected. However, no QTL for grain number per plant, thousand grain weight or flowering time was recovered when plants were grown in phytochambers (personal communication, Dr Winfriede Weschke). The reason for this is still unclear. Despite the absence of QTL for agronomic traits, it was tested in the following whether QTL for protein expression could be detected in these lines and if the method of 2-D gel electrophoresis is capable to detect these single features in a reproducible manner in both sets of grown plants.

Calculation of QTL for protein expression

Molecular markers are short (single nucleotides) or long (microsatellites with up to 6 nucleotides) DNA sequences used to study the relationship between a trait and its underlying genomic region. Markers are associated to a specific locus in the genome and due to polymorphism within a population they are used to determine the distribution of parental genomes in progeny lines. ILs from the Brenda x HS213 population were genotyped with 60 microsatellite markers (Li et al., 2005) and 30 single nucleotide polymorphism markers that were developed within the Gabi SEED II project (unpublished data) in order to determine the position of introgressions from the wild type donor in the genome of progeny lines. This provided the basis for QTL detection. Dr Christof Pietsch from the Gene and Genome Mapping group from IPK conducted the genotyping and the pQTL calculation.

From the first experiment, a subset of 40 ILs was used to estimate pQTL. In this calculation the abundance of each spot visualized on 2-D gels is treated as a phenotypic parameter and its expression in the whole population is related to the introgressions from the wild type barley genome. In total, 1,050 phenotypes from 40 introgression lines were incorporated into the pQTL analysis meaning that expression values for 1,050 detected spots on 2-D gels were used for the calculation.

As a result, 70 pQTL from ILs grown in the first experiment were detected with a significant LOD score ($\text{LOD} \geq 3$). The LOD score (logarithm of odds) is used in genetics to estimate recombination frequency. In QTL analysis this score is used to express the linkage between a trait and a molecular marker. A LOD score greater than 3.0 means that the probability of linkage between trait and marker by chance is less than 1 in 1,000. MS-based identification

was successful for all selected spots. According to their appearance on the 2-D gel, the group was divided into 35 single and 12 multiple protein observations (Table A2, Figure 22). Protein z-type serpin was identified in 10 spots and the respective markers were located on chromosomes 4H, 5H and 6H. Peroxidase and peroxidase precursor were also highly abundant in pQTL analysis. From these protein species 6 protein spots were identified with the respective molecular marker on chromosome 7H.

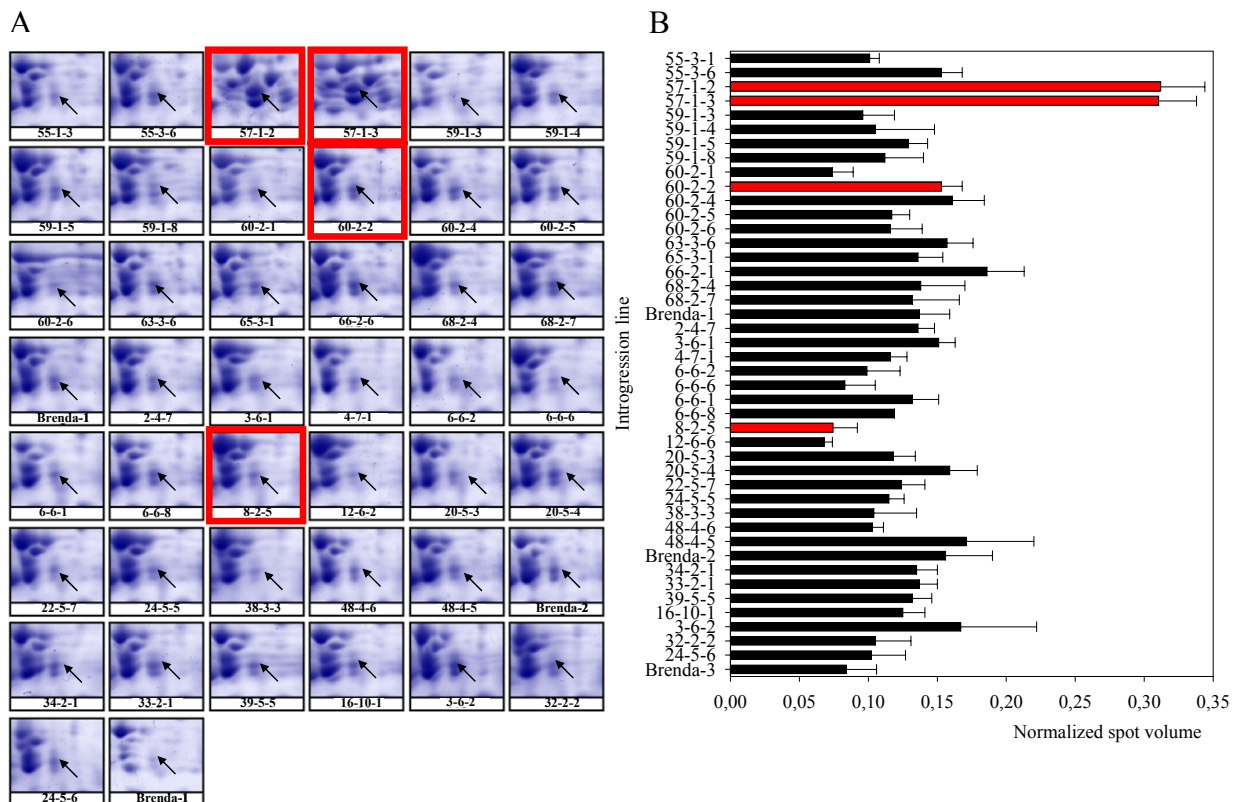


Figure 22: Detection of pQTL in barley grain proteome analysis. Shown is a close-up view on 2-D gels from ILs used for pQTL analysis (A). A pQTL signal was derived from spot 1040 (arrow), identified as protein z-type serpin (gi:1310677), with a significant LOD score (5.978) at marker position Bmac303 on chromosome 5H. Those lines are marked with red boxes having an introgression of the wild type parent genome at this distinct marker position. Shown in B is the normalized volume of spot 1040; marked in red are the respective lines as in A. The higher abundance of spot 1040 in lines 57-1-2 and 57-1-3 is apparent.

For most pQTL a distinct chromosomal region was pinpointed based on the LOD score of the respective marker. However, the segregation pattern for some markers did not reveal a distinct location and therefore the exact position of a number of pQTL could not be determined precisely. This is probably due to linkage disequilibrium of some molecular markers within the population and therefore, these markers were combined into haplotypes ('composed marker' C). For instance spot 1315, identified as peroxidase, had the same LOD score in the

region of marker Bmac090 on chromosome 1H and marker Ebmac674 on chromosome 6H. Hence it is not possible to verify the chromosomal position of this pQTL using the Brenda x HS213 mapping population.

From the second experiment, 36 ILs were incorporated into the pQTL analysis. The calculation was based on 2,718 phenotypes for protein expression, meaning a 2.5 fold increase in phenotypes derived from the second experiment as compared to the first one, due to the higher separation capacity of large-format 2-D gels. But despite this increased input, the number of estimated pQTL was similar in both experiments. Out of 67 detected pQTL with a significant LOD score ($\text{LOD} \geq 3$) in the second experiment, 65 could be assigned to an identifier from public databases and these could be divided into 38 single and 10 multiple protein identifications (Table A3).

The same observations were made as compared to the first experiment in terms of multiple protein spots and variable genomic localisation. For instance, three pQTL were estimated for an Hsp 70 (spots 703, 2332, 2411) with three different molecular markers (Ebmac684, Bmag613, K117_2s) on three different chromosomes (5H, 6H, 4H). Also in the second experiment, the segregation pattern for some molecular markers did not reveal a precise chromosomal position, hampering the determination of the genomic localisation of 7 pQTL. Because of the lower environmental variance of the second experiment, the resulting pQTL were investigated in more detail. Functional classification revealed most spots belonging to metabolism and disease/defence related processes in the mature grain (Figure 23). But also proteins functioning in energy and protein synthesis pathways were identified.

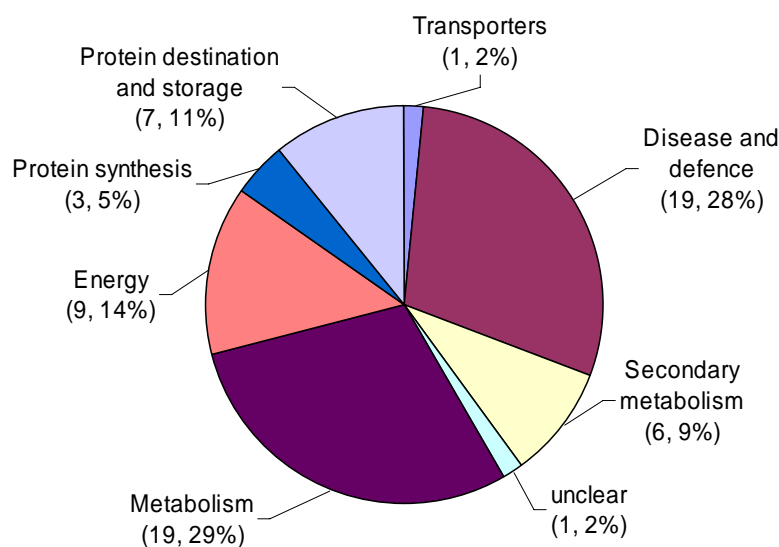


Figure 23: Functional classification of pQTL detected in the second experiment using comparative protein profiling of the Brenda x HS213 mapping population. A complete list of identified proteins that gave a QTL signal is provided in Table A3.

In order to detect hotspots for pQTL in the genome, the distribution of the estimated pQTL was analysed. In case that a pQTL could not be pinpointed to a distinct chromosomal position due to the segregation pattern of the marker, the respective markers were grouped to an artificial 'composed marker'. The pQTL signals were distributed evenly over the molecular marker positions indicating that no pronounced hotspot for inherited protein expression was found in the analysis (Figure 24).

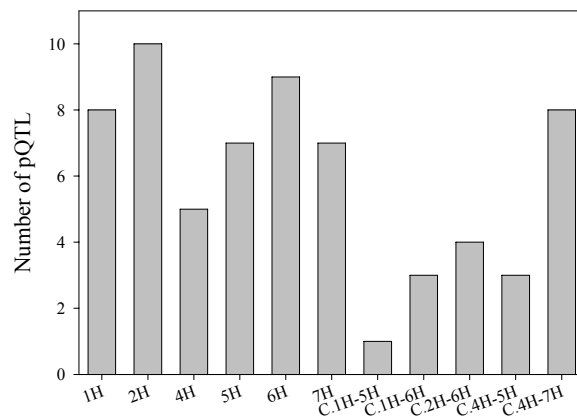


Figure 24: pQTL distribution in the second experiment. pQTL that could not be related to one distinct chromosomal region (molecular marker) were grouped and termed 'composed marker'. The pQTL were evenly distributed among the genome and no hotspot region was found in the analysis.

Due to the impact of environmental effects on protein expression in the first experiment the recovery of only a low number of pQTL is not surprising. When comparing both experiments, 15 protein identifiers appear in both sets of pQTL, regardless of the respective position on the 2-D gel. The matching of the spot positions on the 2-D gels is complicated by the different separation methods used in both experiments. This is probably one reason why pQTL were estimated with different markers on different chromosomes but leading to the same identifier. It is also likely that different isoforms of the same protein were detected in the analysis. For instance, in the first experiment one pQTL for a spot identified as beta amylase was calculated for the marker GBMS062 on chromosome 1H. But in the second experiment one pQTL, also identified as beta amylase, was estimated for the marker GBMS077 on chromosome 2H. In this case, no conclusions can be drawn regarding to the reproducibility of pQTL detection. But for some pQTL a clear correlation is visible, one is presented in Figure 25. Here, a protein spot identified as B-hordein gave pQTL signals in both experiments for the same marker (GBMS062) on the same chromosome (1H). Although hordeins are normally extracted with 55% 2-propanol, this protein spot appears in the water-soluble protein fraction of grains, indicating isoform-specific biochemical properties.

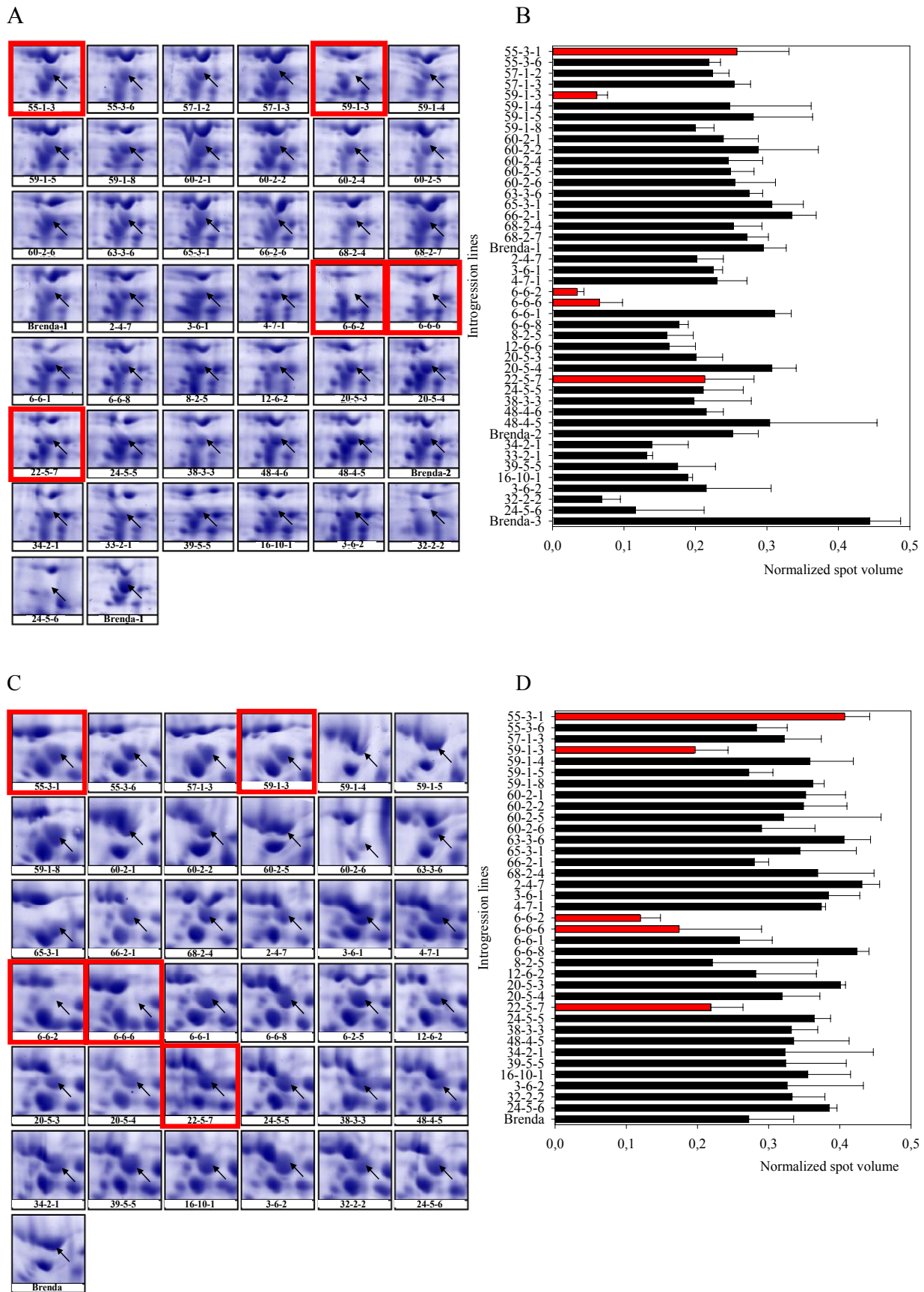


Figure 25: Description next page

Figure 25: Replication of pQTL signals in two independent experiments. Shown are enlargements of 2-D gels to follow the expression of the same spot (arrows) in all lines under investigation in the first experiment (A) and in the second experiment (C). The spot abundance is given as normalized volume for each experiment in B and D, respectively. Protein extract from lines grown in the first experiment were separated on 13 cm IPG strips and from lines grown in the second experiment on 24 cm IPG strips. In both experiments pQTL signals for a protein spot (arrows), identified as B-hordein, was derived from the segregation pattern of marker GBMS062 on chromosome 1H. Those lines are marked with red boxes that were genotyped with an introgression of the wild type genome at this marker position. In 3 lines (59-1-3, 6-6-2, 6-6-6) the protein expression of B hordein is reduced as compared to the remaining population.

The recovery of pQTL signals in two biological experiments demonstrates that, despite the challenges due to the environmental conditions on plant growth in the different sets, the techniques used in the separation and quantification of proteins were highly reproducible in detecting single features in the overall protein complement.

Analysis of alcohol-soluble grain storage proteins

In barley, prolamins represent the vast majority of proteins in the mature grain and they account for 30-50 % of total grain protein. During germination and seedling growth these storage proteins function as source of amino acids and they contribute to the nutritional quality of grains. In order to gain insight into the alcohol-soluble prolamins complement of the parent Brenda, several highly abundant spots separated by 2-D gel electrophoresis were selected for initial protein identification. Characteristic for most members of the prolamins family is the high number of cysteine residues in the amino acid sequence, resulting in numerous intramolecular disulfide bonds. Therefore, it was necessary to apply a modified protocol for tryptic digest to obtain a sufficient number of peptides for mass spectrometry database search. An additional reduction and alkylation of cysteine residues prior to the tryptic digest resulted in an increase of peptide masses detected in MALDI-TOF measurements (Figure 26). However, most of the highly abundant proteins could be identified with LC-ESI-Q-TOF MS/MS exclusively. *De novo* sequencing of tryptic peptides led to the identification of B- and γ -hordeins in multiple spots, confirming the high level of polymorphism in amino acid sequence, which is known from the literature, rather than posttranslational modifications (Figure 27, Table 2).

Because a direct comparison of 2-D gel patterns between Brenda and a subset of introgression lines did not reveal differential expression of single spots, the overall amount of storage proteins extracted from mature grains was determined and compared between both sets

(Figure 28). The protein content was reproducible for most of the ILs, but also lines were found where the prolamin content differed considerably between both sets, indicating environmental effects on prolamin accumulation during grain maturation or effects of the introgressions from the wild type parent. To test the latter, the storage protein content in mature barley grains was used for QTL analysis. However, no QTL signal for storage proteins was detected in either the experiments using the Brenda x HS213 mapping population.

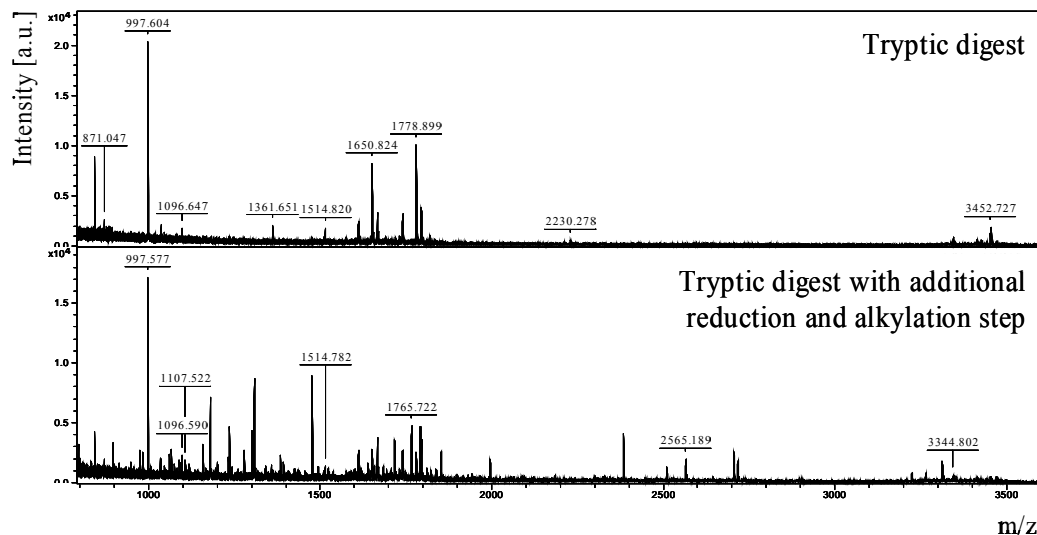


Figure 26: MALDI-TOF MS analysis of tryptic digests from a protein spot of the alcohol-soluble fraction of mature barley kernels. The same spot was excised from two replicate gels and digested following the conventional protocol for tryptic digests (upper row) and with an additional reduction and alkylation step (lower row). The number of detected peptide masses was higher when the modified digest protocol was applied. The spot was identified as B1-hordein precursor (TC138708) by peptide mass fingerprinting.

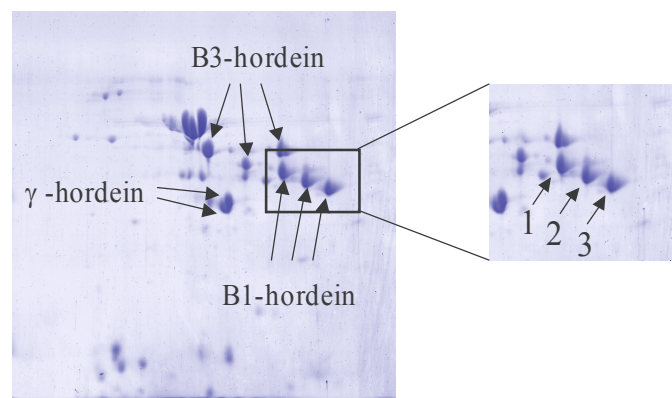


Figure 27: Spot pattern of the prolamin fraction from mature barley grains. The protein extract was separated on 13 cm IPG strips with pH gradient 3–10 in the first dimension and 12.5 % SDS-PAGE. Identification of major spots present in extracts from the parent line Brenda revealed a high level of polymorphism among B1-, B3- and γ -hordeins. The close-up view shows protein spots identified as B1-hordeins using LC-ESI-Q-TOF-MS/MS. The amino acid sequence of peptides that led to the identification is given in Table 2.

Table 2: Identification of B1-hordeins from mature barley grains cv. Brenda by LC-ESI-Q-TOF MS/MS. Given are the spot number as indicated in Figure 27, the protein name and accession number, the peptide sequence revealed by ESI MS/MS and the detected peptide modifications.

Spot	Protein name	Accession number	Identified peptides	Modifications
1	probable hordein B1 (fragment)	T04473	(K)VFLQQQCSPVR(M)	Carbamidomethyl C (7)
2	probable hordein B1 (fragment)	T04473	(K)VFLQQQCSPVR(M)	Carbamidomethyl C (7)
3	B1-hordein (clone pB11) (fragment)	S07976	(R)TLPMMCSVNVPLYR(I)	Carbamidomethyl C (6)
			(R)TLPMMCSVNVPLYR(I)	Oxidation M (5), Carbamidomethyl C (6)
			(R)TLPMMCSVNVPLYR(I)	Oxidation M (4), Oxidation M (5), Carbamidomethyl C (6)

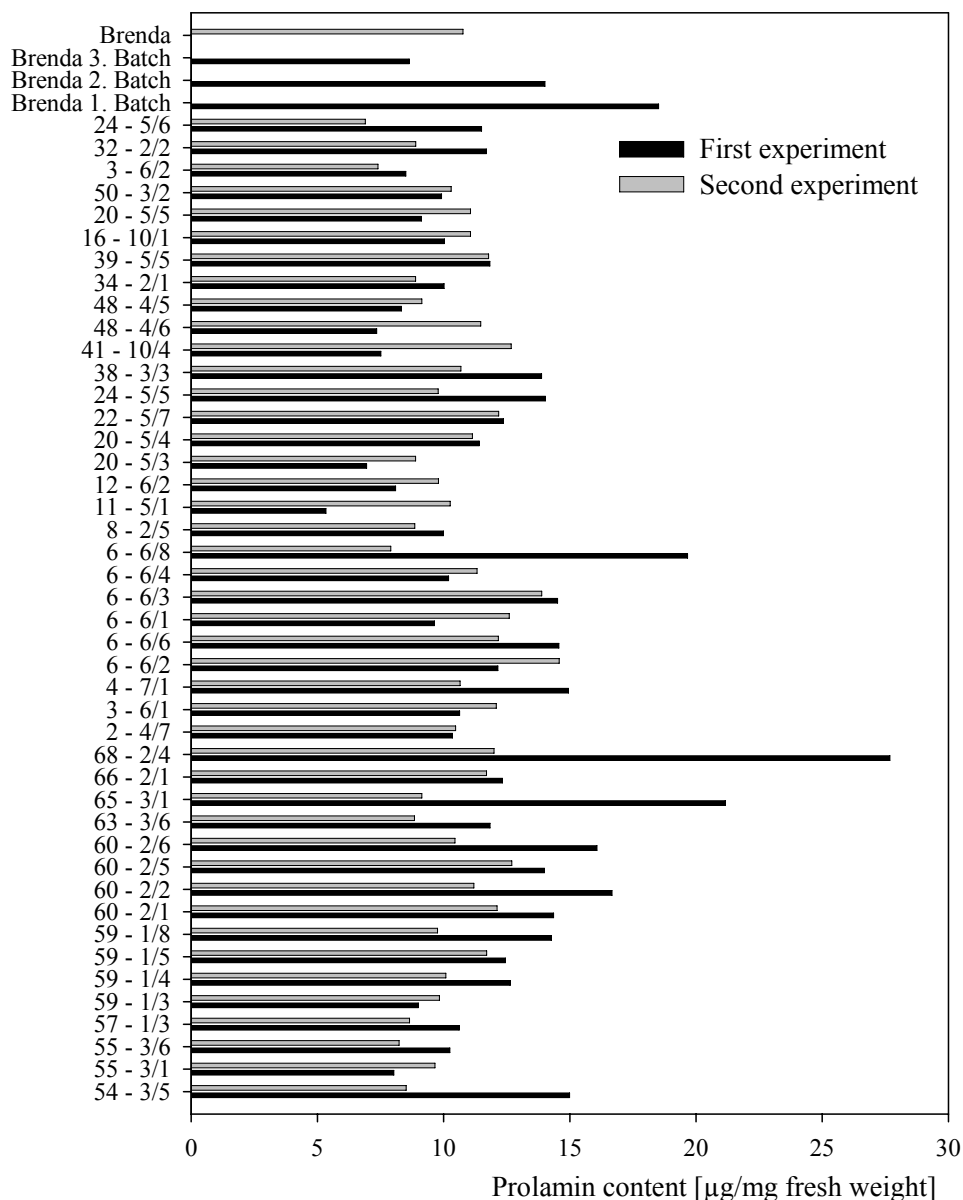


Figure 28: Description next page

Figure 28: Determination of total storage protein content in mature grains of introgression lines and the Brenda parent in both experiments. Alcohol-soluble prolamins were extracted from grains of ILs grown in two independent experiments and the total protein content was related to the fresh weight of flour as it was used for the protein extraction.

4.2. Grain proteome analysis of accessions from the Oregon Wolfe Barley mapping population differing in salt stress response

Salinity is one of the most severe abiotic factors threatening agriculture worldwide, hence there is a high interest in unraveling the mechanisms leading to salt tolerance and improve plant performance on saline soil in crop species. Salt tolerance is a multigenic trait, including salt partitioning within the plant, osmotic adjustment as well as cellular and subcellular morphological changes (Munns, 2005). Although the physiology of salt tolerance is well investigated in barley, little is known about the molecular mechanisms determining salt tolerance. Due to the fact, that barley is one of the most salt-tolerant crops and that cultivars display different levels of tolerance, it is an appropriate tool to study qualitative and quantitative changes in protein abundance in response to salt stress. In order to utilize the large diversity of barley accessions stored at the IPK Genebank, germination assays under various stress conditions are performed at the Resources Genetics and Reproduction group. When salinity stress is applied during germination, it was found that there is a great array of stress responses, ranging from highly sensitive to notably tolerant towards stress treatment.

Indeed, the parental lines of the OWB mapping population, DOM and REC, display contrasting salt tolerance on the basis of germination experiments (Weidner et al., 2005). Results indicate a higher tolerance in germinating grains of REC toward salt stress as compared to DOM. In order to identify proteins conferring salt tolerance during germination, a comparative proteome analysis of mature grains of DOM and REC was conducted.

4.2.1. Comparative proteome profiling

Using 2-D gel electrophoresis for the separation of the water-soluble protein fraction on mid-scale 2-D gels (IPG strips of 13 cm length), a new staining method was established, applying the fluorescent dye ruthenium(II)-tris-(bathophenanthroline-disulphonate) (RuBP). The advantages of fluorescent staining techniques are the greater sensitivity for low abundant proteins as well as the better linearity between protein amount and primary signal as compared to Coomassie Brilliant Blue or silver stain. Overall, about 1,200 spots could be

detected on 2-D gels of DOM and REC and triplicate gels confirmed the spot patterns. The Phoretix software with processing parameters as described in Materials and Methods section (3.5.1) was applied for image analysis, including spot detection and quantification. The comparative image analysis of the grain protein patterns from DOM and REC revealed 336 spots that were differentially expressed when applying a threshold of 1.5 fold. Actually, 228 spots were more abundant in the salt sensitive parent DOM and only 108 spots were higher expressed in the salt tolerant parent REC. It is not very likely that all differentially expressed proteins contribute to the contrasting response toward salt stress in both cultivars. In fact, the parent lines of the OWB population display an exceptional degree of phenotypic variation, so it can be assumed that the majority of proteins contribute to morphological or other characteristics. Therefore, four accessions from the OWB population were added to the analysis showing an even stronger trait for salt response than the parent lines (see Figure 3). Members of the Resources Genetics and Reproduction group at IPK tested the germination ability under stress conditions of 94 accessions from the OWB population and revealed a great range of natural variation for salt tolerance in progeny lines. As a result, lines were identified exhibiting a higher tolerance toward salt stress than the tolerant parent REC or that were more sensitive than the parent DOM. In order to limit the number of candidate proteins, lines OWB21 and OWB73, reacting more sensitive in the germination assay than DOM, and lines OWB34 and OWB59, reacting more tolerant than REC, were included in the comparative proteome analysis (Figure 29).

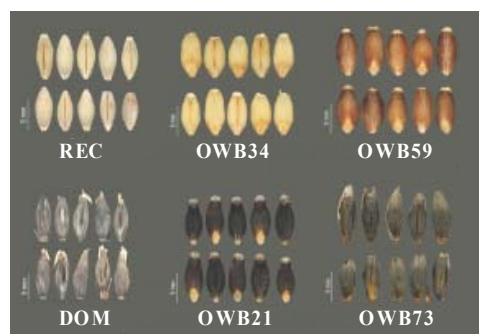


Figure 29: The grain phenotype of the selected lines for proteome analysis. Depicted in the upper row are salt tolerant lines (REC, OWB34, OWB59) and in the lower row salt sensitive lines (DOM, OWB21, OWB73).

The protein patterns of the four progeny lines revealed distinct differences when compared with the patterns of the parent lines. These cultivar-specific protein spots were excluded from the comparison, because only protein spots with similar expression levels in the same group

of tolerant or sensitive lines were of interest. As a result, the numbers of differentially expressed spots in salt tolerant and salt sensitive lines decreased considerably (Table 3).

Table 3: Differential protein expression in barley genotypes with contrasting response towards salinity stress. Given in the table are the number of differentially expressed protein spots revealed by direct comparison of the parental lines DOM with REC or by comparing groups of salt tolerant (REC+OWB34+OWB59) with salt sensitive genotypes (DOM+OWB21+OWB73). Differential protein expression was judged based on a 1.5 fold change in abundance.

	Spots with increased abundance	
	Salt sensitive cultivars	Salt tolerant cultivars
Comparison of parent lines (DOM vs. REC)	228	108
Comparison including additional accessions (DOM+OWB21+OWB73 vs. REC+OWB34+OWB59)	6	5

Due to the addition of progeny lines, sharing the same trait for salt responsiveness as the respective parent, the number of higher expressed spots was 6 and 5 for sensitive and tolerant genotypes, respectively. Two examples for protein expression are given in Figure 30. Spot # 8 (Figure 30A) was detected only in salt sensitive cultivars, whereas spot # 9 (Figure 30B) showed a 1.5 fold increase in salt tolerant lines.

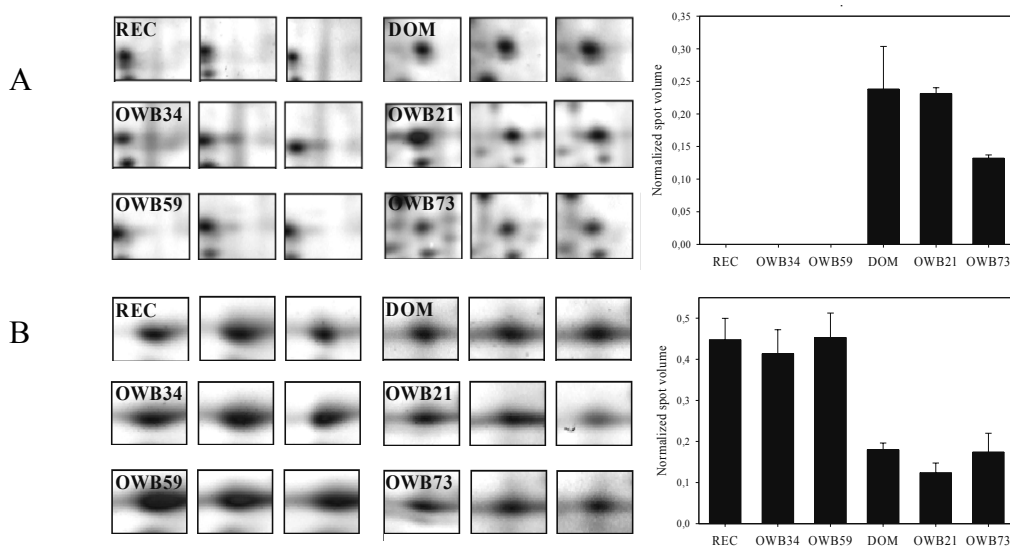


Figure 30: Expression of selected spots in the grain proteome of salt tolerant and salt sensitive barley cultivars. The enlarged 2-D gel sections show spots # 8 (A) and # 9 (B) in all lines under examination on triplicates per sample. The histogram gives the spot quantities as normalized volumes calculated by image analysis software as mean of three replicates.

4.2.2. Identification of candidate proteins by mass spectrometry

The position of differentially regulated proteins selected for identification by MS is indicated in Figure 31.

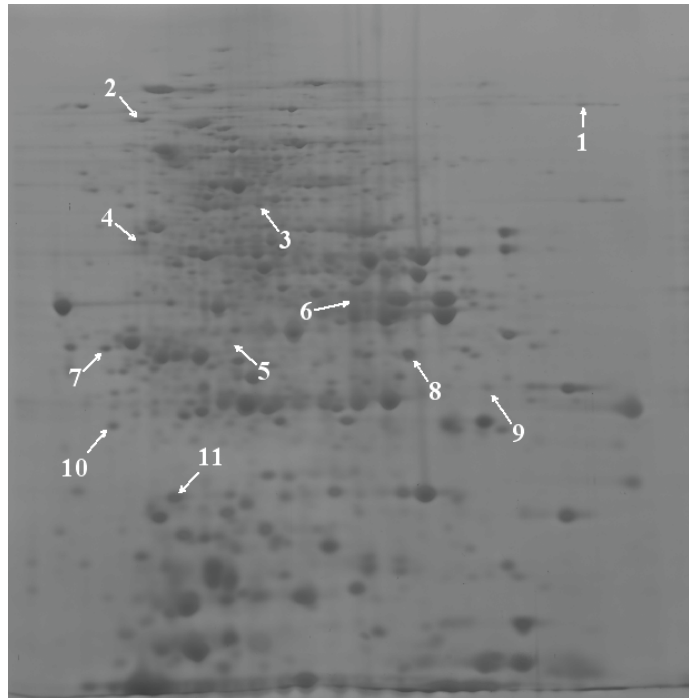
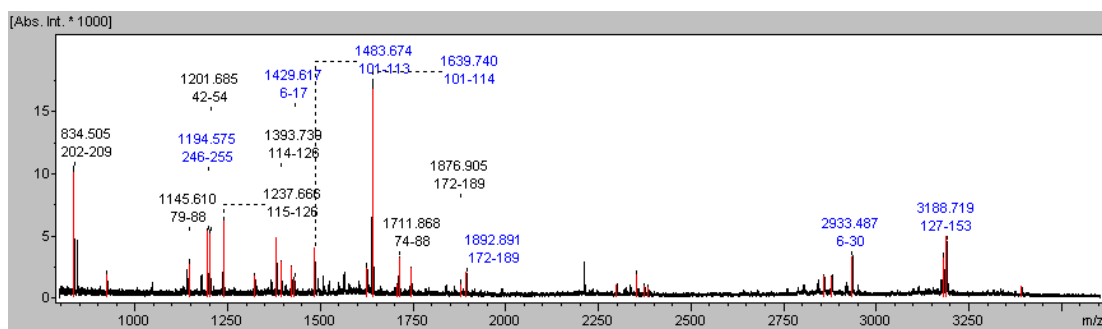


Figure 31: Representative 2-D gel from the analysis of soluble protein fractions from mature barley grains. Arrows indicate the position of 11 protein spots with differential expression in salt tolerant and sensitive lines selected for identification via mass spectrometry.

These 11 spots were excised manually from gels of all lines under investigation in order to verify the spot identity. The gel plugs were digested with trypsin and subjected to MS. Samples that could not be identified by MALDI-TOF MS peptide mass fingerprinting were subsequently analyzed by LC-ESI-Q-TOF MS/MS using the derived *de novo* sequence of tryptic peptides for homology-based database search. The identification of spot # 6 is shown in Figure 32 as an example for protein identification via MALDI-TOF MS and LC-ESI-Q-TOF MS/MS. This protein spot was more abundant in salt tolerant genotypes and due to the higher concentration of the protein in the spot, peptide masses acquired using MALDI-TOF MS were sufficient for identification (Figure 32A). However, the protein concentration was lower in salt sensitive lines and here, LC-ESI-Q-TOF MS/MS had to be applied (Figure 32B). The workflow yielded in the identification of 6 spots (Table 4). This is due to the relatively limited entry numbers of barley protein and EST sequences in databases, but also a hit was rejected when the identity was not confirmed in all lines where this spot was detected. The proteins identified included a cytosolic 6-phosphogluconate dehydrogenase (# 3), elongation

factor 1 (# 7), Hsp 70 (# 8) and translationally controlled tumor protein homolog (# 10). A glucose and ribitol dehydrogenase homolog was found in two different spots (# 6 and 9), indicating posttranslational processing. In general, the theoretical biochemical properties (molecular mass, isoelectric point) were in agreement with the position of the respective spot on the 2-D gel, except for spot # 8 that displayed a lower molecular mass than estimated from the amino acid sequence.

A MASQK**FPPQQ QDCQPGKEHA MDPRPEAIK** NYKSANKLQG **KVALVTGGDS GIGRAVCLCL**
 ALEGATVNFT YVKG**HEDKDA EETLQALRDI** KSRTGAGEPK **ALSGDLGYEE NCRRVVEEVA**
NAHGGRVDIL VNNAEQYVR PCITEITEQD LERVFRTNIF SYFLMTKFAV **KHMGPSSII**
NTTSVNAYKG NATLLDYTAT **KGAIVAFTRA** LSMQLAEKGI RVNGVAPGPI WTPLIPASFP
 EEKVK**QFGSE VPMKRAGQPS** EVAPSFVFLA SEQDSSYISG QILHPNGGTI VNS



B MASQK**FPPQQ QDCQPGKEHA MDPRPEAIK** NYKSANKLQG **KVALVTGGDS GIGRAVCLCL**
 ALEGATVNFT YVKG**HEDKDA EETLQALRDI** KSRTGAGEPK **ALSGDLGYEE NCRRVVEEVA**
NAHGGRVDIL VNNAEQYVR PCITEITEQD LERVFRTNIF SYFLMTKFAV **KHMGPSSII**
NTTSVNAYKG NATLLDYTAT **KGAIVAFTRA** LSMQLAEKGI RVNGVAPGPI WTPLIPASFP
 EEKVK**QFGSE VPMKRAGQPS** EVAPSFVFLA SEQDSSYISG QILHPNGGTI VNS

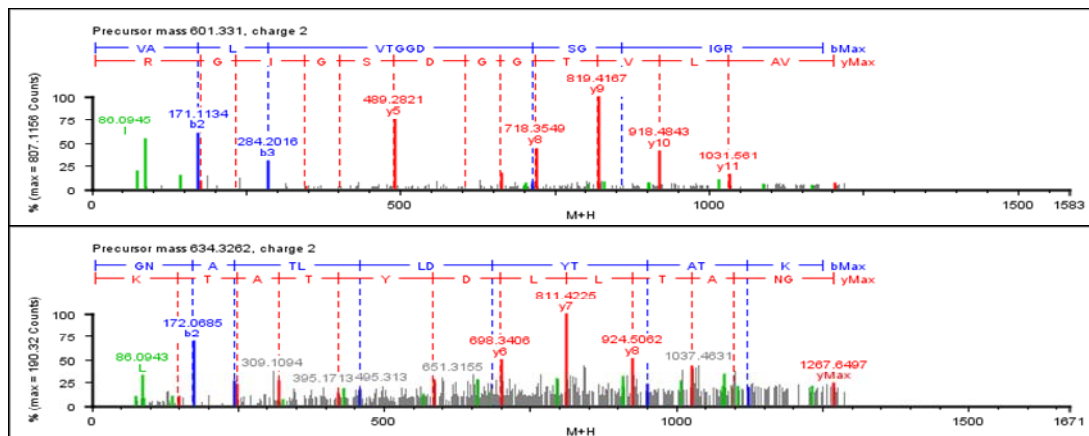


Figure 32: Identification of protein spot # 6 as glucose and ribitol dehydrogenase homolog using MALDI-TOF MS and LC-ESI-Q-TOF MS/MS. A: Identification of spot # 6 that was excised from 2-D gels from line OWB34. Shown is the amino acid sequence (black) and matching tryptic peptides (red) and below the MALDI-TOF spectrum of the tryptic digest. B: Identification of spot # 6 that was excised from 2-D gels from line OWB21. The amino acid sequence (black) and tryptic peptides sequenced by LC-ESI-Q-TOF MS/MS (red) and below the ESI-MS/MS spectra of the m/z 601.331 $[M+H]^+$ and m/z 634.326 $[M+H]^+$ peptide ions derived from in-gel digestion are shown. Protein identification via MALDI-TOF MS and LC-ESI-Q-TOF MS/MS was performed by searching *Viridiplantae* of the NCBI nr database.

Table 4: Identification of differentially expressed proteins using MALDI-TOF MS and LC-ESI-Q-TOF MS. Presented are spot numbers from the comparative 2-D gel analysis, the regulation of the respective spot as more (↑) or less (↓) abundant in salt tolerant lines or present only in salt sensitive lines (*), fold change of the corresponding spot based on normalized spot volumes from two gel groups (salt tolerant vs. salt sensitive lines) consisting of three cultivars with triplicate 2-D gels each. Spot identity based on MS analysis and the species from which the sequence homolog was identified, accession number from TIGR EST or NCBI nr protein database as well as the theoretical isoelectric point (pI) and molecular weight (MW) as calculated using ExPASy tools (<http://www.expasy.ch>) are given.

Spot number	Expression in salt tolerant lines	Fold change	Protein name	Accession number	Theoretical pI/MW (kDa)
3	↑	4.4	Cytosolic 6-phosphogluconate dehydrogenase, <i>Oryza sativa</i>	TC146849	5.9/52.7
6	↑	3.2	Glucose and ribitol dehydrogenase homolog, <i>Hordeum vulgare</i>	gi:7431022	6.5/31.6
7	↓	4.4	Putative elongation factor 1 beta, <i>Hordeum vulgare</i>	gi:7711024	4.5/24.5
8	*	-	Hsp 70, <i>Triticum aestivum</i>	gi:2827002	5.2/70.9
9	↑	1.5	Glucose and ribitol dehydrogenase homolog, <i>Hordeum vulgare</i>	gi:7431022	6.5/31.6
10	↓	3.1	Translationally-controlled tumor protein homolog, <i>Hordeum vulgare</i>	gi:20140865	4.5/18.8

4.2.3. Cloning and overexpression of candidate proteins

In the comparative proteome analysis of accessions from the OWB mapping population, two proteins, cytosolic 6-phospho-gluconate dehydrogenase and glucose/ribitol dehydrogenase homolog, were identified showing a higher abundance in salt tolerant cultivars. Their biological function is discussed later on, but it is very likely that they contribute to salt tolerance. The test the latter, a more detailed characterization was initiated by cloning and overexpression studies.

To obtain barley full-length clones, the nucleotide sequence of the identified proteins was blasted against the barley EST database CR-EST (<http://pgrc.ipk-gatersleben.de/cr-est/index.php>, release v1.5). This tool provides sequence and annotation data from crop EST projects at the IPK Gatersleben and contains about 40,280 barley consensus sequences. Clones with the highest similarity to the proteins identified by the proteome approach were ordered and the sequences were verified by DNA sequencing. Comparison at the nucleotide level revealed a 99 % identity of the clone HS09N23 when compared to barley glucose/ribitol dehydrogenase homolog mRNA (gi:633889) and a 88 % nucleotide identity of the clone

HI05J23 when compared to *Oryza sativa* cytosolic 6-phosphogluconate dehydrogenase mRNA (gi:30313360). Based on these high similarities both clones were selected for overexpression in the salt sensitive barley cv. Golden Promise.

Each clone was fused to the promoter of the maize ubiquitin for constitutive expression (Ubi1p) or to the promoter of the wheat α -gliadin for grain-specific expression (AGp) (Figure 33). This approach should allow the functional characterisation of candidate proteins not only overexpressed in the whole plant, but also confined to grain-specific cell types.

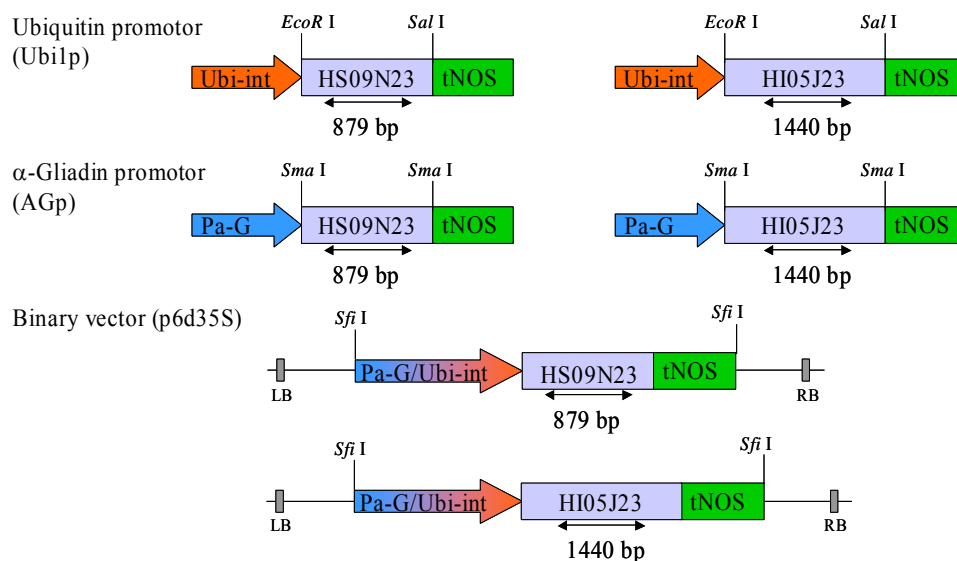


Figure 33: Schematic diagrams of expression vectors used for barley transformation. Clones coding for glucose/ribitol dehydrogenase homolog (HS09N23) and cytosolic 6-phosphogluconate dehydrogenase (HI05J23) were fused to the maize ubiquitin promoter or to the wheat α -gliadin promoter, respectively. Expression cassettes were subcloned into a binary vector for *Agrobacterium tumefaciens*-based transformation. The vectors were kindly provided by Drs Götz Hensel (Lig154(pNOS+PaG) containing AGp) and Axel Himmelbach (pUBI-ABM containing Ubi1p), IPK and DNA Cloning Service, Hamburg (p6d35S).

The resulting expression cassettes were finally cloned into a binary vector (p6d35S). The Plant Reproductive Biology group at IPK performed the *A. tumefaciens*-based gene transfer to immature barley embryos resulting in stable transgenic plants. About 100 immature embryos were used for transformation and subsequent selection on hygromycin containing media. Between 15 and 26 T₀-lines were generated per construct and verified by PCR for the hygromycin resistance gene. Transgene copy numbers were assessed by hybridisation of *Hind*III digested DNA with a (³²P)-dCTP-labelled probe for hygromycin resistance gene (Figures 34 and 35). In order to analyse the transgene expression of constructs driven by the ubiquitin promoter, total RNA from leaf tissue was hybridised with the respective gene-

specific probe (Figure 34). In leaves of Golden Promise wild type plants, no transcript for glucose/ribitol dehydrogenase homolog was detected and the expression level of 6-phosphogluconate dehydrogenase transcripts was also very low in this tissue. When compared to wild type plants, most transgenic plants showed an accumulation of transcripts for glucose/ribitol dehydrogenase homolog and 6-phosphogluconate dehydrogenase, respectively, although no apparent phenotype was observed.

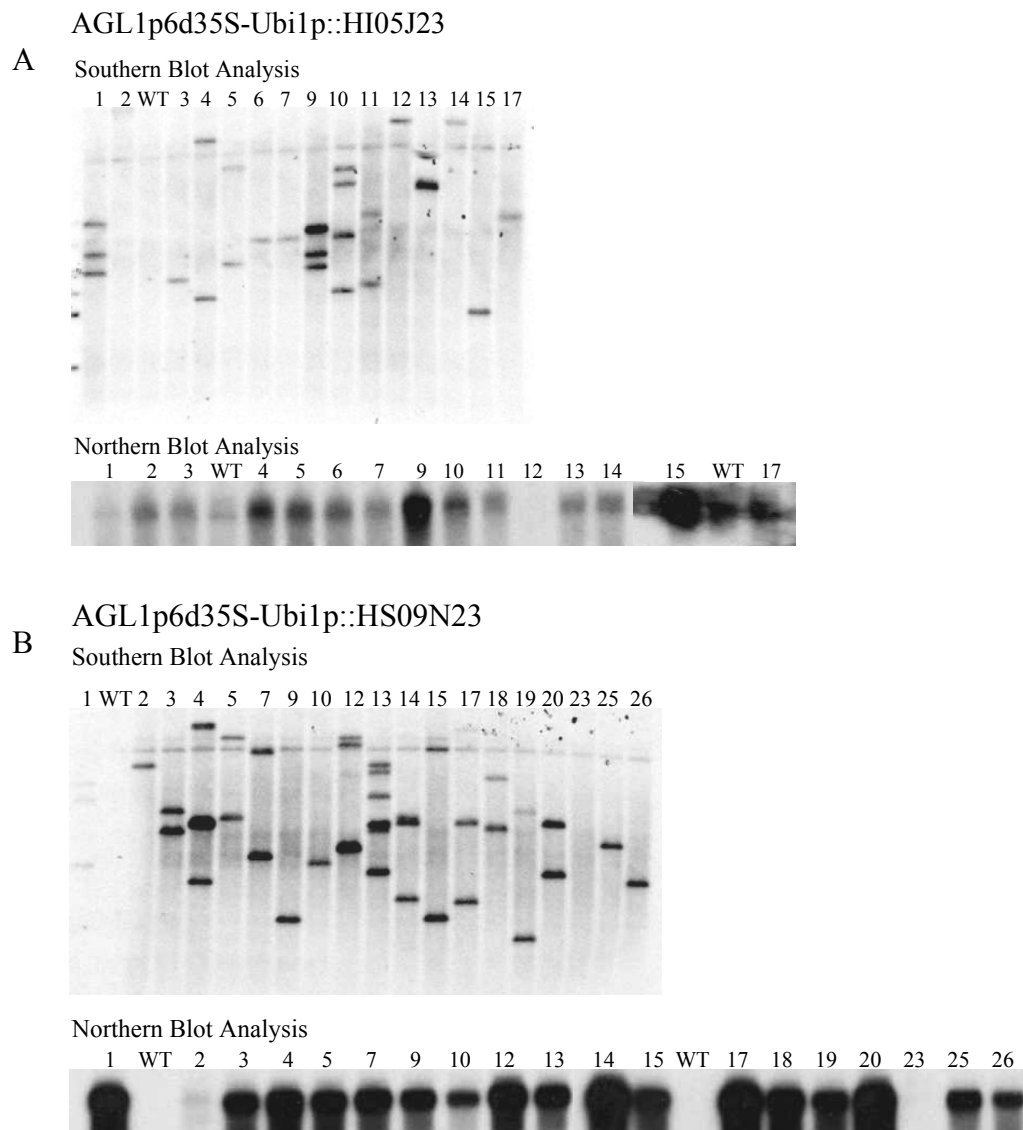


Figure 34: Southern and Northern blot analysis of ubiquitin promoter-driven expression cassettes for glucose/ribitol dehydrogenase homolog (AGL1p6d35S-Ubi1p::HS09N23) (A) and 6-phosphogluconate dehydrogenase (AGL1p6d35S-Ubi1p::HI05J23) (B). DNA and RNA were extracted from leaf material. Digested DNA was hybridized with a probe for hygromycin resistance gene, RNA blots were hybridized with the respective gene-specific probe. Transcripts for glucose/ribitol dehydrogenase homolog and 6-phosphogluconate dehydrogenase were more abundant in transgenic barley as compared to wild type (WT) plants.

The transcript levels of barley lines transformed with constructs driven by the α -gliadin promoter were evaluated by RNA analysis of mature grains (Figure 35).

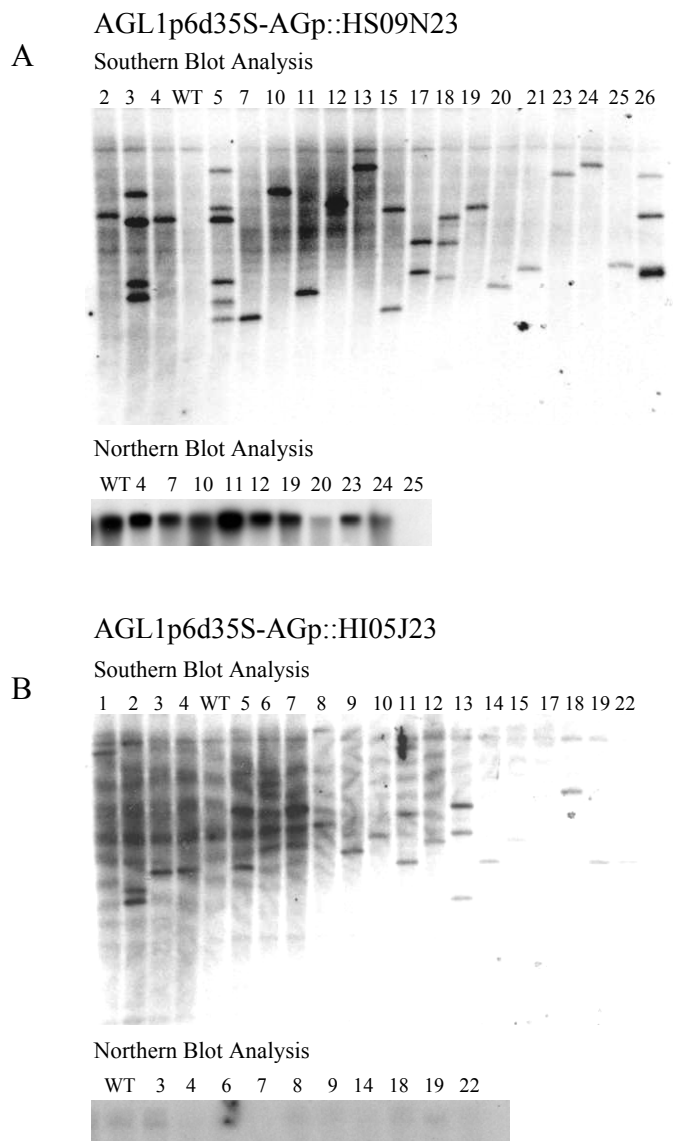


Figure 35: Southern and Northern blot analysis of the α -gliadin-driven expression cassettes for glucose/ribitol dehydrogenase homolog (AGL1p6d35S-AGp::HS09N23) (A) and 6-phosphogluconate dehydrogenase (AGL1p6d35S-AGp::HI05J23) (B). DNA was extracted from leaf material and RNA was extracted from mature grains. Digested DNA was hybridized with a probe for hygromycin resistance gene, RNA blots were hybridized with the respective gene-specific probe. Transcripts for glucose/ribitol dehydrogenase homolog were more abundant in transgenic barley as compared to wild type (WT) plants. mRNA abundance of 6-phosphogluconate dehydrogenase in transgenic lines was not altered to the same extent.

Here, several plants failed to develop grains, which is probably due to the transformation process, rather than to transgene expression. For that reason Northern Blot analysis was

performed for a smaller number of transgenic plants as compared to the ubiquitin promoter-driven transgenic plants. A high abundance of glucose/ribitol dehydrogenase homolog transcripts was found in non-transgenic grains of the cultivar Golden Promise, indicating a grain-specificity of this gene. When the gene was fused to a α -gliadin promoter for overexpression of glucose/ribitol dehydrogenase homolog, transgenic lines were identified with a higher transcript level as compared to wild type plants. In wild type plants, the expression of 6-phosphogluconate dehydrogenase was lower in mature grains as compared to leaf tissue. The transcript accumulation was only moderately enhanced by overexpression of this gene under control of the grain-specific α -gliadin promoter.

Currently, the next generation of transgenic lines is growing and grains of this generation will be characterized in future stress experiments.

4.3. Proteome analysis of accessions from the Steptoe Morex mapping population with contrasting response towards salt stress at different developmental stages

Although the grain proteome analysis of accessions from the OWB mapping population revealed potential candidates for salt tolerance improvement, this population was developed to map phenotypic traits and the resulting high phenotypic variance within this population might be limiting for in-depth investigation of agronomic traits (Dr Andreas Börner, personal communication). For further experiments on the salt response at the germination stage of barley, the SM mapping population, which was derived from a cross of a high yielding feed barley (Steptoe) with a malting quality standard (Morex), was selected. This population consists of 150 doubled haploid (DH) lines with low phenotypic variation and detailed molecular marker maps are available which are of special interest for QTL analysis of agronomic characteristics.

4.3.1. Comparative proteome profiling of mature grains

Similar as it was done for the OWB population members of the Resources Genetics and Reproduction group at IPK tested the complete SM population for the ability to germinate under salt stress conditions. Germination tests during salt stress demonstrated a contrasting response of the parental lines towards the stress. The Steptoe parent reacted more sensitive to the stress applied as compared to the Morex parent. Also accessions were found showing a greater or lower tolerance towards stress as Morex or Steptoe, respectively (Dr Annette Weidner, unpublished data). In order to follow the experimental set-up from the comparative

grain protein profiling of accessions from the OWB population, four progeny lines from the SM population were selected with a more contrasting salt response trait as compared to the parent lines.

In order to improve the protein separation and visualization, large-format 2-D gels (IPG strips of 24 cm length) and the highly sensitive fluorescent RuBP stain were employed in the profiling of the water-soluble protein fraction. Overall, 1,400 protein spots were detected on the 2-D gels and for the estimation of spot quantities the SameSpots software was used. PCA on the protein patterns of all lines under investigation revealed a clear separation between accessions that were salt sensitive (Step toe, DH14, DH93) or salt tolerant during germination (Morex, DH80, DH187) (Figure 36).

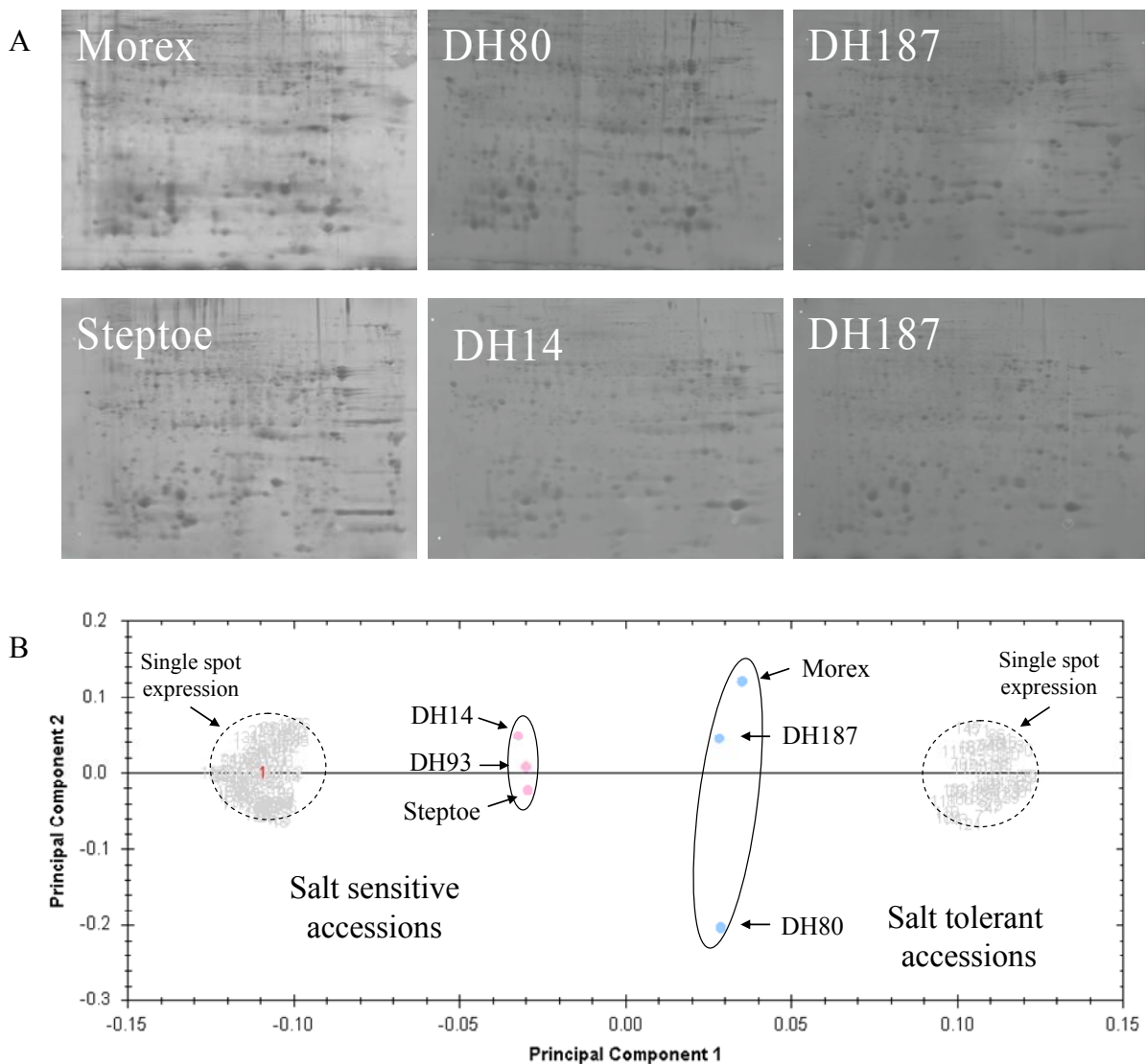


Figure 36: Description next page

Figure 36: 2-D gel electrophoresis of the water-soluble fraction of mature grains from accession of the SM population. A: Protein extracts from grains of salt tolerant (Morex, DH80, DH187) and salt sensitive genotypes (Steptoe, DH14, DH187) were separated in the first dimension on IPG strips ranging from 3-11 and in the second dimension using a 12.5 % SDS-PAGE. B: Grouping of protein patterns of salt tolerant and sensitive accessions from the SM population. PCA of protein spots from one 2-D gel per sample displayed a clear separation between accessions showing a good (Morex, DH80, DH187) or poor performance (Steptoe, DH14, DH93) in germination tests during salt application. Encircled with a dashed line are the single spots that are differentially regulated. Only spots with a significant change in abundance ($p < 0.05$) were used for calculation.

Based on image analysis, 8 protein spots were selected for mass spectrometry-based identification. Those spots showed a similar expression either in the groups of tolerant or sensitive accessions but differed in abundance between the groups. Two examples are given in Figure 37. Spot # 1 was found 2.7 fold more abundant in salt tolerant lines, whereas spot # 5 was 2.5 fold less expressed in these accessions.

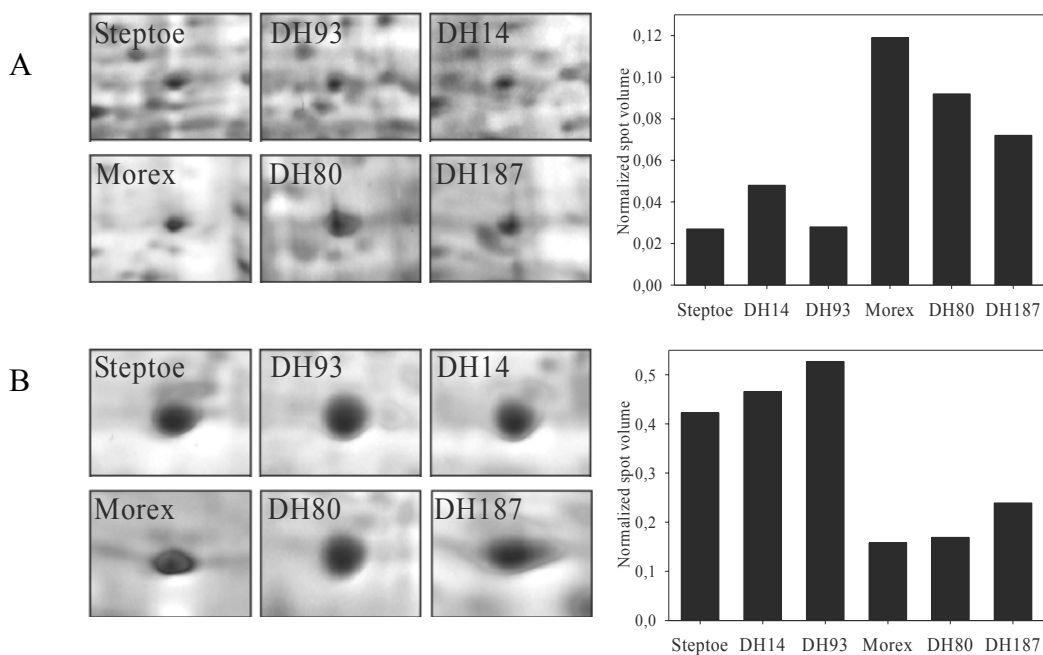


Figure 37: Expression of selected spots in the grain proteome of salt tolerant and salt sensitive accessions from the SM population. The enlarged 2-D gel sections show spot # 1 (A) and # 5 (B) in all lines under examination. The histogram gives the spot quantities as normalized volumes estimated by image analysis software.

Identification of candidate proteins by mass spectrometry

The location of protein spots selected for identification using mass spectrometry is indicated in Figure 38. These 8 spots were excised manually from gels of all lines under investigation in order to confirm the spot identity.

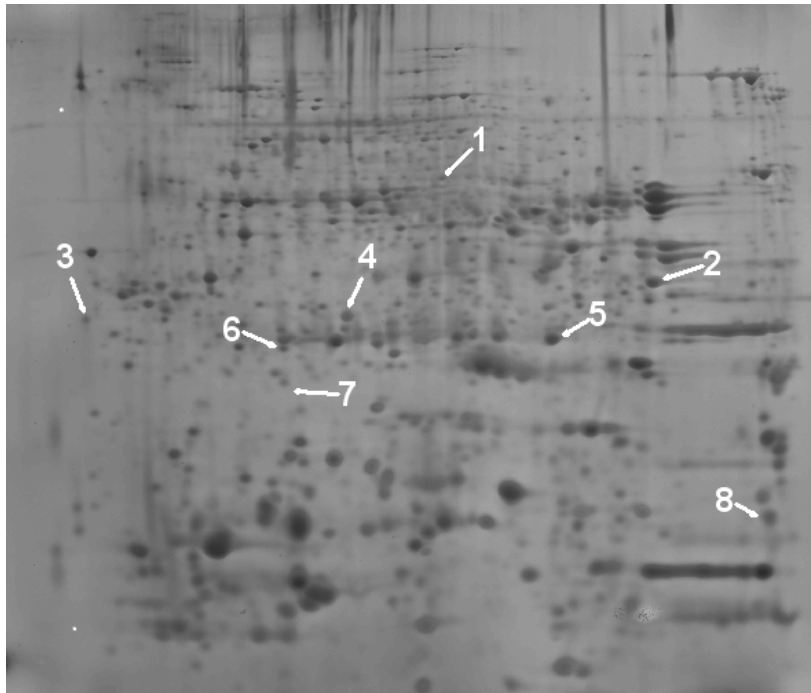


Figure 38: 2-D gel from the water-soluble grain protein fraction from the Steptoe parent. Arrows indicate the position of 8 protein spots with differential expression in salt tolerant and sensitive lines that were selected for identification.

Protein identification via MALDI-TOF MS and LC-ESI-Q-TOF MS/MS was successful for 7 spots (Table 5). Protein # 7 was identified as putative ripening-related protein 2 precursor (*Oryza sativa*, TC139695) only from the 2-D gel fabricated from Morex and DH14 protein extracts, but the identity could not be confirmed in the remaining lines probably due to very low protein expression in these lines. Therefore this protein spot was rejected from further investigations. The other protein spots contained an isocitrate dehydrogenase (# 1), lipoprotein-like protein (# 2), Rab28 protein (# 3), embryo-specific protein (# 4), 1-Cys peroxiredoxin PER1 (# 5), chitinase (# 6) and LEA protein (# 8). To a large extent, the theoretical values for *pI* and MW correspond to the position of the protein spot in the 2-D gel. Slight deviations were observed for the *pI* from LEA protein since this parameter was deduced from the amino acid sequence of a homologous protein from another species.

Table 5: Identification of protein spots by MALDI-TOF MS and LC-ESI-Q-TOF MS. Spot numbers from the comparative 2-D gel analysis, the abundance of the respective spot as more (↑) or less (↓) accumulated in salt tolerant lines and the fold change of the corresponding spot based on normalized spot volumes from two gel groups (salt tolerant vs. salt sensitive lines) consisting of three cultivars with one 2-D gel each are given in the table. Furthermore, spot identity based on MS analysis and the species from which the sequence homolog was identified, accession number from TIGR EST or NCBI nr protein database, theoretical pI and MW as calculated using ExPASy tools (<http://www.expasy.ch>) are shown.

Spot number	Expression in salt tolerant lines	Fold change	Protein name	Accession number	Theoretical pI/MW (kDa)
1	↑	+2.7	Isocitrate dehydrogenase, <i>Arabidopsis thaliana</i>	gi:20260384	6.1/45.7
2	↓	-3.0	Lipoprotein-like protein, <i>Oryza sativa</i>	TC132560	7.8/ 28.1
3	↑	+2.5	Rab28 protein, <i>Zea mays</i>	TC141145	4.9/27.7
4	↓	-1.9	Embryo-specific protein, <i>Oryza sativa</i>	TC147106	5.6/26.4
5	↓	-2.5	1-Cys peroxiredoxin PER1, <i>Hordeum vulgare</i>	gi:1710077	6.3/23.9
6	↓	-1.9	Chitinase, <i>Hordeum vulgare</i>	gi:563489	6.1/26.6
8	↓	-3.6	LEA protein, <i>Bromus inermis</i>	TC132485	6.9/18.5

Cloning and overexpression of candidate proteins

The proteome analysis of mature grains from SM population accessions revealed two proteins that were more abundant in lines performing well in germination tests under salt stress application. The possible function of both proteins in the context of defence against salt stress is discussed later on. But for the detailed characterization of isocitrate dehydrogenase and Rab28 protein, both proteins were selected for cloning and overexpression studies in the salt sensitive barley cultivar Golden Promise.

In order to obtain full-length clones, the nucleotide sequence of the identified proteins was blasted against the CR-EST database (<http://pgrc.ipk-gatersleben.de/cr-est/index.php>, release v1.5) and clones with the highest similarity on the nucleotide level were ordered and sequenced. The alignment of subject and query showed a 78 % identity of the clone HO26C23 with the *Arabidopsis* NADP-specific isocitrate dehydrogenase (gi:20260384) and a 59 % identity of the clone HS09M23 with the Rab28 protein from maize (gi:22459). To permit the tissue-specific functional characterization, each clone was not only fused to the

maize ubiquitin promoter for constitutive overexpression (Ubi1p), but also to the wheat α -gliadin promoter (AGp) for grain-specific overexpression. The resulting expression cassettes were subcloned into the binary vector p6d35S. The transformation of immature barley embryos at the Plant reproductive biology group at IPK is under way.

4.3.2. Assessment of salt tolerance at the seedling stage of the Steptoe and Morex parental lines

Germination rate is an easy trait to score for salt tolerance and the analysis of the grain proteome of accessions with contrasting response to salt stress revealed a number of interesting and potential candidate proteins relevant for further characterisation studies. But in fact, the ability of a crop to germinate does not predict the capability to grow or set seed in saline soil. This means that tolerance at germination may not confer tolerance at the seedling stage. In order to assess salt stress responses at later developmental stages, experiments are conducted with plants grown in saline conditions. Reviewing the literature on salt stress experiments, in most cases the stress is applied at high dosage and only for a short period of time. The resulting growth reduction is assumed to be salt stress induced, but it is more likely that short-term water deficit and unspecific stress responses caused the reduced biomass production. Even more challenging is the request to quantify salt stress response at later stages in different genotypes as growth behaviour might differ between the investigated accessions. Therefore, for the investigation of salt stress response at the seedling stage in the Steptoe and Morex parental lines, long-term salt stress experiments were conducted using hydroponic culture systems (Figure 39). This system allows the controlled application of NaCl to plants via a nutrient solution and makes the harvest of roots less difficult.

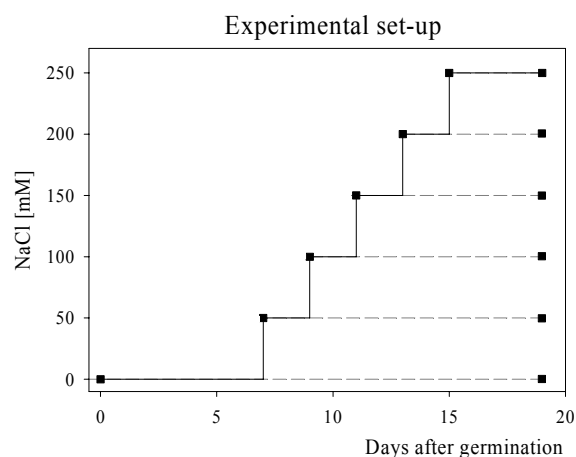


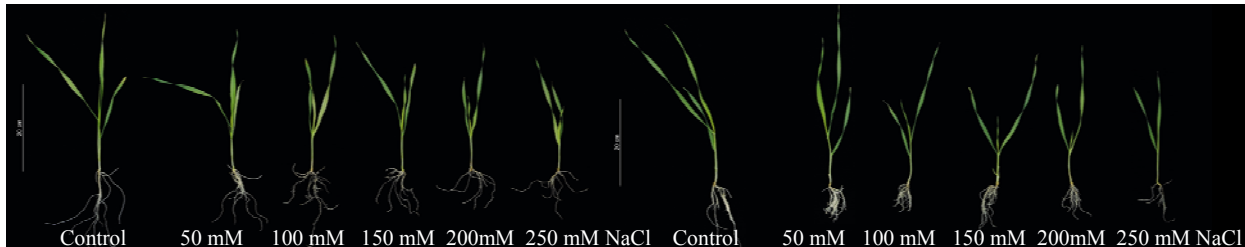
Figure 39: Schematic diagram of salt stress application using hydroponic culture. NaCl concentration was increased 7 days after germination and plants were harvested after 13 days of stress treatment at indicated concentration levels. The experiment was designed following the set-up of Walia et al. (2006).

At the harvest time point both cultivars showed a delay in growth when salt stress was applied (Figure 40A). This observation was supported by biometric data determined from stressed plants (Figure 40B) and these data were confirmed in three independent experiments.

A

Morex

Step toe



Morex

Step toe

B

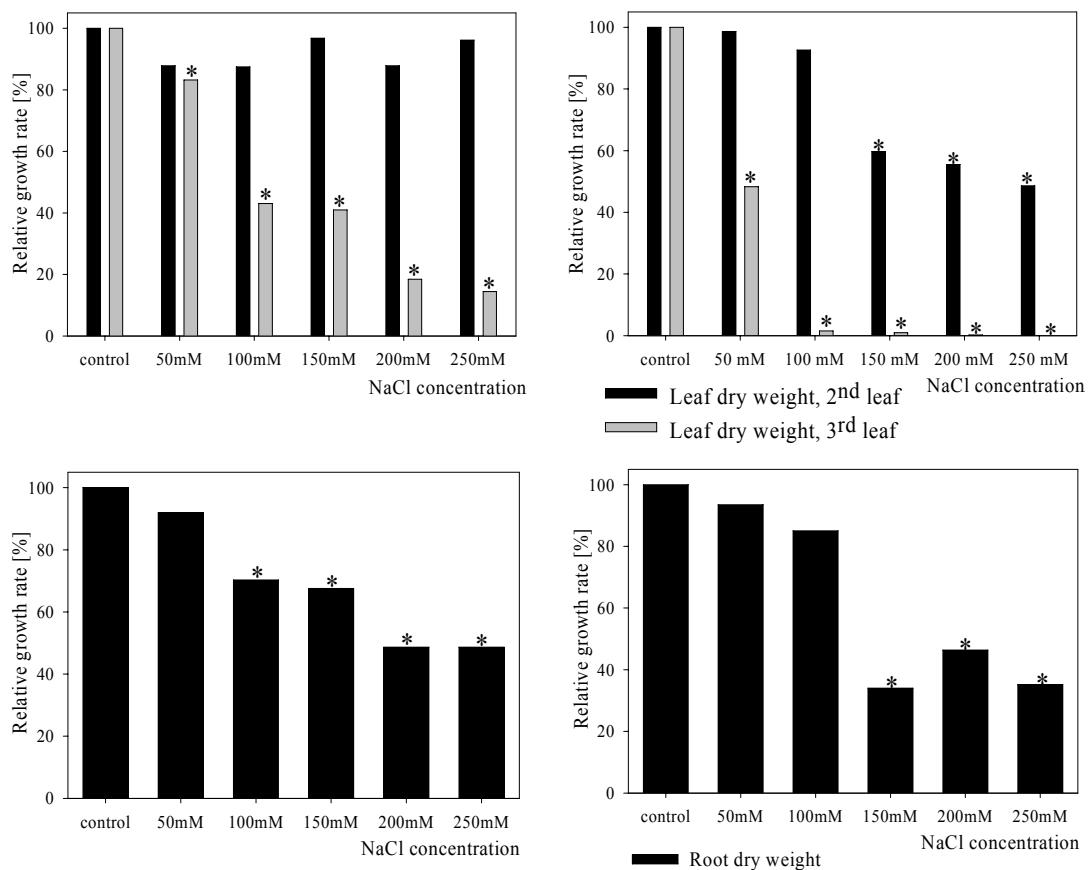


Figure 40: Effect of NaCl on the growth of seedlings from accessions with contrasting salt tolerance. Growth inhibition in both barley cultivars was already visible at 50 mM NaCl treatment and was increasing with higher salt concentrations (A). Growth measurements of leaf and root tissue indicate the better performance of Morex compared to Step toe with respect to the development of the secondary and tertiary leaf, but not to root development (B). The data represents the relative growth rate as compared to control plants of the respective cultivar. Means of $n = 20$ plants per treatment were used for calculation. Statistical differences between treatments were analyzed following the Duncan multiple range tests (Duncan, 1955). Asterisks indicate significant differences at $p < 0.05$ as compared to control.

Measurements of root length, root fresh weight and root dry weight as well as leaf length, fresh weight and dry weight of the second and third leaf were performed. The growth inhibition is clearly visible for both cultivars, although even at high salt concentrations no sign of leaf senescence was noticed. Based on the dry weight, no significant change in the expansion of the second leaf was detected for Morex, whereas a significant reduction in growth in the same leaf was shown for Steptoe, starting from 150 mM NaCl. In Steptoe, the development of the third leaf was diminished at 150 mM NaCl and almost completely inhibited at 200 and 250 mM NaCl. In contrast to this, the Morex cultivar was able to develop the third leaf even at 250 mM NaCl, although there was a growth reduction of nearly 90 %. The root development was also affected by salt treatment, but dry weight measurement did not reveal a cultivar-specific response as both genotypes decrease in biomass production to a similar extent of 40–50 % as compared to control plants.

4.3.3. Cultivar-specific and salt stress-affected protein expression in roots of Steptoe and Morex

In order to unravel cultivar-specific salt stress responses, a proteome analysis was initiated. Significant changes in growth upon stress treatment were shown for leaf tissue and therefore the proteome of second and third leaves was investigated on mid-scale 2-D gels in preliminary experiments. Surprisingly, only a small number of differentially expressed protein spots were detected, indicating that the proteome of leaves was affected only to a small extent by the stress treatment. Subsequently, the protein expression in roots was analysed and here, a considerable amount of differentially expressed protein spots was found in both cultivars after salt stress application. Based on these findings, an in-depth proteome analysis in root tissue of Steptoe and Morex was conducted to analyse proteins in response to salt stress in both genotypes. The experimental design is shown in Figure 41.

2-D gels (pH gradient 3-10 with IPG strips of 13 cm length) from three biological experiments were analysed independently to detect proteins that were reproducibly regulated in the same manner either cultivar-specific or in response to the stress treatment. For protein visualisation, cCBB was applied as the staining procedure for this large number of 2-D gels is shorter as compared to RuBP staining. The protein pattern was consistent throughout the biological replicates although the number of detected spots on 2-D gels varied (experiment 1: 990 spots, experiment 2: 840 spots, experiment 3: 640 spots). The introduction of two genotypes and three treatments lead to the generation of a highly dimensional data set, since the comparisons between genotypes under control conditions, between control and stress

treatment in each genotype as well as between genotypes under stress conditions complicated the pair-wise evaluation of differentially expressed protein spots. In order to reduce the data set and to eliminate false-positives, analysis of variance (ANOVA) was applied with a threshold of $p > 0.05$. Using this approach, only spots with significant change in abundance either between genotypes or that are responsive to the salt treatment and that were replicated in three biological experiments were selected for mass spectrometry-based identification.

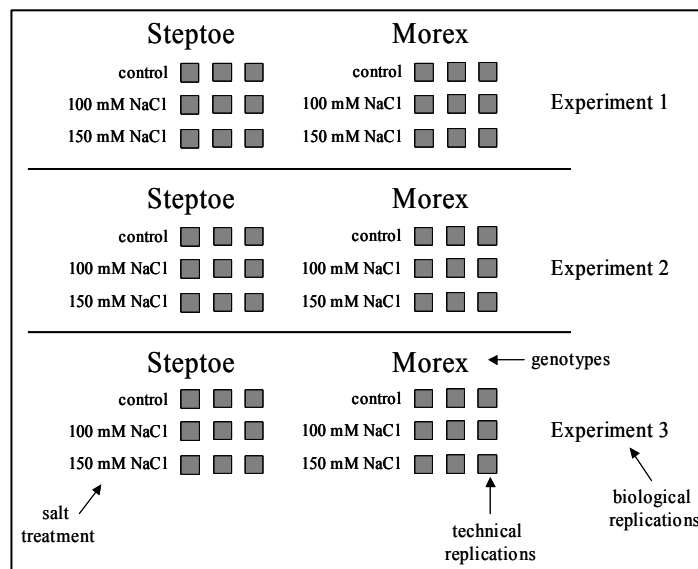


Figure 41: Experimental design of the 2-D gel electrophoresis of barley root tissue. Indicated are the three independent biological experiments with both genotypes under three conditions (control, 100 mM NaCl, 150 mM NaCl) and three technical replicates of 2-D gels per sample. Plants were grown and stressed as shown in Figure 39.

This thorough investigation led to the detection of 39 proteins with differential expression between the salt tolerant and salt sensitive genotype under control conditions, after stress treatment or in both groups. One example is shown in Figure 42, where the reproducibility of the results is demonstrated. PCA revealed a strong grouping according to genotypes and treatment (Figure 43). Based on PCA, the expression patterns of the selected spots in the salt sensitive line Steptoe were grouped according to the three growing conditions. In contrast to this, there was a grouping only into control and salt treated samples for Morex, indicating little difference for protein expression in this cultivar after 100 mM and 150 mM NaCl stress treatment.

Based on the expression profiles, the protein spots were grouped into 5 classes (Figure 44). Proteins in class 1 follow an expression pattern characterized by a genotype-specific expression, which was not significantly affected by salt stress treatment. Proteins in class 2

are significantly higher expressed in both genotypes under stress conditions. Proteins that were down regulated upon stress treatment were grouped into class 3. Class 4 consisted of proteins up or down regulated after stress application only in the Morex genotype, whereas class 5 proteins were up or down regulated after treatment in the Steptoe genotype.

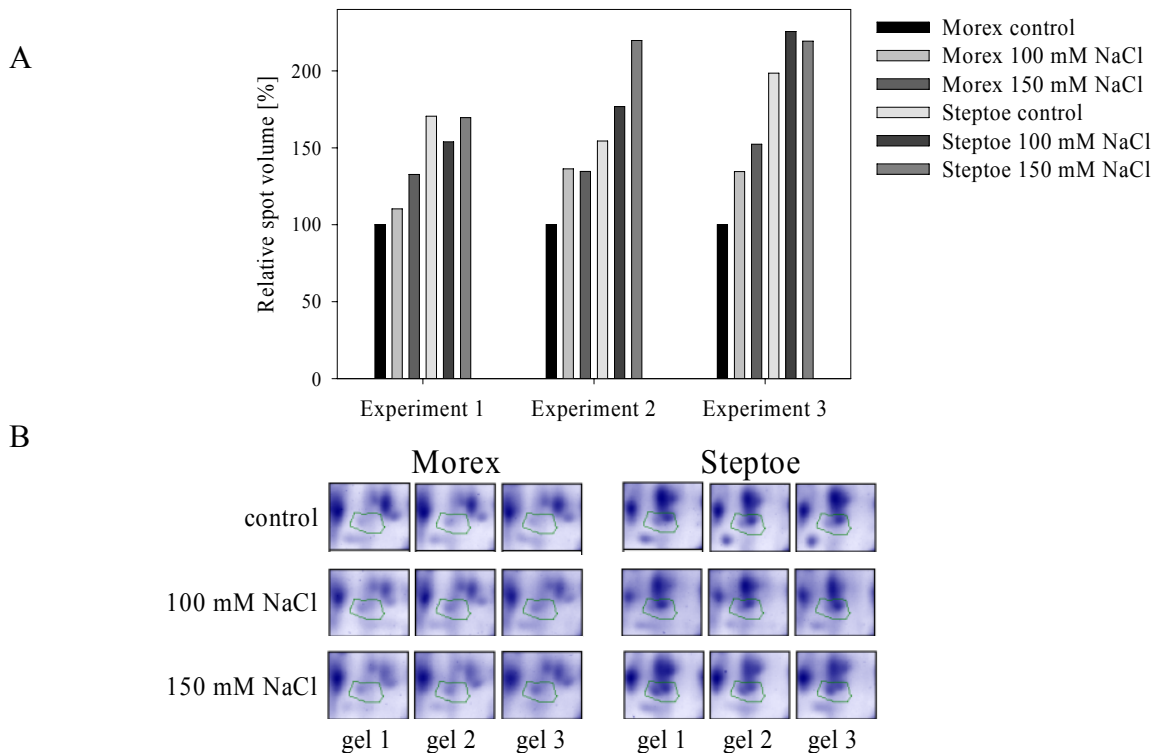


Figure 42: Protein expression of spot # 208 in three independent biological experiments. Protein abundance increased after stress application in both genotypes, but to a higher extent in Steptoe than in Morex. A: Protein expression values are given as relative spot volumes related to the normalised spot volume of the Morex control. B: Close-up view of the expression of spot # 208 in the second experiment.

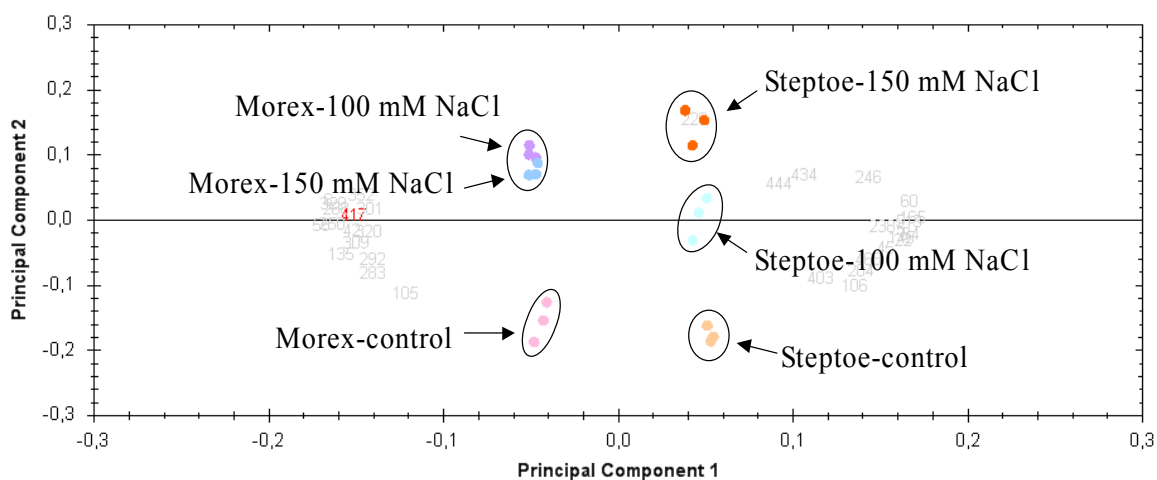


Figure 43: Grouping of protein expression profiles of the salt tolerant line Morex and sensitive line Steptoe. PCA of protein spots from three 2-D gels per sample show a clear class-separation between genotypes as well as treatment. Used for calculation were only spots with $p < 0.05$.

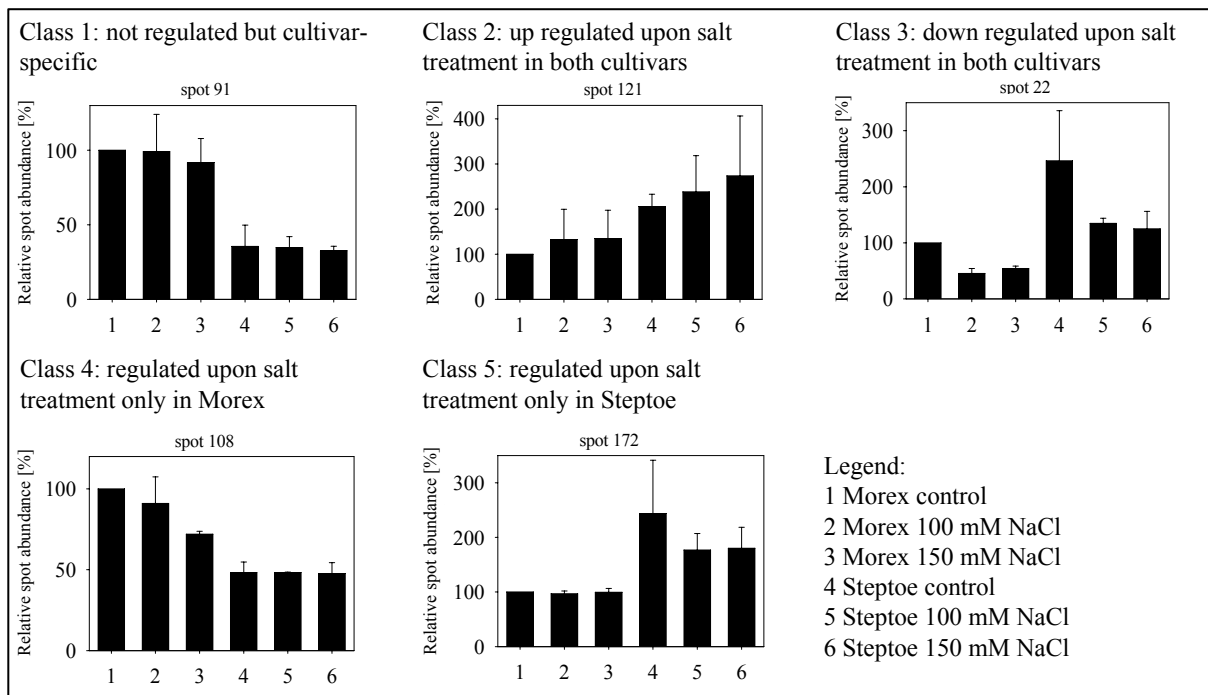


Figure 44: Grouping of protein spot expression patterns based on normalized spot volumes. The expression patterns of differentially expressed protein spot were grouped into five categories. For each class, the expression of one protein spot is shown. Given are relative spot volumes with Morex control as set to 100 %. The spot volumes were calculated as the mean of normalized spots volumes from at least two independent experiments. The identification of proteins belonging to the respective groups can be found in Table 6.

Mass spectrometry-based identification was successful for 28 out of 39 selected protein spots. To confirm the protein identity, the spots were identified from all genotypes and treatments, where they were detected, as well as from two independent biological experiments. The position of the respective spots on 2-D gels is shown in Figure 45 and the results of the comparative proteome analysis are presented in Table 6. The expression of proteins assigned to the first cluster was rather cultivar-specific than responsive towards stress treatment. Three proteins were found following the expression pattern of class 1, namely two LEA proteins and a poly(A)-binding protein. The expression of seven proteins correlated with class 2, which were S-adenosylmethionine synthetase 1, carboxymethylenebutenolidase-like protein, peroxidase, lactoylglutathione lyase, a probable L-ascorbate peroxidase 7, poly(A)-binding protein and endo-1,3-beta glucosidase.

Protein in class 3 were grouped based on down regulation in both genotypes after stress treatment and these were a putative nuclear RNA binding protein, lactoylglutathione lyase, 23 kDa jasmonate-induced protein, iron-deficiency specific (IDS) proteins IDS2 and IDS3, 6-phosphogluconate dehydrogenase, a putative monodehydroascorbate reductase and a probable

nicotianamine synthase 7. For one EST (spot # 239) it was not possible to find a protein with significant similarity from any other organisms. Class 4 consisted of proteins revealing a cultivar-specific expression in Morex and including a probable L-ascorbate peroxidase 7, glutathione transferase F5, lipoxygenase 1 and a stress-inducible protein F23N19.10. Proteins that were significantly differentially expressed in the Steptoe cultivar, grouped in class 5, were fructokinase 2, Osr40g2 protein, which was found as a salt stress-responsive cDNA in rice (Moons et al., 1996), iron-deficiency induced (IDI) proteins IDI1, IDI2 as well as catalase 1.

According to their functional characterization, most protein spots identified in the analysis function in oxidative stress responses. Nine protein spots that are differentially regulated upon salinity treatment are involved in redox regulation. The remaining groups, representing protein synthesis, primary and secondary metabolism as well as disease/defence-related proteins contain 4 of the identified proteins, respectively.

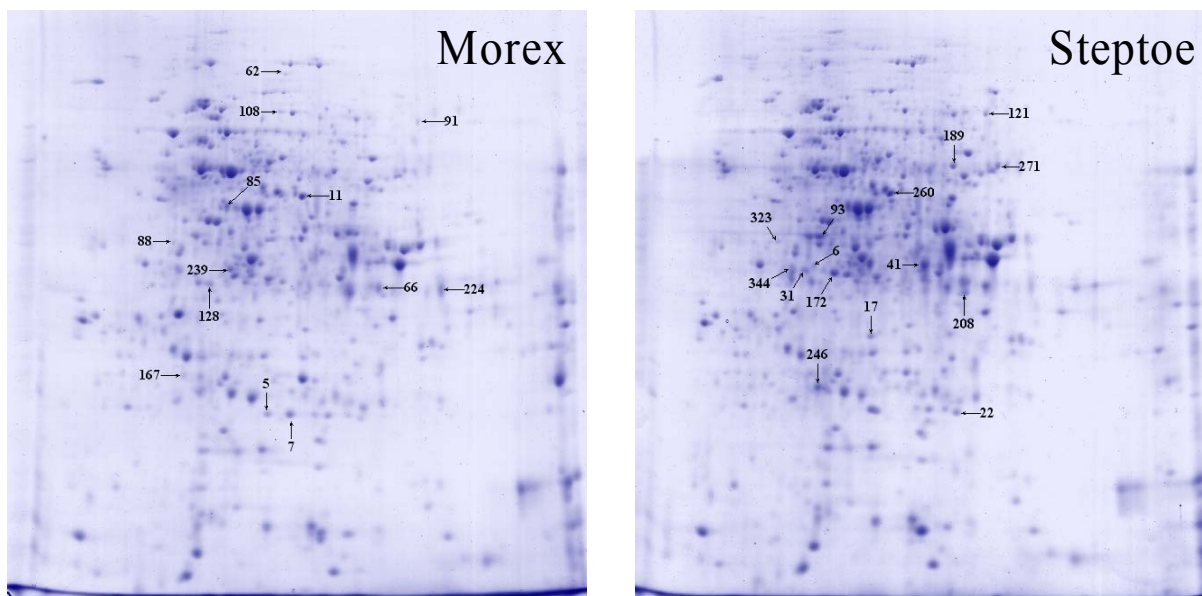
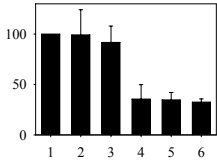
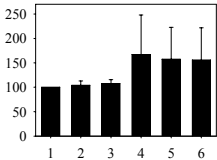
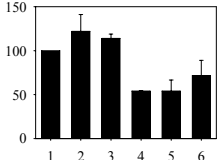
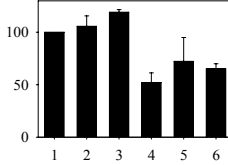
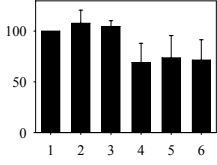
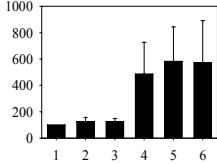
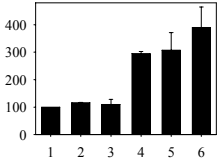
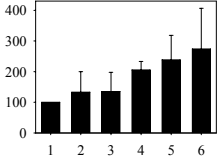
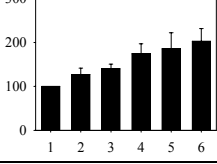


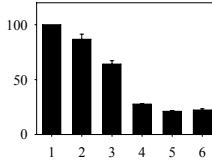
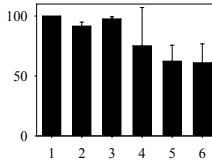
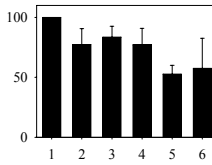
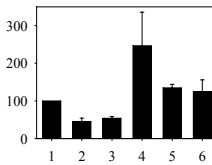
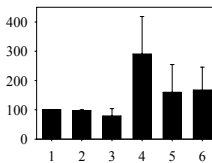
Figure 45: Representative Coomassie-stained 2-D gels from root samples of Morex (left) and Steptoe (right) show the position of the spots from Table 7. The spot is indicated in the genotype where the expression was highest.

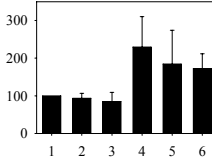
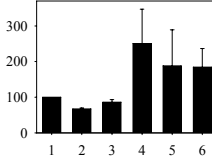
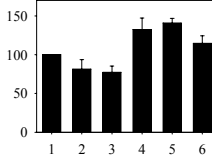
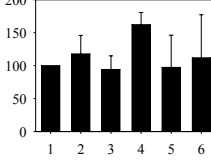
Table 6: Differentially expressed protein spots revealed by the comparative proteome analysis of salt-stressed roots from salt tolerant Morex and salt sensitive Steptoe. Proteins are grouped into expression classes. Given are the protein identifiers from EST (TIGR gene index for barley) and protein databases (Uni-Prot), biochemical properties (MW, pI) as calculated with ExPASy tools and the functional category. The expression pattern is given as the relative ratio [%] of the mean of the normalized spot volumes from at least two experiments (first column: Morex control as set to 100 %, second column: Morex 100 mM NaCl, third column: Morex 150 mM NaCl, fourth column: Steptoe control, fifth column: Steptoe 100 mM NaCl, sixth column: Steptoe 150 mM NaCl treatment).

Spot number	TIGR	Uni-Prot	Description	MW (kDa)	pI	Functional category	Expression pattern
Class 1: cultivar-specific proteins							
88	TC139604	Q6Z4J9	Late embryogenesis abundant protein, <i>Oryza sativa</i>	41.07	4.98	Desiccation tolerance	
91	TC139323	P93616	Poly(A)-binding protein, <i>Triticum aestivum</i>	70.82	6.60	Protein synthesis	
323	TC139604	Q6Z4J9	Late embryogenesis abundant protein, <i>Oryza sativa</i>	41.07	4.98	Desiccation tolerance	
Class 2: up-regulated proteins							
85	TC131046	P50299	S-adenosylmethionine synthetase 1, <i>Hordeum vulgare</i>	42.84	5.49	Primary metabolism	

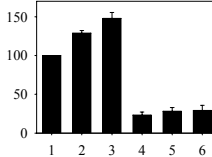
167	TC139656	Q8LQS5	Carboxymethylenebutenolidase-like protein, <i>Oryza sativa</i>	30.41	6.31	Redox regulation	
224	TC140370	O49866	Peroxidase, <i>Hordeum vulgare</i>	36.55	5.91	Redox regulation	
6	TC130772	Q9ZWJ2	Lactoylglutathione lyase, <i>Oryza sativa</i>	32.55	5.51	Redox regulation	
17	TC131931	Q7XJ02	Probable L-ascorbate peroxidase 7, <i>Oryza sativa</i>	38.32	8.76	Redox regulation	
121	TC139323	P93616	Poly(A)-binding protein, <i>Triticum aestivum</i>	70.82	6.60	Protein synthesis	
208	TC149802	Q02438	(1→3)-β-glucanase GV, <i>Hordeum vulgare</i>	34.41	6.91	Disease/defence	

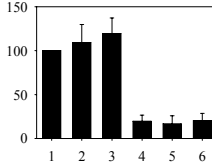
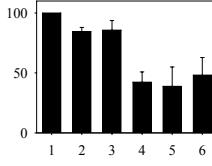
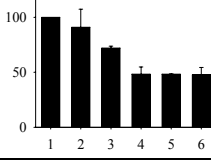
Class 3: down-regulated proteins

11	35_16328	Q8W0D1	Putative nuclear RNA binding protein A, <i>Oryza sativa</i>	40.42	6.37	Protein synthesis	
128	TC130772	Q9ZWJ2	Lactoylglutathione lyase, <i>Oryza sativa</i>	32.55	5.51	Redox regulation	
239	TC137024		Not found			Unknown	
22	TC138639	P32024	23 kDa jasmonate-induced protein, <i>Hordeum vulgare</i>	22.84	5.92	Disease/defence	
41	TC142112	Q9LU11	Iron-deficiency specific protein IDS3, <i>Hordeum vulgare</i>	37.85	5.81	Secondary metabolism	

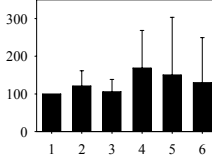
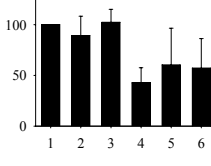
93	TC137786	Q40061	Iron-deficiency specific protein IDS2, <i>Hordeum vulgare</i>	37.57	5.17	Secondary metabolism	
189	TC133105	Q7Y248	Cytosolic 6-phosphogluconate dehydrogenase, <i>Oryza sativa</i>	51.58	6.58	Primary metabolism	
260	TC132873	Q84PW3	Putative monodehydroascorbate reductase, <i>Oryza sativa</i>	52.75	6.84	Redox regulation	
344	NP315772	Q9ZWH8	Probable nicotianamine synthase 7, <i>Hordeum vulgare</i>	35.24	5.10	Secondary metabolism	

Class 4: Proteins regulated in the salt tolerant cultivar

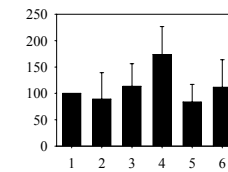
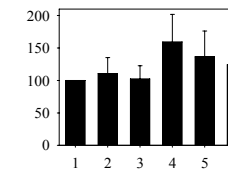
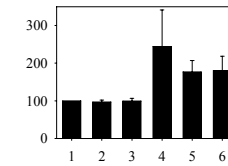
5	TC131931	Q7XJ02	Probable L-ascorbate peroxidase 7, <i>Oryza sativa</i>	38.32	8.76	Redox regulation	
---	----------	--------	--	-------	------	------------------	---

7	TC146774	Q8GTB8	Glutathione transferase F5, <i>Triticum aestivum</i>	23.43	5.78	Redox regulation	
62	TC146955	P29114	Lipoxygenase 1, <i>Hordeum vulgare</i>	96.39	5.73	Primary metabolism	
108	TC139384	Q9SI76	F23N19.10 stress-inducible protein, <i>Arabidopsis thaliana</i>	67.32	6.24	Disease/defence	

Class 5: Proteins regulated in the salt sensitive cultivar

31	TC147014	A2YQL4	Fructokinase 2, <i>Oryza sativa</i>	35.51	5.02	Primary metabolism	
66	CA023164	O24212	Osr40g2 protein, <i>Oryza sativa</i>	38.65	7.28	Disease/defence	

172	TC147167	Q9AYT7	Iron-deficiency induced protein IDI2, <i>Hordeum vulgare</i>	38.57	5.44	Protein synthesis
246	TC145151	Q93XJ5	Iron-deficiency induced protein IDI1, <i>Hordeum vulgare</i>	23.46	5.23	Secondary metabolism
271	TC139229	P55307	Catalase 1, <i>Hordeum vulgare</i>	56.58	6.68	Redox regulation



4.3.4. Identification of progeny lines showing a similar response towards salt stress at the seedling stage as the parent lines

The strategy to include progeny lines showing a similar response towards salt stress as the parental lines for limiting the number of candidate proteins conferring salt tolerance during germination was proven to be successful for the comparative proteome analysis of mature grains from the OWB and SM mapping populations. To apply this strategy for the investigation of salt tolerance at the seedling stage in the SM population, progeny lines were tested using the hydroponic system for long-term stress experiments. Recorded biometric data were root length, root fresh and dry weight, length of the second and third leaf as well as fresh and dry weight of the second and third leaf. Indicative for the differentiation between salt tolerant and salt sensitive genotypes was the development of the second and third leaf from plants treated with 100 and 150 mM NaCl. As expected, not all genotypes showed the same response toward stress application during germination and at seedling stage. From the four lines (DH14, DH93, DH80, DH187) that were used for the grain proteome analysis, only DH187 displayed a comparable reaction as the salt tolerant Morex parent and DH14 as the sensitive Steptoe parent (Figure 46).

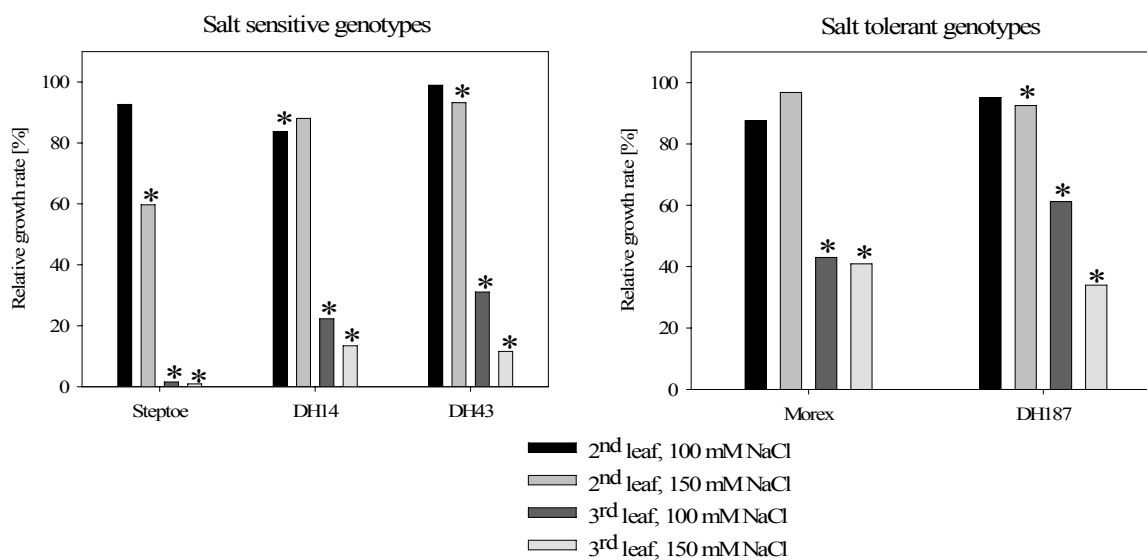


Figure 46: Effect of NaCl on the growth of seedlings from accessions with contrasting salt tolerance at the seedling stage. Growth measurements of the second and third leaf indicate the comparable performance of Steptoe, DH14 and DH43 as well as of Morex and DH187. The data shown represents the relative growth rate as compared to control plants of the respective genotype. Means of $n = 20$ plants per treatment were used for calculation. Statistical differences between treatments were analyzed following the Duncan multiple range tests (Duncan, 1955). Asterisks indicate significant differences at $p < 0.05$ as compared to control.

Additionally, a further progeny line DH43 was identified as salt sensitive at the seedling stage. The hydroponic stress experiments were performed in two independent experiments to confirm the results.

The growth reduction that was found for Steptoe of more than 95 % upon stress treatment with 150 mM NaCl was not found in the progeny lines tested. DH14 and DH43 exhibited a growth inhibition of about 85-90 % as compared to control plants of the same genotype and were therefore considered as salt sensitive genotypes. In contrast to this, the Morex parent displayed a growth reduction of the third leaf of 60 % after treatment with 150 mM NaCl. The line DH187 reacted in a similar way and growth inhibition was determined to be between 40 % at 100 mM NaCl and 70 % at 150 mM NaCl. Hence, this line was considered as salt tolerant genotype.

The identified lines are used in future hydroponic stress experiments for the comparative analysis of the root proteome in order to limit the number of candidate proteins as it was shown for the analysis of the proteome from mature grains.

4.3.5. Plasma membrane protein expression in roots of Steptoe and Morex subjected to salt stress

Roots control the ion uptake from soil as well as the transport within the plant and are exposed directly to salt. Especially proteins attached to or embedded in the lipid bilayer of plasma membranes (PMs) are known to act as sensors and facilitators of transport processes. However, the analysis of those proteins is hampered by their heterogeneous biochemical properties and low abundance. The method of choice for enrichment of PMs from various tissues is aqueous two-phase partitioning (Schindler et al., 2008). Here, membranes separate between two different polymer phases according to their surface properties. The lower phase contains dextran and becomes enriched with endomembranes, while in the upper phase PMs will accumulate due to the more hydrophobic PEG-phase (see Figure 9).

In order to investigate the PM proteome under salt stress conditions in the two barley cultivars with contrasting tolerance towards salinity treatment (Steptoe, Morex), a time-course experiment with hydroponic culture was conducted. Seven days after germination the NaCl concentration was increased in a stepwise manner (see Figure 39) up to 100 mM and 150 mM NaCl. Plants were harvested after 1, 3, 6 and 8 days of stress application. The samples were pooled resulting in one batch of control plants and one of stressed plants. The reason for pooling different time points was to increase the starting material needed for the two-phase

partitioning method and to detect proteins that might be differentially regulated at early or late time points at once. The time-course experiment was performed twice.

Enrichment of plasma membranes using two-phase partitioning method

The 2-phase partitioning method was optimised for barley root tissue. The resulting protein fractions were separated on SDS-PAGE and revealed distinct differences in protein patterns (Figure 47). The quality of PM preparation was verified using Western blotting for marker proteins in cytosolic, endomembrane and plasma membrane fractions.

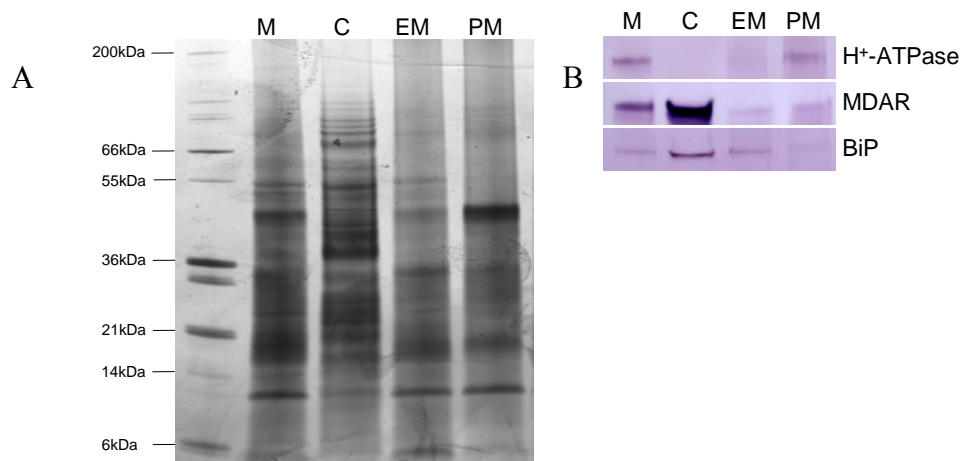


Figure 47: Protein patterns of 2-phase partitioning fractions and immunoblotting using marker proteins of Steptoe root sample. A: Five μg of protein from microsomal (M), cytosolic (C), endomembrane (EM) and plasma membrane (PM) fractions were separated on SDS-PAGE and visualized by silver staining. B: Western blot analysis with antisera against plasma membrane specific H^+ -ATPase, cytosol specific monodehydroascorbate reductase (MDAR) and endomembrane specific luminal binding protein (BiP) reveal an enrichment of H^+ -ATPase and a depletion of MDAR as well as BiP in the PM fraction.

Patterns of microsomal and endomembrane fraction were highly similar because the latter represents the vast majority of microsomal membrane proteins. The fraction of soluble cytosolic proteins was collected as supernatant after pelleting the microsomal fraction and the protein pattern differed from all other fractions. Furthermore, protein bands with differing intensity can be observed between endomembrane and PM fraction. Immunoblot analysis confirmed the enrichment of plasma membrane H^+ -ATPase in the upper phase as compared to the lower endomembrane phase. The soluble protein monodehydroascorbate reductase (MDAR) was used as a marker for contaminations from cytosolic proteins. As expected, the strongest signal was detected in the cytosolic fraction, but traces were also present in endo- and PM fractions. This indicates only little contamination of the membrane fractions by soluble proteins. Luminal binding protein BiP was detected with the same intensity in the

endomembrane fraction as in the original microsomal fraction, but was barely detected in the plasma membrane fraction indicating a depletion in this fraction. Overall, the yield of PM protein was between 25-30 $\mu\text{g/g}$ root fresh weight.

Subsequent to 2-phase partitioning of plasma membranes, integral hydrophobic proteins were further enriched by reversed-phase chromatography. First, lipids were extracted from PM fraction by precipitation in chloroform/methanol mixture. After resolubilisation, samples were loaded on a column filled with C4-resin and proteins were stepwise eluted with different concentrations of 2-propanol. Eluates were separated by SDS-PAGE to verify the elution pattern (Figure 48). Abundance of H^+ -ATPase in the various eluates was confirmed using immunoblotting. This procedure resulted in a further enrichment for hydrophobic integral membrane proteins.

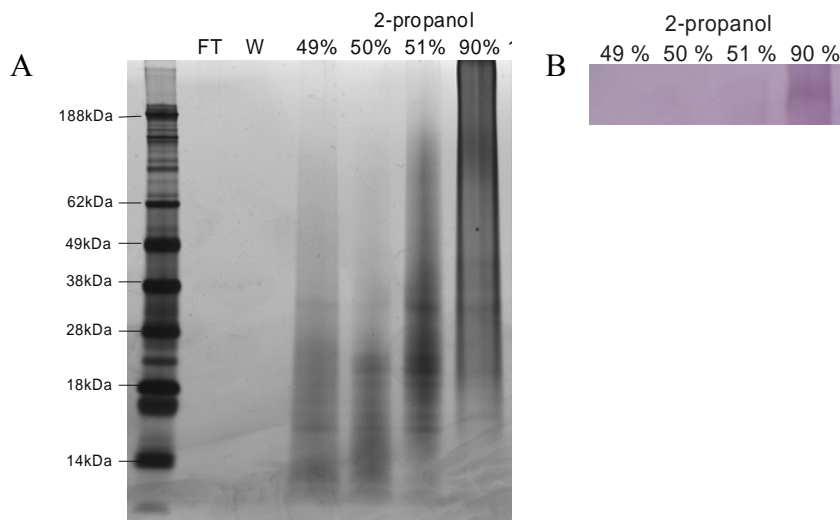


Figure 48: Elution profile of batch reversed-phase chromatography of root plasma membrane fraction from Steptoe cultivar and western blotting of fractions with antisera against H^+ -ATPase. A: Fractionation of proteins according to their hydrophobicity by reversed-phase chromatography. After sample application (flow-through, FT), the column was washed with 0.15 % TFA (W) and proteins were eluted using 49 %, 50 %, 51 % and 90 % 2-propanol. Two μg of protein were loaded on SDS-PAGE and proteins were visualized by silver staining. B: Western blotting of fractions eluted by 49 %, 50 %, 51 % and 90 % 2-propanol using antiserum against H^+ -ATPase on 4 μg of protein separated by SDS-PAGE confirmed that the highest concentration of H^+ -ATPase was in the 90% 2-propanol fraction.

Identification of plasma membrane proteins by LC-based mass spectrometry

The standard method for separation and quantification of proteins is 2-D gel electrophoresis. Following this approach, proteins are separated by isoelectric point and subsequently by

molecular weight. However, solubility of proteins at the isoelectric point is lowest and this would cause the precipitation of highly hydrophobic integral PM proteins. Therefore, relative quantification and identification of differentially expressed proteins in the comparative analysis of root plasma membrane proteins was performed using label-free LC-based separation method (LC-MS^E). Here, the protein sample is completely digested with trypsin and the resulting tryptic peptides are separated via liquid chromatography (LC). An electrospray-ionisation mass spectrometer (ESI-MS) is coupled to the LC detecting the peptide (so-called precursor) in MS mode and carrying out the collision-induced dissociation of all precursors for *de novo* sequencing and subsequent homology-based database search (Figure 49).

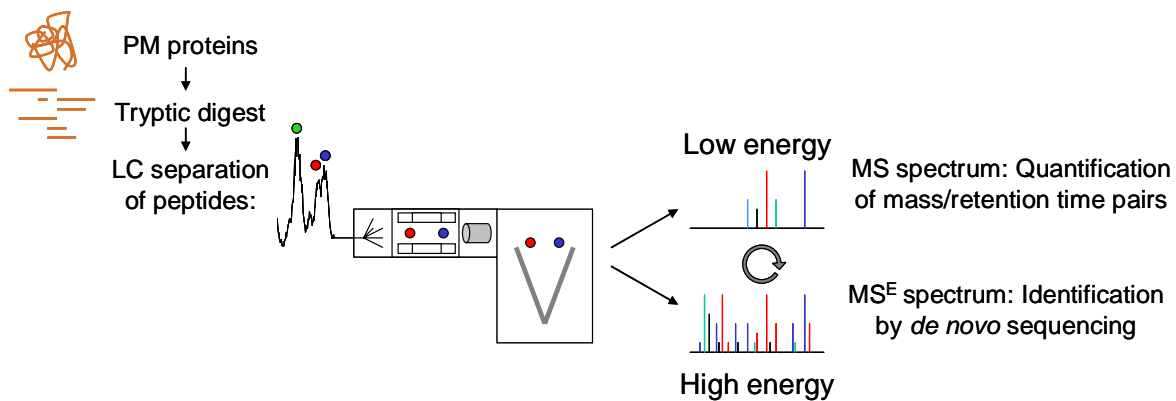


Figure 49: Principles of the LC-MS-based method for quantitation and identification of plasma membrane proteins. Fractions of plasma membrane proteins are digested with trypsin and the resulting peptides are separated via liquid chromatography. MS data are collected in an alternating low energy (MS) and elevated energy (MS^E) mode of acquisition. In the MS^E mode all ions are selected and fragmented in parallel. The produced fragment ions from any given precursor will have the same chromatographic profile and retention time as the originated precursor ion and for that reason, the signal intensity of a peptide can be related to the respective amino acid sequence. The intensity of peptides are compared to determine their relative abundance. The diagram is modified after L. Pollack, Waters.

The method is based on the assumption that changes in the peptide signal from each exact mass and retention time (EMRT) pair in LC-MS/MS experiments directly reflects their concentration in the sample (Silva et al., 2005) (Figure 50).

Plasma membrane proteins from roots of control and salt stressed plants from the genotypes Steptoe and Morex were tryptically digested and the resulting complex peptide mixture was analysed by LC-MS^E. Each sample was injected three times and LC chromatograms were consistent over all injections of the same sample (Figure 51). To assess the reproducibility of intensity measurements, binary comparisons of the intensity of peptide precursors of two

injections were used (Figure 52). Plotting resulted in a diagonal line with only little variation throughout the detected range and this quality control was applied for all samples and injections. The LC-MS^E data from each run were processed using the Protein Expression software (Waters) to produce EMRT cluster and to determine the relative abundance of peptides and proteins across genotypes and treatments.

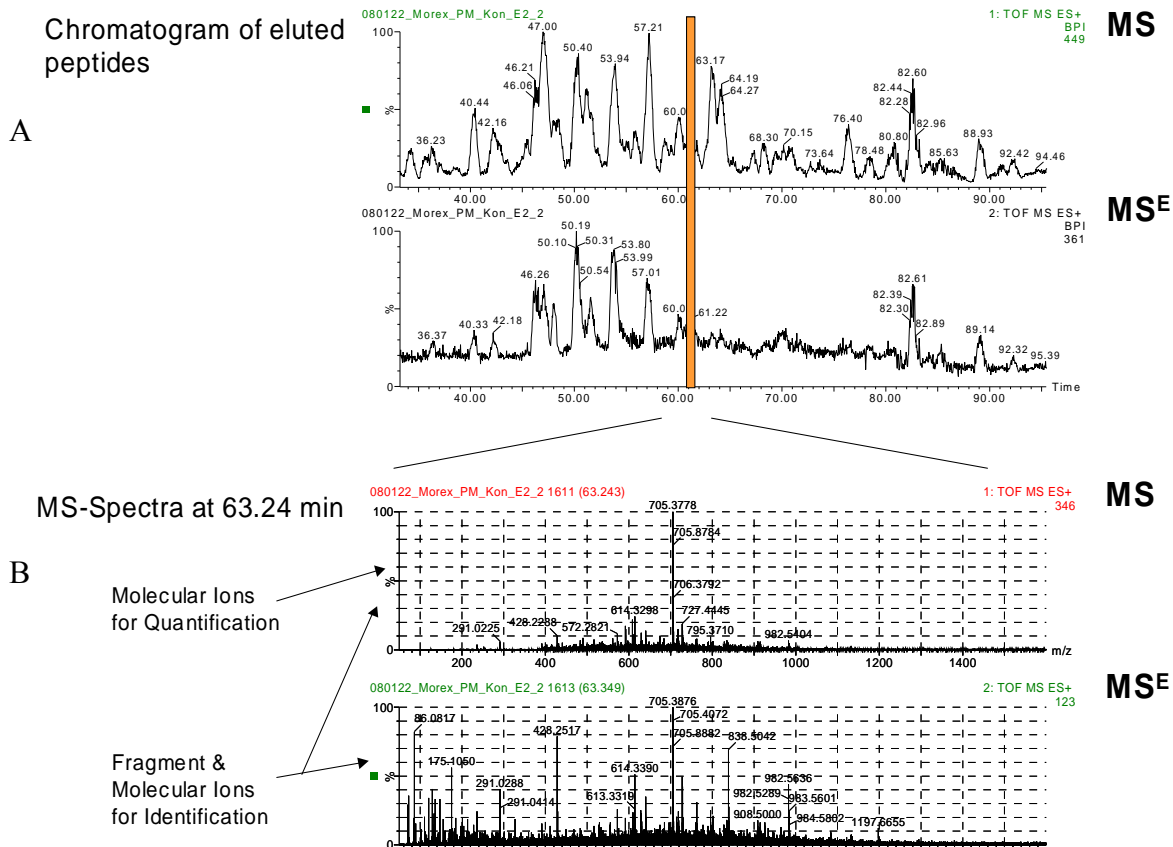


Figure 50: The base peak intensity chromatogram of an LC-MS^E experiment contains a low energy function (MS) for the intact peptides (upper row) and an elevated function (MS^E) for the associated fragment ions (lower row) (A). MS spectra for both functions are acquired at any given retention time point. Shown in the figure are the mass spectra for MS and MS^E at the retention time 63.24 min (B). The intensity of the precursor ion in the MS spectrum is used for the quantification of the respective peptide and the fragment ions derived from the precursor in the MS^E spectrum are used for the identification of the peptide.

Prior to the comparative analysis of control and stressed samples from both genotypes, the capacity of the LC-MS^E approach to analyse a proteome complement was evaluated. To determine, how many proteins could be identified from a total digest of root PM proteins from both barley genotypes, a database search was performed using the SwissProt *Viridiplantae* and TrEMBL *Poales* protein index for control samples from two independent experiments.

Replica filter were applied to reduce the number of false-positive protein identifications, which is an issue in LC-MS^E experiments. Only proteins identified on the basis of two independent peptides as well as in 2 out of 3 injections were considered for further analysis. In total, 159 proteins were identified from root plasma membrane samples of Steptoe and Morex; the complete list of proteins is provided in the appendix (Table A4). No protein was detected in only one genotype meaning that all proteins were detected in Morex and in Steptoe PM samples.

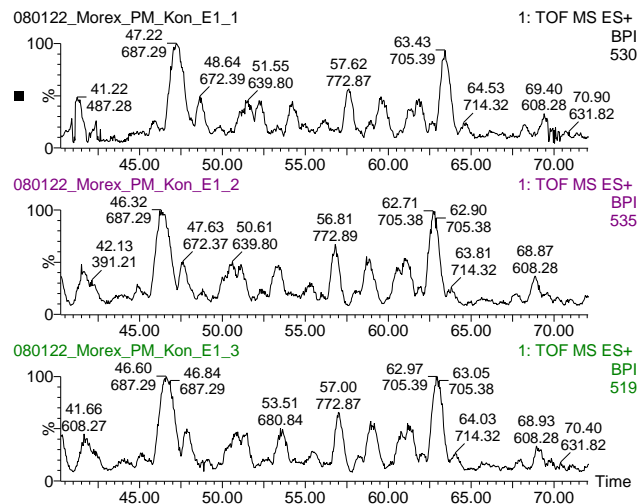


Figure 51: Chromatogram of LC-separated peptide mixture from Morex PMs in triplicate. The close-up view at the base peak intensity chromatogram displays a high degree of similarity across single injections from one sample.

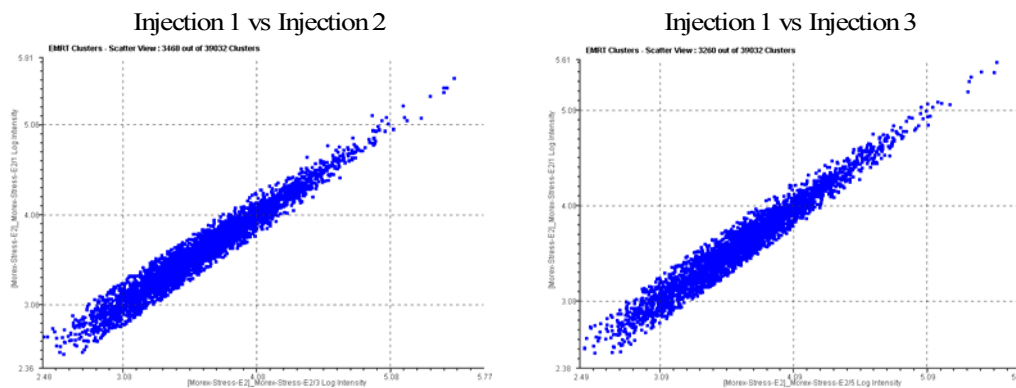


Figure 52: Log intensity of EMRT clusters for injection 1 vs. injection 2 (left-hand side) and for injection 1 vs. injection 3 (right-hand side) of Morex plasma membrane sample. Only little variation in intensity between runs was noticed.

One or more transmembrane domains (TMD) were predicted for 88 (56 %) of these proteins using the online tools DAS (<http://www.sbc.su.se/~miklos/DAS/>) and TMPred (http://www.ch.embnet.org/software/TMPRED_form.html). Allocation to subcellular compartments was achieved using WoLF PSORT (<http://wolfsort.org/>) and revealed 39

proteins (25 %) assigned to the PM. The remaining proteins were assigned to the cytosol (83, 53 %), mitochondria (15, 9 %), vacuole (16, 10 %), Golgi complex (2, 1 %), nucleus (2, 1 %) and endoplasmatic reticulum (1, 1 %) (Figure 53).

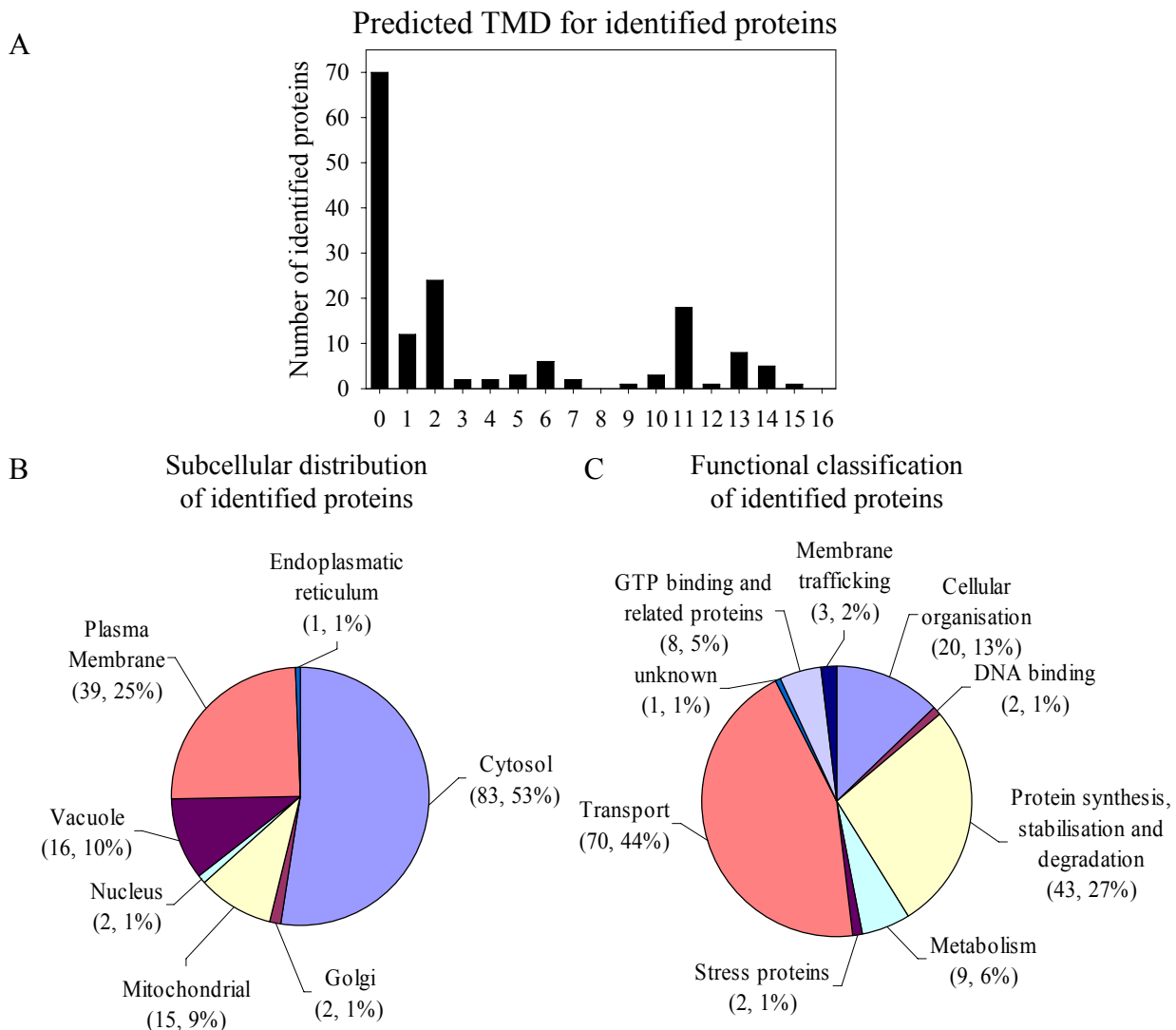


Figure 53: Comparison of predicted TMD (A), subcellular distribution (B) and functional classification (C) of identified proteins from barley root plasma membranes.

The identified proteins were grouped according to their functional annotation into nine classes. The largest group was assigned to transport processes. Among them were proteins involved in proton transport (ATPase, ATP synthase), water transport (aquaporins), ADP/ATP translocation (ADP/ATP carrier protein) or hexose transport (glucose-6-phosphate translocator). Proteins in the second largest group play a role in protein synthesis (elongation factor, initiation factors, ribosomal proteins), stabilisation (heat shock proteins) and degradation (ubiquitin). Several proteins were identified that are structural proteins, such as

tubulin and actin isoforms. Furthermore, proteins were identified involved in cell signalling by GTP binding (Ras-related proteins) and in membrane trafficking (ADP-ribosylation factors). Some proteins could be considered as contaminants as they function in metabolic pathways and have no described interaction with the plasma membrane (aspartate aminotransferase, glyceraldehyde-3-phosphate dehydrogenase). This was the case for only 6 % of all identified proteins.

Comparative analysis of the plasma membrane proteome of Steptoe and Morex roots under salt stress conditions

Subsequently to the evaluation of the plasma membrane proteome from control samples of Steptoe and Morex, a comparative analysis of both genotypes under control and stress conditions was initiated. As quality and outlier control, PCA was performed on triplicate LC runs of control and stress treated samples of both genotypes from two independent experiments. The intensity data from EMRT clusters was extracted from the Expression software (Waters) and loaded into CSVed 1.4.4 (<http://csved.sjfranke.nl/index.html>) for editing. In order to reduce the number of missing values, 5,000 EMRT clusters with highest intensity were further processed. Missing values that were still present were replaced by the number of 1 and the data set was lg transformed. PCA was performed using R software (www.R-project.org). The PCA scores plot showed a tight clustering of biological and technical replicates of all samples and a clear separation of LC runs in groups of genotypes and treatments was observed (Figure 54). The result of PCA indicated high sample reproducibility and therefore, the data set was further analyzed for differentially expressed peptides.

For the comparative analysis proteins replica filter and P-value filter were applied in order to reduce the number of false-positives and detect significantly regulated peptides and proteins. Furthermore, differentially expressed proteins had to be detected in both biological experiments with the same regulation pattern.

In the comparative analysis, the intensity signals of the precursor ions are compared based on the log ratio. The probability of regulation is given by the Expression software as P-value. The P-value is ranging between 0 and 1; 0 means that there is a 100 % probability of down regulation, 1 means that there is a 100 % of up regulation and 0.5 represents no significant change in expression. Only peptides were used for further evaluation detected in 2 out of 3 injections and regulated with a probability of up regulation with $P > 0.95$ or down regulation

with $P < 0.05$. Overall, between 35,000 and 40,000 peptide clusters were replicated across the 2/3 runs per sample, but only a small fraction of these clusters were assigned to a database entry using the *Viridiplantae* database from Swiss-Prot and the *Poales* database from TrEMBL. Between 2,000 and 2,600 regulated peptides were identified and out of these, about 100 peptides were replicated in two independent biological experiments under control or under stress conditions, respectively.

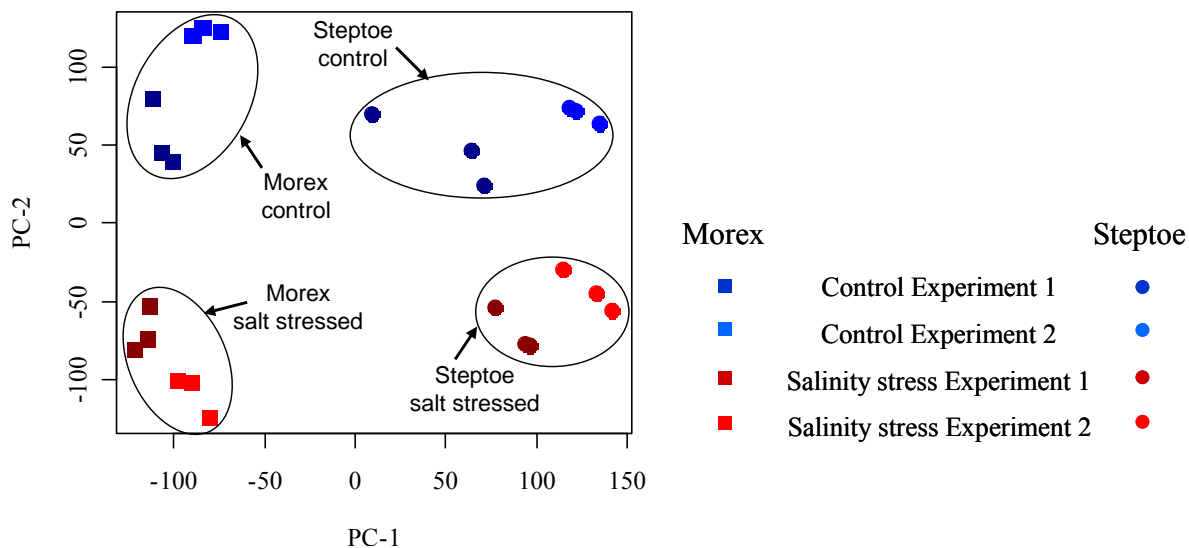


Figure 54: PCA for the assessment of technical and biological variation in peptide profiles (Dr Marc Strickert, Data Inspection group, IPK). Plasma membrane proteins from plants grown under control and salt stress conditions in two independent biological experiments were digested with trypsin. The resulting peptide mixture was analyzed in triplicates by LC-based label-free mass spectrometry. The first two principle components accounted for the highest variation in the data set and a clustering into genotypes (Steptoe and Morex) and treatments (control and salinity stress) was observed.

Following the workflow for data processing that is given by the Expression software, two lists are generated for each comparison. A schematic diagram of the workflow is depicted in Figure 55. The first generated list is the protein list. For all peptides that could be assigned to a single protein identifier, the mean of the average intensity ratio of each peptide was determined. The ratio was also affected by the probability score of an individual peptide. Taking this into account, the protein was accepted when it passed the P-value filter. Because mean values are considered, it is possible that the expression change of single peptides varies or that single peptides have a contrasting expression as compared to the remaining peptides. This is taken into account in the second generated list, the peptide list. This list is based on the expression change of each single EMRT cluster, which equals to one peptide, detected in the analysis and is called peptide list. Here, each single peptide has to pass the filter criteria and

has to reveal the same regulation in the two biological repetitions. Subsequently, peptides leading to the same protein identifier were grouped. Only proteins identified with at least two independent peptides were accepted. The protein list and the peptide list are generated using different algorithms and should be considered as complementary to each other. The protein identifiers are summarized in Table 7, for the protein list and the peptide list separately. Additional information, such as the respective average intensity ratios of all peptides and proteins, the identification score as well as the P-values, are provided in the Appendix (Table A5 and A6).

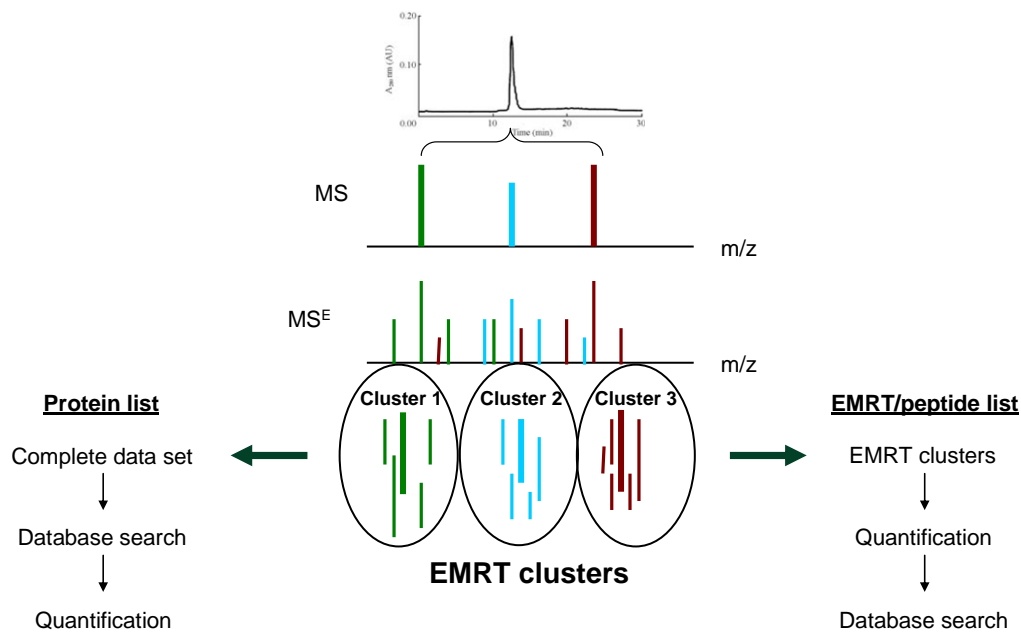


Figure 55: Schematic diagram of data preparation by the ProteinLynx Global Server software (Waters). Eluted peptides were analyzed using low energy mode (MS) and high energy mode (MS^E). Precursor ion and the respective fragment ions of the same eluted peptide form one EMRT cluster. Applying the protein route, all EMRT clusters were subjected to database search and the mean value of the expression change of all peptides that could be assigned to one protein is used for the comparison. Contrary to this, in the EMRT or peptide list all clusters are quantified first and database search is performed for each EMRT cluster individually. The diagram is courtesy of S. Kaspar, IPK.

When salt stress-responsive proteins were analysed for each genotype, it was noticed that a smaller number of proteins was differentially expressed after stress treatment in Morex than compared to Steptoe. In the salt tolerant line Morex only 5 proteins and 101 peptides were regulated upon stress treatment. Proteins induced upon treatment were ATP synthase subunit alpha and beta, pyrophosphatase, NAR2 and ADP/ATP carrier protein. Among the down regulated proteins upon stress treatment were several aquaporin isoforms, such as PIP1, PIP2 and PM intrinsic protein, and IDS3. Interestingly, IDS3 was also detected as down-regulated

in both genotypes in the comparative analysis of the root proteome. In the PM fraction of the sensitive line Steptoe, 14 proteins and 118 peptides were found as differentially expressed. Proteins identified as higher expressed upon treatment were 5 different pyrophosphatases, plastid ATP/ADP transporter and others. Hypersensitive response protein, aquaporins and tubulin were identified as down-regulated after salinity treatment.

Table 7: Summary of the comparative proteome analysis of plasma membrane proteins from the salt tolerant barley line Morex and the salt sensitive line Steptoe under control and stress conditions. Given in the protein list are accession and protein name as well as the relative ratio. When the protein was detected in only one group, no ratio can be given. Indicated in the peptide list are the protein name, the number of independent peptides detected in the analysis and the change in abundance. The score for protein and peptide identification and the P-values are provided in the Appendix (Tables A5 and A6).

Protein list:

Morex		Ratio Stress:Control	
Accession	Protein name	Experiment 1	Experiment 2
<i>Up-regulated under salt stress:</i>			
Q01859	ATP synthase subunit beta mitochondrial precursor, <i>O. sativa</i>	1.06	1.11
<i>Down-regulated under salt stress:</i>			
P24459	ATP synthase subunit alpha mitochondrial, <i>P. vulgaris</i>	0.74	0.27
P62787	Histone H4, <i>Z. mays</i>	0.46	Control
Q4LDT4	PIP aquaporin isoform, <i>H. vulgare</i>	0.90	0.36
Q5PSM6	Plasma membrane H ⁺ -ATPase, <i>T. aestivum</i>	0.92	0.27
Steptoe		Ratio Stress:Control	
Accession	Protein name	Experiment 1	Experiment 2
<i>Up-regulated under salt stress:</i>			
Q7XAC0	H ⁺ -pyrophosphatase, <i>O. sativa</i>	1.28	1.97
P12862	ATP synthase subunit alpha mitochondrial, <i>T. aestivum</i>	1.92	1.46
Q06572	Pyrophosphate energized vacuolar membrane proton pump, <i>H. vulgare</i>	1.34	1.92
Q6YZC3	Glucose-6-phosphate/phosphate translocator, <i>O. sativa</i>	1.25	1.9
P43281	S-adenosylmethionine synthetase 2, <i>S. lycopersicum</i>	Stress	1.9
O80384	Ovp1 pyrophosphatase, <i>O. sativa</i>	1.27	2.01
Q704F4	Proton translocating pyrophosphatase, <i>O. sativa</i>	1.27	2.12
Q6H883	Putative inorganic diphosphatase, <i>O. sativa</i>	1.28	1.93
Q9FS12	Vacuolar proton-inorganic pyrophosphatase, <i>H. vulgare</i>	1.31	1.92
<i>Down-regulated under salt stress:</i>			
P83970	Plasma membrane ATPase, <i>T. aestivum</i>	0.7	0.44
Q08IH3	Aquaporin, <i>H. vulgare</i>	0.52	0.82
Q84L97	Proton-exporting ATPase (Fragment), <i>Z. mays</i>	0.47	0.54
Q43271	H ⁺ -transporting ATPase, <i>Z. mays</i>	0.51	0.31

A5HE90	Hypersensitive response protein, <i>T. aestivum</i>	Control	Control
--------	---	---------	---------

Peptide list:

Morex				
Accession	Protein name	Number of peptides	Average ratio Stress:Control	
			Experiment 1	Experiment 2
<i>Up-regulated under salt stress:</i>				
P31167	ADP/ATP carrier protein 1 mitochondrial precursor, <i>A. thaliana</i>	12	3.18	3.15
P28734	Aspartate aminotransferase cytoplasmic, <i>D. carota</i>	5	1.5	1.26
Q06735	ATP synthase subunit alpha mitochondrial, <i>B. vulgaris</i>	12	Stress	Stress
Q01859	ATP synthase subunit beta mitochondrial precursor, <i>O. sativa</i>	18	Stress	Stress
P25861	Glyceraldehyde-3-phosphate dehydrogenase cytosolic, <i>A. majus</i>	7	3.11	5.7
P26413	Heat shock 70 kDa protein, <i>G. max</i>	5	2.40	1.54
Q6X677	NAR2, <i>H. vulgare</i>	2	1.48	2.56
P31414	Pyrophosphate energized vacuolar membrane proton pump, <i>A. thaliana</i>	5	Stress	2.86
P50299	S-adenosylmethionine synthetase, <i>H. vulgare</i>	3	3.675	Stress
Q7Y070	Vacuolar proton inorganic pyrophosphatase, <i>T. aestivum</i>	4	1.64	1.79
<i>Down-regulated under salt stress:</i>				
Q0J4P2	Heat shock protein 81 kDa, <i>O. sativa</i>	6	0.57	0.49
Q41811	Histone H4, <i>Z. mays</i>	7	0.43	0.20
Q9LU11	Iron-deficiency specific cDNA IDS3, <i>H. vulgare</i>	2	0.57	0.5
O48518	PIP1 protein, <i>H. vulgare</i>	6	0.69	0.46
O48517	PIP2 protein, <i>H. vulgare</i>	4	0.63	0.43
A7J2I1	Plasma membrane intrinsic protein, <i>T. aestivum</i>	3	0.52	0.58
Steptoe				
Accession	Protein name	Number of peptides	Average ratio Stress:Control	
			Experiment 1	Experiment 2
<i>Up-regulated under salt stress:</i>				
Q2TJ67	Plastid ATP/ADP transporter, <i>O. sativa</i>	3	Stress	2.76
<i>Down-regulated under salt stress:</i>				
P49690	60S ribosomal protein, <i>A. thaliana</i>	3	0.65	0.49
P53504	Actin, <i>S. bicolor</i>	8	Control	Control
P27080	ADP/ATP carrier protein, <i>C. reinhardtii</i>	5	0.67	Control
Q08IH3	Aquaporin, <i>H. vulgare</i>	8	0.34	0.6
A7J2I1	Plasma membrane intrinsic protein, <i>T. aestivum</i>	7	0.25	0.45

O48518	PIP1 protein, <i>H. vulgare</i>	2	0.265	Control
O48517	PIP2 protein, <i>H. vulgare</i>	4	0.30	0.56
P11143	Heat shock protein 70 kDa, <i>Z. mays</i>	4	0.59	0.57
Q69QQ6	Heat shock protein 81 kDa, <i>O. sativa</i>	3	0.54	0.57
A5HE90	Hypersensitive response protein, <i>T. aestivum</i>	4	0.25	0.41
P20649	Plasma membrane ATPase, <i>A. thaliana</i>	51	0.44	0.44
A3A343	Putative uncharacterized protein, <i>O. sativa</i> , Helicase C-related	2	0.57	0.54
P28188	Ras-related protein, <i>A. thaliana</i>	3	Control	Control
A4K4Y4	Tubulin alpha, <i>T. aestivum</i>	5	Control	Control
P12411	Tubulin beta, <i>A. thaliana</i>	6	0.39	0.52

The expression of a number of proteins was affected in both genotypes upon stress application, *e.g.* ATP synthase, aquaporins, S-adenosylmethionine synthetase and pyrophosphatase. Although the expression of numerous proteins was affected in both genotypes, there were also proteins identified revealing differential expressions in only one barley genotype. For example, the expression of a hypersensitive response protein was decreased only in Steptoe and NAR2, a protein involved in nitrate uptake, was higher expressed upon treatment exclusively in Morex.

5. Discussion

5.1. Detection of QTL for protein expression in mature grains of the Brenda x HS213 mapping population

Transcript or protein expression in a mapping population can be considered as a quantitative trait and its variation among members of a population is used to map the location of the gene or protein in the genome. In this respect, the genetic position of the gene or protein itself can be mapped (*cis*QTL) or of genes or gene products regulated by a factor that controls the expression level at a position different from the genetic position of the QTL (*trans*QTL). In recent years the ‘Genetical Genomics’ concept was successfully applied for QTL analysis of gene expression (eQTL), either for genome-wide expression analysis (Keurentjes et al., 2007; West et al., 2007) or for the analysis of agronomic traits (Shi et al., 2007). But to this moment, QTL analysis for protein expression (pQTL) did not receive the same attention although proteins are the major determinants for yield quality in crop plants. Especially proteins in barley grains are of economic importance as they define the nutritional quality of the cereal for livestock as well as the malting quality for industrial processes.

The aim of the investigation of the proteome of mature barley kernels was the molecular characterization of ILs through proteome profiling. In previous experiments, this population was used for QTL analysis of agronomic parameters and a number of QTL for yield, yield components and malting quality were detected (Li et al., 2005). Therefore this population seemed highly suited for further in-depth QTL analysis on the transcriptome and proteome level. In parallel to the proteome profiling of the grains, the doubled-haploid Brenda x HS213 mapping population was analysed for eQTL in developing grains. The resulting eQTL should then be aligned with pQTL representing the final stage of protein expression in mature grains. But in the course of the experiments, both approaches had to cope with a number of constraints, such as the limited sample size of only 2-3 plants per line, the relatively small population size and the low number of molecular markers that left intervals of QTL at a considerable width. Also the population was unbalanced, meaning that a small number of lines contained the majority of introgressions (Dr Christof Pietsch, personal communication). Furthermore the growth conditions in the first experimental set were biased, which led to strong environmental influences on the samples. But despite these caveats, it was possible to detect QTL for 67 proteins from the second experiment, which was more homogenous in growing conditions. Also, a number of pQTL could be replicated in both sets and this clearly

points towards a good reproducibility of 2-D gels, as it was shown in the cluster analysis of the 2-D gel protein patterns.

Among the proteins, for which QTL signals were detected, are interesting candidates for the construction of near-isogenic lines for fine mapping of the respective QTL locus. Two distinct pQTL for beta-amylase on chromosomes 2H and 6H were identified. Beta-amylase catalyses the degradation of starch during germination and therefore it is important for malting quality. Also, pQTL for several heat shock proteins and late embryogenesis abundant proteins were found. These proteins are known for their role in protein folding and stability during grain desiccation and other stresses. Hence, a better understanding of their functionality could confer stress resistance and increase the germination rate.

Although it was one of the major aims of the GABI-SEED II project, the association of eQTL data with pQTL data posed several issues. For the eQTL analysis, 12k-grain array data hybridised with samples taken at four developmental stages (4, 8, 16, 25 days after fertilization) of grain development (Sreenivasulu et al., 2006) resulted in 47,144 and 43,405 gene expression phenotypes. The subsequent eQTL analysis revealed 7,059 eQTL detected in the first experiment and 3,014 eQTL in the second experiment; recovered in both experiments on the same chromosome were 179 QTL (Dr Christof Pietsch, Gene and Genome Mapping group, IPK; unpublished data). It is clear that far more QTL can be detected on the transcript level than on the protein level due to the higher number of phenotypes detected with the different methods. But the detection of posttranslational modifications in the proteome analysis represents additional information that cannot be gained with transcriptome analysis. However, this was also the point where it became difficult to merge data from eQTL and pQTL analysis. In order to classify the detected eQTL and pQTL according to their molecular function, gene ontology terms were used to map the respective genes and proteins onto pathways. So far, no correlation was found indicating the complementary nature of both data sets. This has already been shown by Stylianou et al. (2008). Data obtained by microarray analysis, single nucleotide polymorphism analysis and proteome analysis, were incorporated in QTL analysis of inbred mouse strains. As a result, some candidates were identified by all three methods, but each approach yielded unique candidates not detected with the other methods. Therefore, authors suggested that QTL candidate genes should be assessed for changes both on transcript and protein levels.

5.2. Proteome analysis of mature grains from contrasting genotypes reveals candidate proteins conferring salt tolerance during germination

The mature barley grain is of high importance in feed and malting processes, and proteins present in the grain also determine the plant's performance during germination and affect the final crop productivity. In that context, mapping populations represent a valuable resource of germplasm that can be exploited in the search of genes and proteins conferring tolerance to biotic and abiotic stresses. In mapping populations, a high degree of natural variation for a certain trait is often found, especially when both parents show a contrasting phenotype for the respective trait. At the IPK Genebank about 21,000 barley accessions are stored and, in order to utilize these resources for the improvement of crop performance under unfavourable environmental conditions, these accessions are tested under various stress conditions.

5.2.1. Candidate proteins retrieved in the Oregon Wolfe Barley population

Barley accessions from the OWB mapping population exhibit a contrasting response towards salinity stress during germination. In a comparative proteome analysis of mature grains from these genotypes 6 protein spots were identified differing in abundance between salt tolerant and salt sensitive genotypes.

In germination assays it could be shown that the parent lines of the OWB population, DOM and REC, display a contrasting response for salinity at the germination stage (Weidner et al., 2005). Therefore, mature grains were chosen for a comparative proteome approach aiming at the identification of proteins conferring salt tolerance during germination. A comparison of the protein patterns of the parent lines DOM and REC revealed a high number of spots differentially expressed in the grain. To limit the number of candidate proteins and to take advantage of the huge genetic resource that mapping populations represent, 4 additional lines were added to the comparison showing an even stronger trait for salt response as the parent lines. In the comparative proteome analysis including all 6 lines, only 11 spots showed differential expression between groups of salt tolerant and salt sensitive lines. The reason for this reduction is the large heterogeneity of the spot patterns due to genotype-specific protein spots. By excluding these spots, presumably contributing to morphological or other characteristics, and by comparing only spots that were common to all lines, the number of candidate spots was limited to a feasible size with the protein identification successful for 6 spots (Table 8).

Table 8: Summary of identified proteins from the comparative analysis of mature grains from accessions of the OWB population showing contrasting response towards salinity at the germination.

Spot number	Protein name	Expression in salt tolerant genotypes
3	Cytosolic 6-phosphogluconate dehydrogenase	↑
6	Glucose and ribitol dehydrogenase homolog	↑
7	Putative elongation factor β	↓
8	Hsp 70	↓
9	Glucose and ribitol dehydrogenase homolog	↑
10	Translationally-controlled tumor protein homolog	↓

Among these identified protein spots, spot # 3 showed a higher abundance in salt tolerant lines and was identified as cytosolic 6-phosphogluconate dehydrogenase (6PGDH). This enzyme plays a key role in the pentose phosphate pathway, which provides reduced nicotinamide adenine dinucleotide phosphate (NADPH) for metabolic and detoxification reactions (Figure 56).

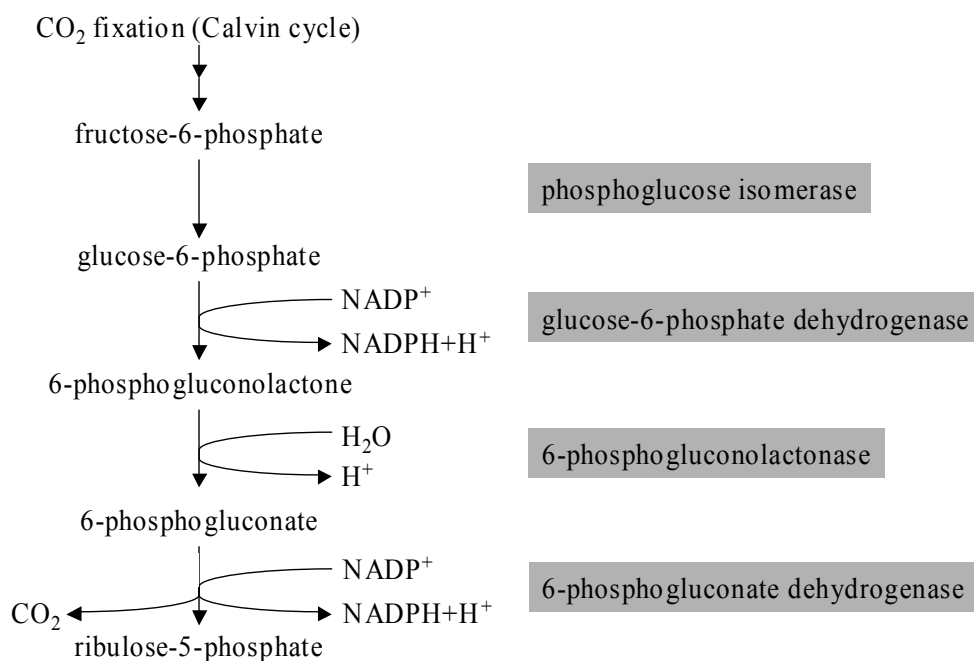


Figure 56: Schematic diagram of the oxidative pentose phosphate pathway. While CO₂ fixation takes place in the reductive pentose phosphate pathway, the oxidative pentose phosphate pathway yields in the oxidation of a hexosephosphate to a pentosephosphate under the release of CO₂. The significance of this pathway is the production of NADPH.

NADPH is a reducing equivalent necessary as electron donor in reductive biosynthetic reactions like synthesis of lipids, aromatic amino acids and coenzymes. It is also essential in the ascorbate-glutathione cycle, which is an important antioxidant protection system (Corpas et al., 1998). Recent studies confirmed the relation between oxidative stress upon salt treatment and enhanced expression of NADPH-dependent dehydrogenases. Olive plants were subjected to salt stress and consequently, the protein content and activity of glucose-6-phosphate dehydrogenase, isocitrate dehydrogenase and malic enzyme, all NADPH-recycling enzymes, increased significantly (Valderrama et al., 2006). In shoots of salt-treated rice plants, transcripts of 6PGDH were up regulated under stress conditions as early as 30 min after treatment (Huang et al., 2003). The accumulation of 6PGDH in grains of salt-tolerant barley lines could therefore indicate an enhanced pentose phosphate pathway and a better supply with NADPH leading to an accelerated germination under stress conditions. Furthermore, the protein could function as protection against oxidative damage caused by salinity.

Two spots (# 6 and 9) were identified as glucose and ribitol dehydrogenase homolog (GlucDH) that were more abundant in salt tolerant lines. The sequence of the identified protein shared similarities with glucose dehydrogenase and ribitol dehydrogenase from bacteria, which are structurally related and belong to the short alcohol dehydrogenases (Jornvall et al., 1984). Transcripts and protein of GlucDH were found exclusively in developing barley embryos and levels decreased during germination (Alexander et al., 1994). Enzymatic measurements revealed the restriction of dehydrogenase activity to the oxidation of D-glucose, but not sugar-phosphates, using NAD as co-substrate (Alexander et al., 1994). This points to a metabolic pathway not yet described in barley and could indicate a specific carbohydrate metabolism important for early embryo development. The higher abundance of GlucDH in grains of salt tolerant genotypes points to an enhanced carbohydrate metabolism. The identification of GlucDH in two distinct protein spots with different pI and molecular weight could result from posttranslational modifications or an additional isoform. In fact, the position of spot # 6 corresponds to the theoretical biochemical properties deduced from the amino acid sequence, whereas spot # 9 shows a lower molecular weight and a higher isoelectric point. Peptide mass fingerprinting and *de novo* sequencing did not reveal further insights into the structural integrity of the protein and it remains open whether a protein modification or an enzyme isoform is responsible for the multiple observation of this protein.

Spot # 7 was less abundant in salt tolerant lines and identification revealed a putative elongation factor 1 β (EF-1 β). This protein appeared as low temperature responding in cold-treated barley leaves (Baldi et al., 2001). Components of the protein translational apparatus, including EF-1 β , showed an accumulation at the transcript level in frost sensitive and resistant plants and authors concluded that the up regulation of translation machinery for synthesis of soluble proteins during cold acclimation is a general response reaction. The findings from the comparative proteome approach could indicate an enhanced synthesis of stress-related proteins in the sensitive accessions.

A translationally controlled tumor protein homolog (TCTP, spot # 10) was more abundant in salt-sensitive lines. TCTP is described as a calcium-binding protein abundant in various animal tumor cells and homologous proteins have been found in a wide range of organisms including human, mouse, yeast and plants. The expression of TCTP in *Pharbitis* was related to photoperiodism (Sage-Ono et al., 1998) and in soybean, transcripts accumulated after aluminum-induced stress (Ermolayev et al., 2003). The high level of conservation indicates an essential function, but at this stage it is difficult to suggest a possible function during salt-stress in susceptible plants.

Spot # 8 was exclusively found in salt-sensitive barley lines and identified as Hsp 70, a molecular chaperone that is highly conserved in plants. In *Arabidopsis*, at least 18 genes encoding members of a 70 kDa heat shock protein family are known with developmental and environmental regulated expression (Lin et al., 2001). Besides the known induction by heat and cold stresses, it plays also an important role in grain development and germination (Sung et al., 2001). During grain desiccation, proteins are unfolded or misfolded and Hsp 70 might be necessary to ensure proper protein aggregation in the ripening grain. The accumulation of Hsp 70 in the salt sensitive line is in contrast to the previous findings, but it could confer tolerance to other stress factors, like drought, which has not been tested yet.

The comparative proteome analysis with accessions from the OWB population was performed to identify proteins that might confer salt tolerance during germination. Two proteins were found higher expressed in salt tolerant lines as compared to salt sensitive accessions. These were 6PGDH and GlucDH and both were selected for stable transformation experiments to test the effect of constitutive and grain-specific overexpression in a salt sensitive barley cultivar (Golden Promise). Northern blot analysis of non-transgenic plants revealed a transcript accumulation of GlucDH in mature grains, but not in leaf tissue, whereas 6PGDH transcripts were detected in grains and leaves to a similar extent. This indicates the grain-

specificity for GlucDH, but not for 6PGDH. After screening the T0 generation of transgenic plants on the genome and transcriptome level, transgenic lines were selected for propagation. The T1 and T2 progeny will be used in prospective experiments to test the transgenic plants for their enhanced ability to germinate during salt stress application.

5.2.2. Candidate proteins detected in the Steptoe Morex population

In contrast to the OWB population, the SM population possesses a lower phenotypic diversity and the selection of parental lines was based on agricultural relevance. The population was developed to accumulate favorable economic traits and has been the subject for genome mapping and QTL analysis by the North American Barley Genome Mapping Project (Hayes et al., 1996).

For the analysis of the grain proteome of accessions from the SM population with contrasting response towards salinity stress, the same experimental set-up was chosen as it has been applied for the investigation of kernels from lines of the OWB population. Out of seven protein spots with differential abundance between salt tolerant (Morex, DH80, DH187) and salt sensitive lines (Steptoe, DH14, DH93), two and five protein spots were more and less abundant in genotypes showing a higher tolerance towards salt stress during germination, respectively (Table 9).

Table 9: Summary of identified proteins revealed by a comparative analysis of mature grains from accessions of the SM population that show contrasting response towards salinity during germination.

Spot number	Protein name	Expression in salt tolerant genotypes
1	Isocitrate dehydrogenase	↑
2	Lipoprotein-like protein	↓
3	Rab28 protein	↑
4	Embryo-specific protein	↓
5	1-Cys peroxiredoxin PER1	↓
6	Chitinase	↓
8	LEA protein	↓

Among the identified protein spots, two spots (lipoprotein like protein, spot # 2, embryo-specific protein, spot # 4) were detected with lower expression in salt tolerant lines. Although

their function is not yet described, both share the same conserved domain DUF1264. Some members of this family are annotated as putative lipoproteins that are posttranslationally modified by the attachment of lipids or fatty acids for cell membrane binding. Currently, there are 153 protein sequences sharing this conserved domain in the NCBI database from organisms like fungi (*Aspergillus niger*), bacteria (*Xanthomonas campestris*) and plants (*A. thaliana*, *O. sativa*), with some of them annotated as embryo-specific. But although this high level of conservation among prokaryotes and eukaryotes indicates essential function, further characterization is still absent. Therefore, it remains open what functions those proteins have under salinity stress in salt sensitive lines.

Spot # 8 was identified as LEA protein. In plant seed development, these unstructured proteins are highly abundant during the final stage of desiccation (Ingram and Bartels, 1996), but recently group 3 LEA proteins were also identified in invertebrates (Browne et al., 2002; Hand et al., 2007; Kikawada et al., 2006). Besides the general adjustment of metabolic processes as well as the osmotic and structural alteration throughout the final maturation stage, these proteins play an important role aiming at dehydration tolerance of the mature grain. LEA proteins are expressed at the onset of desiccation, presenting the majority of proteins in dehydrated tissues (Roberts et al., 1993) with the degradation occurring as soon as 12 h post imbibition (Bønsager et al., 2007). Because of their hydrophilic amino acid composition and high concentration in the cell, they are supposed to bind water in order to avoid total desiccation and stabilize proteins as well as the cell wall. In fact, Chakrabortee et al. (2007) could demonstrate the *in vivo* antiaggregant and osmoprotective role of overexpressed LEA protein from the nematode *Aphelenchus avenae* in human cell lines. Moons et al. (1995) showed the correlation of group 3 LEA protein accumulation with stress tolerance. Furthermore, overexpression of a barley group 3 LEA protein, HVA1, increased tolerance to water deficit and salt stress in T1 progeny of rice (Xu et al., 1996). But at the same time, the presence of other LEA is not correlated with stress tolerance (Still et al., 1994) or it was shown that they act together with sugars in order to contribute to tolerance (Blackman et al., 1991). The LEA protein detected in the analysis as differentially expressed between groups of salt tolerant and salt sensitive barley lines showed high sequence similarity with group 3 LEA proteins from wheat and rice. The lower protein expression in salt tolerant lines could indicate a protective role of this protein under other stress conditions during germination.

Spot # 5 was also less abundant in salt tolerant lines and mass spectrometry lead to the identification of 1-Cys peroxiredoxin PER1. Peroxiredoxins are considered as LEA proteins because they follow the same expression pattern resulting in high abundance at the stage of grain development followed by a strong decrease in expression during germination. PER1 was detected specifically in barley aleurone layer and embryo (Stacy et al., 1996; Stacy et al., 1999). In order to protect the grains from reactive oxygen species, which are produced in mitochondrial respiration processes during grain dormancy, 1-Cys peroxiredoxin dimers mediate the detoxification of peroxides like H_2O_2 (Figure 57).

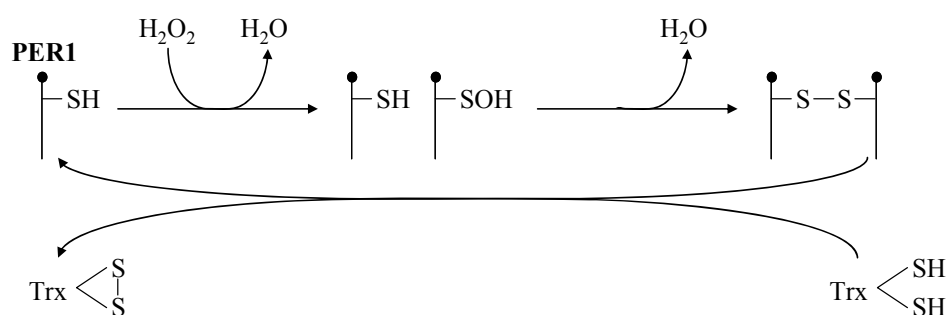


Figure 57: Peroxidase mechanism for 1-Cys peroxiredoxin PER1. H_2O_2 is detoxified by the oxidation of the PER1 cysteine residue and water is released after the formation of a disulfide bond with a second PER1. Regeneration of peroxiredoxins is mediated by the thioredoxin (Trx). The diagram is modified after Rouhier et al. (2002).

The reaction mechanism consists of three steps: oxidation of one conserved cysteine residue by a peroxide, formation of disulfide bonds with other thiols, thereby releasing a water molecule, and regeneration of ground state by dithiols (Dietz, 2003). The reduction of PER1 by thioredoxin in mature barley grains was shown recently (Maeda et al., 2004). Although the function of PER1 is clear, the role during dormancy is still questioned. The involvement in maintenance of dormancy was suggested (Stacy et al., 1996), but high expression level of *AtPER1* in a non-dormant mutant indicated that *AtPER1* alone was not sufficient to induce dormancy (Haslekas et al., 1998). Interestingly, it was shown that overexpression of *AtPER1* inhibits germination under abiotic stress conditions such as salt or osmotic treatments (Haslekas et al., 2003) and this finding would correlate with the result from the comparative proteome analysis. Here, the protein abundance of PER1 was higher in lines showing a reduced germination and seedling growth in salt stress experiments. These results can be explained by the fact that the *AtPER1* promoter contains an ABA-responsive element (Aalen, 1999). ABA concentration increases in response to salt stress or other unfavorable germination conditions and the induction of barley PER1 gene expression by ABA was

shown (Espelund et al., 1995). In order to prevent germination under stress conditions, PER1 could remove H₂O₂, which is known to trigger germination (Fontaine et al., 1994), resulting in a reduced germination frequency. In this context, PER1 seems to be involved in sensing environmental conditions and a higher protein expression in mature grains leads to an inhibition of germination under salt stress conditions. To test this hypothesis, stable transformation experiments in a salt sensitive barley cultivar with RNAi or anti-sense constructs for PER1 could be performed.

One protein spot that was more abundant in grains of salt tolerant lines was identified as Rab28 (spot # 3). This protein was initially isolated as an ABA-responsive gene in young embryos and vegetative tissue (Pla et al., 1991). In grains, Rab28 protein accumulates during late embryogenesis and in vegetative tissue, gene expression could be induced by dehydration stress (Niogret et al., 1996). The expression of Rab28 in maize can be regulated by ABA, but the homologous gene in Arabidopsis vegetative tissue cannot be induced by ABA or osmotic stress (Arenas-Mena et al., 1999). Germination tests with Arabidopsis, overexpressing *Atrab28*, gave evidence that the protein confers tolerance towards salt (LiCl, NaCl) and osmotic stress in grains, but also seedlings of transgenic lines were more tolerant toward Li⁺ and continued growing under stress conditions (Borrell et al., 2002). The promoter region of *Zmrab28* contains ABA-responsive elements (ABRE) and transcripts were localized in the nucleus of vascular cells (Niogret et al., 1996; Pla et al., 1991). Recently, two transcription factors were identified interacting as heterodimers with the ABRE and mediate *rab28* transcription through this element (Nieva et al., 2005). Protein localization in the cell nucleus points towards a regulative function in ribosome biogenesis or mRNA stability. The localization of Rab28 in developing tissues of mature grains indicates that Rab28 plays a role in late embryo differentiation processes and localization in vascular tissue could indicate a function in ion homeostasis. Although the exact role of Rab28 still has to be elucidated, it seems to be a promising candidate protein for conferring salt tolerance during germination in barley.

Proteome analysis revealed a higher accumulation of spot # 6 in salt sensitive genotypes and the spot was identified as chitinase. This protein is well known for its antifungal properties by hydrolyzing chitin, the major structural polysaccharid of fungal cell walls. The expression can be induced by various biotic and abiotic stress factors, e.g. pathogens, drought and salinity (Kasprzewska, 2003). Purified chitinase from barley grains was able to inhibit the growth of *Fusarium sporotrichioides*, barley seed rot, significantly (Leah et al., 1991). The chitinase

identified in the comparative proteome analysis showed a 95 % sequence similarity on the amino acid level with a class II endochitinase-antifreeze protein precursor accumulating in cold-acclimated winter rye leaves (Yeh et al., 2000). Antifreeze proteins adsorb onto the surface of intercellular ice crystals and block their further growth and apparently also chitinases have this functionality. The higher abundance of chitinase in grains of salt sensitive barley genotypes could indicate a better seedling growth under low or freezing temperatures. Whether these lines are in fact more frost resistant has not yet been tested, but would provide more information on an agronomic interesting trait.

A spot identified as cytosolic NADP-specific isocitrate dehydrogenase (NADP-ICDH, spot # 1) was higher abundant in salt tolerant lines. This enzyme catalyses the oxidative decarboxylation of isocitrate to 2-oxoglutarate and produces reduced NADPH. Activity of NADP-ICDH has been shown in the cytosol (Palomo et al., 1998), mitochondria (Macherel et al., 2007; Moller, 2001), chloroplasts (Galvez et al., 1994) and peroxisomes (Corpas et al., 1999). The role of NADP-ICDH in mitochondria and peroxisomes in the removal of reactive oxygen species (ROS) is well described (del Rio et al., 2002; Macherel et al., 2007; Moller, 2001). However, in the cytosol several functions of NADP-ICDH have been proposed. Besides the production of the reducing equivalent NADPH, it could also be involved in the amino acid synthesis (Figure 58). Following this hypothesis, citrate would leave the mitochondrial TCA cycle to be used for the production of isocitrate in the cytosol. 2-oxoglutarate would be imported into chloroplast via a specific transporter and enter the glutamine synthase/glutamate synthase pathway (Hodges et al., 2003).

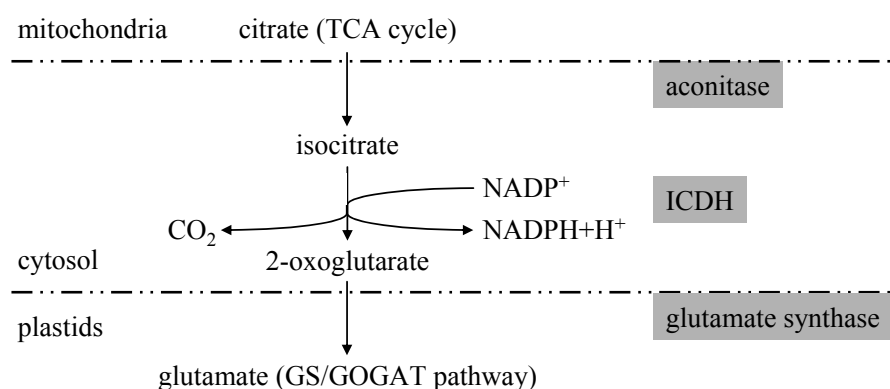


Figure 58: Schematic diagram for the function of ICDH in ammonium assimilation and the production of NADPH. Citrate is transported from the mitochondria to the cytosol via a di/tricarboxylate transporter (Picault et al., 2002) and metabolized to 2-oxoglutarate under catalytic activity of aconitase and ICDH. 2-oxoglutarate is imported into plastids by a 2-oxoglutarate/malate translocator (Weber and Flügge, 2002) and enters the glutamine synthase/glutamate synthase cycle. NADPH is used for plant responses to oxidative stress, such as ascorbate/glutathione cycle. The diagram is modified after Hodges et al. (2003).

In leaves of salt-stressed olive plants, NADP-ICDH as well as other NADP-generating dehydrogenases accumulated upon stress treatment (Valderrama et al., 2006). In *Mesembryanthemum crystallinum*, a facultative halophyte, transcript, protein and enzyme activity increased in leaves after salt stress treatment and authors suggested a function in ROS removal rather than in amino acid biosynthesis since no increase in protein abundance in the vascular tissue for long-distance transport of nitrogen compounds was detected (Popova et al., 2002). The possible role of NADP-ICDH in barley grains still has to be determined, but the higher abundance of NADP-ICDH in grains of salt tolerant genotypes could be responsible for a faster germination rate because of the better supply with nitrogen and NADPH as well as for an enhanced detoxification of ROS during germination.

In conclusion, investigations of the grain proteome from genotypes with contrasting salt tolerance from the OWB and SM mapping populations revealed proteins with differential expression. Proteins that were higher abundant in salt tolerant genotypes are putative candidates and could confer salt tolerance in seedlings. There was no overlap between the proteins differentially expressed in lines from the OWB population as compared to the SM population. But, since salt tolerance is a multigenic trait, that finding is not unexpected. Higher abundant in salt tolerant lines were 6PGDH, GluDH, NADP-ICDH and Rab28. In order to test their functionality, those proteins were selected for overexpression studies using a strong ubiquitous and an endosperm-specific promoter. At the moment, transgenic plants are in preparation and germination tests will be used to validate if the selected proteins confer salt tolerance in barley.

5.3. Hydroponic long-term salt stress experiments using the parent genotypes of the Steptoe Morex population confirm the results of the germination assay

The parent lines Steptoe and Morex were subjected to salt stress at the seedling stage in order to verify their contrasting salt response at this developmental stage. Although germination rate is a simple trait to score, it cannot be used to predict the plant's ability to grow and set grain under salt stress conditions. Therefore, long-term stress experiments were conducted. The NaCl concentration was increased in a step-wise manner and the stress was applied for a maximum of 12 days. The biometric data recorded from these experiments confirmed the findings from the germination assay. There was a growth inhibition in both cultivars, but only

the Morex genotype was able to develop the third leaf at the highest concentration of 250 mM NaCl. Also elongation of the second leaf was strongly inhibited in the sensitive cultivar Steptoe. A growth reduction was noticed for the root, but no cultivar-specific differences were detected. In contrast to the leaf tissue, where growth reduction of up to 90 % was noticed, the growth inhibition of roots was only between 40-50 % of dry weight.

The reduction of water uptake is an early effect of salinity and there are different mechanisms controlling growth at different periods of time for plants that are exposed to salinity. There are rapid changes in leaf and root growth within few minutes to hours after stress application, but this fast response is due to the changes in cell water relation and not to salt stress (Munns, 2002). Some days after the start of salt stress treatment, the leaf and root growth is stably reduced. Here, leaf elongation is more inhibited than root growth. This phenomenon also can be observed for plants subjected to water deficiency (Hsiao and Xu, 2000) and evidence indicate that ABA is mainly responsible for this reaction. The inhibition of ABA synthesis reduced root growth but promoted shoot growth of maize seedlings under low water potential (Saab et al., 1990). However, under normal conditions this reaction was not observed. Also it was shown that ABA is responsible for maintaining root growth but inhibiting shoot growth in maize under water deficiency (Sharp et al., 1994). The reason, why the growth reduction after short-term stress application is rather due to water deficiency stress than to salt stress is also supported by findings that the concentration of Na^+ and Cl^- in the rapid dividing and elongating cells of root and shoot is below toxic levels (Hu and Schmidhalter, 1998). The central role of ABA in mediating salt stress responses in Arabidopsis root was recently investigated on the cell-type-specific level (Dinnyeny et al., 2008). Transcriptome analysis showed the induction of ABA-responsive genes in all cell layers of the root upon salinity treatment, although cell-type-specific responses are noticed at the promoter level. Authors also could show that root epidermis was the most salt stress-responsive cell type indicating essential function in stress sensing and mediating.

Specific salt stress effects become apparent after the prolonged stress application of days to weeks when Na^+ and Cl^- accumulate in leaves to toxic levels. Then, the cell is not longer able to compartmentalize these ions in the vacuole resulting in elevated ion concentration in the cytoplasm inhibiting enzyme activity and in the cell wall dehydrating the cell (Flowers and Yeo, 1986). Subsequent phenotypic indications of salt toxicity are yellowing and death of older leaves.

The conducted salt stress experiments using the contrasting genotypes Steptoe and Morex aimed at the comparative analysis of stress reactions in both genotypes, but not in the analysis of senescence processes. For that reason, the plants were subjected to moderate, but long-term stress conditions where growth persisted and plants were harvested before any indications of leaf injuries were noticeable. Nevertheless, the final conclusion about salt tolerance or sensitivity can only be drawn when plants are stressed throughout the development and the decision is based on the yield. To complete the evaluation of both contrasting barley genotypes at all developmental stages, the reproductive development on saline soil should be analyzed.

As the contrasting response towards salinity stress could be confirmed at the seedling stage, both genotypes were further investigated on the proteome level. In order to identify proteins conferring salt tolerance, the root proteome of Steptoe and Morex was analyzed under control and under salinity stress conditions.

5.4. Root proteome analysis of the parent lines of the Steptoe Morex population after salt stress treatment reveals cultivar-specific protein expression

The analysis of salt stress mechanisms is not restricted to crop plants only. Numerous studies using the genetic model plant *A. thaliana* aimed at the dissection of salinity tolerance and revealed valuable information on the cellular and subcellular Na⁺ transport (reviewed in Moller and Tester, 2007). In crop plants, extensive efforts were made towards the generation of salt tolerant rice (*O. sativa*). Due to the enormous genetic and genomic information on rice, traditional breeding was almost completely replaced by generation of transgenics, large-scale transcript and protein profiling as well as QTL studies (reviewed in Sahi et al., 2006). Especially the improvements of proteomic technologies regarding protein separation and detection, but also mass spectrometry-based protein identification have facilitated the studies of plant responses to salinity stress (Parker et al., 2006; Qureshi et al., 2007). Recent efforts aimed at the analysis of the root proteome since roots are exposed directly to salt and control the ion uptake from the soil as well as the transport within the plant. Comparative proteome studies of salt-stressed roots from Arabidopsis and rice revealed new insight into salt stress responses (Chitteti and Peng, 2007; Jiang et al., 2007; Yan et al., 2005). For both model plants, Arabidopsis and rice, vast molecular genetic resources are available but nevertheless, most genotypes of these species are sensitive to moderate levels of salinity. In contrast to this,

barley is considered to be notably salt tolerant among the cereals and available accessions cover a wide range of responses towards salinity. Recently, several studies took advantage of this system to study large-scale gene expression in barley roots under salt stress (Ozturk et al., 2002; Ueda et al., 2006; Ueda et al., 2002; Walia et al., 2006).

In order to unravel gene function, the analysis of the proteome is targeted. For more than 20 years 2-dimensional gel electrophoresis has dominated the field because of its capability to simultaneously separate and quantify several hundreds of proteins species. For that reason, a proteome study using 2-D gel electrophoresis of barley root tissue from control and salt-treated samples of genotypes with contrasting salt response was initiated. The aim was to identify candidate proteins conferring salt tolerance and to understand the regulation of protein expression and protein function during salt stress. Due to the large data sets acquired from proteome analysis, quality and differential analysis of spot patterns are in the focus of many attempts to add statistical value to proteomic experiments. For a long time, only spot by spot analysis was performed by researches, disregarding dependencies in sample preparation, outlier control or false discovery rate. Now, explorative data analysis in multivariate approaches is supplemented to ease the interpretation of protein expression data, to find relationships in protein expression and finally, to limit the number of proteins for further validation (Chich et al., 2007; Dowsey et al., 2003; Gottlieb et al., 2004).

Therefore, two methods for differential analysis were applied for the analysis of the root proteome of Steptoe and Morex, including analysis of variance (ANOVA) and principle component analysis (PCA). ANOVA tests the significance of the differences in the mean of spot volumes between the groups under investigation. Usually a threshold of $p < 0.05$ is applied in ANOVA as a false discovery rate, meaning that up to 5 % of differentially expressed spots are identified by chance. PCA is an unsupervised technique used for transforming the data set of spot volumes into a new set of variables, the main components, which are then uncorrelated to one another and explain the greatest variance in the data set. The outcome of PCA will provide information about outliers in biological or technical replicates and classes of similar observations. Both methods were used as they are implemented in the SameSpots image analysis software (Nonlinear Dynamics).

PCA with protein spots that matched $p < 0.05$ revealed a strong separation between the Steptoe and Morex genotype in all three experiments and grouping according to the treatments was also clearly visible. Proteins spots accounting for the grouping and that were replicated in three independent experiments were selected for MS-based identification.

Overall, 28 proteins were identified showing a cultivar-specific or salt stress-responsive expression in the salt tolerant Morex and salt sensitive Steptoe genotype. These proteins are summarized in Table 10.

Table 10: Differentially expressed protein spots in roots of barley cv. Morex and cv. Steptoe under control conditions and upon salinity treatment. The functional category for each protein is given as well as the abundance as more (↑), less (↓) or unchanged (-).

Spot number	Description	Functional category	Expression under salt stress conditions	
			Morex	Steptoe
Class 1				
88	Late embryogenesis abundant protein	Desiccation tolerance	-	-
91	Poly(A)-binding protein	Protein synthesis	-	-
323	Late embryogenesis abundant protein	Desiccation tolerance	-	-
Class 2				
85	S-adenosylmethionine synthetase 1	Primary metabolism	↑	↑
167	Carboxymethylenebutenolidase-like protein	Redox regulation	↑	↑
224	Peroxidase	Redox regulation	↑	↑
6	Lactoylglutathione lyase	Redox regulation	↑	↑
17	Probable L-ascorbate peroxidase 7	Redox regulation	↑	↑
121	Poly(A)-binding protein	Protein synthesis	↑	↑
208	(1→3)-β-glucanase GV	Disease/defence	↑	↑
Class 3				
11	Putative nuclear RNA binding protein A	Protein synthesis	↓	↓
128	Lactoylglutathione lyase	Redox regulation	↓	↓
239	Not found	Unknown	↓	↓
22	23 kDa jasmonate-induced protein	Disease/defence	↓	↓
41	Iron-deficiency specific protein IDS3	Secondary metabolism	↓	↓
93	Iron-deficiency specific protein IDS2	Secondary metabolism	↓	↓
189	Cytosolic 6-phosphogluconate dehydrogenase	Primary metabolism	↓	↓
260	Putative monodehydroascorbate reductase	Redox regulation	↓	↓
344	Probable nicotianamine synthase 7	Secondary metabolism	↓	↓
Class 4				
5	Probable L-ascorbate peroxidase 7	Redox regulation	↑	-
7	Glutathione transferase F5	Redox regulation	↑	-
62	Lipoxygenase 1	Primary metabolism	↓	-
108	F23N19.10 stress-inducible protein	Disease/defence	↓	-
Class 5				
31	Fructokinase 2	Primary metabolism	-	↓
66	Osr40g2 protein	Disease/defence	-	↑
172	Iron-deficiency induced protein IDI2	Protein synthesis	-	↓
246	Iron-deficiency induced protein IDI1	Secondary metabolism	-	↓
271	Catalase 1	Redox regulation	-	↓

5.4.1. Proteins non-responsive to salt stress treatment

Three protein spots were identified accountable for the grouping according to genotypes and that were either highly expressed in Morex or in Steptoe. Because their expression was not affected by the salt treatment, these spots formed class 1. Two spots showed a higher abundance in Morex and these were a LEA protein (spot # 88) and a poly(A)-binding protein (spot # 91). The remaining protein in this group was more abundant in Steptoe than in Morex and was identified as a second LEA protein (spot # 323).

MS-based identification of the two LEA proteins in this group led to the same EST entry in the TIGR gene index for barley and their position in the 2-D gel is closely together (see Figure 45). Therefore, it is very likely that these are two isoforms detected in the analysis. The protein belongs to group 2 LEA proteins, so-called dehydrins (Close et al., 1989). Dehydrin expression is ABA responsive and proteins accumulate in response to dehydration (Moons et al., 1995). Interestingly, the identified proteins spots did not show an induced expression upon salt treatment neither in Morex nor in Steptoe. Because of the diverse functions of LEA proteins, the cultivar-specific expression of the group 2 LEA proteins could also be related to other stresses as cold that were not the subject of investigation.

Poly(A)-binding protein was about three-fold more abundant in Morex as compared to Steptoe. This protein binds to the poly(A) tail of an mRNA and interacts with several translation initiation factors to promote translation (reviewed in Gallie et al., 1998). When bound to the mRNA it also prevents the decapping of the 5' cap structure and therefore is functioning in maintaining mRNA integrity (Caponigro and Parker, 1995). Characterization in yeast, human, mouse, Arabidopsis and wheat revealed a high level of conservation on the nucleotide level among eukaryotes and the functional complementation of its homolog in yeast by wheat poly(A)-binding protein could be demonstrated (Le et al., 1997). Multiple protein spots have been observed in wheat ranging in *pI* from 6.0-7.8, but nature and role of the modifications or isoforms are still not known. In Arabidopsis, the highest promoter activity of the poly(A)-binding protein 2 was detected in rapidly growing and dividing cell types, like meristem of root tip and shoots as well as lateral primordial of roots (Palanivelu et al., 2000). The high abundance of this protein in roots of Morex could reflect a higher level of protein synthetic activity in this genotype. As a consequence, this would cause the maintenance of a steady elevated growth rate in Morex even under stress conditions as compared to the sensitive line Steptoe.

5.4.2. Proteins showing the same regulation in both genotypes upon treatment

Proteins in class 2 follow the expression that is characterized by an induction under salt stress conditions. These included S-adenosylmethionine synthase 1 (spot # 85), carboxymethylenebutenolidase-like protein (spot # 167), peroxidase (spot # 224), lactoylglutathione lyase (spot # 6), probable L-ascorbate peroxidase 7 (spot # 17), poly(A)-binding protein (spot # 121) and (1→3)- β -glucanase GV (spot # 208).

S-adenosylmethionine synthase accumulated during salinity treatment. This enzyme catalyzes the attachment of an adenosyl residue to methionine resulting in the formation of S-adenosylmethionine (SAM), which is a universal methyl group donor for DNA, proteins, carbohydrates, membrane lipids, flavonoids and others. SAM is also the precursor of ethylene, polyamides, nicotianamine, phytosiderophores and biotin (reviewed in Roje, 2006). Because of this broad spectrum of catalytic activity, it is difficult to interpret the up regulation of SAM synthase found in the analysis.

The identified carboxymethylenebutenolidase-like protein features a dienelactone hydrolase (DLH) domain, which is responsible for the detoxification of chloroaromatic compounds in bacteria (Bruckmann et al., 1998). In a proteomic study of rice aleurone layer, DLH was found as a putative target for thioredoxin-mediated reduction (Yano and Kuroda, 2006). Thioredoxins reduce disulfide bonds and donate electrons to various enzymes, such as peroxiredoxins functioning in H₂O₂ detoxification (Dietz et al., 2006). To this moment, the substrate of DLH in plants is unknown, but induction upon salt stress treatment could point to a regulatory role in redox metabolism.

Among induced proteins was also peroxidase, a key player in ROS scavenging. The peroxidase identified in the experiment was initially cloned from barley coleoptiles and it was induced after infection with powdery mildew fungus (Kristensen et al., 1999). According to the prediction of the subcellular localization of the identified protein (<http://wolfpsort.org/>), the peroxidase belongs to class III peroxidases that are secreted to the cell wall or surrounding medium. During pathogen attack ROS are supplied by an oxidative burst. At the cell wall peroxidases catalyze the reduction of H₂O₂ by using various molecules, such as phenolic compounds, lignin precursors, auxin or others, as electron donors leading to polymerization reactions as lignification, suberization and cross-linking of cell wall proteins (Kristensen et al., 1999; Passardi et al., 2004). Peroxidases participate not only in plant defense mechanisms but also in other biological processes as growth by cell elongation. As shown for maize roots, ROS are involved in gravitropism and scavenging of ROS resulted in an inhibition of root

gravitropism (Joo et al., 2001). In salt stress experiments with rice seedlings, no change in activity was found for cell wall-bound peroxidase, whereas ionically bound peroxidase activity increased during the treatment (Lin and Kao, 2001). The peroxidase identified in the experiment was initially higher expressed in Morex as compared to Steptoe and did reveal only a slight induction upon treatment. This is in agreement with the previous findings and could point to the maintenance of basal processes in root growth under stress conditions. The higher abundance in Morex could indicate that the salt tolerant genotype is able to maintain a higher growth rate as compared to the sensitive genotype Steptoe, because it prevents the inhibition of root growth due to H₂O₂-induced cell wall stiffening.

Lactoylglutathione lyase is also known as glyoxalase I and is involved in the glutathione-based detoxification of methylglyoxal, a byproduct of carbohydrate and lipid metabolism. Although the physiological role of this enzyme is not clear, tobacco plants overexpressing glyoxalase I possessed a higher tolerance towards salinity as compared to wild type plants (Singla-Pareek et al., 2003). The effect was even more pronounced when plants were transformed with glyoxalase I and II together, because glyoxalase II catalyzes the final step for the release of glutathione. Since glutathione is a key player in the scavenging of ROS it appears that glyoxalase I is involved in detoxification processes during stress application. The study also shows very nicely that in most cases salinity tolerance depends on more than one gene or enzyme activity.

The induction of ascorbate peroxidase (APX) by salt stress treatment is not unexpected. APX catalyzes the reduction of H₂O₂ to water with the concomitant generation of monodehydroascorbate (Figure 59) and is therefore a key component in the scavenging pathway of ROS produced by various stress factors (Shigeoka et al., 2002). APX protein expression was induced in salt stressed Arabidopsis roots along with other members of the ROS scavenging pathway, such as glutathione S-transferase, peroxidase and monodehydroascorbate reductase (Jiang et al., 2007). The accumulation of APX that was found in barley roots is in agreement with the literature, although the initial protein expression level was higher in the sensitive genotype Steptoe than in the tolerant genotype Morex.

The poly(A)-binding protein identified in this group shares the same identifier as the poly(A)-binding protein in class 1. However, the position of the protein on the 2-D gel is less basic (see Figure 45) indicating multiple isoforms or post-translational modifications (PTM) of the protein as described already for wheat (Le et al., 1997). But in contrast to the expression of this protein in class 1, the initial expression level was higher in Steptoe than in Morex. The up

regulation of the poly(A)-binding protein during stress application indicates an enhanced activity of the translational machinery in both genotypes or a higher requirement for protecting the integrity of protein biosynthesis.

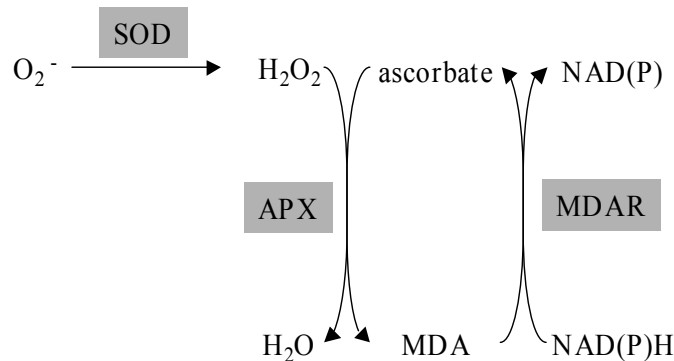


Figure 59: ROS scavenging by ascorbate peroxidase (APX). Two molecules of O_2^- are converted to H_2O_2 by superoxide dismutase (SOD). APX catalyzes the detoxification of H_2O_2 by reduction of ascorbate under the formation of monodehydroascorbate (MDA) and the release of water. Ascorbate is regenerated by monodehydroascorbate reductase under consumption of NAD(P)H. The diagram is modified after Mittler et al. (2004).

The (1→3)- β -glucanase gene family consists of seven members, designated GI to GVII (Xu et al., 1992). These enzymes are classified as pathogenesis-related proteins because of their ability to hydrolyze the (1→3, 1→6)- β -glucans of fungal cell walls (Xu et al., 1994). While some isoenzymes are targeted to vacuoles or the extracellular space for protection against pathogens, others have a cytosolic localization. GV was isolated from barley roots and leaves and did not possess a cellular targeting motif, suggesting its participation in a non-specific protection strategy (Xu et al., 1994). The up regulation in the stress experiment in both genotypes supports this assumption.

Nine proteins were down regulated in barley seedlings of both genotypes upon salinity treatment. These were a putative nuclear RNA binding protein (spot # 11), lactoylglutathione lyase (spot # 128), 23 kDa jasmonate-induced protein (spot # 22), IDS2 (spot # 93) and IDS3 (spot # 41), 6-phosphogluconate dehydrogenase (spot # 189), a putative monodehydroascorbate reductase (spot # 260) and a probable nicotianamine synthase 7 (spot # 344). For one identified EST (spot # 239) no homologous proteins were found in public databases.

The identification of a putative nuclear RNA binding protein indicates the repression of protein synthesis during salt stress treatment. This is in agreement with results from other

studies showing that especially cytosolic and plastidic ribosomal proteins are down regulated under salt stress conditions (Jiang et al., 2007; Jiang and Deyholos, 2006).

Lactoylglutathione lyase (glyoxalase I) was identified in a second protein spot located closely to the respective spot in class 2. While the expression of spot # 6 was induced upon salinity treatment, expression of spot # 128 was inhibited. The occurrence of multiple spot observations with different expression under salt stress conditions points to a regulation mechanism based on multiple isoforms or PTM.

23 kDa jasmonate-induced protein was detected as lower abundant after stress application. A recent study of the shoot transcriptome from the Morex genotype under salinity stress revealed a considerable number of differentially expressed genes related to the jasmonic acid (JA) pathway or responsive to JA (Walia et al., 2006). JA is an important phytohormone produced upon wounding or other stresses via the degradation of membrane lipids. The salinity stress study of Walia et al. revealed that the induction of the JA pathway was most prominent at early sampling time points indicating a cross-talk between JA and other stress-induced plant hormones as ABA or ethylen. In a follow-up study using barley cv. Golden Promise it could be shown that pre-treatment with JA followed by salinity stress resulted in a lower accumulation of Na^+ in shoots as compared to untreated salt stressed plants (Walia et al., 2007). In both studies, the 23 kDa JA-induced protein appeared as differentially regulated by salinity stress, by JA alone as well as by JA-pre-treated salinity stressed plants. The function of this protein has to be determined; so far no homology to annotated proteins was found that could explain the role of 23 kDa JA-induced protein during salt stress responses.

IDS2 and IDS3 are two dioxygenase genes isolated from iron-deficient barley roots (Nakanishi et al., 2000). Under normal conditions, plants reduce Fe^{3+} chelates and take up the more soluble Fe^{2+} via low-affinity iron transport systems. However, under iron-deficiency graminaceous plants produce phytosiderophores (PS) that are secreted into the rhizosphere (Curie and Briat, 2003). PS have a high affinity for Fe and solubilize Fe^{3+} by chelation. The resulting complexes are then transported through the plasma membrane via specific transporters. During the biosynthesis of mugineic acid family PS nicotianamine is metabolized to 2'-deoxymugineic acid, which is the precursor of all other mugineic acids and the substrate of IDS2 and IDS3. Interestingly, the protein expression of IDS2, IDS3 as well as of a probable nicotianamine synthase is repressed under salt stress treatment. The down regulation of the mentioned proteins could point to the salt stress-induced growth inhibition and the concomitant decrease of Fe consumption in stressed plants. It could also be indicative

for the avoidance of metal ion-induced oxidative stress. Although iron is an essential cofactor for many proteins, the reaction with oxygen can lead to the production of hydroxyl and peroxide radicals in the Fenton reaction (Figure 60). These radicals are engaged in secondary reactions as protein oxidation, lipid peroxidation and DNA nicking (Briat, 2002). Limiting iron uptake under salt stress conditions could therefore counteract ROS formation.

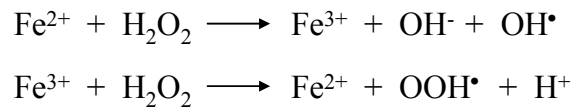


Figure 60: Generation of ROS through iron catalysis in the Fenton reaction.

Furthermore, 6-phosphogluconate dehydrogenase (6PGDH) was lower expressed, which was detected in the comparative analysis of the grain proteome from accession of the OWB mapping population. Protein identification revealed two different ESTs; hence, it is very likely that two different isoforms were detected. But in contrast to the earlier experiment, 6PGDH was more abundant in the salt-sensitive accession. As discussed previously, the enzyme functions in the pentose phosphate pathway providing NADPH for metabolic and detoxification processes. In 24 hours salt-stressed barley root, the gene expression was down-regulated upon stress treatment and to a greater extent in the more salt tolerant barley than in the more susceptible rice (Ueda et al., 2006). Obviously, there are different isoforms of 6PGDH in barley with tissue-specific expression. It has to be determined whether they also have distinctive roles in biosynthetic processes.

Like several others before monodehydroascorbate reductase (MDAR) is involved in the removal of ROS (see figure 44). But unlike peroxidase or ascorbate peroxidase, the abundance of this spot is decreasing after stress application although MDAR catalyzes the important regeneration of ascorbate (Mittler et al., 2004). In a proteome analysis of Arabidopsis roots subjected to salt stress, MDAR expression was also inhibited (Jiang et al., 2007). Authors assumed that although the requirement of reduced ascorbate is high under salt stress, a fine-tuning of the levels of antioxidants is also an important consideration. This could also be the case for salt stressed barley roots.

5.4.3. Proteins exhibiting a cultivar-specific regulation upon treatment

In the analysis, four proteins were detected that revealed a significant change in expression upon salinity stress only in the salt tolerant genotype Morex. Proteins composing class 4 were

a probable L-ascorbate peroxidase 7 (spot # 5), glutathione transferase F5 (spot # 7), lipoxygenase 1 (spot # 62), and a stress-inducible protein F23N19.10 (spot # 108).

Glutathione transferase (GST) catalyzes the conjugation of reduced glutathione to a variety of target compounds. For a long time it was believed that GST is acting only in the detoxification of xenobiotics but recent results indicate the involvement in oxidative stress responses (reviewed in Droog, 1997). Overexpression of a GST, which possesses also glutathione peroxidase activity, in tobacco conferred salt tolerance in transgenic plants during germination (Roxas et al., 1997). The concomitant induction of APX upon stress treatment in Morex leads to the conclusion that the removal of ROS in this genotype is more effective as compared to the sensitive line. Also, a higher initial expression of GST and APX was detected in Morex, which would provide a better starting point for the tolerant genotype in the scavenging of ROS generated upon salinity stress.

Lipoxygenase expression was repressed in Morex and that is in agreement with results from a gene expression study in Morex seedlings (Walia et al., 2006). Lipoxygenase is involved in the generation of JA and its abundance was related to salinity stress as well as JA treatment (Walia et al., 2007). A down regulation was also found for the 23 kDa JA-induced protein, indicating only minor relevance of JA signaling in later stages of salinity stress.

The expression of a stress-inducible protein F23N19.10 was exclusively repressed in Morex. This protein is not yet characterized but sequence comparison on the amino acid level revealed four conserved motifs: three tetratricopeptide repeat (TPR) domains and one heat shock chaperonin-binding motif. TPR motifs mediate protein-protein interactions through helix formations (D'Andrea and Regan, 2003) and it was shown that TPR proteins are involved in the organization of the Hsp70/Hsp90 multiprotein complex (Pratt and Toft, 2003). Recently, a protein with homology to F23N19.10 was detected as highly enriched in trichomes of tobacco leaves, as compared to the remaining leaf tissue, and authors assumed protective function of this protein (Amme et al., 2005). Possible roles of the identified protein from barley roots include protein stabilization and turnover as well as Hsp-involved signal transduction processes (Wang et al., 2004).

Five proteins were found regulated in Steptoe: fructokinase 2 (spot # 31), IDI1 (spot # 246) and IDI2 (spot # 172), Osr40g2 protein (spot # 66) and catalase 1 (spot # 271).

Fructokinase 2 catalyzes the phosphorylation of fructose to fructose-6-phosphate. For the storage of carbohydrates in sink tissues, sucrose is transported via the phloem to the root and

cleaved after phloem unloading into glucose and fructose. Fructose is converted first into fructose-6-phosphate and subsequently into glucose-6-phosphate through hexose-phosphate isomerase. Then, glucose-6-phosphate is transferred into the amyloplast by membrane-bound glucose-phosphate translocator for starch synthesis (Heldt, 2003). The expression of fructokinase was only slightly affected by salt stress conditions and protein abundance was more than two-fold higher in Steptoe than in Morex. Although soluble sugars are involved in signaling processes during biotic or abiotic stresses (Couee et al., 2006), it is more likely that the cultivar-specific and non-responsive expression of fructokinase is related to the root growth performance. A high expression of fructokinase indicates an enhanced storage of soluble sugars in Steptoe, while in the more rapidly growing roots of Morex the soluble sugars are immediately metabolized.

IDI1 and IDI2 were initially isolated as cDNAs from Fe-deficient barley roots. IDI1 encodes for an acireductone dioxygenase that is part of the methionine salvage pathway and converts 5'-methylthioadenosine to methionine for PS production (Yamaguchi et al., 2000a). IDI2 encodes a protein related to the α subunit of eukaryotic translation initiation factor 2B, probably regulating the synthesis of proteins required for stress adaptation (Yamaguchi et al., 2000b). Like IDS2 and IDS3, the protein abundance of IDI1 and IDI2 is negatively affected especially in the Steptoe genotype due to salt treatment indicating a reduced consumption of Fe under stress conditions or the avoidance of iron-induced oxidative stress.

Catalase 1 (CAT1) was also repressed specifically in Steptoe, which is the principal H₂O₂ scavenging enzyme in plant peroxisomes besides APX. CAT catalyzes the breakdown of H₂O₂ into H₂O and O₂. CAT activity is crucial for ROS detoxification and the reduction of CAT1, representing 80 % of leaf CAT activity, leading to an enhanced sensitivity towards light stress, oxidative stress, ozone and salt stress in tobacco could be shown (Willekens et al., 1997). Repression of protein expression in barley roots might be related to the induction of APX (spot # 17) in Steptoe in order to fill the gap in ROS scavenging.

Osr40g2 was the only protein induced in Steptoe exclusively, a protein coding for an ABA and salt stress-responsive cDNA isolated from rice (Moons et al., 1996). Due to the lack of homologous proteins or conserved domains the function and role during salinity stress of this protein is unknown. The role of ABA was discussed earlier and the enhanced expression of Osr40g2 might be related to ABA-specific stress reactions.

In summary, proteomic analysis revealed 28 proteins, including 3 cultivar-specific, 16 salt-responsive and 9 cultivar-specific salt-responsive proteins in roots of Steptoe and Morex. A similar number of proteins was induced or repressed upon salt treatment in the tolerant and in the sensitive genotype, indicating that stress tolerance may not only be due to the constitutive overexpression of many genes functioning in stress tolerance but also to the fine-tuning of a network of regulatory proteins. This would be the case for proteins involved in redox regulation, the group on which salinity stress had highest impact on and where most proteins are induced in the tolerant cultivar. Also, JA- and ABA-responsive proteins were identified as well as proteins associated with gene translation. Overall, the comparative proteome analysis revealed several candidate proteins for further characterization, like GST, APX or poly(A)-binding protein.

5.5. Identification of accessions from the Steptoe Morex population with contrasting response towards salinity treatment

The comparison of the root proteome from the Steptoe and Morex parents revealed a number of candidate proteins that might confer salt tolerance. But because of the effort and time it is not reasonable to investigate all proteins that were differentially expressed either in genotypes or upon stress treatment. In order to limit the number of candidate proteins and to detect proteins related to salt tolerance mechanisms, additional accessions from the SM population should be used showing the same contrasting stress response as compared to the parent lines. As it was done for the comparative analysis of the grain proteome, progeny lines are used as a filter since proteins related to stress response should be expressed at a similar level in genotypes with the same trait for salt stress response. Therefore, a number of progeny lines, showing an equal contrasting phenotype as the parents in the germination assay, were subjected to the long-term salt stress treatment. Three lines were found that maintained the same trait for salt stress response at the seedling stage, indicating that different factors might be responsible for tolerance or sensitivity in the plant at different developmental stages.

The identified lines are to use in hydroponic stress experiments to reduce the number of possible candidate proteins augmenting salt tolerance in barley. Resulting candidate proteins from a comparative proteome analysis of tolerant and sensitive genotypes should be more meaningful and worth for further in-depth studies.

5.6. Proteome analysis of root plasma membranes reveals salt stress-responsive protein expression

As outlined before, roots are responsible for ion uptake, transport and the regulation of the water status. 2-D gel electrophoresis of roots from Steptoe and Morex revealed potential candidates conferring salt tolerance in barley for further in-depth characterization. However, due to certain constraints of the 2-D technique, the analysis of proteins attached to or embedded in the lipid bilayer of plasma membranes is hampered by their heterogeneous biochemical properties and general low abundance. But as they are of great biological importance in signalling and transport processes under salt stress, a comparative analysis of root plasma membrane proteins using a subcellular proteomics approach was initiated. The aim was not only to gain knowledge of the plasma membrane profile from the tolerant and the sensitive genotype but also to detect proteins differing in expression in response towards to salt stress treatment.

5.6.1. Identification of plasma membrane proteins from barley root tissue

Sample preparation is a critical issue for membrane proteomics and different strategies are established to enrich samples for plasma membranes. Aqueous 2-phase partitioning has been used for a number of years and, although it requires a certain degree of expertise as well as optimisation for each sample, it provides the highest purity of plasma membranes when compared to other methods (Santoni, 2007). The preparation of plasma membranes from control and salt stressed root of Steptoe and Morex was verified by immunoblotting of marker proteins for cytosolic, endomembrane and plasma membrane fractions. For most preparations, the intensity of western blot signal from the plasma membrane specific H⁺-ATPase was similar between the microsomal fraction and the plasma membrane fraction, indicating a limited enrichment of plasma membranes. However, immunoblotting also revealed a highly reduced signal intensity for endomembrane and cytosolic marker proteins in the plasma membrane fraction and this indicated a successful depletion of these classes of proteins during the 2-phase partitioning. Subsequently, the plasma membrane fraction was enriched for hydrophobic integral membrane proteins by reversed-phase chromatography and results were confirmed by western blotting using anti-H⁺-ATPase antibodies.

The most commonly used method for the separation of complex protein samples is 2-D gel electrophoresis. However, this method is not suited for highly hydrophobic proteins. In the first dimension of 2-D gel electrophoresis, proteins are introduced to a pH gradient and

separate according to their isoelectric point (pI) under application of electrical current. But under neutral conditions, in other words on the respective pI , solubility is at a minimum and hydrophobic proteins tend to precipitate, preventing the transfer into the second dimension (reviewed in Speers and Wu, 2007). Therefore, the gel-free method of LC-MS^E was applied for the separation and quantification of proteins and peptides. In recent years numerous improvements in MS technology facilitated the rise of this highly advanced separation, quantitation and identification approach. The challenges that were faced were related to the accuracy in retention time, mass and signal response as well as to software solutions for spectra alignment, clustering of EMRT pairs and normalisation algorithm. This approach was already used for relative and absolute quantitation of proteins in complex mixtures as well as for the search for biomarkers (Silva et al., 2005; Silva et al., 2006b; Vissers et al., 2007). The dynamic range of the system was demonstrated in a feeding experiment with *Escherichia coli* grown with different carbon sources and protein expression changes were determined from 0.1- to 90-fold in relative abundance (Silva et al., 2006a).

The identification of plasma membrane proteins from both genotypes was successful for 159 proteins and out of these, 56 % had one or more predicted TMD. The high amount of proteins that did not have a TMD could arise from contamination of cytosolic or other proteins. However, because of the additional enrichment using reversed-phase chromatography, it is more likely that these proteins have been coenriched with plasma membrane proteins due to a close interaction of both. For instance, a number of ribosomal proteins and elongation factors were found in the analysis sharing no TMD. They probably originate from polysomes that are bound to the cytoskeleton via actin filaments, which are attached to the plasma membrane (Medalia et al., 2002). Membrane-anchored small GTP-binding proteins and ADP-ribosylation factors were identified playing a role in signalling pathways and targeting to the plasma membrane (Lee et al., 2002). A recent study on the plasma membrane proteome of *Arabidopsis* cell culture revealed similar findings. Also here, half of the proteins identified had no TMD indicating close interaction of the plasma membrane with other cellular compartments, such as cytoskeleton and endomembrane systems (Marmagne et al., 2007). From all identified proteins of the barley plasma membrane, only 25 % were predicted to be allocated to the plasma membrane; the rest was assigned to cellular compartments like vacuole or cytosol. However, it is very likely that some proteins are actually located in the plasma membrane despite their annotation in protein databases. Examples for this are ATP synthase subunits α and β that were identified in plasma membrane fractions before although both proteins were allocated to the mitochondria according to WoLF Psort (Hynek et al.,

2006; Katz et al., 2007). Whether these are persistent contaminants, since no localisation at the plasma membrane was shown before in subcellular characterization studies, or the proteome analysis results reflect the *in vivo* distribution within the cell has to be investigated in more detail.

The analysis yielded in a broad coverage of cellular processes on the plasma membrane. The proteins identified have function in transport and signalling processes, protein synthesis and stabilisation, cellular organisation and metabolism. However, no transporters for ions or other GTP-binding receptors were detected in the analysis. This is probably due to their low abundance. Protein identification was most effective for highly abundant proteins, as H⁺-ATPase or aquaporins. Therefore, improvements in the separation of tryptic peptides from the total digest of plasma membrane samples should enable the detection of proteins with low abundance in the plasma membrane. Prefractionation of the protein sample using SDS-PAGE would result in a less complex peptide mixture for LC-MS^E providing the possibility of detecting proteins at low concentrations. Furthermore, only a small fraction of *de novo* sequences derived from LC-MS^E experiments could be related to a protein database entry. To overcome this issue, EST databases, such as TIGR gene index, could be used for the identification as these databases comprise of considerably more sequences for barley genes. Currently attempts are made to extract *de novo* sequences from the Expression software and to search EST databases using bioinformatic means.

5.6.2. Salt-induced changes in the plasma membrane proteome of barley genotypes with contrasting response towards salinity stress

The comparative analysis of plasma membrane proteins revealed that more proteins showed altered expression upon salt treatment in the sensitive genotype Steptoe as compared to the tolerant genotype Morex reflecting the higher stress potential of salinity for the susceptible genotype.

The plasma membrane H⁺-ATPase is one of the best-studied enzymes in plants. This membrane-integral proton pump drives the nutrient transport by generating an electrochemical gradient between the apoplast and the cytosol. The proton pump exports H⁺ from the cytosol into the apoplast under the consumption of ATP, which is provided by ATP synthase activity (Sondergaard et al., 2004). The proton gradient energizes channel proteins and carriers to facilitate the nutrient uptake in roots, where plasma membrane H⁺-ATPase is highly expressed, and the long-distance transport within the plant (Palmgren, 2001). It was shown that pump activity changes in response to various stress factors (Ashraf and Harris,

2004; Palmgren, 2001). The comparative proteome analysis revealed that plasma membrane H⁺-ATPase abundance decreased in the salt sensitive and the salt tolerant genotype under salt stress conditions. This could lead to a reduction in nutrient uptake and transport in seedling roots.

Aquaporins mediate the transport of water and small neutral molecules across the plasma membrane. In maize roots it was shown that salinity stress inhibits the expression of aquaporin in a salt tolerant variety in order to promote cellular water conservation (Martinez-Ballesta et al., 2008). The activity of aquaporins is modulated by post-translational modifications of the non-membrane integral N- and C-terminal domains and recently, methylation of N-terminal amino acid residues was detected (Santoni et al., 2006). SAM is the universal donor of methyl groups and it was found as salt-stress induced in the comparative proteome analysis of root soluble proteins. Interestingly, this protein was also found as up-regulated in the plasma membrane protein fraction of both genotypes. Whether this is due to contaminations with soluble proteins or it was coenriched with plasma membranes has to be determined. Overall, aquaporin expression decreased in both genotypes under salinity conditions. This is in agreement with the literature and suggests a regulatory role in water transport during stress treatment (Boursiac et al., 2005).

Numerous proteins (60S ribosomal protein, Hsp 70, Hsp 81) that were detected as salt stress-responsive are integrated in protein synthesis and stability processes. Orthologs of heat shock proteins in other species associate with plasma membrane proteins and indeed Hsp 70 abundance was induced in plasma membrane preparations of the halotolerant alga *Dunaliella salina* upon salinity stress (Aoki et al., 2002; Katz et al., 2007). Therefore, findings that Hsp 70 was higher expressed in Morex under stress conditions but was lower expressed in Steptoe are in agreement with the literature and could point to an enhanced protein stabilisation in the tolerant genotype.

Several ATP synthase-related proteins were detected in the analysis as salt stress-responsive. This is in accordance with recent findings where the expression of ATP synthase subunits α and β was induced in *Dunaliella* under salt stress conditions (Katz et al., 2007). Although ATP synthase is allocated to mitochondria, some studies revealed a possible plasma membrane localisation (Hynek et al., 2006; Katz et al., 2007; Schindler et al., 2008). Enhanced expression of ATP synthase-related proteins would lead to an elevated energy supply in form of ATP for ATPases.

The H⁺-pyrophosphatase transfers protons into the vacuole through the cleavage of pyrophosphate to phosphate and is the second proton-transporting enzyme in the vacuole besides the vacuolar H⁺-ATPase. The protein was induced after salinity treatment in both genotypes that were examined. The vacuolar H⁺-pyrophosphatase has been immunogold-localized to the plasma membrane of cauliflower inflorescence cells (Ratajczak et al., 1999). But although the protein is present in the plasma membrane it failed to pump protons through the plasma membrane. Therefore it is doubtful that the protein functions in the acidification of the apoplast and possible roles at the plasma membrane remain to be examined.

NAR2 was higher abundant in the salt tolerant genotype Morex. This protein is part of a two-component nitrate uptake system where one protein is a nitrate carrier with 12 TMD and the other protein is considerably smaller in size and has only one TMD. NAR2 was identified in barley and possessed one TMD (Tong et al., 2005). How both proteins interact is still unclear. The higher expression in Morex could point to an elevated nitrogen uptake and the maintenance of a higher growth rate as compared to Steptoe.

Some proteins were detected as differentially expressed that might be considered as probable contaminants. Among them were the mitochondrial ADP/ATP and ATP/ADP carrier proteins and the cytosolic glyceraldehyde-3-phosphate dehydrogenase that were earlier found in plasma membrane preparations (Alexandersson et al., 2004; Hynek et al., 2006). Aspartate aminotransferase catalyses the formation of aspartate and α -ketoglutarate from oxalacetate and glutamate and isoforms in Arabidopsis were detected in the cytosol, mitochondria and plastids (Schultz and Coruzzi, 1995). Also the presence of histone H4 in the PM fraction poses questions. Although these proteins were detected reproducibly in different PM preparations, barley genotypes and treatments, validation of the findings by independent biochemical methods is inevitable.

Taken together, the characterization of protein expression changes in plasma membrane fractions demonstrates genotype-specific response towards salinity by altering transport activities, signaling processes as well as protein synthesis and stabilization. Possible candidate proteins for further in-depth studies in order to improve salt tolerance in barley include aquaporin isoforms, NAR2 and pyrophosphatase.

5.7. Summary: what are the characteristics of a salt tolerant barley genotype and how can salt tolerance be improved?

Salt tolerance is a multigenic trait where different mechanisms have been evolved for adaptation. Barley grains undergo specific alterations in the transcriptome during germination that have an impact on storage mobilization, activation of photosynthesis and hormone biosynthetic pathways (Sreenivasulu et al., 2008). Previously, also the proteome of different grain tissues was analyzed and differentially regulated proteins were involved in desiccation, osmotic and oxidative stress, protein synthesis and metabolism (Bønsager et al., 2007).

The comparative proteome analysis of grains from contrasting genotypes in salt stress response from two different mapping populations revealed 5 potential candidates that might confer salt tolerance (Figure 61).

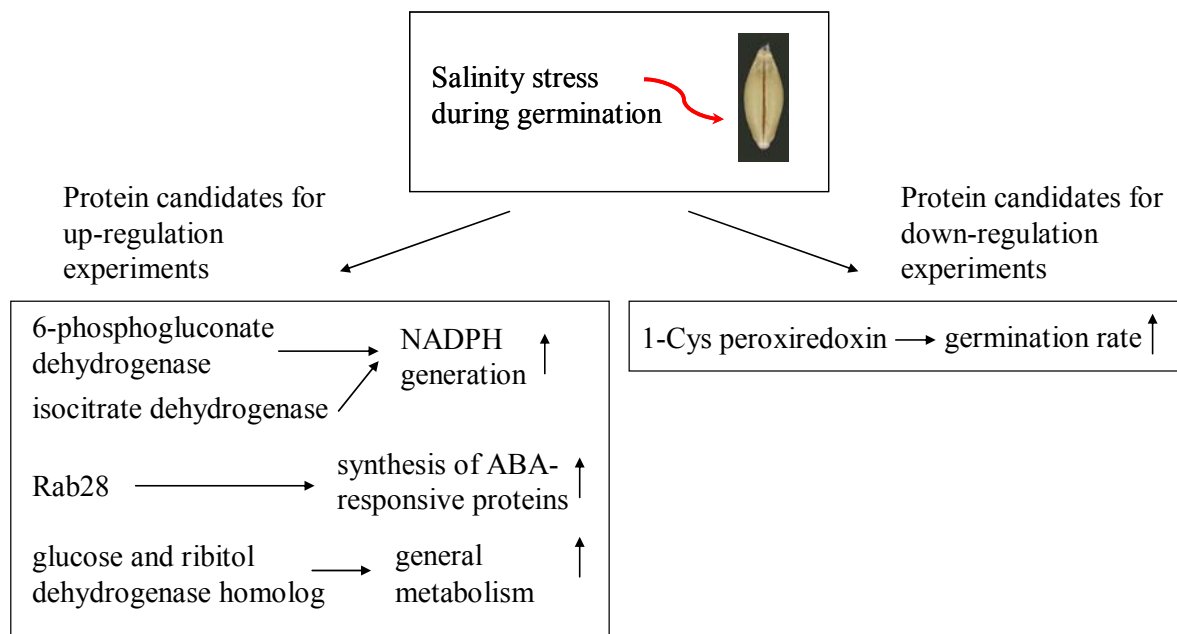


Figure 61: Candidate proteins for up regulation or down regulation experiments in barley grains. The proteins were detected in the comparative grain proteome analysis of accessions from the OWB and the SM population showing a contrasting response to salt stress during germination. Proteins and the possible impacts on the metabolism for conferring salt tolerance are depicted.

Enhanced expression of 6-phosphogluconate dehydrogenase and isocitrate dehydrogenase would result in a better supply of NADPH for metabolic and stress-related pathways. The function of Rab28 has not been elucidated completely, but it is very likely that the up regulation of the ABA-responsive Rab28 affects the synthesis of other ABA-responsive proteins and therefore confers resistance towards osmotic stress that is accompanied by salinity stress. Also the possible role of glucose and ribitol dehydrogenase homolog is not

fully understood, but the increased consumption of glucose could be beneficial for growth rates under stress conditions. 1-Cys peroxiredoxin seems to be a sensor for unfavorable environmental conditions, such as salinity stress. The down regulation of this protein in grains might increase the germination rate under stress conditions.

In addition to the comparative grain proteome, also root proteins were analyzed from barley genotypes with contrasting response towards salinity. In the comparison of Steptoe with Morex under control and stress condition, numerous proteins were detected as higher expressed in the salt tolerant line playing a role in the detoxification of ROS, protein synthesis, ATP production, hormone signaling and others. The possible function of some differentially regulated proteins is shown in Figure 62. These proteins are promising candidates for the generation of transgenic plants in order to test their functionality in a salt sensitive barley cultivar ('Golden Promise').

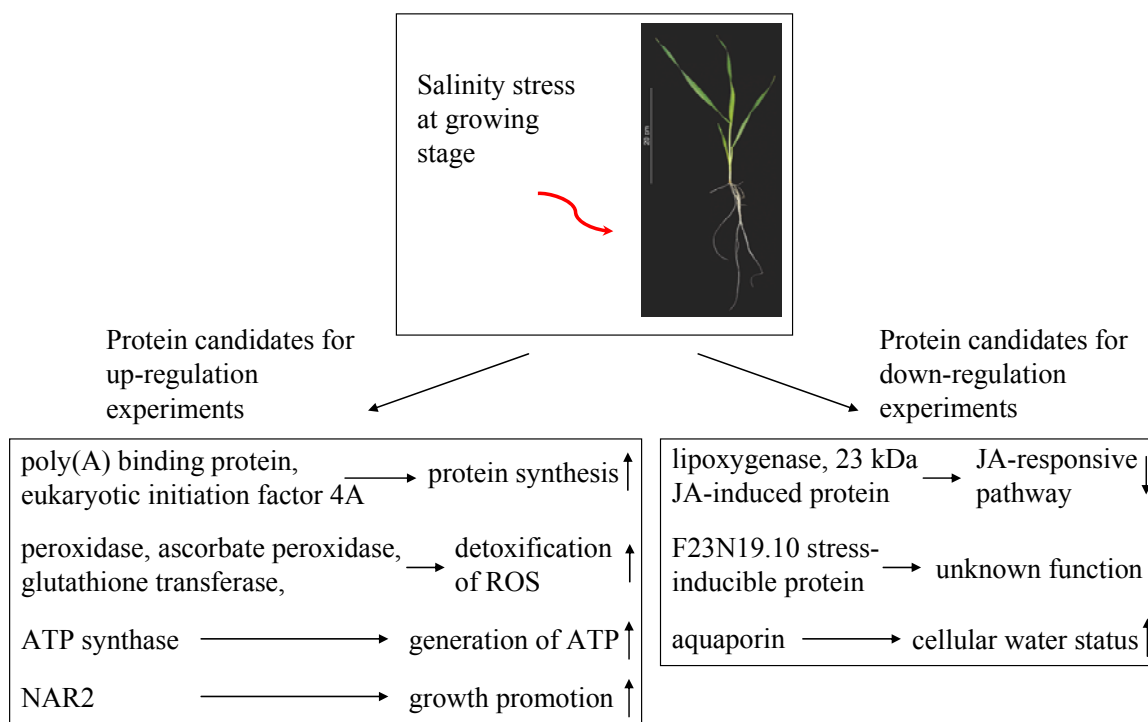


Figure 62: Potential candidates for up regulation or down regulation experiments in barley plants. A small assortment of proteins detected as differentially expressed in the crude extract and in plasma membrane fractions of roots from two genotypes with contrasting response towards salinity is shown. Proteins that have the potential for augmenting salt tolerance and the possible effects on the metabolism are presented.

Transgenic approaches with proteins shown in Figures 59 and 60 would give valuable information about salt tolerance mechanisms in barley. This has been already initiated, but

due to the time-consuming transformation procedure and the long life cycle of barley, transgenic plants have to be analyzed in prospective experiments. Since salt tolerance requires a concerted adaptation of numerous proteins to the stress, the generation of transgenic plants carrying multiple transgenes should also be considered, e.g. proteins involved in ROS scavenging or NADPH generation.

6. References

- Aalen, R. B.** (1999). Peroxiredoxin antioxidants in seed physiology. *Seed Science Research* **9**, 285-295.
- Abebe, T., Guenzi, A. C., Martin, B. and Cushman, J. C.** (2003). Tolerance of mannitol-accumulating transgenic wheat to water stress and salinity. *Plant Physiology* **131**, 1748-1755.
- Alexander, R., Alamilla, J. M., Salamini, F. and Bartels, D.** (1994). A novel embryo-specific barley cDNA clone encodes a protein with homologies to bacterial glucose and ribitol dehydrogenase. *Planta* **192**, 519-25.
- Alexandersson, E., Saalbach, G., Larsson, C. and Kjellbom, P.** (2004). Arabidopsis plasma membrane proteomics identifies components of transport, signal transduction and membrane trafficking. *Plant and Cell Physiology* **45**, 1543-1556.
- Amme, S., Matros, A., Schlesier, B. and Mock, H.-P.** (2006). Proteome analysis of cold stress response in Arabidopsis thaliana using DIGE-technology. *Journal of Experimental Botany* **57**, 1537-46.
- Amme, S., Rutten, T., Melzer, M., Sonsmann, G., Vissers, J. P. C., Schlesier, B. and Mock, H.-P.** (2005). A proteome approach defines protective functions of tobacco leaf trichomes. *Proteomics* **5**, 2508-2518.
- Aoki, K., Kragler, F., Xoconostle-Cazares, B. and Lucas, W. J.** (2002). A subclass of plant heat shock cognate 70 chaperones carries a motif that facilitates trafficking through plasmodesmata. *Proceedings of the National Academy of Sciences of the United States of America* **99**, 16342-16347.
- Apse, M. P., Aharon, G. S., Snedden, W. A. and Blumwald, E.** (1999). Salt tolerance conferred by overexpression of a vacuolar Na⁺/H⁺ antiport in Arabidopsis. *Science* **285**, 1256-1258.
- Arenas-Mena, C., Raynal, M., Borrell, A., Varoquaux, F., Cutanda, M. C., Stacy, R. A. P., Pages, M., Delseny, M. and Culiñez-Macia, F. A.** (1999). Expression and cellular localization of Atrab28 during Arabidopsis embryogenesis. *Plant Molecular Biology* **40**, 355-363.
- Ashraf, M. and Harris, P. J. C.** (2004). Potential biochemical indicators of salinity tolerance in plants. *Plant Science* **166**, 3-16.
- Baldi, P., Valegrave, G., Mazzucotelli, E., Govoni, C., Faccioli, P., Stanca, A. M. and Cattivelli, L.** (2001). The transcripts of several components of the protein synthesis machinery are cold-regulated in a chloroplast-dependent manner in barley and wheat. *Journal of Plant Physiology* **158**, 1541-1546.
- Bevan, M., Bancroft, I., Bent, E., Love, K., Goodman, H., Dean, C. and Bergkamp, R.** (1998). Analysis of 1.9 Mb of contiguous sequence from chromosome 4 of Arabidopsis thaliana. *Nature* **391**, 485-8.
- Bewley, J. D.** (1997). Seed germination and dormancy. *Plant Cell* **9**, 1055-1066.
- Blackman, S. A., Wettlaufer, S. H., Obendorf, R. L. and Leopold, A. C.** (1991). Maturation proteins associated with desiccation tolerance in soybean *Plant Physiology* **96**, 868-874.
- Bolstad, B. M., Irizarry, R. A., Astrand, M. and Speed, T. P.** (2003). A comparison of normalization methods for high density oligonucleotide array data based on variance and bias. *Bioinformatics* **19**, 185-193.
-

- Bønsager, B. C., Finnie, C., Roepstorff, P. and Svensson, B.** (2007). Spatio-temporal changes in germination and radicle elongation of barley seeds tracked by proteome analysis of dissected embryo, aleurone layer, and endosperm tissues. *Proteomics* **7**, 4528-4540.
- Borrell, A., Cutanda, M. C., Lumbreras, V., Pujal, J., Goday, A., Culiñez-Macia, F. A. and Pages, M.** (2002). Arabidopsis thaliana Atrab28: a nuclear targeted protein related to germination and toxic cation tolerance. *Plant Molecular Biology* **50**, 249-259.
- Boursiac, Y., Chen, S., Luu, D. T., Sorieul, M., van den Dries, N. and Maurel, C.** (2005). Early effects of salinity on water transport in Arabidopsis roots. Molecular and cellular features of aquaporin expression. *Plant Physiology* **139**, 790-805.
- Bradford, M.** (1976). A rapid and sensitive method for the quantitation of microgram quantities of protein utilizing the principle of protein-dye binding. *Anal Biochem* **7**, 248-54.
- Briat, J.-F.** (2002). Metal ion-activated oxidative stress and its control. In *Oxidative Stress in Plants*, eds. D. Inze and M. van Montagu). London: Taylor & Francis Inc.
- Browne, J., Tunnacliffe, A. and Burnell, A.** (2002). Anhydrobiosis: Plant desiccation gene found in a nematode. *Nature* **416**, 38.
- Bruckmann, M., Blasco, R., Timmis, K. N. and Pieper, D. H.** (1998). Detoxification of protoanemonin by dienelactone hydrolase. *Journal of Bacteriology* **180**, 400-402.
- Campo, S., Carrascal, M., Coca, M., Abian, J. and San Segundo, B.** (2004). The defense response of germinating maize embryos against fungal infection: A proteomics approach. *Proteomics* **4**, 383-396.
- Caponigro, G. and Parker, R.** (1995). Multiple functions for poly(A)-binding protein in messenger-RNA decapping and deadenylation in yeast. *Genes & Development* **9**, 2421-2432.
- Casati, P., Zhang, X., Burlingame, A. L. and Walbot, V.** (2005). Analysis of leaf proteome after UV-B irradiation in maize lines differing in sensitivity. *Molecular & Cellular Proteomics* **4**, 1673-1685.
- Chakrabortee, S., Boschetti, C., Walton, L. J., Sarkar, S., Rubinsztein, D. C. and Tunnacliffe, A.** (2007). Hydrophilic protein associated with desiccation tolerance exhibits broad protein stabilization function. *Proceedings of the National Academy of Sciences* **104**, 18073-18078.
- Chich, J. F., David, O., Villers, F., Schaeffer, B., Lutomski, D. and Huet, S.** (2007). Statistics for proteomics: Experimental design and 2-DE differential analysis. *Journal of Chromatography B-Analytical Technologies in the Biomedical and Life Sciences* **849**, 261-272.
- Chitteti, B. R. and Peng, Z. H.** (2007). Proteome and phosphoproteome differential expression under salinity stress in rice (*Oryza sativa*) roots. *Journal of Proteome Research* **6**, 1718-1727.
- Christensen, A. H. and Quail, P. H.** (1996). Ubiquitin promoter-based vectors for high-level expression of selectable and/or screenable marker genes in monocotyledonous plants. *Transgenic Research* **5**, 213-218.
- Close, T. J., Kortt, A. A. and Chandler, P. M.** (1989). A cDNA-based comparison of dehydration-induced proteins (dehydrins) in barley and corn. *Plant Molecular Biology* **13**, 95-108.
-

- Corpas, F. J., Barroso, J. B., Sandalio, L. M., Distefano, S., Palma, J. M., Lupiáñez, J. A. and Del Río, L. A.** (1998). A dehydrogenase-mediated recycling system of NADPH in plant peroxisomes. *Biochem J.* **330**(Pt2), 777-84.
- Corpas, F. J., Barroso, J. B., Sandalio, L. M., Palma, J. M., Lupianez, J. A. and del Rio, L. A.** (1999). Peroxisomal NADP-dependent isocitrate dehydrogenase. Characterization and activity regulation during natural senescence. *Plant Physiology* **121**, 921-928.
- Costa, J. M., Corey, A., Hayes, P. M., Jobet, C., Kleinhofs, A., Kopisch-Obusch, A., Kramer, S. F., Kudrna, D., Li, M., , Riera-Lizarazu, O., Sato, K. et al.** (2001). Molecular mapping of the Oregon Wolfe Barleys: a phenotypically polymorphic doubled-haploid Population. *Theor. Appl. Genet.* **103**, 415-24.
- Couee, I., Sulmon, C., Gouesbet, G. and El Amrani, A.** (2006). Involvement of soluble sugars in reactive oxygen species balance and responses to oxidative stress in plants. *Journal of Experimental Botany* **57**, 449-459.
- Curie, C. and Briat, J.-F.** (2003). Iron transport and signaling in plants. *Annual Review of Plant Biology* **54**, 183-206.
- D'Andrea, L. D. and Regan, L.** (2003). TPR proteins: the versatile helix. *Trends in Biochemical Sciences* **28**, 655-662.
- Dani, V., Simon, W., Duranti, M. and Croy, R.** (2005). Changes in the tobacco leaf apoplast proteome in response to salt stress. *Proteomics* **5**, 737-45.
- de Hoon, M. J. L., Imoto, S., Nolan, J. and Miyano, S.** (2004). Open source clustering software. *Bioinformatics* **20**, 1453-1454.
- de Koning, D. J. and Haley, C. S.** (2005). Genetical genomics in humans and model organisms. *Trends in Genetics* **21**, 377-381.
- del Rio, L. A., Corpas, F. J., Sandalio, L. M., Palma, J. M., Gomez, M. and Barroso, J. B.** (2002). Reactive oxygen species, antioxidant systems and nitric oxide in peroxisomes. *Journal of Experimental Botany* **53**, 1255-1272.
- Dietz, K.-J.** (2003). Plant Peroxiredoxins. *Annual Review of Plant Biology* **54**, 93-107.
- Dietz, K. J., Jacob, S., Oelze, M. L., Laxa, M., Tognetti, V., de Miranda, S. M. N., Baier, M. and Finkemeier, I.** (2006). The function of peroxiredoxins in plant organelle redox metabolism. *Journal of Experimental Botany* **57**, 1697-1709.
- Dinneny, J. R., Long, T. A., Wang, J. Y., Jung, J. W., Mace, D., Pointer, S., Barron, C., Brady, S. M., Schiefelbein, J. and Benfey, P. N.** (2008). Cell identity mediates the response of Arabidopsis roots to abiotic stress. *Science* **320**, 942-945.
- Donnelly, B. E., Madden, R. D., Ayoubi, P., Porter, D. R. and Dillwith, J. W.** (2005). The wheat (*Triticum aestivium* L.) leaf proteome. *Proteomics* **5**, 1624-1633.
- Dowsey, A. W., Dunn, M. J. and Yang, G. Z.** (2003). The role of bioinformatics in two-dimensional gel electrophoresis. *Proteomics* **3**, 1567-1596.
- Droog, F.** (1997). Plant glutathione S-transferases, a tale of theta and tau. *Journal of Plant Growth Regulation* **16**, 95-107.
- Duncan, D. B.** (1955). Multiple range and multiple F tests. *Biometrics* **11**, 1-42.
- Eisen, M. B., Spellman, P. T., Brown, P. O. and Botstein, D.** (1998). Cluster analysis and display of genome-wide expression patterns. *Proceedings of the National Academy of Sciences of the United States of America* **95**, 14863-14868.
- Ermolayev, V., Weschke, W. and Manteuffel, R.** (2003). Comparison of Al-induced gene expression in sensitive and tolerant soybean cultivars. *Journal of Experimental Botany* **54**, 2745-2756.
-

- Espelund, M., Debedout, J. A., Outlaw, W. H. and Jakobsen, K. S.** (1995). Environmental and hormonal-regulation of barley late-embryogenesis-abundant (Lea) messenger-RNAs is via different signal-transduction pathways. *Plant Cell and Environment* **18**, 943-949.
- Fiehn, O., Kopka, J., Dormann, P., Altmann, T., Trethewey, R. N. and Willmitzer, L.** (2000). Metabolite profiling for plant functional genomics. *Nature Biotechnology* **18**, 1157-1161.
- Flowers, T. J.** (2004). Improving crop salt tolerance. *Journal of Experimental Botany* **55**, 307-319.
- Flowers, T. J. and Yeo, A. R.** (1986). Ion relations of plants under drought and salinity. *Australian Journal of Plant Physiology* **13**, 75-91.
- Fontaine, O., Huault, C., Pavis, N. and Billard, J. P.** (1994). Dormancy breakage of *Hordeum-vulgare* seeds - Effects of hydrogen-peroxide and scarification on glutathione level and glutathione-reductase activity. *Plant Physiology and Biochemistry* **32**, 677-683.
- Fricke, W.** (2004). Rapid and tissue-specific accumulation of solutes in the growth zone of barley leaves in response to salinity. *Planta* **219**, 515-525.
- Gallie, D. R., Le, H., Tanguay, R. L. and Browning, K. S.** (1998). Translation initiation factors are differentially regulated in cereals during development and following heat shock. *The Plant Journal* **14**, 715-722.
- Galvez, S., Bismuth, E., Sarda, C. and Gadal, P.** (1994). Purification and Characterization of Chloroplastic NADP-Isocitrate Dehydrogenase from Mixotrophic Tobacco Cells - Comparison with the Cytosolic Isoenzyme. *Plant Physiology* **105**, 593-600.
- Garg, A. K., Kim, J. K., Owens, T. G., Ranwala, A. P., Do Choi, Y., Kochian, L. V. and Wu, R. J.** (2002). Trehalose accumulation in rice plants confers high tolerance levels to different abiotic stresses. *Proceedings of the National Academy of Sciences of the United States of America* **99**, 15898-15903.
- Gaxiola, R. A., Li, J. S., Undurraga, S., Dang, L. M., Allen, G. J., Alper, S. L. and Fink, G. R.** (2001). Drought- and salt-tolerant plants result from overexpression of the AVP1 H⁺-pump. *Proceedings of the National Academy of Sciences of the United States of America* **98**, 11444-11449.
- Giavalisco, P., Nordhoff, E., Kreitler, T., Kloppel, K. D., Lehrach, H., Klose, J. and Gobom, J.** (2005). Proteome analysis of *Arabidopsis thaliana* by two-dimensional gel electrophoresis and matrix-assisted laser desorption/ionisation-time of flight mass spectrometry. *Proteomics* **5**, 1902-1913.
- Gottlieb, D. M., Schultz, J., Bruun, S. W., Jacobsen, S. and Sondergaard, I.** (2004). Multivariate approaches in plant science. *Phytochemistry* **65**, 1531-1548.
- Han, F., Romagosa, I., Ullrich, S. E., Jones, B. L., Hayes, P. M. and Wesenberg, D. M.** (1997). Molecular marker-assisted selection for malting quality traits in barley. *Molecular Breeding* **3**, 427-437.
- Hand, S. C., Jones, D., Menze, M. A. and Witt, T. L.** (2007). Life without water: expression of plant LEA genes by an anhydrobiotic arthropod. *Journal of Experimental Zoology Part A: Ecological Genetics and Physiology* **307A**, 62-66.
- Haslekas, C., Stacy, R. A. P., Nygaard, V., Cullianez-Macia, F. A. and Aalen, R. B.** (1998). The expression of a peroxiredoxin antioxidant gene, AtPer1, in *Arabidopsis thaliana* is seed-specific and related to dormancy. *Plant Molecular Biology* **36**, 833-845.
- Haslekas, C., Viken, M. K., Grini, P. E., Nygaard, V., Nordgard, S. H., Meza, T. J. and Aalen, R. B.** (2003). Seed 1-Cysteine Peroxiredoxin Antioxidants Are Not Involved in

Dormancy, But Contribute to Inhibition of Germination during Stress. *Plant Physiology* **133**, 1148-1157.

Hausmann, L. and Toepfer, R. (1999). Entwicklung von Plasmidvektoren. In *Vorträge für Pflanzenzüchtung: Bioengineering für Rapsorten nach Maß*, vol. 45 eds. D. Brauer G. Röbbelen and R. Toepfer), pp. 155-172. Göttingen.

Hayes, P., Chen, F., Kleinhofs, A., Kilian, A. and Mather, D. (1996). Barley genome mapping and its applications. In *Method of genome analysis in plants*, (ed. P. Jauhar), pp. 229-49. Boca Raton: CRC Press.

Heldt, H. (2003). Pflanzenbiochemie. Heidelberg, Berlin: Spektrum Akademischer Verlag.

Hensel, G., Valkov, V., Middlefell-Williams, J. and Kumlehn, J. (2008). Efficient generation of transgenic barley: The way forward to modulate plant-microbe interactions. *Journal of Plant Physiology* **165**, 71-82.

Hoagland, D. and Arnon, D. (1950). The water culture method for growing plants without soil. *Calif Agric Exp Stn Circ.* **347**.

Hodges, M., Flesch, V., Galvez, S. and Bismuth, E. (2003). Higher plant NADP(+)-dependent isocitrate dehydrogenases, ammonium assimilation and NADPH production. *Plant Physiology and Biochemistry* **41**, 577-585.

Hong, Z. L., Lakkineni, K., Zhang, Z. M. and Verma, D. P. S. (2000). Removal of feedback inhibition of Delta(1)-pyrroline-5-carboxylate synthetase results in increased proline accumulation and protection of plants from osmotic stress. *Plant Physiology* **122**, 1129-1136.

Hsiao, T. C. and Xu, L. K. (2000). Sensitivity of growth of roots versus leaves to water stress: biophysical analysis and relation to water transport. *Journal of Experimental Botany* **51**, 1595-1616.

Hu, Y. and Schmidhalter, U. (1998). Spatial distributions of inorganic ions and sugars contributing to osmotic adjustment in the elongating wheat leaf under saline soil conditions. *Australian Journal of Plant Physiology* **25**, 591-597.

Huang, J., Zhang, H., Wang, J. and Yang, J. (2003). Molecular cloning and characterization of rice 6-phosphogluconate dehydrogenase gene that is up-regulated by salt stress. *Molecular Biology Reports* **30**, 223-227.

Huang, S., Spielmeyer, W., Lagudah, E. S. and Munns, R. (2008). Comparative mapping of HKT genes in wheat, barley, and rice, key determinants of Na⁺ transport, and salt tolerance. *Journal of Experimental Botany* **59**, 927-937.

Hynek, R., Svensson, B., Jensen, O. N., Barkholt, V. and Finnie, C. (2006). Enrichment and identification of integral membrane proteins from barley aleurone layers by reversed-phase chromatography, SDS-PAGE, and LC-MS/MS. *Journal of Proteome Research* **5**, 3105-3113.

Ingram, J. and Bartels, D. (1996). The Molecular Basis of Dehydration Tolerance in Plants. *Annual Review of Plant Physiology and Plant Molecular Biology* **47**, 377-403.

Jansen, R. C. and Nap, J.-P. (2001). Genetical genomics: the added value from segregation. *Trends in Genetics* **17**, 388-391.

Jiang, Y., Yang, B., Harris, N. S. and Deyholos, M. K. (2007). Comparative proteomic analysis of NaCl stress-responsive proteins in Arabidopsis roots. *Journal of Experimental Botany* **58**, 3591-3607.

Jiang, Y. Q. and Deyholos, M. K. (2006). Comprehensive transcriptional profiling of NaCl-stressed Arabidopsis roots reveals novel classes of responsive genes. *BMC Plant Biology* **6**.

- Joo, J. H., Bae, Y. S. and Lee, J. S.** (2001). Role of Auxin-Induced Reactive Oxygen Species in Root Gravitropism. *Plant Physiology* **126**, 1055-1060.
- Jornvall, H., von Bahr-Lindstrom, H., Jany, K.-D., Ulmer, W. and Froschle, M.** (1984). Extended superfamily of short alcohol-polyol-sugar dehydrogenases: structural similarities between glucose and ribitol dehydrogenases. *FEBS Letters* **165**, 190-196.
- Jorin, J. V., Rubiales, D., Dumas-Gaudot, E., Recorbet, G., Maldonado, A., Castillejo, M. A. and Curto, M.** (2006). Proteomics: a promising approach to study biotic interaction in legumes. A review. *Euphytica* **147**, 37-47.
- Kasprzewska, A.** (2003). Plant chitinases - Regulation and function. *Cellular & Molecular Biology Letters* **8**, 809-824.
- Katz, A., Waridel, P., Shevchenko, A. and Pick, U.** (2007). Salt-induced changes in the plasma membrane proteome of the halotolerant alga *Dunaliella salina* as revealed by blue native gel electrophoresis and nano-LC-MS/MS analysis. *Molecular & Cellular Proteomics* **6**, 1459-1472.
- Keurentjes, J. J. B., Fu, J., Terpstra, I. R., Garcia, J. M., van den Ackerveken, G., Snoek, L. B., Peeters, A. J. M., Vreugdenhil, D., Koornneef, M. and Jansen, R. C.** (2007). Regulatory network construction in *Arabidopsis* by using genome-wide gene expression quantitative trait loci. *PNAS* **104**, 1708-1713.
- Kikawada, T., Nakahara, Y., Kanamori, Y., Iwata, K.-I., Watanabe, M., McGee, B., Tunnacliffe, A. and Okuda, T.** (2006). Dehydration-induced expression of LEA proteins in an anhydrobiotic chironomid. *Biochemical and Biophysical Research Communications* **348**, 56-61.
- Kristensen, B. K., Bloch, H. and Rasmussen, S. K.** (1999). Barley coleoptile peroxidases. Purification, molecular cloning, and induction by pathogens. *Plant Physiology* **120**, 501-512.
- Lamanda, A., Zahn, A., Röder, D. and Langen, H.** (2004). Improved Ruthenium II tris (bathophenanthroline disulfonate) staining and destaining protocol for a better signal-to-background ratio and improved baseline resolution. *Proteomics* **4**, 599-608.
- Le, H., Chang, S.-C., Tanguay, R. L. and Gallie, D. R.** (1997). The wheat poly (A)-binding protein functionally complements Pab1 in yeast. *European Journal of Biochemistry* **243**, 350-357.
- Leah, R., Tommerup, H., Svendsen, I. and Mundy, J.** (1991). Biochemical and molecular characterisation of three barley seed proteins with antifungal properties. *Journal of Biological Chemistry* **266**, 1564-73.
- Lee, K. H., Kim, Y. S., Park, C. M. and Kim, H. J.** (2008). Proteomic identification of differentially expressed proteins in *Arabidopsis* mutant ntm1-D with disturbed cell division. *Molecules and Cells* **25**, 70-77.
- Lee, M. H., Min, M. K., Lee, Y. J., Jin, J. B., Shin, D. H., Kim, D. H., Lee, K. H. and Hwang, I.** (2002). ADP-ribosylation factor 1 of *Arabidopsis* plays a critical role in intracellular trafficking and maintenance of endoplasmic reticulum morphology in *Arabidopsis*. *Plant Physiology* **129**, 1507-1520.
- Li, J. and Burmeister, M.** (2005). Genetical genomics: combining genetics with gene expression analysis. *Human Molecular Genetics* **14**, R163-R169.
- Li, J., Huang, X. Q., Heinrichs, F., Ganai, M. W. and Röder, M. S.** (2005). Analysis of QTLs for yield, yield components, and malting quality in a BC3-DH population of spring barley. *Theoretical and Applied Genetics* **110**, 356-363.
-

- Lin, B.-L., Wang, J.-S., Liu, H.-C., Chen, R.-W., Meyer, Y., Barakat, A. and Delseny, M.** (2001). Genomic analysis of the Hsp70 superfamily in *Arabidopsis thaliana*. *Cell Stress Chaperones*, 201–8.
- Lin, C. C. and Kao, C. H.** (2001). Cell wall peroxidase activity, hydrogen peroxide level and NaCl-inhibited root growth of rice seedlings. *Plant and Soil* **230**, 135-143.
- Macherel, D., Benamar, A., Avelange-Macherel, M.-H. and Tolleter, D.** (2007). Function and stress tolerance of seed mitochondria. *Physiologia Plantarum* **129**, 233-241.
- Maeda, K., Finnie, C. and Svensson, B.** (2004). Cy5 maleimide labelling for sensitive detection of free thiols in native protein extracts: identification of seed proteins targeted by barley thioredoxin h isoforms. *Biochem J.* **1**, 497–507.
- Marmagne, A., Ferro, M., Meinel, T., Bruley, C., Kuhn, L., Garin, J., Barbier-Brygoo, H. and Ephritikhine, G.** (2007). A high content in lipid-modified peripheral proteins and integral receptor kinases features in the *Arabidopsis* plasma membrane proteome. *Molecular & Cellular Proteomics* **6**, 1980-1996.
- Martinez-Ballesta, M. d. C., Bastias, E., Zhu, C., Schaffner, A. R., Gonzalez-Moro, B., Gonzalez-Murua, C. and Carvajal, M.** (2008). Boric acid and salinity effects on maize roots. Response of aquaporins ZmPIP1 and ZmPIP2, and plasma membrane H⁺-ATPase, in relation to water and nutrient uptake. *Physiologia Plantarum* **132**, 479-490.
- Medalia, O., Weber, I., Frangakis, A. S., Nicastro, D., Gerisch, G. and Baumeister, W.** (2002). Macromolecular architecture in eukaryotic cells visualized by cryoelectron tomography. *Science* **298**, 1209-1213.
- Mittler, R., Vanderauwera, S., Gollery, M. and Van Breusegem, F.** (2004). Reactive oxygen gene network of plants. *Trends in Plant Science* **9**, 490-498.
- Moller, I. M.** (2001). Plant mitochondria and oxidative stress: Electron transport, NADPH turnover, and metabolism of reactive oxygen species. *Annual Review of Plant Physiology and Plant Molecular Biology* **52**, 561-591.
- Moller, I. S. and Tester, M.** (2007). Salinity tolerance of *Arabidopsis*: a good model for cereals? *Trends in Plant Science* **12**, 534-540.
- Moons, A., Bauw, G., Prinsen, E., Vanmontagu, M. and Vanderstraeten, D.** (1995). Molecular and physiological-responses to abscisic-acid and salts in roots of salt-sensitive and salt-tolerant indica rice varieties. *Plant Physiology* **107**, 177-186.
- Moons, A., Gielen, J., Vandekerckhove, J., Gheysen, G. and Van Montagu, M.** (1996). An abscisic acid and salt stress-responsive rice cDNA from a novel plant gene family. Submitted (OCT-1996) to the EMBL/GenBank/DDBJ databases, Cited for: NUCLEOTIDE SEQUENCE.
- Munns, R.** (2002). Comparative physiology of salt and water stress. *Plant, Cell & Environment* **25**, 239-250.
- Munns, R.** (2005). Genes and salt tolerance: bringing them together. *New Phytologist* **167**, 645-663.
- Munns, R., Husain, S., Rivelli, A. R., James, R. A., Condon, A. G. T., Lindsay, M. P., Lagudah, E. S., Schachtman, D. P. and Hare, R. A.** (2002). Avenues for increasing salt tolerance of crops, and the role of physiologically based selection traits. *Plant and Soil* **247**, 93-105.
- Munns, R., James, R. A. and Lauchli, A.** (2006). Approaches to increasing the salt tolerance of wheat and other cereals. *Journal of Experimental Botany* **57**, 1025-1043.
- Nakanishi, H., Yamaguchi, H., Sasakuma, T., Nishizawa, N. K. and Mori, S.** (2000). Two dioxygenase genes, *Ids3* and *Ids2*, from *Hordeum vulgare* are involved in the

biosynthesis of mugineic acid family phytosiderophores. *Plant Molecular Biology* **44**, 199-207.

Nieva, C., Busk, P., Dominguez-Puigjaner, E., Lumbreras, V., Testillano, P., Risueno, M.-C. and Pages, M. (2005). Isolation and functional characterisation of two new bZIP maize regulators of the ABA responsive gene rab28. *Plant Molecular Biology* **58**, 899-914.

Niogret, M. F., Culianez-Macia, F. A., Goday, A., Alba, M. M. and Pages, M. (1996). Expression and cellular localization of rab28 mRNA and Rab28 protein during maize embryogenesis. *The Plant Journal* **9**, 549-557.

O'Farrell, P. H. (1975). High-resolution 2-dimensional electrophoresis of proteins. *Journal of Biological Chemistry* **250**, 4007-4021.

Østergaard, O., Melchior, S., Roepstorff, P. and Svensson, B. (2002). Initial proteome analysis of mature barley seeds and malt. *Proteomics* **2**, 733-739.

Ozturk, Z. N., Talame, V., Deyholos, M., Michalowski, C. B., Galbraith, D. W., Gozukirmizi, N., Tuberosa, R. and Bohnert, H. J. (2002). Monitoring large-scale changes in transcript abundance in drought- and salt-stressed barley. *Plant Mol Biol* **48**, 551-73.

Palanivelu, R., Belostotsky, D. A. and Meagher, R. B. (2000). Conserved expression of Arabidopsis thaliana poly-(A) binding protein 2 (PAB2) in distinct vegetative and reproductive tissues. *The Plant Journal* **22**, 199-210.

Palmgren, M. G. (2001). Plant plasma membrane H⁺-ATPases: Powerhouses for nutrient uptake. *Annual Review of Plant Physiology and Plant Molecular Biology* **52**, 817-845.

Palomo, J., Gallardo, F., Suarez, M. F. and Canovas, F. M. (1998). Purification and characterization of NADP(+)-linked isocitrate dehydrogenase from Scots pine - Evidence for different physiological roles of the enzyme in primary development. *Plant Physiology* **118**, 617-626.

Pandey, A. and Mann, M. (2000). Proteomics to study genes and genomes. *Nature* **405**, 837-846.

Parker, R., Flowers, T. J., Moore, A. L. and Harpham, N. V. J. (2006). An accurate and reproducible method for proteome profiling of the effects of salt stress in the rice leaf lamina. *Journal of Experimental Botany* **57**, 1109-1118.

Passardi, F., Penel, C. and Dunand, C. (2004). Performing the paradoxical: how plant peroxidases modify the cell wall. *Trends in Plant Science* **9**, 534-40.

Picault, N., Palmieri, L., Pisano, I., Hodges, M. and Palmieri, F. (2002). Identification of a novel transporter for dicarboxylates and tricarboxylates in plant mitochondria. *J Biol Chem* **277**, 24204-11.

Pla, M., Gomez, J., Goday, A. and Pages, M. (1991). Regulation of the Abscisic Acid-Responsive Gene Rab28 in Maize Viviparous Mutants. *Molecular & General Genetics* **230**, 394-400.

Popov, N., Schmitt, M., Schulzeck, S. and Matthies, H. (1975). Reliable micromethod for determination of the protein content in tissue homogenates. *Acta Biol Med Ger* **34**, 1441-6.

Popova, O., Ismailov, S., Popova, T., Dietz, K.-J. and Gollidack, D. (2002). Salt-induced expression of NADP-dependent isocitrate dehydrogenase and ferredoxin-dependent glutamate synthase in *Mesembryanthemum crystallinum*. *Planta* **215**, 906-913.

- Pratt, W. B. and Toft, D. O.** (2003). Regulation of signaling protein function and trafficking by the hsp90/hsp70-based chaperone machinery. *Experimental Biology and Medicine* **228**, 111-133.
- Prioul, J. L., Quarrie, S., Causse, M. and deVienne, D.** (1997). Dissecting complex physiological functions through the use of molecular quantitative genetics. *Journal of Experimental Botany* **48**, 1151-1163.
- Qureshi, M. I., Qadir, S. and Zolla, L.** (2007). Proteomics-based dissection of stress-responsive pathways in plants. *Journal of Plant Physiology* **164**, 1239-1260.
- Rabilloud, T., Strub, J.-M., Lucbe, S., Dorselaer, A. v. and Lunardi, J.** (2001). A comparison between Sypro Ruby and ruthenium II tris (bathophenanthroline disulfonate) as fluorescent stains for protein detection in gels. *Proteomics* **1**, 699-704.
- Ratajczak, R., Hinz, G. and Robinson, D. G.** (1999). Localization of pyrophosphatase in membranes of cauliflower inflorescence cells. *Planta* **208**, 205-211.
- Roberts, J. K., DeSimone, N. A., Lingle, W. L. and Dure III, L.** (1993). Cellular concentrations and uniformity of cell-type accumulation of two *Lea* proteins in cotton embryos. *Plant Cell* **5**, 769-780.
- Roje, S.** (2006). S-Adenosyl-l-methionine: Beyond the universal methyl group donor. *Phytochemistry Rod Croteau Special Issue, Part 1* **67**, 1686-1698.
- Rouhier, N. and Jacquot, J. P.** (2002). Plant peroxiredoxins: alternative hydroperoxide scavenging enzymes. *Photosynthesis Research* **74**, 259-268.
- Roxas, V. P., Smith, R. K., Allen, E. R. and Allen, R. D.** (1997). Overexpression of glutathione S-transferase glutathione peroxidase enhances the growth of transgenic tobacco seedlings during stress. *Nature Biotechnology* **15**, 988-991.
- Rus, A., Lee, B. H., Munoz-Mayor, A., Sharkhuu, A., Miura, K., Zhu, J. K., Bressan, R. A. and Hasegawa, P. M.** (2004). AtHKT1 facilitates Na⁺ homeostasis and K⁺ nutrition in planta. *Plant Physiology* **136**, 2500-2511.
- Saab, I. N., Sharp, R. E., Pritchard, J. and Voetberg, G. S.** (1990). Increased endogenous abscisic-acid maintains primary root-growth and inhibits shoot growth of maize seedlings at low water potentials. *Plant Physiology* **93**, 1329-1336.
- Sage-Ono, K., Ono, M., Harada, H. and Kamada, H.** (1998). Dark-induced accumulation of mRNA for a homolog of translationally controlled tumor protein (TCTP) in *Pharbitis*. *Plant Cell Physiol.* **39**, 357-360.
- Sahi, C., Singh, A., Kumar, K., Blumwald, E. and Grover, A.** (2006). Salt stress response in rice: genetics, molecular biology, and comparative genomics. *Funct Integr Genomics* **6**, 263-84.
- Saijo, Y., Hata, S., Kyojuka, J., Shimamoto, K. and Izui, K.** (2000). Overexpression of a single Ca²⁺-dependent protein kinase confers both cold and salt/drought tolerance on rice plants. *Plant Journal* **23**, 319-327.
- Saldanha, A. J.** (2004). Java Treeview-extensible visualization of microarray data. *Bioinformatics* **20**, 3246-3248.
- Salekdeh, G., Siopongco, J., Wade, L., Ghareyazie, B. and Bennett, J.** (2002). A proteomic approach to analyzing drought- and salt-responsiveness in rice. *Field Crops Research* **76**, 199-219.
- Sambrook, J. and Russell, D. W.** (2001). *Molecular Cloning: A Laboratory Manual*: Cold Spring Harbor Laboratory Press.

Santoni, V. (2007). Plant plasma membrane protein extraction and solubilization for proteomic analysis. In *Methods in Molecular Biology*, vol. 335 eds. H. Thiellement M. Zivy C. Damerval and V. Méchin), pp. 93-109: Humana Press Inc.

Santoni, V., Verdoucq, L., Sommerer, N., Vinh, J., Pflieger, D. and Maurel, C. (2006). Methylation of aquaporins in plant plasma membrane. *Biochemical Journal* **400**, 189-197.

Schindler, J., Lewandrowski, U., Sickmann, A. and Friauf, E. (2008). Aqueous polymer two-phase systems for the proteomic analysis of plasma membranes from minute brain samples. *Journal of Proteome Research* **7**, 432-442.

Schlesier, B. and Mock, H.-P. (2006). Protein isolation and 2-D electrophoretic separation. In *Arabidopsis protocols*, eds. J. Sanchez-Serrano and J. Salinas).

Schultz, C. J. and Coruzzi, G. M. (1995). The aspartate aminotransferase gene family of Arabidopsis encodes isoenzymes localized to three distinct subcellular compartments. *The Plant Journal* **7**, 61-75.

Sharp, R. E., Wu, Y. J., Voetberg, G. S., Saab, I. N. and Lenoble, M. E. (1994). Confirmation that abscisic-acid accumulation is required for maize primary root elongation at low water potentials. *Journal of Experimental Botany* **45**, 1743-1751.

Shi, C., Uzarowska, A., Ouzunova, M., Landbeck, M., Wenzel, G. and Lubberstedt, T. (2007). Identification of candidate genes associated with cell wall digestibility and eQTL (expression quantitative trait loci) analysis in a Flint x Flint maize recombinant inbred line population. *BMC Genomics* **8**, 22.

Shi, H. Z., Lee, B. H., Wu, S. J. and Zhu, J. K. (2003). Overexpression of a plasma membrane Na⁺/H⁺ antiporter gene improves salt tolerance in Arabidopsis thaliana. *Nature Biotechnology* **21**, 81-85.

Shigeoka, S., Ishikawa, T., Tamoi, M., Miyagawa, Y., Takeda, T., Yabuta, Y. and Yoshimura, K. (2002). Regulation and function of ascorbate peroxidase isoenzymes. *Journal of Experimental Botany* **53**, 1305-1319.

Silva, J. C., Denny, R., Dorschel, C., Gorenstein, M. V., Li, G. Z., Richardson, K., Wall, D. and Geromanos, S. J. (2006a). Simultaneous qualitative and quantitative analysis of the Escherichia coli Proteome - A sweet tale. *Molecular & Cellular Proteomics* **5**, 589-607.

Silva, J. C., Denny, R., Dorschel, C. A., Gorenstein, M., Kass, I. J., Li, G. Z., McKenna, T., Nold, M. J., Richardson, K., Young, P. et al. (2005). Quantitative proteomic analysis by accurate mass retention time pairs. *Analytical Chemistry* **77**, 2187-2200.

Silva, J. C., Gorenstein, M. V., Li, G. Z., Vissers, J. P. C. and Geromanos, S. J. (2006b). Absolute quantification of proteins by LC-MS^E - A virtue of parallel MS acquisition. *Molecular & Cellular Proteomics* **5**, 144-156.

Singla-Pareek, S. L., Reddy, M. K. and Sopory, S. K. (2003). Genetic engineering of the glyoxalase pathway in tobacco leads to enhanced salinity tolerance. *Proceedings of the National Academy of Sciences* **100**, 14672-14677.

Sondergaard, T. E., Schulz, A. and Palmgren, M. G. (2004). Energization of transport processes in plants. Roles of the plasma membrane H⁺-ATPase. *Plant Physiology* **136**, 2475-2482.

Speers, A. E. and Wu, C. C. (2007). Proteomics of integral membrane proteins - Theory and application. *Chemical Reviews* **107**, 3687-3714.

Sreenivasulu, N., Radchuk, V., Strickert, M., Miersch, O., Weschke, W. and Wobus, U. (2006). Gene expression patterns reveal tissue-specific signaling networks

controlling programmed cell death and ABA-regulated maturation in developing barley seeds. *Plant Journal* **47**, 310-327.

Sreenivasulu, N., Usadel, B., Winter, A., Radchuk, V., Scholz, U., Stein, N., Weschke, W., Strickert, M., Close, T. J., Stitt, M. et al. (2008). Barley grain maturation and germination: Metabolic pathway and regulatory network commonalities and differences highlighted by new MapMan/PageMan profiling tools. *Plant Physiology* **146**, 1738-1758.

Stacy, R., Munthe, E., Steinum, T., Sharma, B. and Aalen, R. (1996). A peroxiredoxin antioxidant is encoded by a dormancy-related gene, *Per1*, expressed during late development in the aleurone and embryo of barley grains. *Plant Molecular Biology* **31**, 1205-16.

Stacy, R. A. P., Nordeng, T. W., Culianez-Macia, F. A. and Aalen, R. B. (1999). The dormancy-related peroxiredoxin anti-oxidant, *PER1*, is localized to the nucleus of barley embryo and aleurone cells. *The Plant Journal* **19**, 1-8.

Still, D. W., Kovach, D. A. and Bradford, K. J. (1994). Development of desiccation tolerance during embryogenesis in rice (*Oryza sativa*) and wild rice (*Zizania palustris*) (Dehydrin expression, abscisic acid content, and sucrose accumulation). *Plant Physiology* **104**, 431-438.

Stylianou, I. M., Affourtit, J. P., Shockley, K. R., Wilpan, R. Y., Abdi, F. A., Bhardwaj, S., Rollins, J., Churchill, G. A. and Paigen, B. (2008). Applying gene expression, proteomics and SNP analysis for complex trait gene identification. *Genetics*, 107.081216.

Sung, D. Y., Vierling, E. and Guy, C. L. (2001). Comprehensive expression profile analysis of the Arabidopsis Hsp70 gene family. *Plant Physiology* **126**, 789-800.

Taiz, L. and Zeiger, E. (2006). *Plant Physiology*. Sunderland, Massachusetts: Sinauer Associates, Inc.

Tanksley, S. D. and Nelson, J. C. (1996). Advanced backcross QTL analysis: A method for the simultaneous discovery and transfer of valuable QTLs from unadapted germplasm into elite breeding lines. *Theoretical and Applied Genetics* **92**, 191-203.

Tohge, T., Nishiyama, Y., Hirai, M. Y., Yano, M., Nakajima, J., Awazuhara, M., Inoue, E., Takahashi, H., Goodenowe, D. B., Kitayama, M. et al. (2005). Functional genomics by integrated analysis of metabolome and transcriptome of Arabidopsis plants over-expressing an MYB transcription factor. *Plant Journal* **42**, 218-235.

Tong, Y., Zhou, J.-J., Li, Z. and Miller, A. J. (2005). A two-component high-affinity nitrate uptake system in barley, vol. 41, pp. 442-450.

Ueda, A., Kathiresan, A., Bennett, J. and Takabe, T. (2006). Comparative transcriptome analyses of barley and rice under salt stress. *Theor Appl Genet* **112**, 1286-94.

Ueda, A., Shi, W., Nakamura, T. and Takabe, T. (2002). Analysis of salt-inducible genes in barley roots by differential display. *J Plant Res* **115**, 119-130.

Valderrama, R., Corpas, F. J., Carreras, A., Gomez-Rodriguez, M. V., Chaki, M., Pedrajas, J. R., Fernandez-Ocana, A., Del Rio, L. A. and Barroso, J. B. (2006). The dehydrogenase-mediated recycling of NADPH is a key antioxidant system against salt-induced oxidative stress in olive plants. *Plant, Cell & Environment* **29**, 1449-1459.

Varshney, R. K., Graner, A. and Sorrells, M. E. (2005). Genomics-assisted breeding for crop improvement. *Trends in Plant Science 10th Anniversary Issue - Feeding the World: Plant Biotechnology Milestones* **10**, 621-630.

- Vickers, C., Xue, G. and Gresshoff, P. (2006). A novel cis-acting element, ESP, contributes to high-level endosperm-specific expression in an oat globulin promoter. *Plant Molecular Biology* **62**, 195-214.
- Vij, S. and Tyagi, A. K. (2007). Emerging trends in the functional genomics of the abiotic stress response in crop plants. *Plant Biotechnology Journal* **5**, 361-380.
- Vissers, J. P. C., Langridge, J. I. and Aerts, J. M. F. G. (2007). Analysis and quantification of diagnostic serum markers and protein signatures for gaucher disease. *Mol Cell Proteomics* **6**, 755-766.
- Walia, H., Wilson, C., Condamine, P., Liu, X., Ismail, A. M. and Close, T. J. (2007). Large-scale expression profiling and physiological characterization of jasmonic acid-mediated adaptation of barley to salinity stress. *Plant, Cell & Environment* **30**, 410-421.
- Walia, H., Wilson, C., Wahid, A., Condamine, P., Cui, X. and Close, T. (2006). Expression analysis of barley (*Hordeum vulgare* L.) during salinity stress. *Funct Integr Genomics* **6**, 143-56.
- Wang, M.-C., Peng, Z.-Y., Li, C.-L., Li, F., Liu, C. and Xia, G.-M. (2008). Proteomic analysis on a high salt tolerance introgression strain of *Triticum aestivum*/*Thinopyrum ponticum*. *Proteomics* **8**, 1470-1489.
- Wang, W. X., Vinocur, B., Shoseyov, O. and Altman, A. (2004). Role of plant heat-shock proteins and molecular chaperones in the abiotic stress response. *Trends in Plant Science* **9**, 244-252.
- Weber, A. and Flügge, U. (2002). Interaction of cytosolic and plastidic nitrogen metabolism in plants. *J Exp Bot* **53**, 865-74.
- Weidner, A., Dadshani, S., Hakizimana, S., Buck-Sorlin, G. and Boerner, A. (2005). Möglichkeiten der Nutzung von Genbankmaterial zur Steigerung der Salztoleranz im Weizen und der Gerste. *Vortr. Pflanzenzüchtg.* **67**, 53-5.
- West, M. A. L., Kim, K., Kliebenstein, D. J., van Leeuwen, H., Michelmore, R. W., Doerge, R. W. and St. Clair, D. A. (2007). Global eQTL Mapping Reveals the Complex Genetic Architecture of Transcript-Level Variation in *Arabidopsis*. *Genetics* **175**, 1441-1450.
- Willekens, H., Chamnongpol, S., Davey, M., Schraudner, M., Langebartels, C., VanMontagu, M., Inze, D. and VanCamp, W. (1997). Catalase is a sink for H₂O₂ and is indispensable for stress defence in C-3 plants. *Embo Journal* **16**, 4806-4816.
- Witzel, K., Surabhi, G.-K., Jyothsnakumari, G., Sudhakar, C., Matros, A. and Mock, H.-P. (2007). Quantitative Proteome Analysis of Barley Seeds Using Ruthenium(II)-tris-(bathophenanthroline-disulphonate) Staining. *J. Proteome Res.* **6**, 1325-33.
- Xu, D., Duan, X., Wang, B., Hong, B., Ho, T. and Wu, R. (1996). Expression of a Late Embryogenesis Abundant Protein Gene, HVA1, from Barley Confers Tolerance to Water Deficit and Salt Stress in Transgenic Rice. *Plant Physiology* **110**, 249-257.
- Xu, P., Harvey, A. J. and Fincher, G. B. (1994). Heterologous expression of cDNAs encoding barley (*Hordeum vulgare*) (1 → 3)-[beta]-glucanase isoenzyme GV. *FEBS Letters* **348**, 206-210.
- Xu, P. L., Wang, J. and Fincher, G. B. (1992). Evolution and Differential Expression of the (1- 3)-Beta-Glucan Endohydrolase-Encoding Gene Family in Barley, *Hordeum vulgare*. *Gene* **120**, 157-165.
- Yamaguchi, H., Nakanishi, H., Nishizawa, N. K. and Mori, S. (2000a). Induction of the IDI1 gene in Fe-deficient barley roots: A gene encoding a putative enzyme that catalyses the methionine salvage pathway for phyto siderophore production. *Soil Science and Plant Nutrition* **46**, 1-9.
-

Yamaguchi, H., Nakanishi, H., Nishizawa, N. K. and Mori, S. (2000b). Isolation and characterization of IDI2, a new Fe-deficiency-induced cDNA from barley roots, which encodes a protein related to the alpha subunit of eukaryotic initiation factor 2B. *Journal of Experimental Botany* **51**, 2001-2007.

Yan, S., Tang, Z., Su, W. and Sun, W. (2005). Proteomic analysis of salt stress-responsive proteins in rice root. *Proteomics* **5**, 235-44.

Yano, H. and Kuroda, M. (2006). Disulfide proteome yields a detailed understanding of redox regulations: A model study of thioredoxin-linked reactions in seed germination. *Proteomics* **6**, 294-300.

Yeh, S., Moffatt, B. A., Griffith, M., Xiong, F., Yang, D. S. C., Wiseman, S. B., Sarhan, F., Danyluk, J., Xue, Y. Q., Hew, C. L. et al. (2000). Chitinase genes responsive to cold encode antifreeze proteins in winter cereals. *Plant Physiology* **124**, 1251-1264.

7. Abbreviations

(m)RNA	(messenger) ribonucleic acid
6PGDH	6-phosphogluconate dehydrogenase
ABA	abscisic acid
ANOVA	analysis of variance
APX	ascorbate peroxidase
ATP	adenosine triphosphate
BiP	luminal binding protein
BSA	bovine serum albumin
cCBB	colloidal Coomassie Brilliant Blue
CHAPS	3-[(3-cholamidopropyl)dimethylammonio]-1-propansulfonate
Da	Dalton
DLH	dienelactone hydrolase
DNA	desoxyribonucleic acid
DTT	1,4-dithiothreitol
EF	elongation factor
EMRT	exact mass retention time
EST	expressed sequence tag
g	gram
GA	giberellic acid
GlucDH	glucose and ribitol dehydrogenase homolog
GST	glutathione transferase
GTP	guanosine triphosphate
h	hour
HKT	high-affinity K ⁺ transporter
Hsp	heat shock protein
IEF	isoelectric focussing
IL	introgression line
IPG	immobilised pH gradient
IPK	Leibniz-Institute for Plant Genetics and Cop Plant Research
JA	jasmonic acid
k	kilo
l	litre
LC-ESI-Q-TOF MS	liquid chromatography electrospray-ionisation quadrupole time-of-flight mass spectrometry
LEA	late embryogenesis abundant
m	milli or meter
M	mol
MALDI-TOF MS	matrix-assisted laser disorption ionisation time-of-flight mass spectrometry

MDAR	monodehydroascorbate dehydrogenase
min	minute
MOPS	3-(N-mMorpholino)-propansulfonate
MS ^E	mass spectrometry with elevated energy
MW	molecular weight
NADPH	nicotinamide adenine dinucleotide phosphate
NADP-ICDH	NADP-specific isocitrate dehydrogenase
OWB population	Oregon Wolfe Barley population
PCA	principle component analysis
PEG	polyethylene glycol
pI	isoelectric point
PM	plasma membrane
PS	phytosiderophore
PTM	post-translational modification
QTL analysis	quantitative trait loci analysis
ROS	reactive oxygen species
RuBP	ruthenium II tris (bathophenanthroline disulfonate)
SAM	S-adenosylmethionine
SDS-PAGE	sodium dodecyl polyacrylamide gel electrophoresis
SM population	Steptoe Morex population
SOD	superoxide dismutase
TCA	trichloroacetic acid or tricarboxylic acid cycle
TCTP	translationally controlled tumor protein homolog
TFA	trifluoroacetic acid
TMD	transmembrane domain
TPR	tetratricopeptide repeat
UPLC	ultra performance liquid chromatography
v/v	volume-to-volume ratio
Vol	volume
w/v	weight-to-volume ratio
x g	gravitation force

8. Acknowledgements

At this point I would like to express my thanks to all colleagues contributing to this thesis by any means.

I would like to thank my PhD supervisor Dr Hans-Peter Mock for giving me the opportunity to work in his group on this interesting topic and to share the outcome with the scientific community at meetings. His advice and suggestions with the experimental design and data analysis as well as his support in writing this thesis are highly appreciated.

For reviewing my thesis I'm very grateful to Prof Dr Klaus Humbeck at the Martin-Luther-University in Halle.

Part of my work was embedded in the GABI-SEED II project at IPK and I would like to thank all members of the GABI consortium for their cooperation, especially the coordinator of the project, Prof Dr Ulrich Wobus. I also would like to thank Drs Christof Pietsch and Marc Strickert not only for the bioinformatic processing of proteome data but also for making the results understandable for a biologist.

The second part of my work was addressed to investigate salt tolerance mechanisms using mapping populations. Here I would like to thank Drs Annette Weidner and Andreas Börner for sharing the results of the germination assays, for providing barley grain material and for helpful discussions on the work.

I'm very grateful to Prof Dr Birte Svensson and Assoc. Prof Dr Christine Finnie for supervising my work during my stay at the Enzyme and Protein Chemistry group at the Technical University of Denmark. For his advice while I was trying to become familiar with plasma membranes I would like to thank Dr Anders Møller.

For providing the transformation vectors and for performing the stable plant transformations I would like to thank Dr Götz Hensel and Conny Marthe. As the mentor of my PhD work I'm grateful to Dr Jochen Kumlehn for helpful discussions and comments on this thesis.

I would like to express my special thanks to all members of the Applied Biochemistry group at IPK for their support and cooperation. I thank Drs Andrea Matros and Bernhard Schlesier for valuable advice with handling the MS instrumentation and Stephanie Kaspar for her help with the Expression system. I'm also grateful to Christiane Hedtmann for her assistance with the molecular cloning and the inevitable distraction from work. For excellent technical assistance I would like to thank Petra Linow and especially Annegret Wolf.

Highly appreciated is the work carried out by the technical staff of the Molecular Cell Biology department at IPK, Christa Kallas, Elis Fraust and Dagmar Böhmert. For plant photographs I'm grateful to Heike Ernst.

Financial support of the work from BMBF (FKZ 0313115) and COST organisation (FA0603-03178) is gratefully acknowledged.

Last but not least, I would like to thank my parents and my sisters for their constant support throughout the years.

9. Curriculum vitae

Name : Katja Witzel
Date of Birth: 07.04.1978
Place of Birth: Nordhausen
Nationality: German
Marital Status: Unmarried

Scientific Career

01/2005	PhD student	Leibniz Institute of Plant Genetics and Crop Plant Research Gatersleben, Dept. Molecular Cell Biology, Applied Biochemistry Group
12/2003-12/2004	PhD student	Leibniz Institute of Plant Genetics and Crop Plant Research Gatersleben, Dept. Molecular Cell Biology, Molecular Plant Physiology Group
02/-11/2003	Graduate Research Assistant, Research Associate	Friedrich-Schiller-University Jena, Dept. of Biology and Pharmacy, General Plant Biology Group
08/2000-08/2001, 02/-09/2003	Graduate Research Assistant	Max-Planck-Institute of Chemical Ecology Jena, Department of Biochemistry

Education

10/-12/2007	Visit of the laboratory of Prof. Birte Svensson (Enzyme and Protein Chemistry group, Technical University of Denmark, Lyngby, Denmark) as recipient of a Short Term Scientific Fellowship by the COST Organisation
08/2002- 09/2003	Diploma thesis 'Comparative Analysis of Gene Expression of Prenyltransferases in Norway Spruce (Picea abies)' at the Max-Planck-Institute of Chemical Ecology, Department of Biochemistry Graduation: Diploma
09/2001-	Postgraduate studies at the University Vigo, Spain, as recipient of the

-
- 03/2002 ERASMUS fellowship by the European Commission
- 1997-2003 Study of Biology, Friedrich-Schiller-University Jena, Department of Biology and Pharmacy
- 1997 Final secondary-school examinations, Staatliche Berufsbildende Schule Nordhausen

Peer Reviewed Publications

Strickert, M., Witzel, K., Keilwagen, J., Mock, H.-P., Schneider, P., Biehl M. and Villmann, T. (2008) Adaptive Matrix Metrics for Attribute Dependence Analysis in Differential High-Throughput Data. Fifth International Workshop on Computational Systems Biology (WCSB 2008), Leipzig.

Witzel, K., Surabhi, G.-K., Jyothsnakumari, G., Sudhakar, C., Matros, A. and Mock, H.-P. (2007) Quantitative Proteome Analysis of Barley Seeds Using Ruthenium(II)-tris-(bathophenanthroline-disulphonate) Staining. *J. Proteome Res.*, 6, 1325-1333.

Strickert, M., Witzel, K., Mock, H.-P., Schleif, F.-M. and Villmann, T. (2007) Supervised Attribute Relevance Determination for Protein Identification in Stress Experiments. Proceedings of the International Workshop on Machine Learning in Systems Biology (MLSB 2007), Paris.

Oral presentations

Proteomic Approaches to Evaluate Agronomic Traits in Crop and Model Plants. – Plant Proteomics in Europe, COST Action Meeting FA0603, Munich, 20.-21.09.2007

Proteome Analysis of a Barley Mapping Population. - IPK Student Conference, Gatersleben, 29.05.-01.06.2006

Proteome Analysis of a Barley Mapping Population. - Proteomlux Conference, Luxembourg, 11.-14.10.2006

Proteome Analysis of Barley Seeds. - IPK Student Conference, Gatersleben, 22.-25.06.2005

Poster presentations

K. Witzel, A. Møller, C. Finnie, A. Boerner, A. Matros, B. Svensson and H.-P. Mock. Proteome Analysis of Plasma Membrane Proteins in Barley Cultivars with Different Tolerance Towards Salt Stress. - Plant Proteomics in Europe, COST Action Meeting FA0603, Cordoba, 06.-08.02.2008

A. Møller, K. Witzel, R. Hynek, B. Andersen, B. Svensson, D. B. Collinge, J. D. Jensen, J. K. Schjoerring and C. Finnie. Barley Plasma Membrane Proteomics: Identification of Protein Targets for Improvement of Crop Plants. - Plant Proteomics in Europe, COST Action Meeting FA0603, Cordoba, 06.-08.02.2008

A. Kaczmarczyk, K. Witzel, A. Matros and H.-P. Mock. Investigations on cryopreservation of potato shoot tips – new results using a proteomics approach. - Institut's Day IPK, Gatersleben, Germany, 22.-23.10.2007

K. Witzel, M. Strickert, A. Weidner, A. Boerner and H.-P. Mock. Proteomic Investigation of Salt Tolerance Mechanisms of Barley Using the Genetic Variation of Mapping Populations. - Plant Proteomics in Europe, COST Action Meeting FA0603, Munich, 20.-21.09.2007

K. Witzel, A. Matros and H.-P. Mock. Proteome Analysis of a Barley Mapping Population. - DGMS (German Association for Mass Spectrometry), 40th Annual Meeting, Bremen, 11.-14.03.2007

K. Witzel, C. Klukas, F. Schreiber, C. Pietsch, M. Röder, U. Seiffert, A. Matros and H.-P. Mock. Proteome Analysis of a Barley Mapping Population. - 7th GABI Status Seminar, Potsdam, 06.-08.03.2007

K. Witzel, A. Weidner, A. Matros and H.-P. Mock. Seed Proteome Analysis of Accessions from the Oregon Wolfe Barley Mapping Population Differing in their Salt Tolerance. -

DGMS (German Association for Mass Spectrometry), 39th Annual Meeting, Mainz, 05.-08.03.2006

K. Witzel, A. Matros and H.-P. Mock. Proteome Analysis of a Barley Mapping Population. - HUPO, 4th Annual World Congress, Munich, 28.08-01.09.2005

10. Affirmation

Hereby, I declare that all the work presented in this dissertation is my own, carried out solely with the help of the literature and the aids cited.

Ich erkläre hiermit, dass ich mich mit der vorliegenden wissenschaftlichen Arbeit erstmals um die Erlangung des Doktorgrades bewerbe. Ich erkläre die Arbeit selbstständig und ohne fremde Hilfe verfasst, nur die von mir angegebenen Quellen und Hilfsmittel benutzt und die den benutzten Werken wörtlich oder inhaltlich entnommenen Stellen als solche kenntlich gemacht habe.

Gatersleben, Juni 2008

Katja Witzel

11. Appendix

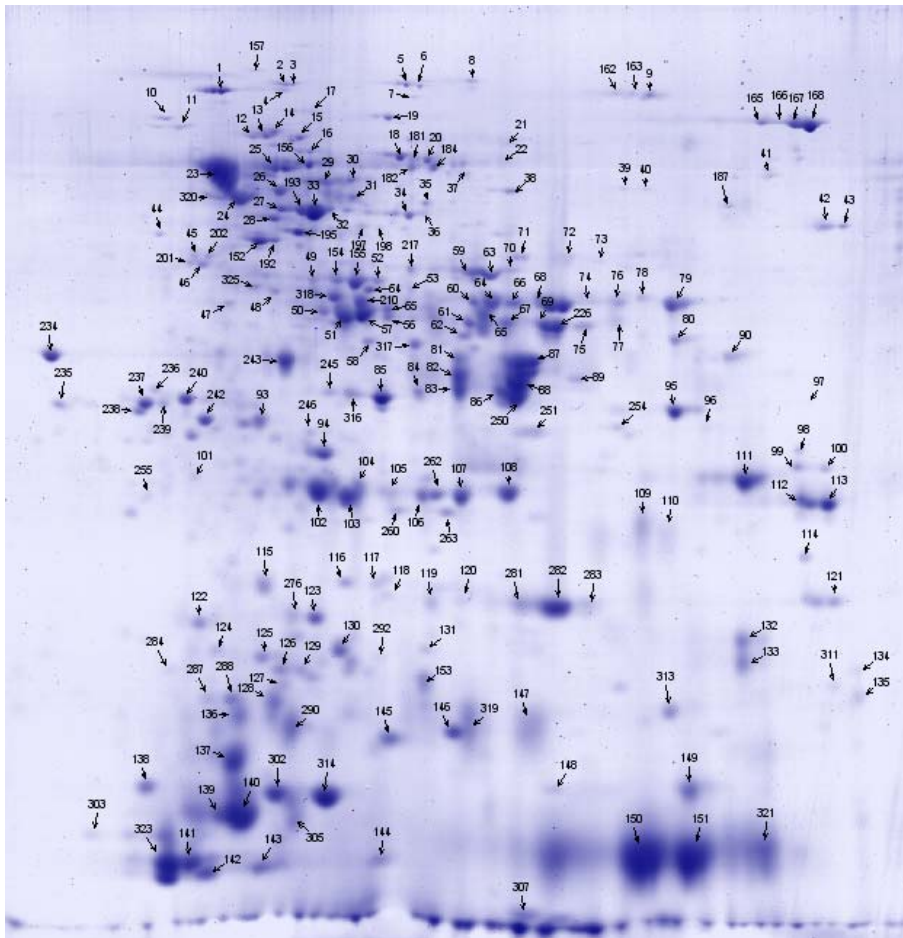


Figure A1: Proteins identified in the water-soluble seed proteome of barley cv. Brenda.

Table A1: Proteins identified from the barley cv. Brenda seed proteome. Given are the name, the organism the protein identity came from and the protein accession number. ExPASy tools were used for the calculation of the theoretical values for Mw and pI (http://us.expasy.org/tools/pi_tool.html). The proteins were assigned to functional categories. When identification via MALDI-TOF MS and ESI-Q-TOF MS/MS failed, proteins were referred as not identified (ni).

Spot	Name	Protein source	Accession	Mw (kDa)	pI	Classification
1	Hypothetical protein	Oryza sativa	TC143234	48.34	4.85	unclear
2	Pyruvate phosphate dikinase	Zea mays	gi:62738112	95.19	5.27	Energy
3	Orthophosphate dikinase	Oryza sativa	TC146954	102.80	5.89	Energy
4	cDNA clone	Hordeum vulgare	AJ466073			unclear
5	Putative aconitate hydratase	Oryza sativa	TC146875	98.08	5.67	Energy
6	Aconitate hydratase	Cucurbita maxima	TC139409	98.00	5.74	Energy
7	ni					
8	ni					
9	D hordein	Hordeum vulgare	gi:671537	50.78	7.60	Protein destination and storage
10	ni					
11	Heat shock protein 70	Triticum aestivum	gi:6670931	39.70	4.56	Disease and defence
12	Heat shock protein cognate 70	Oryza sativa	TC138914	71.31	5.10	Disease and defence
13	Heat shock protein 70	Zea mays	gi:59799993	40.98	4.78	Disease and defence
14	Heat shock protein 70 precursor	Hordeum vulgare	TC147130	67.01	5.76	Disease and defence
15	Putative heat shock protein 70	Oryza sativa	TC139412	70.44	5.45	Disease and defence
16	Phosphoglucomutase	Triticum aestivum	TC146784	62.78	5.66	Energy
17	Methionine synthase	Sorghum bicolor	TC131380	83.78	5.93	Metabolism
18	Phosphoglyceromutase	Ricinus communis	TC136118	60.81	5.52	Energy
19	ni					
20	NADP malic enzyme	Oryza sativa	TC139309	64.26	6.50	Metabolism
21	ni					
22	Putative tDET1 protein	Oryza sativa	TC142571	59.25	7.65	Signal transduction
23	Protein disulfide-isomerase precursor	Hordeum vulgare	TC146674	56.46	5.02	Protein destination and storage
24	Protein disulfide-isomerase	Hordeum vulgare	gi:493591	33.22	4.81	Protein destination and storage
25	Protein disulfide-isomerase precursor	Hordeum vulgare	TC146674	56.46	5.02	Protein destination and storage

26	Beta-amylase	Hordeum vulgare	gi:113786	59.64	5.58	Metabolism
27	Enolase	Oryza sativa	gi:55297212	47.93	5.38	Energy
28	UTP-glucose-1-phosphate uridylyltransferase	Hordeum vulgare	TC139210	51.64	5.20	Metabolism
29	Beta-amylase	Hordeum vulgare	TC146664	59.57	5.51	Metabolism
30	Beta-amylase	Hordeum vulgare	TC146664	59.57	5.51	Metabolism
31	Leucine aminopeptidase	Oryza sativa	TC147191	61.81	8.29	Protein destination and storage
32	Enolase	Oryza sativa	TC138581	47.97	5.41	Energy
33	Enolase	Oryza sativa	gi:780372	47.98	5.42	Energy
34	Alanine aminotransferase 2	Hordeum vulgare	TC146731	52.60	5.93	Energy
35	Glutathione reductase	Triticum monococcum	TC131783	53.01	5.93	Metabolism
36	Gamma-1-coat protein	Oryza sativa	TC147625	98.60	5.11	Intracellular traffic
37	Pyrophosphate-fructose-6-phosphate-1-phosphotransferase	Ricinus communis	TC139326	60.11	6.19	Energy
38	Putative dihydrolipoamide dehydrogenase	Oryza sativa	TC147317	52.73	7.63	Energy
39	Putative late embryogenesis abundant protein	Oryza sativa	gi:47497112	47.31	6.40	unclear
40	ni					
41	F-box protein family-like	Oryza sativa	TC140872	28.02	4.62	unclear
42	Enhancer of zeste protein	Oryza sativa	gi:29565495	99.77	8.00	unclear
43	Putative enolase	Oryza sativa	gi:31430374	45.94	5.16	Energy
44	Putative RAD23 protein	Oryza sativa	gi:53793163	43.07	4.70	Transcription
45	ni					
46	Putative heat shock protein 70	Hordeum vulgare	gi:2695923	12.14	6.23	Disease and defence
47	ni					
48	Protein disulfide-isomerase precursor	Triticum aestivum	gi:7437387	56.53	4.99	Protein destination and storage
49	Succinyl-CoA ligase precursor	Oryza sativa	TC146930	44.86	5.80	Metabolism
50	Malate dehydrogenase	Zea mays	TC146609	35.58	5.77	Energy
51	Malate dehydrogenase	Zea mays	TC146609	35.58	5.77	Energy
52	Protein z-type serpin	Hordeum vulgare	TC139095	43.22	5.61	Protein destination and storage

53	Putative receptor-like kinase	<i>Oryza sativa</i>	gi:50900768	59.32	8.61	unclear
54	Phosphoglycerate kinase	<i>Triticum aestivum</i>	TC146369	42.12	5.64	Energy
55	Protein z-type serpin	<i>Hordeum vulgare</i>	TC139095	43.22	5.61	Protein destination and storage
56	Protein z-type serpin	<i>Hordeum vulgare</i>	TC139095	43.22	5.61	Protein destination and storage
57	Protein z-type serpin	<i>Hordeum vulgare</i>	gi:1310677	43.22	5.61	Protein destination and storage
58	ni					
59	Alcohol dehydrogenase	<i>Hordeum vulgare</i>	TC146599	40.90	6.28	Energy
60	Glyceraldehyde-3-phosphate dehydrogenase	<i>Hordeum vulgare</i>	TC131363	36.51	6.67	Energy
61	Glyceraldehyde-3-phosphate dehydrogenase	<i>Hordeum vulgare</i>	gi:167044	33.23	6.20	Energy
62	Malate dehydrogenase	<i>Oryza sativa</i>	TC146529	35.46	8.74	Energy
63	Late embryogenesis abundant protein-like	<i>Arabidopsis thaliana</i>	TC132136	52.08	5.29	Disease and defence
64	Actin 1	<i>Zea mays</i>	TC131421	41.61	5.22	Cell structure
65	Fructose-1-6-bisphosphate aldolase	<i>Oryza sativa</i>	TC146546	38.86	6.96	Energy
66	Glyceraldehyde-3-phosphate dehydrogenase	<i>Hordeum vulgare</i>	TC131363	36.51	6.67	Energy
67	Glyceraldehyde-3-phosphate dehydrogenase	<i>Hordeum vulgare</i>	gi:167044	33.23	6.20	Energy
68	Glyceraldehyde-3-phosphate dehydrogenase	<i>Hordeum vulgare</i>	gi:18978	36.51	6.67	Energy
69	Putative glyceraldehyde-3-phosphate dehydrogenase	<i>Oryza sativa</i>	TC146536	36.56	7.69	Energy
70	Seed maturation protein PM34	<i>Glycine max</i>	TC131559	31.76	6.60	Metabolism
71	Heat shock protein 70 precursor	<i>Hordeum vulgare</i>	TC147130	67.01	5.76	Disease and defence
72	P0485G01 23	<i>Oryza sativa</i>	NP_916883	119.52	9.46	unclear
73	Putative nucleic acid binding protein	<i>Oryza sativa</i>	NP_922754	48.41	5.21	unclear
74	Viviparous 1 protein	<i>Hordeum vulgare</i>	gi:57282034	72.66	7.25	Transcription
75	B3 hordein	<i>Hordeum vulgare</i>	gi:123459	30.19	7.74	Protein destination and storage
76	Fructose-1-6-bisphosphate aldolase	<i>Oryza sativa</i>	TC146554	38.86	6.96	Energy
77	Fructose-1-6-bisphosphate aldolase	<i>Oryza sativa</i>	TC146554	38.86	6.96	Energy

78	B3 hordein	<i>Hordeum vulgare</i>	gi:123459	30.19	7.74	Protein destination and storage
79	B hordein	<i>Hordeum vulgare</i>	gi:1103203A	30.40	7.74	Protein destination and storage
80	B1 hordein	<i>Hordeum vulgare</i>	gi:809031	30.80	7.55	Protein destination and storage
81	Peroxidase BP 1 precursor	<i>Hordeum vulgare</i>	TC132499	38.82	7.57	Secondary metabolism
82	Peroxidase BP 1 precursor	<i>Hordeum vulgare</i>	TC132499	38.82	7.57	Secondary metabolism
83	Peroxidase BP 1 precursor	<i>Hordeum vulgare</i>	TC132499	38.82	7.57	Secondary metabolism
84	Hypothetical protein	<i>Oryza sativa</i>	gi:45736078	9.99	8.66	unclear
85	Meiotic recombination protein DMC1 homolog	<i>Arabidopsis thaliana</i>	gi:21903409	37.51	5.54	Cell growth/division
86	Glucose and ribitol dehydrogenase homolog	<i>Hordeum vulgare</i>	gi:7431022	31.64	6.54	Metabolism
87	Aldose reductase	<i>Hordeum vulgare</i>	TC139599	35.80	6.51	Metabolism
88	Peroxidase BP 1 precursor	<i>Hordeum vulgare</i>	TC132499	38.82	7.57	Secondary metabolism
89	Glucan endo-1-3-beta-glucosidase	<i>Hordeum vulgare</i>	TC130869	35.03	9.80	Metabolism
90	Unknown protein	<i>Oryza sativa</i>	gi:46390660	181.80	6.84	unclear
93	Glyoxalase I	<i>Oryza sativa</i>	TC131211	32.55	5.51	Metabolism
94	Embryo-specific protein	<i>Oryza sativa</i>	TC147106	26.41	5.58	unclear
95	Lipoprotein-like	<i>Oryza sativa</i>	TC132560	28.05	7.79	unclear
96	Peroxidase	<i>Hordeum vulgare</i>	gi:22587	32.97	6.07	Secondary metabolism
97	ni					
98	ABA inducible protein PHV A1	<i>Hordeum vulgare</i>	gi:126081	21.81	9.02	Disease and defence
99	WSI18 protein	<i>Oryza sativa</i>	TC148721	22.13	9.14	Disease and defence
100	WSI18 protein	<i>Oryza sativa</i>	TC148721	22.13	9.14	Disease and defence
101	Putative chaperonin 21 precursor	<i>Oryza sativa</i>	gi:51091339	25.49	5.97	Protein destination and storage
102	Triosephosphate isomerase	<i>Hordeum vulgare</i>	TC150359	26.73	5.39	Metabolism
103	Dehydroascorbate reductase	<i>Triticum aestivum</i>	TC139245	23.35	5.88	Metabolism
104	Dehydroascorbate reductase	<i>Triticum aestivum</i>	TC139245	23.35	5.88	Metabolism
105	Peroxiredoxin	<i>Hordeum vulgare</i>	gi:1694833	23.96	6.31	Secondary metabolism
106	Peroxiredoxin	<i>Hordeum vulgare</i>	gi:1694833	23.96	6.31	Secondary metabolism
107	Peroxiredoxin	<i>Hordeum vulgare</i>	TC131600	23.96	6.31	Secondary metabolism
108	Peroxiredoxin	<i>Hordeum vulgare</i>	gi:1694833	23.96	6.31	Secondary metabolism

109	Barperm1	Hordeum vulgare	gi:2454602	21.65	8.15	Disease and defence
110	Thaumatococcus protein TLP8	Hordeum vulgare	gi:14164983	24.31	7.83	Disease and defence
111	Endochitinase	Hordeum vulgare	gi:18972	19.22	8.55	unclear
112	ABA inducible protein PHV A1	Hordeum vulgare	gi:126081	21.81	9.02	Disease and defence
113	ABA inducible protein PHV A1	Hordeum vulgare	gi:126081	21.81	9.02	Disease and defence
114	ABA inducible protein	Triticum aestivum	gi:33342178	17.52	5.95	Disease and defence
115	Protein disulfide-isomerase	Triticum aestivum	gi:48093450	11.57	7.92	Protein destination and storage
116	Unknown protein	Arabidopsis thaliana	TC142011	16.73	5.24	unclear
117	ni					
118	Aldose reductase	Hordeum vulgare	TC139599	35.80	6.51	Metabolism
119	ni					
120	Putative SP2G	Oryza sativa	TC146705	19.35	6.91	unclear
121	ABA inducible protein	Triticum aestivum	TC132484	17.52	5.95	unclear
122	Cold-regulated protein	Hordeum vulgare	TC147205	17.61	4.93	Disease and defence
123	Em H5 protein	Triticum aestivum	gi:6138910	10.05	5.14	unclear
124	ni					
125	ni					
126	Late embryogenesis abundant protein B19.3	Hordeum vulgare	TC149478	14.60	5.38	Disease and defence
127	Protein disulfide-isomerase precursor	Hordeum vulgare	TC146674	56.46	5.02	Protein destination and storage
128	ni					
129	EST		TC148236			unclear
130	16.9 kDa class I heat shock protein	Triticum aestivum	TC139954	16.87	5.83	Disease and defence
131	Cp31AHv protein	Hordeum vulgare	TC139537	31.92	4.61	Transcription
132	Cyclophilin	Triticum aestivum	gi:14334173	14.07	8.37	Protein destination and storage
133	Cyclophilin A-3	Triticum aestivum	gi:13925737	18.39	8.53	Protein destination and storage
134	RGH1A	Hordeum vulgare	gi:20513867	109.21	6.34	Disease and defence
135	ni					
136	Alpha amylase inhibitor BMAI 1	Hordeum vulgare	gi:2506771	15.81	5.36	Disease and defence
137	Trypsin/amylase inhibitor pUP13	Hordeum vulgare	gi:225102	14.74	5.35	Disease and defence
138	Seed maturation protein PM41	Glycine max	TC132166	8.17	4.86	unclear

139	Subtilisin chymotrypsin inhibitor CI-1C	Hordeum vulgare	gi:124129	8.25	6.79	Disease and defence
140	Alpha-amylase inhibitor BDAI-I precursor	Hordeum vulgare	TC146614	16.42	5.36	Disease and defence
141	Subtilisin-chymotrypsin inhibitor CI-1A	Hordeum vulgare	TC140132	8.88	5.24	Disease and defence
142	Subtilisin-chymotrypsin inhibitor CI-1B	Hordeum vulgare	gi:82382	8.96	5.33	Disease and defence
143	Subtilisin-chymotrypsin inhibitor CI-1A	Hordeum vulgare	TC140132	8.88	5.24	Disease and defence
144	Subtilisin-chymotrypsin inhibitor CI-2A	Hordeum vulgare	gi:124122	9.38	6.58	Disease and defence
145	Putative glyoxalase	Arabidopsis thaliana	TC132259	15.38	6.20	unclear
146	Nucleoside diphosphate kinase	Lolium perenne	TC139131	16.50	6.30	Metabolism
147	Unknown protein	Oryza sativa	TC131152	22.47	9.15	Secondary metabolism
148	10 kDa chaperonin	Oryza sativa	TC146885	10.64	7.97	Protein destination and storage
149	Pathogenesis related protein 4	Hordeum vulgare	gi:1808651	15.69	8.50	Disease and defence
150	Non-Specific lipid transfer protein 1	Hordeum vulgare	gi:47168353	12.30	8.70	Transporters
151	Non-Specific lipid transfer protein 1	Hordeum vulgare	gi:47168353	12.30	8.70	Transporters
152	Group 3 late embryogenesis abundant protein	Triticum aestivum	TC142378	33.36	5.01	Disease and defence
153	Superoxide dismutase	Oryza sativa	gi:34899232	15.08	5.92	Metabolism
154	Protein z-type serpin	Hordeum vulgare	TC139095	43.22	5.61	Protein destination and storage
155	Protein z-type serpin	Hordeum vulgare	TC139095	43.22	5.61	Protein destination and storage
156	Putative phosphoglycerate mutase	Oryza sativa	TC146528	60.78	5.42	Metabolism
157	ni					
162	ni					
163	ni					
165	Putative late embryogenesis abundant protein	Oryza sativa	gi:50906715	47.28	6.78	Disease and defence
166	Putative late embryogenesis abundant protein	Oryza sativa	gi:50906715	47.28	6.78	Disease and defence
167	Putative late embryogenesis abundant protein	Oryza sativa	gi:50906715	47.28	6.78	Disease and defence
168	Putative late embryogenesis abundant protein	Oryza sativa	gi:50906715	47.28	6.78	Disease and defence
181	Phosphoglyceromutase	Ricinus communis	TC136118	60.81	5.52	Energy

182	NADP malic enzyme	<i>Oryza sativa</i>	TC139309	64.26	6.50	Metabolism
184	Putative NADP malic enzyme	<i>Oryza sativa</i>	gi:34909414	59.25	6.49	Disease and defence
187	Beta-glucosidase	<i>Hordeum vulgare</i>	gi:804656	57.44	7.18	Metabolism
192	Group 3 late embryogenesis abundant protein	<i>Triticum aestivum</i>	TC142378	33.36	5.01	Disease and defence
193	Enolase	<i>Oryza sativa</i>	gi:90110845	47.97	5.41	Energy
195	Enolase	<i>Oryza sativa</i>	gi:90110845	47.97	5.41	Energy
197	Succinate-semialdehyde dehydrogenase	<i>Arabidopsis thaliana</i>	TC132154	56.55	6.51	Metabolism
198	Alanine aminotransferase	<i>Hordeum vulgare</i>	gi:469148	52.87	5.93	Energy
201	ni					
202	39 kDa EF-Hand containing protein	<i>Solanum tuberosum</i>	TC132862	38.91	4.65	unclear
210	Protein z-type serpin	<i>Hordeum vulgare</i>	gi:1310677	43.22	5.61	Protein destination and storage
217	Isocitrate dehydrogenase precursor	<i>Medicago sativa</i>	gi:2497259	48.38	6.15	Energy
226	Glyceraldehyde-3-phosphate dehydrogenase	<i>Hordeum vulgare</i>	gi:120668	33.23	6.20	Energy
234	Rab28 protein	<i>Zea mays</i>	TC141145	27.70	4.90	Disease and defence
235	NAC domain containing protein	<i>Arabidopsis thaliana</i>	gi:10177651	17.88	5.10	Protein destination and storage
236	ni					
237	Rab28 protein	<i>Zea mays</i>	TC141145	27.70	4.90	Disease and defence
238	Rab28 protein	<i>Zea mays</i>	TC141145	27.70	4.90	Disease and defence
239	Cysteine-rich extensin-like protein-1	<i>Nicotiana tabacum</i>	TC148494	23.35	8.53	unclear
240	ni					
242	Late embryogenesis abundant protein D-34	<i>Gossypium hirsutum</i>	TC142245	26.91	4.85	Disease and defence
243	Glyoxalase I	<i>Oryza sativa</i>	TC131211	32.55	5.51	Metabolism
245	ni					
246	ni					
250	Peroxidase 1	<i>Hordeum vulgare</i>	gi:2624498	33.82	6.51	Secondary metabolism
251	Heat shock protein 70	<i>Spinacia oleracea</i>	TC142296	71.49	5.09	Disease and defence
254	Heat shock protein 70	<i>Spinacia oleracea</i>	TC142296	71.49	5.09	Disease and defence

Table A2: Identification of pQTL from the first experiment of introgression lines. The table provides the spot number from 2-D gels, the marker position of the introgression as well as the chromosomal location, the LOD score and the protein identity with name and database entry.

Spot number	Marker.Spot number	Chromosomal position	LOD	Annotationen	Identifier
882	Ebmac674.p882	6H	4.796	39 kDa EF-Hand containing protein	TC132862
1233	K117_2s.p1233	4H	3.245	6-phosphogluconolactonase-like protein	TC139824
	TF132_1s.p1233	5H	3.245		
513	Bmag007.p513	7H	3.138	70 kDa peptidylprolyl isomerase	TC139525
1694	Bmac031.p1694	7H	3.487	ABA inducible protein	gi:33342178
1035	Bmag516.p1035	7H	3.113	Adenosine kinase	gi:21698922
1843	eQTL225_1s.p1843	6H	6.085	Alpha hordothionin precursor	CAA29330.1
2076	Bmac316.p2076	6H	6.435	Alpha-amylase inhibitor BDAI-I precursor	gi:123970
1696	Bmac090.p1696	1H	3.841	Amylase subtilisin inhibitor	gi:225172
	Ebmac674.p1696	6H	3.841		
1050	GBMS062.p1050	1H	4.190	B hordein	gi:18929
1179	Bmag007.p1179	7H	7.648	B hordein	gi:73427781
1182	GBMS062.p1182	1H	5.765	B1 hordein	gi:809031
1133	GBMS062.p1133	1H	6.923	B1 hordein	gi:809031
1023	GBMS062.p1023	1H	5.418	B3 hordein	gi:18914
1090	GBMS096.p1090	4H	3.024	B3 hordein	gi:18914
1533	GBMS096.p1533	4H	4.060	Barperm1	gi:2454602
687	GBMS062.p687	1H	5.046	Beta amylase	gi:18918
1721	eQTL433_1s.p1721	2H	3.293	Cold-regulated protein	gi:10799810
1223	Ebmac674.p1223	6H	3.723	Cysteine-rich extensin-like protein 1	TC148494
1259	GBMS096.p1259	4H	5.382	Cysteine-rich extensin-like protein 1	TC148494
1273	GBMS096.p1273	4H	3.410	Cysteine-rich extensin-like protein 1	TC148494
508	TF129_1s.p508	8H	3.880	Cytosolic NADP malic enzyme	TC139309
1643	GBMS096.p1643	4H	3.805	Eukaryotic translation initiation factor 5A1	gi:74048999
1009	Ebmac674.p1009	6H	6.408	Glutamine synthetase	TC130809
1061	Bmac303.p1061	5H	5.012	Glyceraldehyde-3-phosphate dehydrogenase	TC131363

1025	GBMS087.p1025	4H	10.217	Glyceraldehyde-3-phosphate dehydrogenase	gi:18978
1026	GBMS087.p1026	4H	8.167	Glyceraldehyde-3-phosphate dehydrogenase	TC131363
1341	Bmag613.p1341	6H	4.132	Late embryogenesis abundant protein D-34	TC142245
1891	GBMS079.p1891	4H	3.964	LEA protein	TC132484
1771	GBMS065.p1771	1H	4.140	LEA protein	TC132485
1647	Bmag518.p1647	2H	6.951	No description given, EST	gi:15081660
2128	AF43094A.p2128	5H	3.564	Non-Specific lipid transfer protein 1	gi:47168353
	Hvole.p2128	4H	3.564		
2142	GBMS002.p2142	2H	4.156	Non-Specific lipid transfer protein 1	gi:47168353
377	Bmac031.p377	7H	3.915	Orthophosphate dikinase	TC146954
1315	Bmac090.p1315	1H	3.573	Peroxidase	gi:22587
	Ebmac674.p1315	6H	3.573		
1172	Bmag007.p1172	7H	8.947	Peroxidase 1	gi:2624498
1227	Bmag007.p1227	7H	6.096	Peroxidase 1	gi:167081
1247	Bmag007.p1247	7H	7.109	Peroxidase 1	gi:2624498
1153	Bmag007.p1153	7H	4.246	Peroxidase BP 1 precursor	gi:167081
1197	Bmag007.p1197	7H	6.587	Peroxidase BP 1 precursor	TC132499
1211	Bmag007.p1211	7H	5.148	Peroxidase BP 1 precursor	TC132499
1461	GBMS087.p1461	4H	4.855	Peroxiredoxin	gi:1694833
552	Bmac181.p552	4H	4.481	Phosphoglyceromutase	gi:1346735
807	Bmac090.p807	1H	3.024	Proline-rich protein	TC143234
	Ebmac674.p807	6H	3.024		
1664	GBMS077.p1664	5H	3.510	Protein disulfide-isomerase	gi:48093450
813	GBMS065.p813	1H	4.063	Protein disulfide-isomerase precursor	TC146674
962	Bmac090.p962	1H	4.122	Protein disulfide-isomerase precursor	TC146674
	Ebmac674.p962	6H	4.122		
629	GBMS065.p629	1H	3.223	Protein disulfide-isomerase precursor	gi:493587
721	GBMS062.p721	1H	3.686	Protein disulfide-isomerase precursor	gi:493587
1356	Bmag516.p1356	7H	3.006	Protein synthesis inhibitor I	gi:132577
1000	Bmac303.p1000	5H	3.549	Protein z-type serpin	TC139095
970	Bmac181.p970	4H	4.966	Protein z-type serpin	TC139095

928	Ebmac674.p928	6H	3.944	Protein z-type serpin	TC139095
967	Bmac181.p967	4H	5.883	Protein z-type serpin	gi:1310677
971	Bmac181.p971	4H	4.151	Protein z-type serpin	gi:1310677
1040	Bmac303.p1040	5H	5.978	Protein z-type serpin	gi:1310677
1064	Bmac303.p1064	5H	6.040	Protein z-type serpin	gi:1310677
693	Bmac090.p693	1H	15.034	Putative dihydrolipoamide dehydrogenase	gi:50932201
751	GBMS035.p751	7H	7.886	Putative enolase	gi:55297212
1342	Bmac090.p1342	1H	3.633	Putative glutathione-S-transferase	TC139406
	Ebmac674.p1342	6H	3.633		
932	Ebmac674.p932	6H	4.155	Putative heat shock cognate protein	gi:2695923
640	Ebmac705.p640	3H	3.148	Pyrophosphate fructose-6-phosphate-1-phosphotransferase	TC139326
601	Bmac316.p601	6H	4.741	Pyruvate decarboxylase	TC130780
338	Bmac090.p338	1H	6.069	Pyruvate phosphate dikinase	gi:62738112
	Ebmac674.p338	6H	6.069		
1250	eQTL433_1s.p1250	2H	4.280	Rab28 protein	gi: 22460
954	Bmac316.p954	6H	3.972	Seed maturation protein PM34	TC131559
2100	Bmac090.p2100	1H	4.624	Subtilisin-chymotrypsin inhibitor CI 1	gi:124129
	Ebmac674.p2100	6H	4.624		
2064	Bmac316.p2064	6H	4.063	Subtilisin-chymotrypsin inhibitor CI 1	gi:124129
1506	Bmac090.p1506	1H	4.780	Superoxide dismutase	gi:1654387
	Ebmac674.p1506	6H	4.780		
1336	Bmac090.p1336	1H	5.589	Translation elongation factor eEF 1	BI948454
1498	Ebmac674.p1498	6H	4.195	Translationally controlled tumor protein	CA002363

Table A3: Identification of pQTL from the second set of introgression lines. Given in the table are the spot numbers from 2-D gels, the marker position of the introgression as well as the chromosomal location, the LOD score, protein identity with name and database entry as well as the functional classification. In the analysis of the second experiment, molecular markers with unclear localisation were grouped (chromosome order).

Spot number	Marker.Spot number	Chromosome order	LOD	Annotationen	Identifier	Classification
2573	eQTL225_1s.p2573	C.2H-6H	3.303	1-Cys peroxiredoxin PER1	TC131600	Secondary metabolism
1276	Ebmac684.p1276	5H	5.137	6-phosphogluconate dehydrogenase	TC146849	Energy
2903	Bmag516.p2903	C.4H-7H	5.754	Adenosine kinase-like protein	TC131518	Metabolism
	AF43094A.p2391				TC139599	Metabolism
2391	Hvole.p2391	C.4H-5H	3.339	Aldose reductase		
	K095_3s.p2391					
3186	eQTL225_1s.p3186	C.2H-6H	3.027	Aldose reductase	gi:110590879	Metabolism
3676	eQTL433_1s.p3676	2H	5.270	Aldose reductase	gi:113595	Metabolism
3894	Bmac316.p3894	6H	3.647	Alpha-amylase inhibitor BDAI-1 precursor	gi:123970	Disease and defence
3866	K025_2s.p3866	2H	3.430	Alpha-amylase inhibitor BMAI-1 precursor	gi:2506771	Disease and defence
3409	eQTL225_1s.p3409	5H	4.542	Arabidopsis thaliana gDNA	TC148235	unclear
1610	GBMS062.p1610	1H	3.680	B hordein	gi:82548223	Protein destination and storage
1905	GBMS062.p1905	1H	4.259	B hordein	gi:73427781	Protein destination and storage
1984	GBMS062.p1984	1H	4.880	B hordein	gi:73427781	Protein destination and storage
2041	GBMS062.p2041	1H	3.863	B hordein	gi:73427781	Protein destination and

						storage
3429	GBMS077.p3429	2H	4.892	Beta amylase	gi:940385	Metabolism
1049	Bmac316.p1049	6H	3.299	Beta glucosidase	gi:804656	Metabolism
785	Bmag490.p785	C.4H-7H	3.692	Cytosolic NADP malic enzyme	TC139309	Metabolism
969	Bmac090.p969	C.1H-6H	3.601	Dihydrolipoamide dehydrogenase	TC147317	Energy
	Ebmac674.p969					
2589	Bmag613.p2589	C.1H-5H	3.106	Endosperm specific beta amylase 1	TC146664	Metabolism
2696	GBMS106.p2696	6H	3.264	Endosperm specific beta amylase 1	TC146664	Metabolism
1167	GBMS035.p1167	7H	3.365	Enolase 1	35_14450	Energy
3198	Bmag490.p3198	C.4H-7H	3.808	Eukaryotic translation initiation factor 4A	gi:2500519	Protein synthesis
3064	Bmag613.p3064	6H	3.745	Eukaryotic translation initiation factor 1A	TC146692	Protein synthesis
2987	eQTL433_1s.p2987	2H	3.926	Eukaryotic translation initiation factor 5A3	gi:74049040	Protein synthesis
2664	Bmag490.p2664	C.4H-7H	3.756	Glucan endo-1,3-beta D glucosidase	gi:29569880	Metabolism
2404	GBMS077.p2404	5H	3.586	Glucose and ribitol dehydrogenase homolog	gi:7431022	Metabolism
3192	Bmac310.p3192	4H	3.374	Glutathione peroxidase-like protein	TC131780	Disease and defence
1648	GBMS062.p1648	1H	4.050	Glyceraldehyde-3-phosphate dehydrogenase	gi:120680	Energy
2362	GBMS077.p2362	5H	4.310	Glyceraldehyde-3-phosphate dehydrogenase	gi:149392290	Energy
2591	Bmac316.p2591	6H	3.080	Glyoxalase I	TC130772	Metabolism
3304	eQTL433_1s.p3304	2H	3.234	Heat shock protein 16.9C	gi:295501	Disease and defence

3356	Bmag613.p3356	C.2H-6H	3.216	Heat shock protein 17	gi:21807	Disease and defence
703	Ebmac684.p703	5H	3.473	HSP70	gi:2827002	Disease and defence
2332	Bmag613.p2332	6H	3.140	HSP70	gi:2827002	Disease and defence
2411	K117_2s.p2411 TF132_1s.p2411	C.4H-5H	4.837	HSP70	gi:2827002	Disease and defence
1286	Bmag613.p1286	6H	3.107	Isocitrate dehydrogenase	gi:3021513	Energy
2432	eQTL433_1s.p2432	2H	3.324	Late embryogenesis abundant protein D 34	TC142245	Disease and defence
3548	Bmac090.p3548 Ebmac674.p3548	C.1H-6H	5.090	LEA protein	35_45168	Disease and defence
2509	GBMS096.p2509	4H	3.849	LEA1	TC139344	Disease and defence
422	eQTL235_3s.p422	4H	3.377	Lipoxygenase 1	35_14194	Metabolism
3001	Bmag516.p3001	C.4H-7H	3.643	Malate dehydrogenase	TC146609	Energy
938	GBMS035.p938		3.215	identification failed		
1236	eQTL433_1s.p1236		3.899	identification failed		
3600	Ebmac684.p3600	5H	4.148	Nucleoside diphosphate kinase	TC139131	Metabolism
3401	Hvole.p3401 K095_3s.p3401	4H	12.331	Nucleoside diphosphate kinase 4	TC147092	Metabolism
2084	Bmag007.p2084	7H	3.487	Peroxidase BP 1 precursor	TC132499	Secondary metabolism
2085	Ebmac415.p2085	2H	3.087	Peroxidase BP 1 precursor	TC132499	Secondary metabolism
2116	Bmag007.p2116	7H	7.074	Peroxidase BP 1 precursor	TC132499	Secondary metabolism
3330	Bmac316.p3330	6H	3.170	Peroxiredoxin	TC146841	Secondary metabolism
3042	Bmag490.p3042	C.4H-7H	4.174	Peroxiredoxin-2E-2	gi:75139348	Secondary metabolism

2786	Bmag490.p2786 AF43094A.p3879	C.4H-7H	4.530	Phosphate transporter HvPT5	NP661956 gi:6048569	Transporter Disease and defence
3879	Hvole.p3879 K095_3s.p3879	C.4H-5H	7.013	PR 4 Fragment		
2159	eQTL225_1s.p2159	C.2H-6H	3.084	Probable 6-phosphogluconolactonase 4	35_15947	Energy
1137	TF129_1s.p1137	1H	4.981	Probable inosine-5-monophosphate dehydrogenase	TC148243	Metabolism
1017	GBMS062.p1017	1H	7.974	Protein disulfide isomerase	gi:1709617	Protein destination and storage
1504	GBMS062.p1504	1H	3.338	Protein z-type serpin	TC139095	Protein destination and storage
1557	K102_4s.p1557	7H	7.759	Protein z-type serpin	gi:1310677	Protein destination and storage
751	GBMS002.p751	2H	5.834	Putative late embryogenesis abundant domain-containing protein	35_16650	Disease and defence
802	GBMS002.p802	2H	3.848	Putative late embryogenesis abundant domain-containing protein	35_16650	Disease and defence
911	GBMS035.p911	7H	3.686	Putative late embryogenesis abundant domain-containing protein	35_16650	Disease and defence
1173	Bmag007.p1173	7H	3.768	Putative late embryogenesis abundant domain-containing protein	35_16650	Disease and defence
2466	Bmac316.p2466	6H	3.901	Putative late embryogenesis abundant protein D 34	gi:113595605	Disease and defence

1292	GBMS035.p1292	7H	3.077	Putative monodehydroascorbate reductase	35_17669	Energy
2974	GBMS087.p2974	4H	3.043	Seed maturation protein PM34	TC131559	Metabolism
4062	Bmac090.p4062	C.1H-6H	7.333	Subtilisin-chymotrypsin inhibitor 2A	TC131963	Disease and defence
	Ebmac674.p4062					
3804	GBMS077.p3804	5H	5.848	Subtilisin-chymotrypsin inhibitor 2B	gi:18953	Disease and defence
2683	Bmag613.p2683	2H	4.631	Triosephosphate isomerase	gi:2507469	Metabolism
2801	Bmag516.p2801	C.4H-7H	3.154	Triosephosphate isomerase	gi:2507469	Metabolism

Table A4: Proteins identified in the barley root plasma membrane fraction of cultivars Steptoe and Morex via LC-based mass spectrometry. Identification was performed using the SwissProt *Viridiplantae* and TrEMBL *Poales* database. Number of transmembrane domains (TMD) was predicted using DAS (<http://www.sbc.su.se/~miklos/DAS/>) and TMPred (http://www.ch.embnet.org/software/TMPRED_form.html). Allocation to subcellular compartments was predicted using WoLF PSORT (<http://wolfpsort.org/>).

Protein number	Entry	Description	TMD	Subcellular localisation	Function
1	Q00985	1 aminocyclopropane 1 carboxylate oxidase 1 <i>Malus domestica</i>	0	Cytosol	Metabolism
2	P19950	40S ribosomal protein S14 <i>Zea mays</i>	0	Cytosol	Protein synthesis, stabilisation and degradation
3	O64650	40S ribosomal protein S27 1 <i>Arabidopsis thaliana</i>	0	Cytosol	Protein synthesis, stabilisation and degradation
4	Q9M339	40S ribosomal protein S3 2 <i>Arabidopsis thaliana</i>	0	Cytosol	Protein synthesis, stabilisation and degradation
5	Q949H0	40S ribosomal protein S7 <i>Hordeum vulgare</i>	0	Cytosol	Protein synthesis, stabilisation and degradation
6	A2YDY2	60S ribosomal protein L11 <i>Oryza sativa</i> subsp <i>indica</i>	0	Cytosol	Protein synthesis, stabilisation and degradation
7	A6N0Q9	60S ribosomal protein l22 2 Fragment <i>Oryza sativa</i> subsp <i>indica</i>	0	Cytosol	Protein synthesis, stabilisation and degradation
8	P49690	60S ribosomal protein L23 <i>Arabidopsis thaliana</i>	0	Cytosol	Protein synthesis, stabilisation and degradation
9	P14695	60S ribosomal protein L40 <i>Chlamydomonas reinhardtii</i>	0	Cytosol	Protein synthesis, stabilisation and degradation
10	P02581	Actin 1 <i>Glycine max</i>	2	Cytosol	Cellular organisation
11	P30172	Actin 100 Fragment <i>Solanum tuberosum</i>	2	Cytosol	Cellular organisation

12	P93375	Actin 104 Fragment <i>Nicotiana tabacum</i>	2	Cytosol	Cellular organisation
13	P53496	Actin 11 <i>Arabidopsis thaliana</i>	2	Cytosol	Cellular organisation
14	P0C539	Actin 2 <i>Oryza sativa</i> subsp <i>indica</i>	2	Cytosol	Cellular organisation
15	A2XNS1	Actin 3 <i>Oryza sativa</i> subsp <i>indica</i>	2	Cytosol	Cellular organisation
16	P30167	Actin 58 <i>Solanum tuberosum</i>	2	Cytosol	Cellular organisation
17	P93372	Actin 66 Fragment <i>Nicotiana tabacum</i>	2	Cytosol	Cellular organisation
18	P0C542	Actin 7 <i>Oryza sativa</i> subsp <i>indica</i>	2	Cytosol	Cellular organisation
19	P30168	Actin 71 <i>Solanum tuberosum</i>	2	Cytosol	Cellular organisation
20	P93584	Actin 82 Fragment <i>Solanum tuberosum</i>	2	Cytosol	Cellular organisation
21	P93371	Actin 93 Fragment <i>Nicotiana tabacum</i>	2	Cytosol	Cellular organisation
22	Q05214	Actin <i>Nicotiana tabacum</i>	2	Cytosol	Cellular organisation
23	Q41629	ADP ATP carrier protein 1 mitochondrial precursor <i>Triticum aestivum</i>	2	Mitochondrial	Transport
24	Q41630	ADP ATP carrier protein 2 mitochondrial precursor <i>Triticum aestivum</i>	2	Mitochondrial	Transport
25	P31691	ADP ATP carrier protein mitochondrial precursor <i>Oryza sativa</i> subsp <i>japonica</i>	2	Mitochondrial	Transport
26	P36397	ADP ribosylation factor 1 <i>Arabidopsis thaliana</i>	0	Golgi	Membrane trafficking
27	P49076	ADP ribosylation factor <i>Zea mays</i>	0	Golgi	Membrane trafficking
28	Q8S4X5	Aquaporin PIP1 <i>Triticum aestivum</i>	7	Plasma Membrane	Transport
29	Q9XF58	Aquaporin PIP2 5 <i>Zea mays</i>	6	Plasma Membrane	Transport
30	P93004	Aquaporin PIP2 7 <i>Arabidopsis thaliana</i>	6	Plasma Membrane	Transport
31	Q67G16	ARF <i>Oryza sativa</i> subsp <i>japonica</i>	0	Cytosol	Membrane trafficking
32	P37833	Aspartate aminotransferase cytoplasmic <i>Oryza sativa</i> subsp <i>japonica</i>	0	Cytosol	Metabolism
33	Q41628	ATP ADP carrier protein <i>Triticum turgidum</i>	5	Mitochondrial	Transport
34	P68538	ATP synthase protein MI25 <i>Triticum aestivum</i>	0	Mitochondrial	Transport
35	P12862	ATP synthase subunit alpha mitochondrial <i>Triticum aestivum</i>	0	Mitochondrial	Transport
36	P83483	ATP synthase subunit beta 1 mitochondrial precursor <i>Arabidopsis thaliana</i>	0	Mitochondrial	Transport
37	P83484	ATP synthase subunit beta 2 mitochondrial precursor <i>Arabidopsis thaliana</i>	0	Mitochondrial	Transport

38	Q9C5A9	ATP synthase subunit beta 3 mitochondrial precursor Arabidopsis thaliana	0	Mitochondrial	Transport
39	Q01859	ATP synthase subunit beta mitochondrial precursor Oryza sativa subsp japonica	0	Mitochondrial	Transport
40	P20649	ATPase 1 plasma membrane type Arabidopsis thaliana	11	Plasma Membrane	Transport
41	Q43128	ATPase 10 plasma membrane type Arabidopsis thaliana	11	Plasma Membrane	Transport
42	P19456	ATPase 2 plasma membrane type Arabidopsis thaliana	11	Plasma Membrane	Transport
43	P20431	ATPase 3 plasma membrane type Arabidopsis thaliana	11	Plasma Membrane	Transport
44	Q9SU58	ATPase 4 plasma membrane type Arabidopsis thaliana	11	Plasma Membrane	Transport
45	Q9SJB3	ATPase 5 plasma membrane type Arabidopsis thaliana	11	Plasma Membrane	Transport
46	Q9SH76	ATPase 6 plasma membrane type Arabidopsis thaliana	11	Plasma Membrane	Transport
47	Q9LY32	ATPase 7 plasma membrane type Arabidopsis thaliana	11	Plasma Membrane	Transport
48	Q9M2A0	ATPase 8 plasma membrane type Arabidopsis thaliana	11	Plasma Membrane	Transport
49	Q42556	ATPase 9 plasma membrane type Arabidopsis thaliana	11	Plasma Membrane	Transport
50	Q70DK2	Blue copper binding protein Hordeum vulgare var distichum	2	Plasma Membrane	GPI-anchored and cell wall-associated proteins
51	P29357	Chloroplast envelope membrane 70 kDa heat shock related protein Spinacia oleracea	0	Cytosol	Protein synthesis, stabilisation and degradation
52	O49342	Cytochrome P450 71A13 Arabidopsis thaliana	2	Mitochondrial	Metabolism
53	Q40034	Elongation factor 1 alpha Hordeum vulgare	0	Cytosol	Protein synthesis, stabilisation and degradation
54	P35683	Eukaryotic initiation factor 4A 1 Oryza sativa subsp japonica	0	Cytosol	Protein synthesis, stabilisation and degradation
55	Q40465	Eukaryotic initiation factor 4A 11 Nicotiana tabacum	0	Cytosol	Protein synthesis, stabilisation and degradation
56	Q40466	Eukaryotic initiation factor 4A 13 Fragment Nicotiana tabacum	0	Cytosol	Protein synthesis, stabilisation and degradation
57	Q40468	Eukaryotic initiation factor 4A 15 Nicotiana tabacum	0	Cytosol	Protein synthesis, stabilisation and degradation
58	P41377	Eukaryotic initiation factor 4A 2 Arabidopsis thaliana	0	Cytosol	Protein synthesis, stabilisation and degradation
59	Q9CA17	Eukaryotic initiation factor 4A 3 Arabidopsis thaliana	0	Cytosol	Protein synthesis, stabilisation and degradation
60	Q40470	Eukaryotic initiation factor 4A 7 Nicotiana tabacum	0	Cytosol	Protein synthesis, stabilisation and degradation
61	P41381	Eukaryotic initiation factor 4A 8 Nicotiana tabacum	0	Cytosol	Protein synthesis, stabilisation and degradation
62	Q40471	Eukaryotic initiation factor 4A 9 Nicotiana tabacum	0	Cytosol	Protein synthesis, stabilisation and degradation
63	P41378	Eukaryotic initiation factor 4A Triticum aestivum	0	Cytosol	Protein synthesis, stabilisation and degradation
64	Q9LSA5	F box Kelch repeat protein At3g18720 Arabidopsis thaliana	0	Cytosol	Protein synthesis, stabilisation and degradation
65	Q6YZC3	Glucose 6 phosphate phosphate translocator Oryza sativa subsp	4	Plasma Membrane	Transport

		japonica				
66	A5YVV3	Glyceraldehyde 3 phosphate dehydrogenase	Triticum aestivum	0	Cytosol	Metabolism
67	P11143	Heat shock 70 kDa protein	Zea mays	0	Cytosol	Protein synthesis, stabilisation and degradation
68	P22953	Heat shock cognate 70 kDa protein 1	Arabidopsis thaliana	0	Cytosol	Protein synthesis, stabilisation and degradation
69	P22954	Heat shock cognate 70 kDa protein 2	Arabidopsis thaliana	0	Cytosol	Protein synthesis, stabilisation and degradation
70	O65719	Heat shock cognate 70 kDa protein 3	Arabidopsis thaliana	0	Cytosol	Protein synthesis, stabilisation and degradation
71	P36181	Heat shock cognate protein 80	Solanum lycopersicum	2	Cytosol	Protein synthesis, stabilisation and degradation
72	A2YWQ1	Heat shock protein 81 1	Oryza sativa subsp indica	2	Cytosol	Protein synthesis, stabilisation and degradation
73	Q69QQ6	Heat shock protein 81 2	Oryza sativa subsp japonica	2	Cytosol	Protein synthesis, stabilisation and degradation
74	Q07078	Heat shock protein 81 3	Oryza sativa subsp japonica	2	Cytosol	Protein synthesis, stabilisation and degradation
75	A3B4W3	Histone H4	Oryza sativa subsp japonica	0	Nucleus	DNA binding
76	Q41811	Histone H4 3	Zea mays	0	Nucleus	DNA binding
77	O48518	HvPIP1 3 protein	Hordeum vulgare	7	Plasma Membrane	Transport
78	O48517	HvPIP2 1 protein	Hordeum vulgare	6	Plasma Membrane	Transport
79	Q8H1V3	Hypersensitive induced reaction protein 1	Hordeum vulgare var distichum	0	Cytosol	Stress proteins
80	A5HE90	Hypersensitive response protein	Triticum aestivum	0	Cytosol	Stress proteins
81	Q9LU11	IDS3	Hordeum vulgare	1	Cytosol	Metabolism
82	Q9GHE4	Maturase K	Alisma canaliculatum	4	Cytosol	Protein synthesis, stabilisation and degradation
83	P93306	NADH ubiquinone oxidoreductase 49 kDa subunit	Arabidopsis thaliana	0	Mitochondrial	Metabolism
84	Q0E3B7	Os02g0184200 protein	Oryza sativa subsp japonica, Inorganic diphosphatase activity	15	Vacuole	Transport
85	Q0DWS9	Os02g0797300 protein	Oryza sativa subsp japonica, ATPase activity	11	Plasma Membrane	Transport
86	Q0J9F5	Os04g0656100 protein	Oryza sativa subsp japonica, ATPase activity	13	Plasma Membrane	Transport
87	Q0DJ73	Os05g0319800 protein	Fragment Oryza sativa subsp japonica, ATPase activity	11	Plasma Membrane	Transport
88	Q0DH67	Os05g0489600 protein	Oryza sativa subsp japonica, Small GTPase mediated signal transduction	0	Cytosol	GPI-anchored and cell wall-associated proteins
89	Q0J0U7	Os09g0482600 protein	Oryza sativa subsp japonica, Protein	1	Cytosol	Protein synthesis, stabilisation and degradation

		folded				
90	Q01KM8	OSIGBa0158D24 1 protein	Oryza sativa, ATPase activity	13	Plasma Membrane	Transport
91	P46274	Outer mitochondrial membrane protein porin	Triticum aestivum	0	Mitochondrial	Transport
92	O80384	Ovp1	Oryza sativa, Inorganic diphosphatase activity	14	Vacuole	Transport
93	Q9FF53	Probable aquaporin PIP2 4	Arabidopsis thaliana	6	Plasma Membrane	Transport
94	Q9ZVX8	Probable aquaporin PIP2 8	Arabidopsis thaliana	6	Plasma Membrane	Transport
95	P93597	PSB5 protein Fragment	Triticum aestivum	3	Plasma Membrane	Transport
96	A2WWU5	Putative uncharacterized protein	Oryza sativa subsp indica, ATP binding	1	Cytosol	Protein synthesis, stabilisation and degradation
97	A2XJ31	Putative uncharacterized protein	Oryza sativa subsp indica, ATP binding	1	Cytosol	Protein synthesis, stabilisation and degradation
98	A2Y5F9	Putative uncharacterized protein	Oryza sativa subsp indica, ATP binding	0	Cytosol	Protein synthesis, stabilisation and degradation
99	A2YA07	Putative uncharacterized protein	Oryza sativa subsp indica, ATPase activity	11	Plasma Membrane	Transport
100	A2XBF8	Putative uncharacterized protein	Oryza sativa subsp indica, ATPase activity	11	Plasma Membrane	Transport
101	A2XKU5	Putative uncharacterized protein	Oryza sativa subsp indica, ATPase activity	10	Plasma Membrane	Transport
102	A2XYF8	Putative uncharacterized protein	Oryza sativa subsp indica, ATPase activity	13	Plasma Membrane	Transport
103	A2Y368	Putative uncharacterized protein	Oryza sativa subsp indica, ATPase activity	14	Plasma Membrane	Transport
104	A2YJ14	Putative uncharacterized protein	Oryza sativa subsp indica, ATPase activity	11	Plasma Membrane	Transport
105	A2YSS7	Putative uncharacterized protein	Oryza sativa subsp indica, ATPase activity	10	Plasma Membrane	Transport
106	A2YSS8	Putative uncharacterized protein	Oryza sativa subsp indica, ATPase activity	11	Plasma Membrane	Transport
107	A2ZN66	Putative uncharacterized protein	Oryza sativa subsp indica, ATPase activity	10	Plasma Membrane	Transport
108	A2XAK8	Putative uncharacterized protein	Oryza sativa subsp indica, ATPase activity	11	Plasma Membrane	Transport

109	A2XN99	Putative uncharacterized protein Calcium ion binding	Oryza sativa subsp indica,	1	Cytosol	GPI-anchored and cell wall-associated proteins
110	A2X6V9	Putative uncharacterized protein Glyceraldehyde-3-phosphate dehydrogenase (phosphorylating) activity	Oryza sativa subsp indica,	0	Cytosol	Metabolism
111	A2XUU7	Putative uncharacterized protein Glyceraldehyde-3-phosphate dehydrogenase (phosphorylating) activity	Oryza sativa subsp indica,	0	Cytosol	Metabolism
112	A2YJJ0	Putative uncharacterized protein GTP binding	Oryza sativa subsp indica,	1	Cytosol	GPI-anchored and cell wall-associated proteins
113	A2YE72	Putative uncharacterized protein Hydrogen ion transporting ATPase activity	Oryza sativa subsp indica,	0	Mitochondrial	Transport
114	A2YFW1	Putative uncharacterized protein Hydrogen ion transporting ATPase activity	Oryza sativa subsp indica,	1	Mitochondrial	Transport
115	A2WUC1	Putative uncharacterized protein Hydrogen-exporting ATPase activity	Oryza sativa subsp indica,	0	Cytosol	Transport
116	A2WPG7	Putative uncharacterized protein Inorganic diphosphatase activity	Oryza sativa subsp indica,	13	Vacuole	Transport
117	A2X1P8	Putative uncharacterized protein Inorganic diphosphatase activity	Oryza sativa subsp indica,	5	Vacuole	Transport
118	A2Y0L3	Putative uncharacterized protein Inorganic diphosphatase activity	Oryza sativa subsp indica,	5	Vacuole	Transport
119	A2Y9Y6	Putative uncharacterized protein Inorganic diphosphatase activity	Oryza sativa subsp indica,	13	Vacuole	Transport
120	A2YG95	Putative uncharacterized protein Protein modification process	Oryza sativa subsp indica,	0	Cytosol	Protein synthesis, stabilisation and degradation
121	A2YNK7	Putative uncharacterized protein Structural constituent of ribosome	Oryza sativa subsp indica,	0	Cytosol	Protein synthesis, stabilisation and degradation
122	A2XFL8	Putative uncharacterized protein Structural constituent of ribosome	Oryza sativa subsp indica,	0	Cytosol	Protein synthesis, stabilisation and degradation
123	A2XIT7	Putative uncharacterized protein Structural constituent of ribosome	Oryza sativa subsp indica,	0	Cytosol	Protein synthesis, stabilisation and degradation
124	A2YPV2	Putative uncharacterized protein Structural constituent of ribosome	Oryza sativa subsp indica,	0	Cytosol	Protein synthesis, stabilisation and degradation

125	A2YRX6	Putative uncharacterized protein Structural constituent of ribosome	Oryza sativa subsp indica,	0	Cytosol	Protein synthesis, stabilisation and degradation
126	A2YKV4	Putative uncharacterized protein Transporter activity	Oryza sativa subsp indica,	6	Plasma Membrane	Transport
127	A2Z2G1	Putative uncharacterized protein Unfolded protein binding	Oryza sativa subsp indica,	2	Cytosol	Protein synthesis, stabilisation and degradation
128	A2Z2G4	Putative uncharacterized protein Unfolded protein binding	Oryza sativa subsp indica,	2	Cytosol	Protein synthesis, stabilisation and degradation
129	A3AY68	Putative uncharacterized protein ATPase activity	Oryza sativa subsp japonica,	13	Plasma Membrane	Transport
130	A3BHE7	Putative uncharacterized protein ATPase activity	Oryza sativa subsp japonica,	11	Plasma Membrane	Transport
131	A3CJU4	Putative uncharacterized protein ATPase activity	Oryza sativa subsp japonica,	12	Plasma Membrane	Transport
132	A3B904	Putative uncharacterized protein ATPase activity	Oryza sativa subsp japonica,	9	Plasma Membrane	Transport
133	A3ANY8	Putative uncharacterized protein GTP binding	Oryza sativa subsp japonica,	0	Cytosol	GPI-anchored and cell wall-associated proteins
134	A3BHW2	Putative uncharacterized protein GTP binding	Oryza sativa subsp japonica,	1	Cytosol	GPI-anchored and cell wall-associated proteins
135	A2ZX43	Putative uncharacterized protein Hydrogen-exporting ATPase activity	Oryza sativa subsp japonica,	0	Cytosol	Transport
136	A3BCW4	Putative uncharacterized protein Hydrogen-exporting ATPase activity	Oryza sativa subsp japonica,	0	Cytosol	Transport
137	A3ACD7	Putative uncharacterized protein Inorganic diphosphatase activity	Oryza sativa subsp japonica,	13	Vacuole	Transport
138	A2ZSP0	Putative uncharacterized protein Inorganic diphosphatase activity	Oryza sativa subsp japonica,	13	Vacuole	Transport
139	A3B055	Putative uncharacterized protein Inorganic diphosphatase activity	Oryza sativa subsp japonica,	14	Vacuole	Transport
140	Q65X89	Putative uncharacterized protein OJ1593 C11 13	Oryza sativa subsp japonica	3	Endoplasmatic reticulum	unknown
141	P31414	Pyrophosphate energized vacuolar membrane proton pump 1 Arabidopsis thaliana		14	Vacuole	Transport

142	Q06572	Pyrophosphate energized vacuolar membrane proton pump Hordeum vulgare	14	Vacuole	Transport
143	P28188	Ras related protein ARA 5 Arabidopsis thaliana	0	Cytosol	GPI-anchored and cell wall-associated proteins
144	Q40723	Ras related protein RGP2 Oryza sativa subsp japonica	0	Cytosol	GPI-anchored and cell wall-associated proteins
145	Q4LB22	S adenosylmethionine synthetase Hordeum vulgare	0	Cytosol	Metabolism
146	O22347	Tubulin alpha 1 chain Eleusine indica	0	Cytosol	Cellular organisation
147	Q96460	Tubulin alpha 2 chain Hordeum vulgare	0	Cytosol	Cellular organisation
148	P20363	Tubulin alpha 3 alpha 5 chain Arabidopsis thaliana	0	Cytosol	Cellular organisation
149	Q9ZPP0	Tubulin beta 1 chain Eleusine indica	1	Cytosol	Cellular organisation
150	P12460	Tubulin beta 2 chain Glycine max	1	Cytosol	Cellular organisation
151	Q9ZPN8	Tubulin beta 3 chain Eleusine indica	1	Cytosol	Cellular organisation
152	Q41784	Tubulin beta 7 chain Zea mays	1	Cytosol	Cellular organisation
153	P69325	Ubiquitin Glycine max	0	Cytosol	Protein synthesis, stabilisation and degradation
154	O23654	Vacuolar ATP synthase catalytic subunit A Arabidopsis thaliana	0	Vacuole	Transport
155	Q38676	Vacuolar ATP synthase catalytic subunit A isoform 1 Acetabularia acetabulum	0	Vacuole	Transport
156	Q38677	Vacuolar ATP synthase catalytic subunit A isoform 2 Acetabularia acetabulum	0	Vacuole	Transport
157	Q40078	Vacuolar ATP synthase subunit B 1 Hordeum vulgare	0	Vacuole	Transport
158	Q40079	Vacuolar ATP synthase subunit B 2 Hordeum vulgare	0	Vacuole	Transport

Table A5: Summary of quantified proteins from two experiments for stress-induced changes in barley root plasma membranes. Given are the Protein accession and description and the score for identification. The relative intensity ratios between the respective groups as well as the P-value are given when the respective protein was detected in both groups. If this is not the case than only the group in which to protein was detected is shown. For processing of LC-MS^E data the Expression software (Waters) was used.

Morex: Control vs Salt Stress

Accession	Description	Score		Ratio Stress:Control		P-value Stress:Control	
		Experiment 1	Experiment 2	Experiment 1	Experiment 2	Experiment 1	Experiment 2
P24459	ATPAM_PHAVU ATP synthase subunit alpha mitochondrial Phaseolus vulgaris	147.65	126.56	0.74	0.27	0.02	0.00
P62787	H4_MAIZE Histone H4 Zea mays	214.33	116.44	0.46	Control	0.00	Control
Q01859	ATPBM_ORYSJ ATP synthase subunit beta mitochondrial precursor Oryza sativa subsp japonica	403.15	324.79	1.06	1.11	0.98	0.99
Q4LDT4	PIP aquaporin isoform - Hordeum vulgare	352.97	408.18	0.90	0.36	0.05	0.00
Q5PSM6	Plasma membrane H ⁺ -ATPase - Triticum aestivum	496.80	727.73	0.92	0.27	0.02	0.00

Step toe: Control vs Salt Stress

Accession	Description	Score		Ratio Stress:Control		P-value Stress:Control	
		Experiment 1	Experiment 2	Experiment 1	Experiment 2	Experiment 1	Experiment 2
Q08IH3	Aquaporin - Hordeum vulgare	417.75	486.05	0.52	0.82	0	0
P12862	ATPAM_WHEAT ATP synthase subunit alpha mitochondrial Triticum aestivum	233.37	296.72	1.92	1.46	1	1
Q06572	AVP_HORVU Pyrophosphate energized vacuolar membrane proton pump Hordeum vulgare	215.31	216.29	1.34	1.92	1	1
Q6YZC3	Glucose-6-phosphate/phosphate translocator - Oryza sativa subsp. japonica	129.09	149.08	1.25	1.9	0.95	1

Q43271	H(+)-transporting ATPase - Zea mays	458.21	591.3	0.51	0.31	0	0
Q7XAC0	H+-pyrophosphatase - Oryza sativa subsp. japonica	199.66	169.01	1.28	1.97	0.98	1
A5HE90	Hypersensitive response protein - Triticum aestivum	210.34	292.4	Control	Control	Control	Control
P43281	METK2_SOLLC S adenosylmethionine synthetase 2 Solanum lycopersicum	118.28	111.92	Stress	1.9	Stress	1
O80384	Ovp1 - Oryza sativa	158.4	158.15	1.27	2.01	0.97	1
P83970	PMA1_WHEAT Plasma membrane ATPase Triticum aestivum	1401.67	2056.91	0.7	0.44	0	0
Q704F4	Proton translocating pyrophosphatase - Oryza sativa	142.68	156.68	1.27	2.12	0.96	1
Q84L97	Proton-exporting ATPase (Fragment) - Zea mays	236.08	331.79	0.47	0.54	0	0.03
Q6H883	Putative inorganic diphosphatase - Oryza sativa subsp. japonica	155.34	150.33	1.28	1.93	0.95	1
Q9FS12	Vacuolar proton-inorganic pyrophosphatase - Hordeum vulgare	164.53	148.97	1.31	1.92	0.98	1

Table A6: Summary of quantified peptides from two experiments for stress-induced changes in barley root plasma membranes. Given are the Protein accession and description. The relative intensity ratios between the respective groups as well as the P-value are given when the respective protein was detected in both groups. If this is not the case than only the group in which to protein was detected is shown. For processing of LC-MS^E data the Expression software (Waters) was used.

Morex: Control vs. Salt Stress

Accession	Description	Peptide	Ratio Stress:Control		P-value Stress:Control	
			Experiment 1	Experiment 2	Experiment 1	Experiment 2
P31167	ADP ATP carrier protein 1 mitochondrial precursor A. thaliana	GNTANVIR	2.12	Stress	1	Stress
P31167	ADP ATP carrier protein 1 mitochondrial precursor A. thaliana	MMMTSGEAVK	1.35	2.89	0.99	1
Q41629	ADP ATP carrier protein 1 mitochondrial precursor T. aestivum	MTQNLGISVPIMSPSPMFANAP PEKK	8.25	Stress	1	Stress

P04709	ADP ATP carrier protein 1 mitochondrial precursor Z. mays	LSEPYKGI VDCFK	1.8	1.48	0.96	0.99
P04709	ADP ATP carrier protein 1 mitochondrial precursor Z. mays	QFNGLVDVYR	Stress	1.77	Stress	1
Q41630	ADP ATP carrier protein 2 mitochondrial precursor T. aestivum	SSLDAFQQIPAKEGAK	Stress	Stress	Stress	Stress
P12857	ADP ATP carrier protein 2 mitochondrial precursor Z. mays	LGGQFHLS S FSEGVR	Stress	Stress	Stress	Stress
P27080	ADP ATP carrier protein C. reinhardtii	GFNISCVGIVVYR	2.29	1.8	1	1
P27080	ADP ATP carrier protein C. reinhardtii	TVREEGFGSLWR	Stress	Stress	Stress	Stress
P27081	ADP ATP carrier protein mitochondrial precursor Fragment S. tuberosum	WFAGNLAGGGAGASSLLFVY SLDYAR	Stress	Stress	Stress	Stress
P27081	ADP ATP carrier protein mitochondrial precursor Fragment S. tuberosum	YFPTQALNFAFK	Stress	Stress	Stress	Stress
P31691	ADP ATP carrier protein mitochondrial precursor O. sativa	NFMIDFLMGGVSAAVSKTAAA PIER	Stress	7.85	Stress	1
P28011	Aspartate aminotransferase 1 M. sativa	LIFGADSPA IQENR	1.75	1.31	1	0.99
P28734	Aspartate aminotransferase cytoplasmic D. carota	APEDPILGVT VAYHK	1.63	Stress	0.95	Stress
P28734	Aspartate aminotransferase cytoplasmic D. carota	DQSPNKLNLG V GAYR	1.17	1.21	1	1
P28734	Aspartate aminotransferase cytoplasmic D. carota	VATVQCLSGT GSLR	1.45	Stress	0.95	Stress
P37833	Aspartate aminotransferase cytoplasmic O. sativa	MFVADGGELLMAQSYAK	Stress	Stress	Stress	Stress
Q67TM4	ATP synthase subunit alpha O. sativa	FGSDLDATTQALLNR	Stress	Stress	Stress	Stress
Q09EN6	ATP synthase subunit alpha T. dactyloides	ISQYEK	3.71	Stress	1	Stress
Q5VKV9	ATP synthase subunit alpha Fragment flavidulus	S. EVAAFAQFGSD LDAATQALLN R	Stress	4.35	Stress	1
A1XIS7	ATP synthase subunit alpha Fragment splendens	V. LTEV PK	1.82	Stress	0.97	Stress
Q06735	ATP synthase subunit alpha mitochondrial vulgaris	B. RPPGREAFPGDV FYLHSR	Stress	Stress	Stress	Stress
P05492	ATP synthase subunit alpha mitochondrial biennis	O. DTILN QK	Stress	Stress	Stress	Stress
P24459	ATP synthase subunit alpha mitochondrial vulgaris	P. IPQYER	Stress	1.55	Stress	0.96

P12862	ATP synthase subunit alpha mitochondrial T. aestivum	AILSTINPELQK	1.23	1.4	1	1
P12862	ATP synthase subunit alpha mitochondrial T. aestivum	EAFPGDVFYLHSR	Stress	Stress	Stress	Stress
P05494	ATP synthase subunit alpha mitochondrial Z. mays	VYGLNEIQAGEMVEFASGVK	Stress	Stress	Stress	Stress
Q06SI2	ATP synthase subunit alpha S. helveticum	MRPEEISSIIMK	Stress	1.45	Stress	1
Q06SI2	ATP synthase subunit alpha S. helveticum	QAITEYLDEFGAK	Stress	Stress	Stress	Stress
Q5N7P8	ATP synthase subunit beta O. sativa	ESVQSFQGVLDGK	Stress	Stress	Stress	Stress
Q0DG48	ATP synthase subunit beta O. sativa	IMNVIGEPIDEK	Stress	1.63	Stress	0.97
Q41534	ATP synthase subunit beta T. aestivum	IINVIGEPIDHKGDIK	Stress	Stress	Stress	Stress
O24346	ATP synthase subunit beta Fragment S. bicolor	VLNTGSPITVPVGR	1.75	2.12	1	0.97
P83483	ATP synthase subunit beta 1 mitochondrial precursor A. thaliana	TIAMDGTEGLVR	1.13	1.82	1	1
Q9C5A9	ATP synthase subunit beta 3 mitochondrial precursor A. thaliana	IMNVLGEPIDER	Stress	1.6	Stress	1
Q9C5A9	ATP synthase subunit beta 3 mitochondrial precursor A. thaliana	VAEYSTSSPANSAPSSAPAK	Stress	Stress	Stress	Stress
P38482	ATP synthase subunit beta mitochondrial precursor C. reinhardtii	MAGEIK	Stress	Stress	Stress	Stress
P29685	ATP synthase subunit beta mitochondrial precursor H. brasiliensis	MLSPHILGEEHYNTARGVQK	1.72	1.38	1	0.95
P17614	ATP synthase subunit beta mitochondrial precursor N. plumbaginifolia	CALVYQGMNEPPGARAR	Stress	Stress	Stress	Stress
P17614	ATP synthase subunit beta mitochondrial precursor N. plumbaginifolia	ESINSFQGVLDGK	Stress	Stress	Stress	Stress
P17614	ATP synthase subunit beta mitochondrial precursor N. plumbaginifolia	FTQANSEVSALLGR	Stress	1.21	Stress	1
P17614	ATP synthase subunit beta mitochondrial precursor N. plumbaginifolia	YVDLKEINSFQGVLDGK	Stress	2.56	Stress	1
Q01859	ATP synthase subunit beta mitochondrial precursor O. sativa	LGDK	Stress	Stress	Stress	Stress
Q01859	ATP synthase subunit beta mitochondrial precursor O. sativa	VVDLLAPYQR	1.36	1.21	1	1

P19023	ATP synthase subunit beta mitochondrial precursor Z. mays	AAAYASSAAAQAAPATPPPAT GK	Stress	Stress	Stress	Stress
P19023	ATP synthase subunit beta mitochondrial precursor Z.mays	IGLFGGAGVGK	Stress	1.88	Stress	1
P19023	ATP synthase subunit beta mitochondrial precursor Z. mays	ITDEFTGAGAIGQVCQVIGAVV DVR	Stress	Stress	Stress	Stress
A6MZB2	Glyceraldehyde 3 phosphate dehydrogenase Fragment O. sativa	GILGYVEEDLVSTDFQGDNR	Stress	Stress	Stress	Stress
P25861	Glyceraldehyde 3 phosphate dehydrogenase cytosolic A. majus	VIISAPSKDAPMFVVGVNEK	Stress	Stress	Stress	Stress
P26517	Glyceraldehyde 3 phosphate dehydrogenase cytosolic H. vulgare	LKGIMGYVEEDLVSTDFVGDSR	1.67	Stress	1	Stress
P17878	Glyceraldehyde 3 phosphate dehydrogenase cytosolic M. crystallinum	DEKTLFGETPVAVFGCR	Stress	1.55	Stress	1
P17878	Glyceraldehyde 3 phosphate dehydrogenase cytosolic M. crystallinum	TLLFGETPVAVFGCR	Stress	Stress	Stress	Stress
P26519	Glyceraldehyde 3 phosphate dehydrogenase cytosolic P. crispum	DELK	6.05	2.61	1	1
P26521	Glyceraldehyde 3 phosphate dehydrogenase cytosolic R. acris	SDIDIVSNASCTTNCLAPLAK	1.62	1.54	1	1
P26413	Heat shock 70 kDa protein G. max	VEIIPNDQGNR	2.2	Stress	0.99	Stress
P11143	Heat shock 70 kDa protein Z. mays	NAVVTVPAYFNDSQR	1.22	1.46	0.98	1
P29357	Heat shock related protein Chloroplast envelope membrane 70 kDa S. oleracea	FSDASVQADMKHRPFK	Stress	Stress	Stress	Stress
P29357	Heat shock related protein Chloroplast envelope membrane 70 kDa S. oleracea	LSEADK	4.85	1.63	1	1
P29357	Heat shock related protein Chloroplast envelope membrane 70 kDa S. oleracea	NQVAMNPINTVFDK	1.34	Stress	0.97	Stress
Q0J4P2	Heat shock protein 81 1 O. sativa	ASNTLSIIDSGIGMTK	0.42	0.57	0	0.01
Q0J4P2	Heat shock protein 81 1 O. sativa	EVSHEWLVNK	Control	Control	Control	Control
Q69QQ6	Heat shock protein 81 2 O. sativa	ASNTLSIIDSGVGMK	0.63	0.44	0.02	0
Q69QQ6	Heat shock protein 81 2 O. sativa	SGDELTSKDYVTR	Control	Control	Control	Control
Q07078	Heat shock protein 81 3 O. sativa	NLKLGIHEDSTNR	Control	0.31	Control	0

Q07078	Heat shock protein 81 3 O. sativa	VVVSDR	0.68	0.64	0.01	0
Q08277	Heat shock protein 82 Z. mays	ELISNASDALDK	0.61	0.53	0	0
Q7XJ80	Heat shock protein 90 cytosolic H. vulgare	EGQNEIYYITGESK	Control	0.79	Control	0.04
Q41811	Histone H4 3 Z. mays	DNIQGITKPAIR	0.47	0.2	0	0
Q41811	Histone H4 3 Z. mays	ISGLIYEETR	0.39	0.17	0	0
Q41811	Histone H4 3 Z. mays	TLYGFGG	0.26	Control	0	Control
Q41811	Histone H4 3 Z. mays	TYTEHAR	0.35	0.23	0	0
P59259	Histone H4 A. thaliana	GLIYEETR	Control	Control	Control	Control
P62785	Histone H4 variant TH011 T. aestivum	SGLIYEETR	Control	Control	Control	Control
P62785	Histone H4 variant TH011 T. aestivum	TVTAMDVVYALK	0.67	0.22	0	0
Q9LU11	IDS3 H. vulgare	ENILHATPAHVSLPESFVFASDK	Control	0.3	Control	0
Q40063	Ids3 H. vulgare	LFSGATYDTGGEK	0.57	0.7	0	0.01
Q6X677	NAR2 3 H. vulgare	VALDIPTATYYVR	1.48	2.77	1	1
Q6X677	NAR2 3 H. vulgare	VSLCYAPVSQK	1.48	2.36	1	1
Q4LDW9	PIP aquaporin H. vulgare	GFQSSYYVR	0.74	0.48	0	0
Q4LDW9	PIP aquaporin H. vulgare	PQGGEFSSK	Control	0.43	Control	0
Q4LDT4	PIP aquaporin isoform H. vulgare	AKDIEAAPPGGEYAAK	Control	0.44	Control	0
Q4LDT4	PIP aquaporin isoform H. vulgare	DIEAAPPGGEYAAK	Control	0.52	Control	0
Q4LDT4	PIP aquaporin isoform H. vulgare	PPPAPLFDAAELTK	0.61	0.33	0	0
O48518	PIP1 3 protein H. vulgare	GFQTTLYQGNGGGANSVAAGY TK	0.74	0.61	0	0
O48517	PIP2 1 protein H. vulgare	DYSDPPPAPIVDFEELTK	0.76	0.37	0	0
Q9FF53	PIP24 ARATH Probable aquaporin PIP2 4 A. thaliana	SFGAAVIYNNEK	0.63	0.54	0	0.01
Q9XF58	PIP25 MAIZE Aquaporin PIP2 5 Z. mays	GTGLAAEIIIGTFVLVYTVFSATD PK	Control	Control	Control	Control
Q9XF58	PIP25 MAIZE Aquaporin PIP2 5 Z. mays	YGGGANELSAGYSK	0.5	0.4	0	0
A7J2I1	Plasma membrane intrinsic protein T. aestivum	EAAPPGGEYAAK	0.67	Control	0.03	Control
A7J2I1	Plasma membrane intrinsic protein T. aestivum	PLFDAEELTK	0.78	0.58	0.01	0
Q9M7C2	Plasma membrane intrinsic protein 3 T. aestivum	MEGKEEDVR	0.13	Control	0	Control
P31414	Pyrophosphate energized vacuolar membrane	AAVIGDTIGDPLK	1.67	1.97	1	1

Q06572	proton pump 1 <i>A. thaliana</i> Pyrophosphate energized vacuolar membrane FTIFNFGAQQ	Stress	4.01	Stress	1
Q06572	proton pump <i>H. vulgare</i> Pyrophosphate energized vacuolar membrane VTPGAASAAAGAK	Stress	2.61	Stress	1
P21616	proton pump <i>P. aureus</i> Pyrophosphate energized vacuolar membrane VFIGLIVGAMPLPYWFSAMTMK	Stress	Stress	Stress	Stress
P21616	proton pump <i>P. aureus</i> Pyrophosphate energized vacuolar membrane YIEAGASEHARSLGPK	Stress	Stress	Stress	Stress
P50299	S adenosylmethionine synthetase 1 <i>H. vulgare</i> ATVDYEK	4.76	1.82	1	0.98
P50299	S adenosylmethionine synthetase 1 <i>H. vulgare</i> TQVTIEYLNEGGAMVPVR	2.59	Stress	1	Stress
P93438	S adenosylmethionine synthetase 2 <i>O. sativa</i> YLDEKTIFHLNPSGR	Stress	Stress	Stress	Stress
Q84QI7	Vacuolar proton inorganic pyrophosphatase <i>H. brevisubulatum</i> TADVGADLVGK	Stress	Stress	Stress	Stress
Q7Y070	Vacuolar proton inorganic pyrophosphatase <i>aestivum</i> T. GTAKPDYATCVK	Stress	1.79	Stress	1
Q7Y070	Vacuolar proton inorganic pyrophosphatase <i>aestivum</i> T. QFNTIPGLMKGTAKPDYATCVK	1.8	1.79	1	1
Q7Y070	Vacuolar proton inorganic pyrophosphatase <i>aestivum</i> T. VTPGAASAAGGGK	1.49	Stress	0.95	v

Steptoe Control vs. Salt Stress

Accession	Description	Peptide	Ratio Stress:Control		P-value Stress:Control	
			Experiment 1	Experiment 2	Experiment 1	Experiment 2
P49690	60S ribosomal protein L23 <i>Arabidopsis thaliana</i>	GSAITGPIGK	Steptoe control 1	0.32	Steptoe control 1	0.01
P14695	60S ribosomal protein L40 <i>Chlamydomonas reinhardtii</i>	EPSLQALAR	0.66	0.52	0.00	0.01
P35296	60S ribosomal protein L40 <i>Oryza sativa</i> subsp japonica	IIEPSLQALAR	0.64	0.64	0.00	0.00
P53504	Actin 1 <i>Sorghum bicolor</i>	LAYIALDYDQEMETAK	0.73	Control	0.03	Control
P53496	Actin 11 <i>Arabidopsis thaliana</i>	VAPEEHPVLLTEAPLNPK	0.21	Control	0.00	Control
P30165	Actin 2 <i>Pisum sativum</i>	NYELPDGQVITIGAER	0.58	0.39	0.00	0.00

P30168	Actin 71	Solanum tuberosum		LDLAGRDLTEYMK	Control	Control	Control	Control
P93584	Actin 82 Fragment	Solanum tuberosum		YSVWIGGSILASLSTFQQ	Control	Control	Control	Control
A3APH0	Putative uncharacterized protein subsp japonica	Actin	Oryza sativa	DLYGNIVLSGGTTMFPGIADRM SK	Control	Control	Control	Control
A3APH0	Putative uncharacterized protein subsp japonica	Actin	Oryza sativa	EITALAPSSMK	Control	Control	Control	Control
A3APH0	Putative uncharacterized protein subsp japonica	ACTIN	Oryza sativa	SSSSVEKSYELPDGQVITIGAER	Control	Control	Control	Control
P27080	ADP ATP carrier protein	reinhardtii	Chlamydomonas	GGGDRQFNGLVDVYR	0.67	Control	0.00	Control
P27080	ADP ATP carrier protein	reinhardtii	Chlamydomonas	TVREEFGSLWR	0.60	Control	0.04	Control
P27080	ADP ATP carrier protein	reinhardtii	Chlamydomonas	WFAGNMGGAAGAVSLSFV YSLDYARTR	Control	Control	Control	Control
P31691	ADP ATP carrier protein mitochondrial precursor	Oryza sativa subsp japonica		MMMTSGEAVK	0.76	Control	0.03	Control
P31691	ADP ATP carrier protein mitochondrial precursor	Oryza sativa subsp japonica		SDGIAGLYR	Control	Control	Control	Control
Q08IH3	Aquaporin	Hordeum vulgare		AKDIEAAPPGEYGAK	0.19		0.00	0.00
Q08IH3	Aquaporin	Hordeum vulgare		DPPPAPLFDAAELTK	0.48	Control	0.03	Control
Q08IH5	Aquaporin	Hordeum vulgare		GFQTTLYMGNGGGANSVAPGY TK	0.29	0.53	0.00	0.00
Q08IH4	Aquaporin	Hordeum vulgare		GFQTTLYQGNGGGANSVAAGY TK	0.39	0.61	0.00	0.00
Q08IH3	Aquaporin	Hordeum vulgare		LGSSASFGR	0.43	Control	0.00	Control
Q08IH3	Aquaporin	Hordeum vulgare		PGGEYGAK	0.29	0.63	0.00	0.00
Q08IH3	Aquaporin	Hordeum vulgare		PPPAPLFDAAELTK	Control	Control	Control	Control
Q08IH5	Aquaporin	Hordeum vulgare		QPIGTAAQGGGADEKDYK	Control	0.63	Control	0.03
A7J2I1	Plasma membrane intrinsic protein	aestivum	Triticum	AKDIEAAPPGEYAAK	0.21	0.53	0.00	0.00
A7J2I1	Plasma membrane intrinsic protein	aestivum	Triticum	ASATEFGSSASFGSN	Control	Control	Control	Control
A7J2I2	Plasma membrane intrinsic protein		Triticum	FGSSASFGSR	Control	Control	Control	Control

	aestivum							
Q9M7C3	Plasma membrane intrinsic protein 2	Triticum	GFQSSYYVR	0.33	0.64	0.00	0.00	
	aestivum							
Q9M7C3	Plasma membrane intrinsic protein 2	Triticum	GTGLAAEIIGPSCSLPVFSATDP	Control	Control	Control	Control	
	aestivum		K					
Q93XC3	Plasma membrane intrinsic protein 2	Fragment	GAAVIYNK	0.41	0.81	0.00	0.03	
	Triticum monococcum subsp aegilopoides							
Q9M7C2	Plasma membrane intrinsic protein 3	Triticum	MEGKEEDVR	0.05	0.30	0.00	0.00	
	aestivum							
O48518	Plasma membrane intrinsic protein	HvPIP1 3	YSEHQPIGTAAQGGGADEK	0.34	Control	0.00	Control	
	Hordeum vulgare							
O48518	Plasma membrane intrinsic protein	HvPIP1 3	YSEHQPIGTAAQGGGADEKDY	0.19	Control	0.00	Control	
	Hordeum vulgare		K					
O48517	Plasma membrane intrinsic protein	HvPIP2 1	DFEELTK	Control	Control	Control	Control	
	Hordeum vulgare							
O48517	Plasma membrane intrinsic protein	HvPIP2 1	DIEAAPQGGEFSSK	0.31	0.38	0.00	0.00	
	Hordeum vulgare							
O48517	Plasma membrane intrinsic protein	HvPIP2 1	DYSDPPPAPIVDFEELTK	0.27	0.60	0.00	0.00	
	Hordeum vulgare							
O48517	Plasma membrane intrinsic protein	HvPIP2 1	SLGAAVIYNTDK	0.34	0.71	0.00	0.01	
	Hordeum vulgare							
P11143	Heat shock 70 kDa protein	Zea mays	NAVVTVPAYFNDSQR	0.50	Control	0.00	Control	
P11143	Heat shock 70 kDa protein	Zea mays	VEIHANDQGNR	Control	0.47	Control	0.00	
A2WWU5	Putative uncharacterized protein	Oryza sativa	NQVAMNPINTVFDAK	0.64	0.63	0.03	0.01	
	subsp indica Hsp70							
Q943K7	Heat shock protein 70	Putative Oryza sativa subsp	MKELESICNPIIAK	0.63	0.61	0.03	0.03	
	japonica							
Q69QQ6	Heat shock protein 81 2	Oryza sativa subsp	ASNTLSIIDSGVGMTK	Control	0.58	Control	0.00	
	japonica							
Q69QQ6	Heat shock protein 81 2	Oryza sativa subsp	SGDELTSKDYVTR	0.54	0.57	0.00	0.00	
	japonica							
Q69QQ6	Heat shock protein 81 2	Oryza sativa subsp	TMEINPENSIMDELRL	Control	Control	Control	Control	
	japonica							
Q8H1V3	Hypersensitive induced reaction protein	1	AVEEELEK	0.33	0.24	0.00	0.00	

	Hordeum vulgare var distichum								
A5HE90	Hypersensitive response protein aestivum			Triticum	AMNEINAAAR	Control	0.34	Control	0.00
A5HE90	Hypersensitive response protein aestivum			Triticum	MNLDDVFEQK	Control	0.61	Control	0.01
A5HE90	Hypersensitive response protein aestivum			Triticum	SSAVFIPHGPGAVK	0.18	0.28	0.00	0.00
Q08435	Plasma membrane ATPase 1 plumbaginifolia			Nicotiana	GHVESVVK	Control	Control	Control	Control
Q08435	Plasma membrane ATPase 1 plumbaginifolia			Nicotiana	GVDADMVVLMAARASR	Control	0.58	Control	0.01
Q08435	Plasma membrane ATPase 1 plumbaginifolia			Nicotiana	LAQQGAIK	Control	Control	Control	Control
P22180	Plasma membrane ATPase 1 lycopersicum			Solanum	EIHFLPFNPTDK	Control	Control	Control	Control
P20649	Plasma membrane ATPase 1 Arabidopsis thaliana				ESPGGPWEFVGLLPLFDPPR	Control	Control	Control	Control
P20649	Plasma membrane ATPase 1 Arabidopsis thaliana				GSYR	Control	Control	Control	Control
P20649	Plasma membrane ATPase 1 Arabidopsis thaliana				HIVGMTGDGVNDAPALK	0.21	0.41	0.00	0.00
P20649	Plasma membrane ATPase 1 Arabidopsis thaliana				HIVGMTGDGVNDAPALKK	0.29	0.17	0.00	0.00
P19456	Plasma membrane ATPase 2 Arabidopsis thaliana				LLEGDPLKVDQSALTGESLPVK	0.30	Control	0.00	Control
P23980	Plasma membrane ATPase 2 Fragment lycopersicum			Solanum	KHICGMTGDGVNDAPALK	Control	Control	Control	Control
Q08436	Plasma membrane ATPase 3 plumbaginifolia			Nicotiana	DEISALPVDELIEK	0.34	Control	0.00	Control
P54211	Plasma membrane ATPase Dunaliella bioculata				ALNIGR	0.55	Control	0.00	Control
P54211	Plasma membrane ATPase Dunaliella bioculata				MGALSANTVTEEPIDMWLWES YPDRETIK	Control	Control	Control	Control
P54211	Plasma membrane ATPase Dunaliella bioculata				SMVVPVGNMGVDEIMR	Control	Control	Control	Control
Q7M290	Plasma membrane ATPase Fragments Avena sativa				ELSEIAEQAK	0.35	0.65	0.00	0.00
Q7M290	Plasma membrane ATPase Fragments Avena sativa				GTLTLNK	Control	0.39	Control	0.00
Q7M290	Plasma membrane ATPase Fragments Avena sativa				LGDIVPADAR	0.48	0.29	0.00	0.00
Q7M290	Plasma membrane ATPase Fragments Avena sativa				PGDIVSIK	0.40	0.36	0.00	0.00

Q7M290	Plasma membrane ATPase Fragments Avena sativa	VPGDIVSIK	Control	Control	Control	Control
Q7XPY2	Plasma membrane ATPase Oryza sativa subsp japonica	IAFTTK	0.63	0.25	0.02	0.00
Q7XPY2	Plasma membrane ATPase Oryza sativa subsp japonica	LGMGTNMYPSSALLGQNK	Control	Control	Control	Control
Q7XPY2	Plasma membrane ATPase Oryza sativa subsp japonica	NPGDEVFSGSTCK	0.57	0.32	0.00	0.00
Q7XPY2	Plasma membrane ATPase Oryza sativa subsp japonica	TALTYIDADGNWHR	Control	0.61	Control	0.00
P83970	Plasma membrane ATPase Triticum aestivum	ALVLGVNVK	0.31	0.36	0.00	0.00
P83970	Plasma membrane ATPase Triticum aestivum	ENYGKGER	0.61	Control	0.00	Control
P83970	Plasma membrane ATPase Triticum aestivum	GGLEEIR	Control	Control	Control	Control
P83970	Plasma membrane ATPase Triticum aestivum	GLDIDTINQNYTV	0.54	Control	0.04	Control
P83970	Plasma membrane ATPase Triticum aestivum	GVPPEHK	Control	0.38	Control	0.01
P83970	Plasma membrane ATPase Triticum aestivum	IDQSGLTGESLPVTK	0.60	0.34	0.00	0.00
P83970	Plasma membrane ATPase Triticum aestivum	KADIGIAVDDATDAAR	0.44	0.84	0.00	0.00
P83970	Plasma membrane ATPase Triticum aestivum	LLEGDPLK	0.33	0.29	0.00	0.00
P83970	Plasma membrane ATPase Triticum aestivum	LRELNTLK	Control	Control	Control	Control
P83970	Plasma membrane ATPase Triticum aestivum	LSVDK	Control	Control	Control	Control
P83970	Plasma membrane ATPase Triticum aestivum	LSVDKNLVEVFAK	0.66	0.73	0.01	0.00
P83970	Plasma membrane ATPase Triticum aestivum	LVLGVNVK	Control	Control	Control	Control
P83970	Plasma membrane ATPase Triticum aestivum	MTAIEELAGMDVLCSDK	0.74	0.44	0.05	0.00
P83970	Plasma membrane ATPase Triticum aestivum	NLVEVFAK	0.22	Control	0.00	Control
P83970	Plasma membrane ATPase Triticum aestivum	PASHTLFNDK	0.44	Control	0.00	Control
P83970	Plasma membrane ATPase Triticum aestivum	PEPASHTLFNDK	0.47	0.81	0.00	0.01
P83970	Plasma membrane ATPase Triticum aestivum	QGLTSDEGAQR	0.69	0.33	0.00	0.00
P83970	Plasma membrane ATPase Triticum aestivum	QWATAQR	0.38	0.73	0.00	0.02
P83970	Plasma membrane ATPase Triticum aestivum	SLAVAR	Control	Control	Control	Control
P83970	Plasma membrane ATPase Triticum aestivum	TGDQLAIGK	0.44	0.30	0.00	0.00
P83970	Plasma membrane ATPase Triticum aestivum	TLHGLQAPEPASHTLFNDK	Control	Control	Control	Control
P83970	Plasma membrane ATPase Triticum aestivum	VEIFGLNK	0.32	0.21	0.00	0.00

P83970	Plasma membrane ATPase	Triticum aestivum	VEIFGLNKLEEK	0.39	0.62	0.00	0.00
P83970	Plasma membrane ATPase	Triticum aestivum	VENQDAIDACMVGLADPK	0.73	0.30	0.03	0.00
P83970	Plasma membrane ATPase	Triticum aestivum	WGEQEASILVPGDIVSIK	0.45	0.42	0.00	0.00
Q0DJ73	Os05g0319800 protein Fragment	Oryza sativa subsp japonica	ATPase_P TAITYIDTKDGSWHR	0.13	Control	0.00	Control
A3B904	Putative uncharacterized protein	Oryza sativa subsp japonica	ATPase_P AEQIIELCNMAADAEK	Control	Control	Control	Control
A3CJU4	Putative uncharacterized protein	Oryza sativa subsp japonica	ATPase_P EGLTTQQAQQR	Control	Control	Control	Control
Q2TJ67	Plastid ATP ADP transporter	Oryza sativa subsp japonica	SGASGGGGGGVSCGAQPAAAA AAGAVPAAQPEGKK	Stress	2.20	Stress	1.00
O24381	Plastidic ATP ADP transporter	Solanum tuberosum	AAIDVVCNPLGK	5.21	1.84	1.00	1.00
O24381	Plastidic ATP ADP transporter	Solanum tuberosum	FNSLSSLKPNPLNGVSLSSNGFQ K	Stress	4.26	Stress	1.00
A2YGP5	Putative uncharacterized protein	Oryza sativa subsp indica	DNA/RNA_helicase_C ITTDLLAR	0.57	0.59	0.02	0.00
A3A343	Putative uncharacterized protein	Oryza sativa subsp japonica	Helicase_C SLER	Control	0.49	Control	0.01
P28188	Ras related protein ARA 5	Arabidopsis thaliana	LLLIGDSGVGK	Control	0.35	Control	0.00
Q0DH67	Os05g0489600 protein	Oryza sativa subsp japonica	small_GTP RAS QDLPNAMNAAEITDK	Control	Control	Control	Control
A3BHW2	Putative uncharacterized protein	Oryza sativa subsp japonica	small_GTP RAS DYISIADVWGR	Control	Control	Control	Control
A4K4Y4	Tubulin alpha 3B	Triticum aestivum	CGINYQPPSVVPGDLAK	Control	Control	Control	Control
O22347	Tubulin alpha 1 chain	Eleusine indica	AVCMISNSTSVVEVFSR	Control	Control	Control	Control
P14640	Tubulin alpha 1 chain	Zea mays	TIGGGDDAFNTFFSETGAGK	Control	Control	Control	Control
Q6VAG0	Tubulin alpha 2 chain	Gossypium hirsutum	FDGALNVDVTEFQTNLVYPR	Control	Control	Control	Control
Q53M52	Tubulin alpha 2 chain	Oryza sativa subsp japonica	GDVVPK	Control	0.47	Control	0.00
P12411	Tubulin beta 1 chain	Arabidopsis thaliana	AVLMDLEPGTMD SIR	0.50	Control	0.00	Control
P25862	Tubulin beta 1 chain	Fragment Avena sativa	GHYTEGAELIDSVLDVVR	Control	Control	Control	Control
P24636	Tubulin beta 4 chain	Arabidopsis thaliana	MASTFIGNSTSIQEMFR	0.28	0.52	0.00	0.00
Q9ZRA9	Tubulin beta 4 chain	Triticum aestivum	EILHIQGGQCGNQIGAK	Control	Control	Control	Control

A5CFY8	Tubulin beta 5	Hordeum vulgare var distichum	ALTVPELTQQMWDAK	Control	0.52	Control	0.01
A3ANA0	Putative uncharacterized protein subsp japonica Tubulin beta	Oryza sativa	YLTASAMFR	Control	Control	Control	Control
